DRAFT

Duke Energy South Bay Power Plant

SBPP Cooling Water System Effects on San Diego Bay

VOLUME I: Compliance with Section 316(a) of the Clean Water Act for the South Bay Power Plant

May 1, 2004

Submitted to:

San Diego Regional Water Quality Control Board
9174 Sky Park Court, Suite 100
San Diego, CA 92123-4340

Submitted by:

Duke Energy South Bay, LLC
990 Bay Blvd.
Chula Vista, CA 91911

Duke Energy South Bay Power Plant

SBPP Cooling Water System Effects on San Diego Bay

VOLUME I: Compliance with Section 316(a) of the Clean Water Act A.2 for the South Bay Power Plant

DRAFT

Submitted to:

Duke Energy South Bay, LLC
990 Bay Blvd.
Chula Vista, CA 91911

Prepared by:

Tenera Environmental
225 Prado Rd. Suite D
San Luis Obispo, CA 93401

971 Dewing Ave. Suite 101
Lafayette, CA 94549

and

Merkel & Associates
5434 Ruffin Rd.
San Diego, CA 92123

Table of Contents

List of Tables iv

List of Figures vi

Executive Summary **ES-1**

1.0 Introduction and Background **1.1-1**

1.1 Introduction 1.1-1
1.2 Background 1.2-1
1.3 Regulatory Setting 1.3-1
1.3.1 Overview 1.3-1
1.3.2 Federal Regulation of Thermal Discharges 1.3-1
1.3.3 California Regulation of Thermal Discharges 1.3-2
1.4 Effects of thermal discharges: Overview 1.4-1
1.5 Study Design 1.5-1
1.5.1 Background 1.5-1
1.5.2 Analysis Rationale 1.5-1
1.5.3 Study Limitations 1.5-2
1.6 Report Organization 1.6-1

2.0 Description of the South Bay Power Plant and Characteristics of the Source Water Body **2.1-1**

2.1 South Bay Power Plant 2.1-1
2.1.1 SBPP Intake 2.1-1
2.1.2 SBPP Discharge 2.1-2
2.1.3 CWP Flows and Point-of-Discharge Water Temperatures 2.1-3
2.2 San Diego Bay Environmental Setting 2.2-1
2.2.1 Physical Description 2.2-1
2.2.2 Biological Description 2.2-2
2.3 Receiving Water Temperature Monitoring 2.3-1
2.3.1 Introduction 2.3-1
2.3.2 Methods 2.3-2
2.3.3 Intertidal Temperature Results 2.3-8
2.3.4 Subtidal Temperature Results 2.3-9
2.3.5 Thermal Gradients: Delta-T° Modeling and Estimation 2.3-13
2.3.6 Temperature Exposure: Frequency and Duration 2.3-16
2.4 Dissolved Oxygen 2.4-1
2.4.1 Introduction 2.4-1
2.4.2 Methods 2.4-2
2.4.3 Results 2.4-6
2.5 Receiving Water Currents and Bathymetry 2.5-1
2.5.1 Introduction 2.5-1
2.5.2 Methods 2.5-2

DRAFT

2.5.3 Results 2.5-6
2.6 Receiving Water Turbidity Monitoring 2.6-1
2.6.1 Introduction 2.6-1
2.6.2 Methods 2.6-2
2.6.3 Results 2.6-5
2.6.4 Numerical Modeling 2.6-7
2.7 Receiving Water Sediment Characteristics 2.7-1
2.7.1 Introduction 2.7-1
2.7.2 Methods 2.7-2
2.7.3 Results 2.7-2
2.8 Receiving Water Chlorine Monitoring 2.8-1
2.8.1 Introduction 2.8-1
2.8.2 Methods 2.8-2
2.8.3 Results 2.8-2

3.0 Biological Studies 3.1-1

3.1 Introduction 3.1-1
3.2 Eelgrass Studies 3.2-1
3.2.1 Introduction 3.2-1
3.2.1 Review of Eelgrass Studies in South San Diego Bay and Vicinity 3.2-2
3.2.2 Methods 3.2-4
3.2.3 Results 3.2-6
3.3 Benthic Invertebrates 3.3-1
3.3.1 Introduction 3.3-1
3.3.2 Review of Benthic Invertebrate Studies in South San Diego Bay 3.3-1
3.3.3 Methods 3.3-4
3.3.4 Results 3.3-7
3.4 Fish Communities 3.4-1
3.4.1 Introduction 3.4-1
3.4.2 Review of Fish Studies in South San Diego Bay 3.4-1
3.4.3 Methods 3.4-3
3.4.4 Results 3.4-5

4.0 Integrated Discussion 4.1-1

4.1 Introduction 4.1-1
4.2 Eelgrass 4.2-1
4.2.1 SBPP Influence on Turbidity 4.2-2
4.2.2 SBPP Influence on Eelgrass Distribution 4.2-3
4.3 Benthic Invertebrates 4.3-1
4.3.1 Discrimination of Discharge and Reference Assemblages 4.3-1
4.3.2 Discharge Effects Gradients 4.3-3
4.3.3 Faunal Associations with Physical Factors 4.3-4
4.3.4 Conclusions 4.3-7
4.4 Effect of Cooling Water Discharges on Fish Communities: Role of Dissolved Oxygen 4.4-1

5.0 Literature Cited 5-1

DRAFT

Appendices

Appendix A	Letter dated May 24, 2002 from John H. Roburtus, California Regional Water Quality Control Board to Donald Weaver, Duke Energy South Bay
Appendix B	Daily Average Temperatures July 17–September 30, 2003
Appendix C1	SBPP Temperature Data/Animations CD
Appendix C2	SBPP Temperature Delta-T˚ Data/Animations CD
Appendix D	SBPP Current Data/Animations CD
Appendix E	Dissolved Oxygen Data
Appendix F	Station Acoustic Doppler Profiler (ADCP) Average and Depth Bin Current Speed and Direction Estimates August 4–5, 2003.
Appendix G	Hourly Acoustic Doppler Profiler (ADP) Average and Depth Bin Current Speed and Direction Estimates July 17–August 14, 2003.
Appendix H	Turbidity Data
Appendix I	Benthic Faunal Data
Appendix J	Fish Sampling Data

DRAFT

List of Tables

2.0 Description of the South Bay Power Plant and Characteristics of the Source Water Body

2.1 Discharge Description
Table 2.1-1. South Bay Power Plant, generating capacity and cooling water flow volumes by unit. 2.1-1

2.3 Receiving Water Temperature Monitoring
Table 2.3-1. Locations of subtidal and intertidal temperature stations 2.3-6
Table 2.3-2. Distance of subtidal and intertidal temperature stations from the SBPP discharge boom 2.3-7
Table 2.3-3. Percent frequency of the 8.3º C delta-Tº discharge excursion distances (m) during July–September 2003 ..... 2.3-16
Table 2.3-4. Comparison of percent frequency delta-Tº discharge excursion distances during July–September 2003 ..... 2.3-18
Table 2.3-5. The number and duration of temperature excursions to 27°C or above.... 2.3-19
Table 2.3-6. The number and duration of temperature excursions to 30°C or above.... 2.3-20

2.5 Receiving Water Currents
Table 2.5-1. Current measurements at Doppler stations during different tidal levels and discharge volume conditions 2.5-9
Table 2.5-2. Cross-section areas and estimated current speeds at locations in the SBPP discharge embayment and intake channel 2.5-12
Table 2.5-3. Area and volume of SBPP discharge embayment for various tidal heights 2.5-13

2.6 Receiving Water Turbidity Monitoring
Table 2.6-1. Manning's roughness coefficients (n) applied to San Diego Bay TRIM-2D model. 2.6-10

3.0 Biological Studies

3.2 Eelgrass Studies
Table 3.2-1. Eelgrass coverage categories and acreages in study area 3.2-7

3.3 Benthic Invertebrates
Table 3.3-1. Benthic infaunal community parameters at SBPP subtidal monitoring stations, July–September 2003.. ..... 3.3-10
Table 3.3-2. Benthic infaunal community parameters at SBPP intertidal monitoring stations, July–September 2003 ..... 3.3-11

DRAFT

Table 3.3-3. Taxa with the 20 highest and 20 lowest pollution tolerance indices (pi) for taxa enumerated in SBPP benthic core samples. 3.3-12
Table 3.3-4. Description of benthic response index (BRI) assessment thresholds..... 3.3-13
Table 3.3-5. Comparison of ten most abundant invertebrate taxa at subtidal benthic stations in south San Diego Bay.. ..... 3.3-15
Table 3.3-6. Comparison of ten most abundant invertebrate taxa at intertidal benthic stations in south San Diego Bay... ..... 3.3-16
Table 3.3-7. Results of SIMPER analysis showing taxa and their relative contributions to the similarity among subtidal stations during the August 2003 survey. 3.3-18
Table 3.3-8. Results of SIMPER analysis showing taxa and their relative contributions to the dissimilarity between subtidal stations during the August 2003 survey. 3.3-19
Table 3.3-9. Results of SIMPER analysis showing taxa and their relative contributions to the dissimilarity between subtidal stations during the July 2003 survey. 3.3-20
Table 3.3-10. Results of SIMPER analysis showing taxa and their relative contributions to the dissimilarity between subtidal stations during the September 2003 survey..... 3.3-21
Table 3.3-11. Results of SIMPER analysis showing taxa and their relative contributions to the similarity among intertidal stations during the August 2003 survey..... 3.3-23
Table 3.3-12. Results of SIMPER analysis showing taxa and their relative contributions to the dissimilarity between intertidal stations during the August 2003 survey..... 3.3-24
Table 3.3-13. Results of SIMPER analysis showing taxa and their relative contributions to the dissimilarity between intertidal stations in the reference and discharge areas based on Bray-Curtis distances of one replicate from the July 2003 survey..... 3.3-25
Table 3.3-14. Results of SIMPER analysis showing taxa and their relative contributions to the dissimilarity between intertidal stations in the reference and discharge areas based on Bray-Curtis distances of one replicate from the September 2003 survey. 3.3-26
Table 3.3-15. Variable loadings for PCA analysis of physical variables measured at subtidal reference and discharge stations during the August 2003 survey. 3.3-27
Table 3.3-16. Variable loadings for PCA analysis of physical variables measured at intertidal reference and discharge stations during the August 2003 survey..... 3.3-28

3.4 Fishes
Table 3.4-1. Summary of fish abundance and density..... 3.4-6
Table 3.4-2. Summary of fish biomass. 3.4-7
Table 3.4-3. List of fish species observed in long term studies at SBPP discharge and other southern California reference sites. 3.4-12

4.0 Integrated Discussion

4.2 Eelgrass
Table 4.2-1. Predicted eelgrass areal coverage based on H_{sat} thresholds. 4.2-6

DRAFT

List of Figures

Executive Summary

Figure ES-1. Station location map of *in situ* temperature recorders, sediment grain size samples, and benthic biological samples. ES-12
Figure ES-2. a) Intake and discharge basins, southerly view from SBPP; b) Intake and discharge channels, southwesterly view from SPBB; c) Shoreline near Station IT1 exposed during low tide; d) SBPP discharge and discharge channel, easterly view near Station ST3.....ES-13
Figure ES-3. Mean, maximum, and minimum water temperatures during August 2003 at intertidal and subtidal stations in SBPP discharge channel and South Bay.....ES-14
Figure ES-4. Percent frequencies of 2.2°C (4°F) discharge delta T° excursion distances at four depths modeled by linear regressions of station temperatures <2.8 km from the discharge boom... .....ES-15
Figure ES-5. Mean hourly dissolved oxygen curves for South Bay open water and SBPP discharge channel monitoring stations plotted over the standard deviation of the mean hourly dissolved oxygen for the reference stations.....ES-16
Figure ES-6. Numeric model results of net predicted turbidity for the SBPP with cooling water flow of 441 mgd versus no cooling water flow and SBPP with cooling water flow of 601 versus no cooling water flow.....ES-17

2.0 Description of the South Bay Power Plant and Characteristics of the Source Water Body

2.1 Discharge Description

Figure 2.1-1. Diagram of cooling water intake and discharge structures 2.1-2
Figure 2.1-2. SBPP daily average circulating water flow from December 1, 1998 through September 30, 2003. ..... 2.1-4
Figure 2.2-1. Map of ecoregions in San Diego Bay..... 2.2-3

2.3 Receiving Water Temperature Monitoring

Figure 2.3-1a. Station location map for in situ temperature recorders, sediment grain size samples and benthic biological samples: all stations..... 2.3-21
Figure 2.3-1b. Station location map for in situ temperature recorders, sediment grain size samples and benthic biological samples: detail of intake channel and near-field stations. 2.3-22
Figure 2.3-2. Diagram of subtidal and intertidal temperature recorder arrays 2.3-23
Figure 2.3-3. Intertidal station temperatures (minimum, maximum and mean) in August 2003..... 2.3-24
Figure 2.3-4. Intertidal station delta-T° in July, August and September 2003 ..... 2.3-25
Figure 2.3-5. Intertidal station temperatures and tidal curve from Sept. 26–30, 2003 .. 2.3-26
Figure 2.3-6. Intertidal station temperatures and tidal curve from Sept. 2–6, 2003 ..... 2.3-26
Figure 2.3-7. Surface, -1 m subsurface, and bottom mean temperatures recorded at five stations from mid-July through September 30, 2003..... 2.3-27

Figure 2.3-8. Maximum, mean, and minimum temperatures at the surface, 1 m subsurface, and bottom levels at the subtidal stations in July 2003. ..... 2.3-28
Figure 2.3-9. Maximum, mean, and minimum temperatures at the surface, 1 m subsurface, and bottom levels at the subtidal stations in August 2003. ..... 2.3-29
Figure 2.3-10. Maximum, mean, and minimum temperatures at the surface, 1-m subsurface, and bottom levels at the subtidal stations in September 2003. ..... 2.3-30
Figure 2.3-11. Surface temperatures recorded at the eight subtidal stations located within 2,000 meters of the SBPP discharge boom, September 26–30, 2003 ..... 2.3-31
Figure 2.3-12. Surface temperatures recorded at the eight subtidal stations located within 2,000 meters of the SBPP discharge boom, September 2–6, 2003..... 2.3-31
Figure 2.3-13. SBPP plant load, tide level and surface temperature at 21 subtidal monitoring stations on September 5, 2003 at 1510 and 2310 (PST). 2.3-32
Figure 2.3-14. Power spectra for surface level temperature recorders of Stations ST1, ST4, SF4, SF2, SR1, and SA3. ..... 2.3-33
Figure 2.3-15. Example of the development of the thermal plume at SBPP on August 16, 2003 showing temperature at depth as a function of distance from the discharge boom.. ..... 2.3-34
Figure 2.3-16. Subtidal station mean delta-T° in August 2003 at surface, 1-meter and bottom levels 2.3-35
Figure 2.3-17. Percent frequency that the delta-T° exceeded 2.2°C (4°F) at various distances from the SBPP discharge boom. 2.3-36
Figure 2.3-18. Example temperatures, 2.2°C (4°F) relative delta T° and excursion distances (ball and arrow) modeled by linear regressions of station temperatures <2.8 km from the discharge boom. 2.3-37
Figure 2.3-19. Comparison of empirical and model linear regressions of percent frequencies of 2.2°C (4°F) discharge delta T° excursion distances at four depths.. 2.3-38
Figure 2.3-20. Percent frequencies of 2.2°C (4°F) discharge delta-T° excursion distances at four depths modeled by linear regressions of station temperatures 2.3-39
Figure 2.3-21. Map of percent frequencies of 2.2°C (4°F) discharge delta T° excursion distances at four depths modeled by linear regressions of station temperatures <2.8 km from the discharge boom. 2.3-40
Figure 2.3-22a. Dynamics of the thermal plume on Sept. 5, 2003; 0100–1100 PST. ... 2.3-41
Figure 2.3-22b. Dynamics of the thermal plume on Sept. 5, 2003; 0100–1100 PST.... 2.3-42
Figure 2.3-23. Autocorrelation functions (ACF) and lines of significance for delta T°, discharge temperature (SE7), delta T° excursion distance and reference..... 2.3-43
Figure 2.3-24. Crosscorrelation functions for delta-Tº vs. distance and discharge temperature (SE7) vs. 2.2º C delta-Tº excursion distance 2.3-44

2.4 Receiving Water Dissolved Oxygen Monitoring
Figure 2.4-1. Temperature and salinity effects on dissolved oxygen saturation curves at sea level pressure. 2.4-10
Figure 2.4-2. Hydrolab Datasonde monitoring station locations in South Bay, Summer 2003. ..... 2.4-11
Figure 2.4-3. Hydrolab Datasonde dissolved oxygen reference monitoring station locations, Summer 2003. ..... 2.4-12

Figure 2.4-4. Mean hourly dissolved oxygen curve for South Bay open water and discharge channel monitoring stations. 2.4-13
Figure 2.4-5. Mean hourly dissolved oxygen curves for each of the study reference stations. 2.4-14
Figure 2.4-6. Mean hourly dissolved oxygen curve for the combined average of the study reference stations. 2.4-15
Figure 2.4-7. Mean hourly dissolved oxygen curves for South Bay open water and SBPP discharge channel monitoring stations plotted over the standard deviation of the mean hourly dissolved oxygen for the reference stations..... 2.4-16
Figure 2.4-8. Mean hourly temperature curves for South Bay open water and discharge channel monitoring stations. 2.4-17
Figure 2.4-9. Mean hourly temperature curves for reference monitoring stations. 2.4-18
Figure 2.4-10. Mean hourly salinity curves for South Bay monitoring stations..... 2.4-19
Figure 2.4-11. Mean hourly salinity curves for reference monitoring stations..... 2.4-20

2.5 Receiving Water Currents and Bathymetry
Figure 2.5-1. Locations of the ADCP and ADP sampling stations..... 2.5-14
Figure 2.5-2. Acoustic doppler current profiler (ADCP) deployment diagram..... 2.5-15
Figure 2.5-3. Acoustic doppler profiler mounted at fixed position. 2.5-15
Figure 2.5-4. Tenera bathymetry survey tracks in the SBPP discharge channel, July 16–17, 2003 ..... 2.5-16
Figure 2.5-5. Bathymetry of the discharge bay at SBPP and sampled locations for current measurements..... 2.5-17
Figure 2.5-6a. Current direction and velocity during ebb tide sampling..... 2.5-18
Figure 2.5-6b. Current direction and velocity during low tide sampling. 2.5-19
Figure 2.5-6c. Current direction and velocity during flood tide sampling. 2.5-20
Figure 2.5-6d. Current direction and velocity during high tide sampling. 2.5-21
Figure 2.5-7. Time series of tide changes, hourly water column average speeds measured by the Acoustic Doppler Profiler, and discharge flow..... 2.5-22
Figure 2.5-8. Autocorrelation functions (ACF) for current speed and, and cross-correlation functions (CCF) for current speed versus tide. 2.5-23
Figure 2.5-9. Current speed and direction at several depths at the ADP current meter station..... 2.5-24
Figure 2.5-10. Current speeds and directions (Acoustic Doppler Profiler station) and temperatures (Stations ST3, ST4 and SE5) two hours before the two high and two low tides..... 2.5-25
Figure 2.5-11. Current speeds and directions (Acoustic Doppler Profiler station) and temperatures (Stations ST3, ST4 and SE5) during the four slack tides..... 2.5-26
Figure 2.5-12. Current speeds and directions (Acoustic Doppler Profiler station) and temperatures (Stations ST3, ST4 and SE5) two hours after the two high and two low tides.. ..... 2.5-27
Figure 2.5-13. General current directions during: a) flooding tide; b) high tide, superimposed on the TRIM-2D computational model. 2.5-28
Figure 2.5-14. General current directions during: a) flooding tide; b) high tide, superimposed on the TRIM-2D computational model. 2.5-29

DRAFT

Figure 2.5-15 Bathymetric cross-sections along transects in the SBPP intake and discharge channels. 2.5-30

2.6 Receiving Water Turbidity Monitoring
Figure 2.6-1. Hydrolab Datasonde Multiprobe, deployed station arrangement..... 2.6-14
Figure 2.6-2. Transects used for towed turbidity data collection..... 2.6-15
Figure 2.6-3. Schematic of equipment used for towed turbidity sampling..... 2.6-16
Figure 2.6-4. Example of Datasonde PAR data 2.6-17
Figure 2.6-5. Relationship between the diffuse attenuation coefficient and turbidity for South San Diego Bay... ..... 2.6-18
Figure 2.6-6. Average calculated DAC for the South Bay deployed equipment monitoring stations.. ..... 2.6-19
Figure 2.6-7. Average calculated DAC for SBPP discharge channel and South Bay open water monitoring station groups.. ..... 2.6-20
Figure 2.6-8. Example towed turbidity data. 2.6-21
Figure 2.6-9. Interpolated map of average observed turbidity in South San Diego Bay, summer 2003..... 2.6-22
Figure 2.6-10. Interpolated map of average DAC between 0900 and 1600 PDT for South San Diego Bay, summer 2003... ..... 2.6-23
Figure 2.6-11. Interpolated map of the calculated PAR reaching eelgrass canopy elevation at mean sea level at 1200 PDT..... 2.6-24
Figure 2.6-12. Wind roses showing the prevailing daily wind direction and average daily wind speed for all wind directions. 2.6-25
Figure 2.6-13. Spring low tide circulation effects of the SBPP as predicted by Trim 2D hydrodynamic modeling 2.6-26
Figure 2.6-14. Spring flood tide circulation effects of the SBPP as predicted by Trim 2D hydrodynamic modeling... ..... 2.6-27
Figure 2.6-15. Spring high tide circulation effects of the SBPP as predicted by Trim 2D hydrodynamic modeling 2.6-28
Figure 2.6-16. Spring ebb tide circulation effects of the SBPP as predicted by Trim 2D hydrodynamic modeling 2.6-29
Figure 2.6-17. Trim 2D modeled bottom shear stress for south San Diego Bay resulting from wind driven waves, tides, and the total of waves and tides..... 2.6-31
Figure 2.6-18. Trim 2D modeled bottom shear stress for total bottom shear with and without the effects of the SBPP. 2.6-32
Figure 2.6-19. Relative bottom suspendability index applied to bottom sediments in south San Diego Bay... ..... 2.6-33
Figure 2.6-20. Predicted sediment re-suspension from combined Trim 2D modeled bottom shear and relative bottom suspendability index. 2.6-34
Figure 2.6-21. Trim 2D predicted patterns of turbidity with and without the influence of the maximum SBPP cooling water flow. 2.6-35
Figure 2.6-22. Numeric model of net predicted turbidity for the SBPP with cooling water flow of 441 mgd versus no cooling water flow and SBPP with cooling water flow of 601 versus no cooling water flow 2.6-36

DRAFT

2.7 Receiving Water Sediment Characteristics
Figure 2.7-1. Percentages of gravel, sand, and silt-clay in sediment samples. 2.7-4
Figure 2.7-2. Sediment gradation curves for subtidal inner discharge stations. 2.7-5
Figure 2.7-3. Sediment gradation curves for subtidal outer discharge stations. 2.7-5
Figure 2.7-4. Sediment gradation curves for intertidal discharge stations..... 2.7-6
Figure 2.7-5. Sediment gradation curves for intertidal reference stations. 2.7-6
Figure 2.7-6. Sediment gradation curves for subtidal north reference stations. 2.7-7
Figure 2.7-7. Sediment gradation curves for subtidal south reference stations. 2.7-7
Figure 2.7-8. Sediment gradation curves for subtidal intake reference stations. 2.7-8

2.8 Receiving Water Chlorine Monitoring
Figure 2.8-1. Location of chlorine monitoring station in relation to the cooling water intake and discharge channels.. ..... 2.8-4
Figure 2.8-2. Total residual chlorine levels for the cooling water intake and discharge channels..... 2.8-5

3.0 Biological Studies

3.2 Eelgrass Studies
Figure 3.2-1. Eelgrass survey area in south San Diego Bay 3.2-8
Figure 3.2-2. Eelgrass coverage in south San Diego Bay, May 2003..... 3.2-9
Figure 3.2-3. Comparisons of eelgrass coverage in south San Diego Bay (1993, 1999, 2003)..... 3.2-10

3.3 Benthic Invertebrates
Figure 3.3-1. Total number of taxa per sample at intertidal discharge (Series IT) and reference (Series IR) stations... ..... 3.3-29
Figure 3.3-2. Polychaete biomass (g / 0.018 m^2) mean and standard deviation at subtidal stations in south San Diego Bay 3.3-30
Figure 3.3-3. Infaunal diversity (H') mean per station at SBPP discharge stations.. ..... 3.3-31
Figure 3.3-4. Benthic response index (BRI) response levels as percent of stations in discharge channel and south San Diego Bay 3.3-32
Figure 3.3-5. Invertebrate density per subtidal station for example taxa with distributions skewed toward the SBPP discharge. 3.3-33
Figure 3.3-6. Invertebrate density per subtidal station for example taxa with distributions skewed toward the SBPP discharge but with depressed abundances at Station SE7..... 3.3-34
Figure 3.3-7. Invertebrate density per subtidal station for example taxa with distributions generally skewed away from the SBPP discharge. 3.3-35
Figure 3.3-8. Invertebrate density per subtidal station for example taxa with no definitive distribution pattern relative to the SBPP discharge. 3.3-36
Figure 3.3-9. Intertidal invertebrate density per intertidal station for example taxa with greater abundances at discharge stations than reference stations 3.3-37
Figure 3.3-10. Intertidal invertebrate density per station for example taxa with greater abundances at reference stations than discharge stations 3.3-38

DRAFT

Figure 3.3-11. Intertidal invertebrate density per station for example taxa with no definitive distribution pattern relative to the SBPP discharge 3.3-39
Figure 3.3-12. MDS analysis of infaunal abundances from 139 invertebrate taxa for subtidal benthic core samples in reference and discharge areas during the August 2003 survey. Replicates plotted separately.. ..... 3.3-40
Figure 3.3-13. MDS analysis of average infaunal abundances from 145 invertebrate taxa at subtidal benthic stations in reference, transition, and discharge areas during the August 2003 survey. 3.3-40
Figure 3.3-14. MDS analysis of average infaunal abundances from 95 invertebrate taxa at subtidal benthic stations in reference, transition, and discharge areas during the July 2003 survey.. ..... 3.3-41
Figure 3.3-15. MDS analysis of average infaunal abundances from 105 invertebrate taxa at subtidal benthic stations in reference, transition, and discharge areas during the September 2003 survey. 3.3-41
Figure 3.3-16. MDS analysis of infaunal abundances from 100 invertebrate taxa for intertidal benthic core samples in reference and discharge areas during the August 2003 survey. Replicates plotted separately. 3.3-42
Figure 3.3-17. MDS analysis of average infaunal abundances from 100 invertebrate taxa at intertidal benthic stations in reference and discharge areas during the August 2003 survey. 3.3-42
Figure 3.3-18. MDS analysis of average infaunal abundances from 57 invertebrate taxa at intertidal benthic stations in reference and discharge areas during the July 2003 survey.. ..... 3.3-43
Figure 3.3-19. MDS analysis of average infaunal abundances from 57 invertebrate taxa at intertidal benthic stations in reference and discharge areas during the September 2003 survey. 3.3-43
Figure 3.3-20. PCA analysis of physical data parameters from subtidal benthic stations in reference, transition, and discharge areas during the August 2003 survey.. ..... 3.3-44
Figure 3.3-21. PCA analysis of physical data parameters from intertidal benthic stations in reference and discharge areas for the August 2003 survey..... 3.3-44

3.4 Fishes
Figure 3.4-1. Location map of fish study sampling stations in San Diego Bay. 3.4-15
Figure 3.4-2. Fish study sampling stations in SBPP discharge channel and Sweetwater River channel 3.4-16
Figure 3.4-3. Density and biomass of fish caught in SBPP discharge channel and Sweetwater River during three sampling events, Summer 2003 ..... 3.4-17
Figure 3.4-4. Number of fish species, density, and biomass at study sites and three reference sites 3.4-18

4.0 Integrated Discussion

4.2 Eelgrass
Figure 4.2-1. Calculated hours of photosynthesis saturating PAR (H_{sat}) reaching the potential eelgrass canopy level for the South Bay study area. 4.2-11

Figure 4.2-2. Relative proportion of eelgrass cover and cumulative proportion cover for South San Diego Bay expressed as a function of the number of hours of saturating PAR received.. ..... 4.2-12
Figure 4.2-3. Numeric model of H_{sat} without SBPP cooling water, with SBPP cooling water flow of 441 mgd, and with SBPP cooling water flow at 601 mgd 4.2-13
Figure 4.2-4. Numeric model of net effect of 441 mgd cooling water flow versus no SBPP cooling flow, and 601 mgd cooling flow versus no SBPP cooling flow. 4.2-14
Figure 4.2-5. Plot of bay area by hours of photosynthesis saturating PAR received at the eelgrass canopy level for the field interpolated data, and the numerical model with SBPP cooling water flows at 441 mgd, 601, mgd, and 0 mgd..... 4.2-15
Figure 4.2-6. Predicted eelgrass distribution for south San Diego Bay with SBPP running at 441 mgd and 601 mgd..... 4.2-16
Figure 4.2-7. Predicted effects of temperature and turbidity on the distribution of eelgrass in south San Diego Bay with the SBPP cooling flow at 441 mgd and 601 mgd 4.2-17

4.4 Fishes
Figure 4.4-1. Dissolved oxygen plotted in increasing value against number of fish species, density, and biomass at study sites and three reference sites..... 4.4-3

DRAFT

Executive Summary

The purpose of this report is to assess the effects of cooling water discharges of the Duke Energy South Bay Power Plant (SBPP) in Chula Vista, California on marine habitats in south San Diego Bay (South Bay). The report is an updated thermal discharge assessment for the SBPP in response to a CWC Section 13267(b) information request by the San Diego Region of the California Regional Water Quality Control Board (RWQCB) dated May 2002. In the request, RWQCB staff concluded that some of the previous studies of the power plant's discharge effects on the water quality and biological resources of South Bay may not reflect current plant operations or be representative of existing conditions. The updated information forms the basis of continuing the National Pollutant Discharge Elimination System (NPDES) permit renewal process for SBPP Permit Number CA0001368.

In response to the RWQCB requests (*see Appendix A*), this volume includes the following information related to potential power plant discharge impacts:

- Updated discharge impact assessment for compliance with Section 316(a) of the Clean Water Act (CWA),
- Updated study on the viability and distribution of eelgrass in South Bay, and
- Updated dissolved oxygen assessment.

A companion volume (*Volume 2: 316(b) Demonstration for the South Bay Power Plant*), addresses related RWQCB questions concerning potential impacts associated with entrainment and impingement of marine organisms by the SBPP cooling water intake system.

Field studies were conducted in 2003 to collect physical and biological data relevant to the study objectives. The approach was to define water quality and other physical parameters in South Bay, describe the effects of SBPP operation on these parameters, and investigate the relationship between the resulting environmental conditions and the distribution and abundance of marine life in the bay. Because there have been several previous studies of SBPP effects on the bay, the present study was able to build on existing data. The present studies include a comprehensive description of eelgrass habitat and bottom-dwelling invertebrate distributions in South Bay, detailed measurements of currents, turbidity patterns, underwater light regimes, and water temperatures, and a study of fish populations in the SBPP discharge channel. By collecting data from areas in the discharge channel with the greatest potential for significant power plant effects and comparing the conditions to reference areas beyond the influence of the discharge (**Figure ES-1**), we were able to define the extent of discharge effects on biota in South

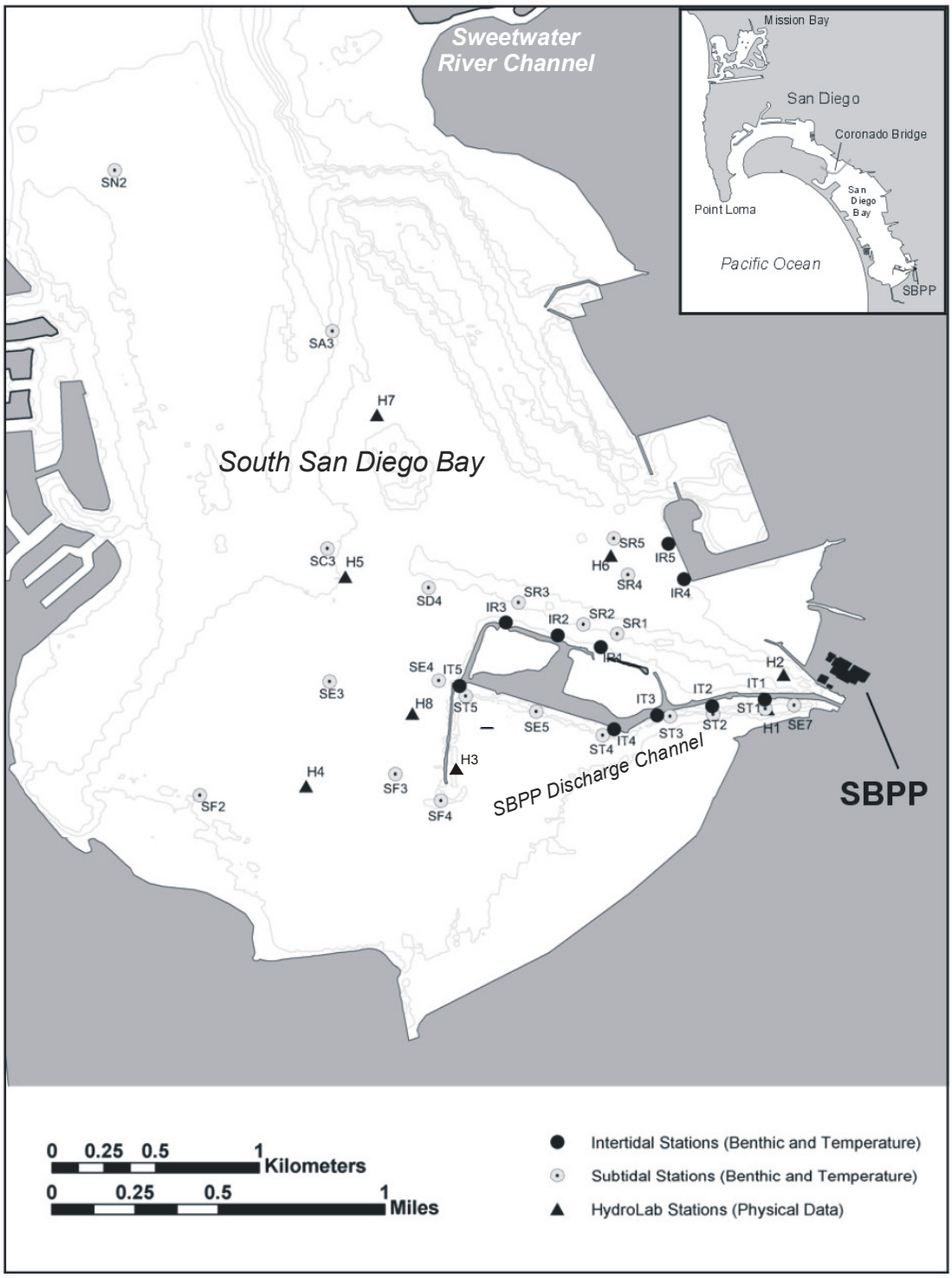

Figure ES-1. Station location map of *in situ* temperature recorders, sediment grain size samples, and benthic biological samples.

Bay. As explained in the following summary of key sections of the report, measurable discharge effects on biota are confined to the discharge channel on the south side of the Chula Vista Wildlife Island (CVWI). Within this area there is a gradient of effects on invertebrate fauna related mainly to elevated temperatures from the SBPP discharge, with the most apparent changes occurring within a distance of approximately one kilometer from the discharge boom at the SBPP property line.

The prior conclusions that areas within the defined discharge channel are wholly unsuitable to support eelgrass due to high temperatures have been called into question by the spring 2003 occurrence of eelgrass in this area. At least portions of the discharge channel appear to be capable of supporting eelgrass for portions of the year. The cumulative conclusions derived from the present and prior study indicate that while turbidity plays the primary role in dictating the distribution of eelgrass in South Bay, the SBPP plays a role in distributing naturally generated turbidity and thus, influencing the distribution of eelgrass. Further, the two studies suggest that there are collective effects of turbidity and temperature within near-field portions of the thermal plume of the SBPP. These effects may result in either an absence of eelgrass, or seasonal die-off or die-back of eelgrass. In the area of the discharge channel nearest the SBPP, it is still believed that warm summer season discharge temperatures alone may limit the occurrence of eelgrass, and turbidity may not be a significant factor in structuring eelgrass habitat within these areas.

Findings on the Physical Characteristics of the Receiving Water Body

The SBPP uses the waters of San Diego Bay for once-through cooling of its four electric generating units (**Figure ES-2**). Each unit is equipped with two circulating water pumps (CWP) that supply cooling water. CWP capacity varies between units, ranging from 148 m^3/min to 259 m^3/min (39,000 gallons per minute [gpm] to 68,400 gpm), based on the manufacturer's pump performance estimates. The quantity of cooling water circulated through the plant is dependent upon the number of pumps in operation. With all eight pumps in operation, the cooling water flow through the plant is 1,580 m^3/min (417,400 gpm) or 2,275,000 m^3/day (601 million gallons per day [mgd]).

Receiving Water Temperatures

The difference in temperature between the intake and discharge water is referred to as 'delta T°'. The warmed water is less dense than the receiving water and tends to form a discrete water mass at the bay surface, except in the inner discharge channel area where, under conditions of low tides and full plant operation, it can contact the bottom. The thermal effluent rises above the cooler bay water, spreading outward, and increasing in surface area while becoming thinner (in depth) and cooler as it moves away from the point of discharge. As the plume mixes with the receiving water, heat dissipates into the receiving water body and the atmosphere.

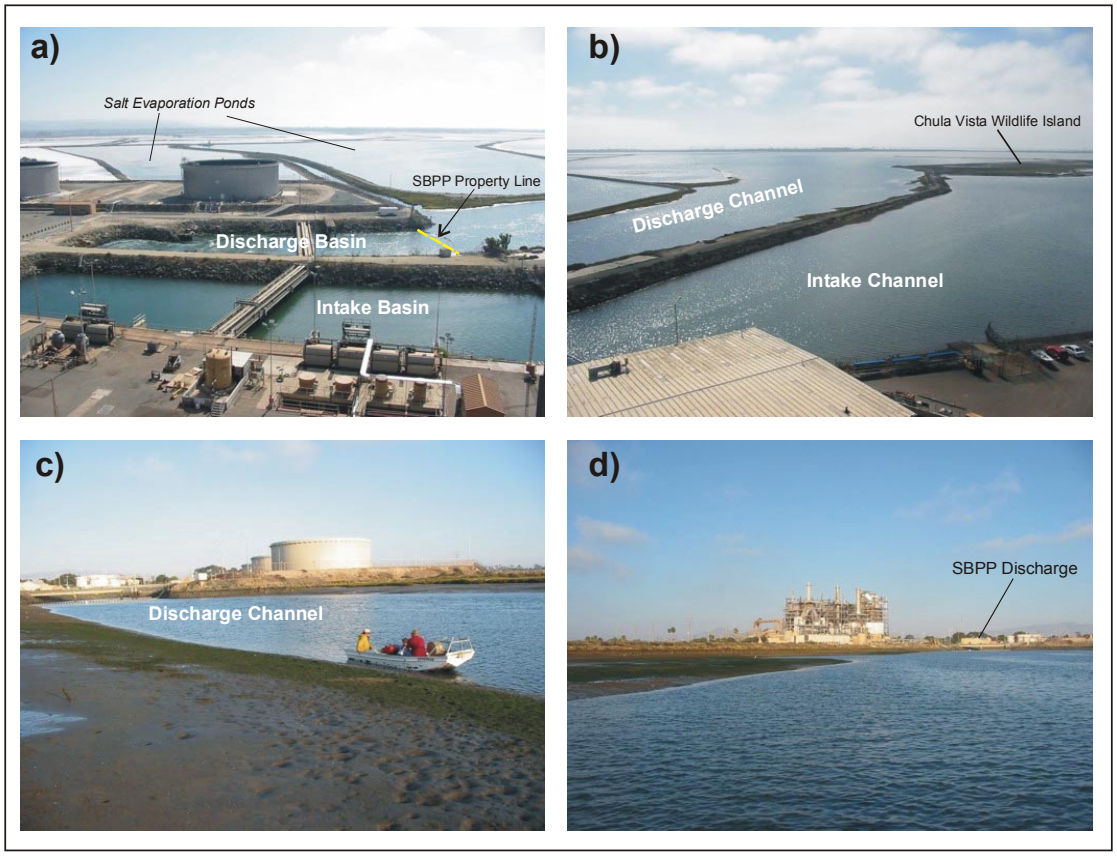

Figure ES-2. a) Intake and discharge basins, southerly view from SBPP; b) Intake and discharge channels, southwesterly view from SPBB; c) Shoreline near Station IT1 exposed during low tide; d) SBPP discharge and discharge channel, easterly view near Station ST3.

Water temperatures at the point of discharge are dependent upon the intake water temperature, the number of circulating water pumps in service, and plant electrical generating load. As the rate of power production increases, greater amounts of heat are transferred into the cooling water discharge. The volume of water discharged varies with the number of circulating water pumps that are in service. The extent and distribution of the thermal plume is dependent upon a variety of environmental factors and the configuration of the receiving water basin. At slack high tide, the plume can be dispersed over a wider expanse of the discharge channel. During an outgoing spring tide, the plume may narrow, but extend further north into San Diego Bay. The receding tide can also bring water that has been heated by solar radiation in the shallows of the bay into contact with the plume.

As expected, the maximum and mean temperatures at the five intertidal stations located in the discharge channel (IT1, IT2, IT3, IT4, and IT5) decreased with increasing distance from the discharge, with the maximum temperature in August declining by 3.4ºC (6.1ºF) over a distance of 1.3 km (0.8 mi) and the mean temperature declining by 2.9ºC (5.2ºF) (**Figure ES-3**). A decrease in mean temperatures between Stations IT3 and IT4 was

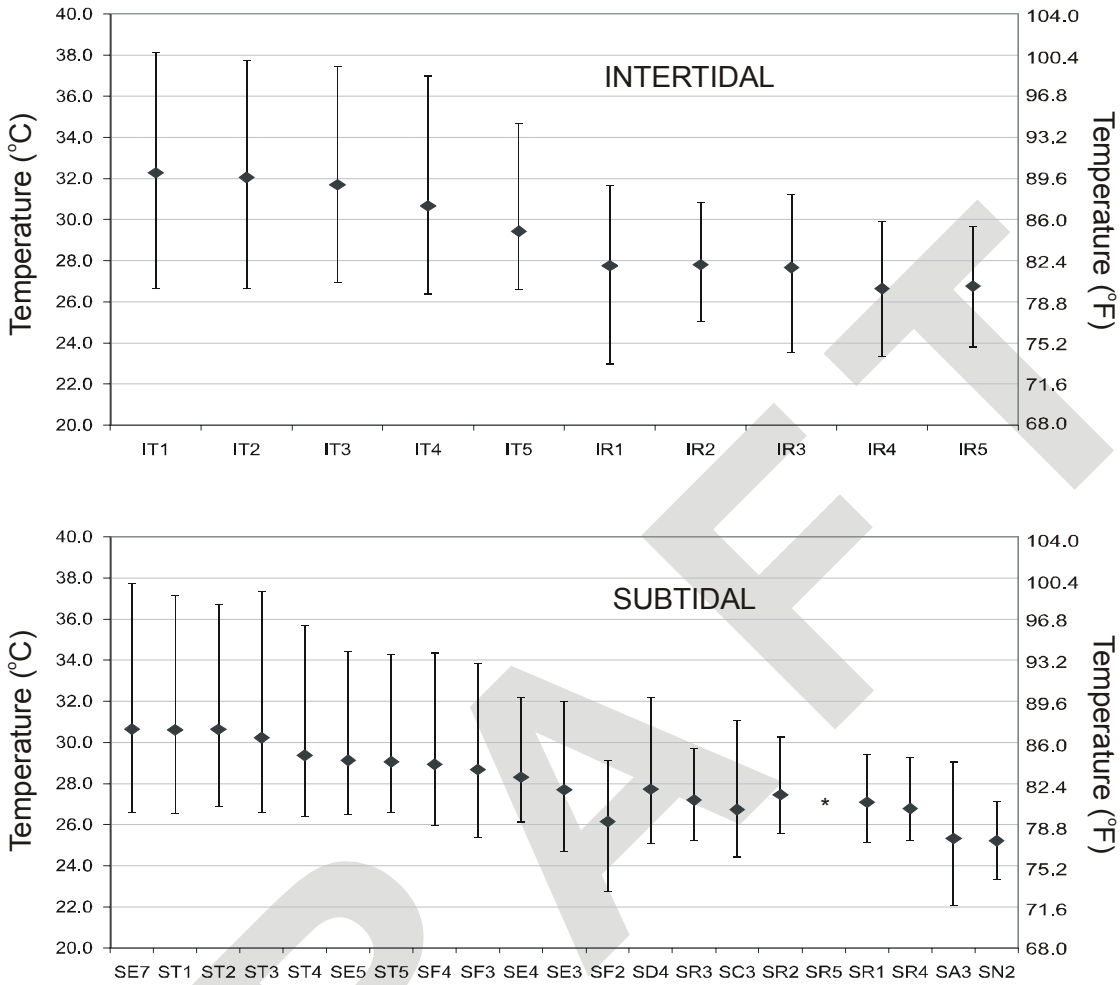

Figure ES-3. Mean, maximum, and minimum water temperatures during August 2003 at intertidal and subtidal stations in SBPP discharge channel and South Bay. Intertidal elevations were +0.3 m (+1.0 ft) above Mean Lower Low Water; subtidal bottom depths ranged from -0.4 m (-1.4 ft) to -4.2 (-13.8 ft) below MLLW. (*) Station SR5 not included due to incomplete data.

related to the shoreline configuration near Station IT4, partially deflecting the momentum of the plume away from that station and the adjacent reach of shoreline. A similar but less distinct temperature break was evident in the subtidal bottom temperatures at this same point. The minimum temperature readings corresponded with periods of low plant generation load and low discharge volumes, usually in the late night and early morning hours when electrical demand was lowest. These are also the intervals when solar heating effects are at a minimum. During these periods no temperature gradient was discernible between the stations.

Temperature dose, the frequency that certain areas were contacted by the thermal plume, was investigated through analysis of field-collected data and modeled temperature distributions. The frequency distribution of the 2.2°C (4°F) discharge delta T° was

selected as an analysis point because it had a wide range of values throughout the discharge channel. The analysis showed that areas on the bottom of the discharge channel were contacted about 75 percent of the time at a distance of 250 m (820 ft) from the point of discharge, about 50 percent of the time at a distance of 0.9 km (0.56 mi), and about 25 percent of the time at a distance of 1.4 km (0.87 mi) (**Figure ES-4**). The distances at which intertidal areas were contacted at these same frequencies were greater than the subtidal areas because of the buoyancy and momentum of the warm water plume.

Receiving Water Dissolved Oxygen

Oxygen is vital to the process of cellular respiration in all species except for the anaerobic bacteria. Environments where dissolved oxygen (DO) levels are significantly or regularly depressed will tend not to support the same biological communities as similar environments with more persistent or higher oxygen levels. DO saturation capacity differs significantly between marine and freshwater systems with saturation capacity decreasing as water temperature and salinity increase. The objective of this study was twofold:

1. Evaluate whether the SBPP causes a decrease in the concentration of DO in South Bay to levels below naturally occurring conditions; and,

2. Determine if any observed declines in DO result in altering biological communities from what might be expected as a balanced indigenous community under natural environmental conditions.

To accomplish the objectives we evaluated how the DO environment of the portions of South Bay that are influenced by the SBPP differ or are similar to back bay environments elsewhere in San Diego Bay and other bays in southern California. The mean hourly DO concentrations for both the South Bay open water stations and the SBPP discharge channel fell within ±1 standard deviation of the mean hourly DO concentration of the reference stations (**Figure ES-5**). In comparison to the mean condition of the combined reference stations, all South Bay stations had greater levels of DO in the morning and lower levels of DO in the afternoon. The mean daily DO concentrations of 5.38 ± 1.01 mg/l (reference sites), 5.52 ± 0.35 mg/l (open San Diego Bay), and 4.99 ± 0.32 mg/l (SBPP discharge channel) do not substantially differ. These ambient DO levels support source water fish populations in the SBPP discharge channel and do not appear to limit their distribution or species composition.

The conditions observed within both the San Diego Bay open water and discharge channel stations were generally reflective of systems with lower primary productivity, larger water volumes, and/or greater aeration or water turnover. It is notable that for reference stations as well as both San Diego Bay open water and discharge channel

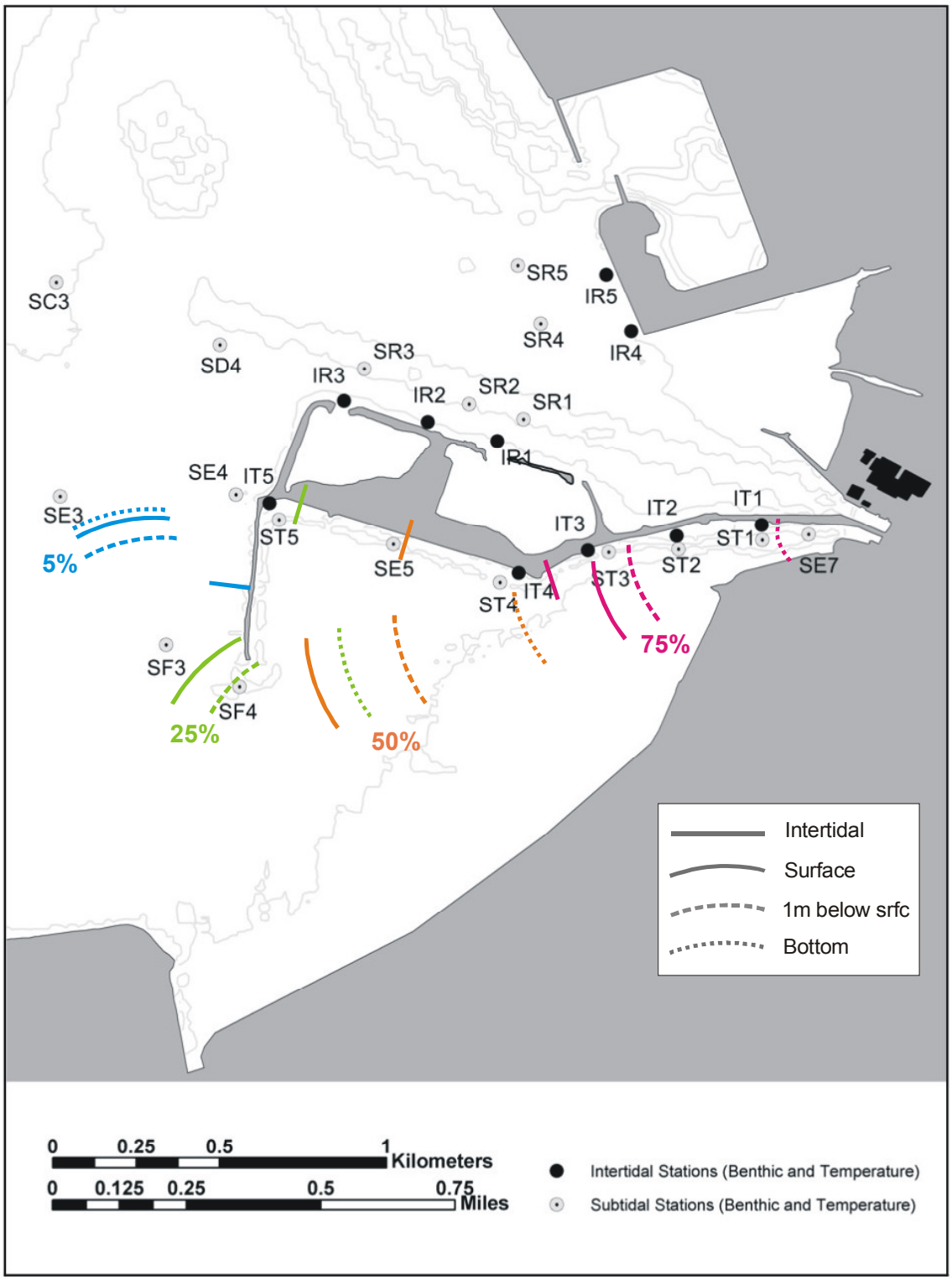

Figure ES-4. Percent frequencies of 2.2°C (4°F) discharge delta T° excursion distances at four depths modeled by linear regressions of station temperatures <2.8 km from the discharge boom. Excursions were modeled from conditions in July–September 2003.

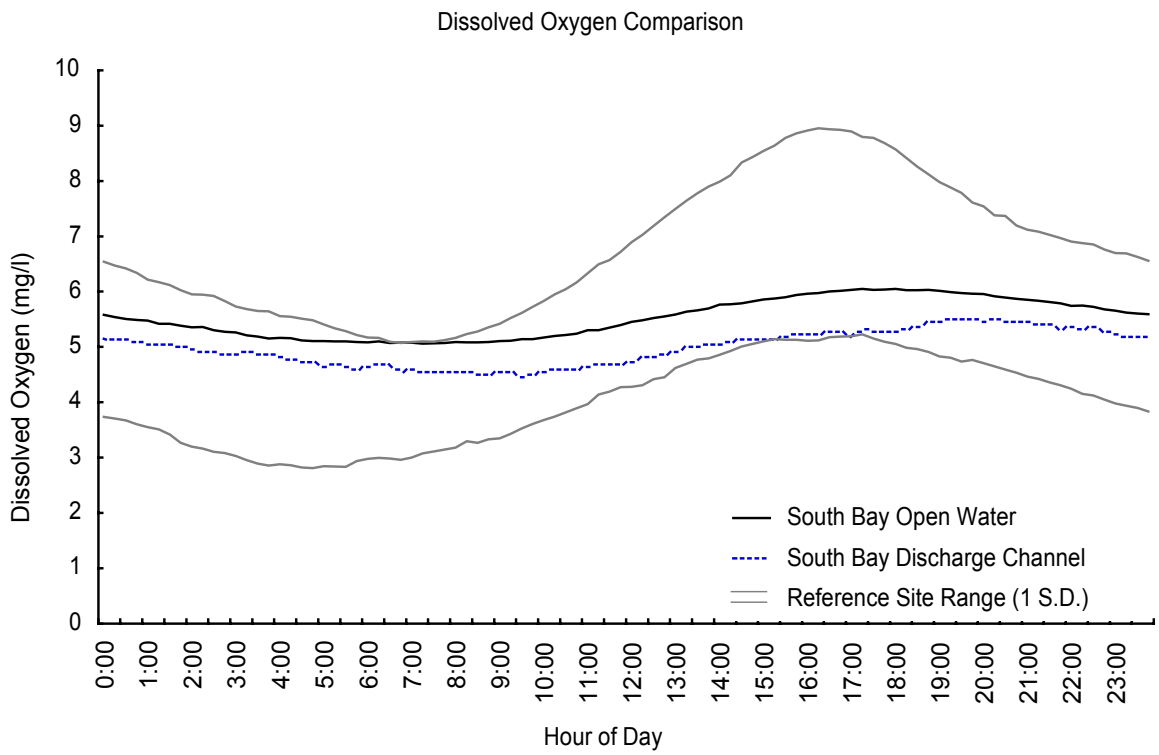

Figure ES-5. Mean hourly dissolved oxygen curves for South Bay open water and SBPP discharge channel monitoring stations plotted over the standard deviation of the mean hourly dissolved oxygen for the reference stations.

stations the mean daily DO curves were consistently below the saturation levels for the mean temperatures experienced at the stations. This suggests that DO consumption was typically higher than production at all locations throughout the study.

Currents and Bathymetry

The purpose of describing current regimes and bathymetry was to provide a more detailed understanding of SBPP discharge plume behavior under a variety of power plant operating conditions and oceanographic conditions in South Bay. The information was used to interpret water temperature and turbidity patterns in the bay.

Our study of current patterns in the SBPP vicinity consisted of three elements:

1) Bathymetry mapping of the South Bay area for modeling circulation patterns;

2) Measurements of current speed and direction at fixed locations during various tide conditions and discharge flow volumes; and

3) Determination of discharge flow contribution to current speeds based on the cross-width area of the receiving water body.

The bathymetry of the South Bay area is characterized by gently sloping mudflat areas transected by dredged and natural channels. The SBPP discharges cooling water along the southern edge of the CVWI, initially through a 15-m (50-ft) wide discharge channel. The depth of the 183-m (600-ft) long discharge channel is -3.8 m (-12.5 ft) mean lower low water (MLLW). The channel continues along the southern edge of the CVWI and turns south along the breakwater. Much of the remaining area in the discharge embayment is shallower and bounded along the southern edge by a wide mudflat that mainly lies below mean sea level (+0.8 m, +2.6 ft). Consequently, discharge water flows over the whole embayment in a westerly and southwesterly direction when tidal levels are above the mean sea level.

Currents in South Bay are largely driven by tidal fluctuations. Once beyond the immediate area of the point of discharge, differing power plant discharge flows did not appear to greatly change current velocities at the locations monitored. Interestingly, bottom and surface vectors often occurred in different directions at times of lower high water and near high tide when the tidal shift was generally smallest and when currents were slowest overall. At tide levels above MLLW, the volume of water leaving the power plant adds less than 0.25 knots (<15 cm per second) to the currents over the most of the area. As the tide level drops, the speed of the discharge water increases due to the smaller confines of the embayment. The strongest currents near the south bank of the CVWI were estimated to exceed 1.5 knots (88 cm s^{-1}) at the lowest tides.

Sediments and Turbidity

The distribution of particle sizes within soft sediment marine environments is a significant factor affecting the composition of infaunal assemblages, and the suspension of fine sediments by currents can decrease light penetration through the water column and affect the growth of bottom vegetation. We measured sediment grain size distributions at each station where benthic faunal samples were collected and used the data to test the relationship between sediment characteristics and infaunal distributions.

The proportions of silt/clay and sand sediments within the discharge channel varied between subtidal stations, with a generally higher percentage of silt/clay particles at the outermost discharge stations but also a higher percentage of gravel and shell debris. There was a gradient of increasingly finer sediments toward the inner intertidal discharge stations. An overall pattern of coarser sediments in the northwestern portions of South Bay grading toward finer sediments in the southeastern portion of the bay was apparent from the data. Earlier studies had attributed this gradient to decreased tidal flushing in the back bay and accumulated sediments from the Otay River Basin.

The turbidity monitoring study was designed to:

1. Map any observed spatial trends in light attenuation and turbidity in South Bay; and,

2. Collect data to support a modeling approach to evaluating the role of the SBPP on turbidity in South Bay.

Typical turbidity conditions measured in South Bay were generally clear water in the northern portion of the bay, and increased turbidity in the southeast portion of the bay corresponding to the general distribution of finer bottom sediments. Although the water was generally more turbid in the southeast portion of the bay, the maximum observed turbidity occurred near a shallow water construction site north of CVWI that was being filled for shallow-water habitat restoration.

Results of bottom-shear modeling support the hypothesis that the SBPP does not contribute to the generation of turbidity in South Bay. The shallow waters to the southeast of the CVWI are probably the single greatest source for turbidity in the southern portion of the South Bay. Although the spatial distribution of turbidity appears correlated with the SBPP discharge channel, the generation of turbidity is almost exclusively explained by wind wave re-suspension of naturally-occurring bottom sediments.

Although the SBPP is not likely to cause increases in the amount of suspended material in the South Bay, it can influence the distribution of turbid water within the South Bay. The power plant cooling water flows contribute to South Bay turbidity distribution by drawing clearer waters southward along the deeper navigational channels on the eastern portion of the bay and expanding natural turbidity plumes along the western portion of the South Bay (**Figure ES-6**). Current and turbidity modeling support the idea that discharged cooling water from the SBPP plays a role in the export of naturally-generated turbidity from the discharge channel and the immediate vicinity of CVWI.

Chlorine

The SBPP currently uses chlorine injections to prevent microfouling of the cooling water condensers, piping, and associated cooling water equipment. Chlorination of the cooling system is permitted under NPDES Permit 96-05. Chlorine is an ideal biocide for cooling water treatment because it is effective against microfouling organisms and most of the residual chemical is consumed through biological and chemical demand within the cooling system resulting in only a small amount of total residual chlorine (TRC) in the receiving waters. SBPP has been capable of maintaining a clean cooling water system with a combination of mechanical cleaning and chlorination at levels at or below those allowed by the NPDES Permit.

The TRC levels measured in the discharge channel during the monitored chlorinations during summer 2003 indicate that the SBPP does little to increase TRC levels above the

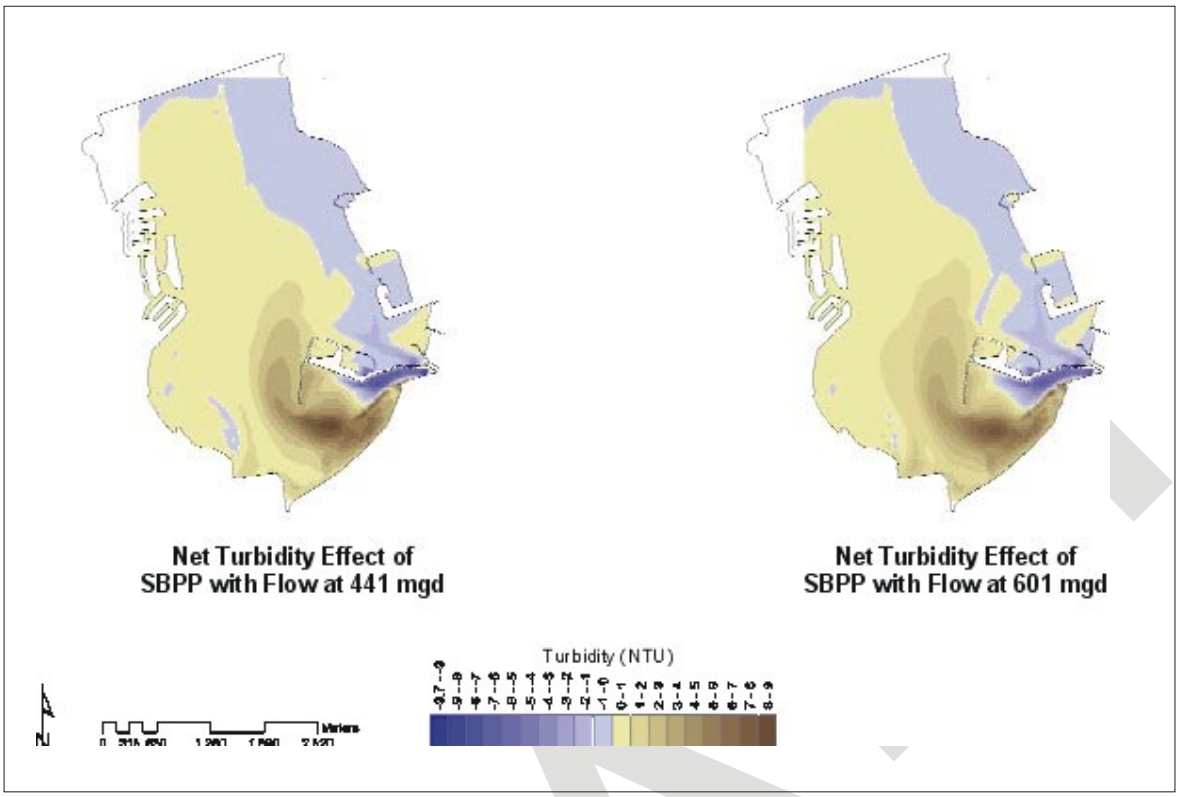

Figure ES-6. Numeric model results of net predicted turbidity for the SBPP with cooling water flow of 441 mgd versus no cooling water flow (left) and SBPP with cooling water flow of 601 versus no cooling water flow (right). Model runs are average difference in turbidity during a 72-hour spring tidal cycle.

detection limit of 40 parts per billion (ppb). Measurements below 40 ppb are considered background variation and are attributed to naturally-occurring halides in the environment. Background TRC levels were similar between the intake and discharge channels. Given the maximum allowable discharge level of 85 ppb when all four generating units are in operation, the power plant was consistently below the established regulatory limits.

The NPDES limit is a water quality based standard developed by the EPA from the results of numerous bioassay experiments using a variety of test species and life stages. Analysis of the impacts of cooling water chlorination on organisms as an isolated stressor in the receiving waters is not possible in a field research context because the measured concentrations were close to, or below, detectable levels and would not be expected to produce any measurable changes in receiving water biota. SBPP tests the potential for synergistic effects of chlorine and other discharge constituents using total toxicity bioassay techniques with sensitive life stages of marine fishes and invertebrates.

Findings on the Biological Characteristics of the Receiving Water Body

Eelgrass

Eelgrass is considered a habitat-forming species that creates unique biological environments in the form of submerged aquatic beds and emergent plant habitat along the shore during low tide. Eelgrass serves as a primary producer in a detrital-based food web, and is further directly grazed upon by invertebrates, fishes, and birds, thus contributing to ecosystem health at multiple trophic levels. It provides physical structure in the form of habitat to the community, and supports epiphytic plants and animals, which in turn are grazed upon by other invertebrates, fishes, and birds. It is also a nursery area for many commercially and recreationally important finfish and shellfish; those that are resident within the bays and estuaries, including oceanic species that enter the estuaries to breed or spawn.

An eelgrass mapping survey was completed in late May 2003 to obtain updated information on eelgrass in South Bay. The survey used the combination of boat-towed side-scan sonar, and single-beam sonar acoustic survey methods. Of the 935 ha (2,310 ac) surveyed, 442 ha (1,094 acres) supported eelgrass. Nearly 80 percent of the eelgrass beds mapped in South Bay had intermediate percent coverage of 26–75 percent. Eelgrass occurred at elevations as high as +0.3 m (+1 ft) MLLW within the southerly portions of the survey area and to as deep as –3.0 m (–10 ft) MLLW near the edges of channels in the northern portions of the survey area.

In the most southern reaches of the South Bay, eelgrass was most widespread west of the CVWI. There was a particularly lush bed near the mouth of the Otay River, with 76–100 percent bottom cover. The eelgrass in this region occurred in depths between about +0.3 m (+1 ft) and –1.2 m (–4 ft) MLLW. The area adjacent to the CVWI was largely devoid of eelgrass except for sparse, isolated patches with less than 25 percent cover. The occurrence of eelgrass within this area has not been previously reported and was unexpected during the present survey since the summer temperatures within the discharge channel are generally too high to support eelgrass year-round. Because prior surveys have generally been conducted during late summer months, it is possible that the presence of eelgrass in this area is seasonal.

The predicted turbidity effects of the SBPP cooling water flows on eelgrass within South Bay suggest that the SBPP, operating at maximum cooling water circulation rates would preclude eelgrass from approximately 41.9 hectares (103.6 acres) of South Bay. At the mean summer 2003 operating conditions of 441 mgd, the SBPP is predicted to preclude eelgrass from approximately 28.9 hectares (71.4 acres) of the Bay through its cooling water discharge effects on naturally-generated turbidity.

The prior conclusions that areas within the defined discharge channel are wholly unsuitable to support eelgrass due to high temperatures have been called into question by

the spring 2003 occurrence of eelgrass in this area. At least portions of the discharge channel appear to be capable of supporting eelgrass for portions of the year. The cumulative conclusions derived from the present and prior Merkel & Associates (2000a) study indicate that while turbidity plays the primary role in dictating the distribution of eelgrass in South Bay, the SBPP plays a role in distributing naturally generated turbidity and thus, influencing the distribution of eelgrass. Further, the two studies suggest that there are collective effects of turbidity and temperature within near-field portions of the thermal plume of the SBPP. These effects may result in either an absence of eelgrass, or seasonal die-off or die-back of eelgrass. In the area of the discharge channel nearest the SBPP, it is still believed that summer season discharge temperatures alone may limit the occurrence of eelgrass, and turbidity may not be a significant factor in structuring eelgrass habitat within these areas.

Benthic Invertebrates

Benthic infauna (e.g., annelid worms, bivalve and gastropod mollusks, crustaceans, echinoderms) have been widely used as pollution indicators because populations are sedentary and respond to local changes in ambient conditions. Together they comprise an important food source for higher trophic level predators such as fishes and shorebirds. The benthic studies in this report supplement earlier monitoring work performed for SBPP from 1968–1994, and further delineate the area affected by discharges from SBPP.

Samples were collected at 21 subtidal stations and 10 intertidal stations during July, August, and September 2003. A total of 163 invertebrate taxa was identified from core samples collected in the SBPP discharge canal and receiving waters of South Bay. A high total abundance of invertebrates at Station E7, the station closest to the discharge, was due to high numbers of nematodes and oligochaetes associated with high concentrations of organic debris in the samples. Abundant subtidal species with distributions skewed away from, or largely absent from, the discharge channel included several species of polychaete worms and amphipods. Most of the taxa sampled in the study had a low frequency of occurrence among all of the stations or low overall densities and consequently their distributions could not be accurately classified according to proximity to the discharge or relationship to temperature variables.

There was no consistent pattern in the distribution of total biomass and no obvious gradient as a function of distance from the discharge. However, when the biomass of polychaete worms was considered separately, there was a trend toward higher biomass values for polychaetes at stations farther from the discharge. Mean diversity at subtidal stations was lowest at the two stations closest to the discharge, SE7 and ST1, and highest at reference station SR4 near the Chula Vista Marina. There was a trend of increasing diversity within the discharge channel as distance from the discharge increased.

A benthic response index (BRI) was calculated for each sample based on taxa abundances and associated pollution tolerance indices (p_i). The index was developed by the Southern California Coastal Water Research Project from empirical data on the abundances of species most likely to occur in polluted or non-polluted areas. The BRI analysis did not distinguish between faunal assemblages at discharge and reference stations. The greater abundances of certain species with high pollution tolerance indices at some reference stations as compared to some discharge stations demonstrated that certain species that are capable of tolerating polluted sediments cannot survive under warm thermal regimes. For the stations sampled, the BRI analysis concluded that the South Bay is not degraded and that any effects produced by the SBPP are not consistent with the shifts in faunal composition seen in polluted areas of other bays in southern California.

Results from this study confirm the general conclusions of earlier benthic monitoring work in South Bay—differences in patterns in species composition between discharge sites and reference sites indicate that the SBPP discharge creates a highly variable environment that favors opportunistic species adapted to a wide range of temperatures. Multivariate statistical analysis clearly demonstrated the dissimilarity among discharge and reference stations at both intertidal and subtidal depths, and also separated stations along a gradient consistent with changes in water temperature resulting from the SBPP discharge. Although there are numerous physical and biological factors that regulate the abundance and distribution of benthic communities, the delineation of sites along a general gradient related to the presence of the SBPP discharge suggests that one or more factors related to the discharge caused the observed patterns. Based on a principal components analysis of the data, differences in sediment type contributed to some of the observed variation in faunal composition, but elevated bottom temperatures were the most important physical factor in determining faunal composition. There were many species in common between the discharge and reference areas suggesting that conditions at the inner discharge stations were not inhibiting the propagation and colonization of many of the same species that occur elsewhere in South Bay. By sampling at a finer spatial scale than earlier studies we were able to delineate a gradient of discharge effects on several individual infaunal taxa, and provide evidence that the greatest departures from the reference communities occurred within an area (primarily within 305 m [1,000 ft] of the SBPP property line) that is smaller than the area thought to be affected by the discharge in previous studies.

Fishes

The present study was designed to more closely characterize the fish community in the discharge channel in comparison to a reference site during the warmest months of the year (July–September) with particular attention to their response to DO regimes. A reference site was selected in the nearby Sweetwater River channel. To make additional comparisons, several past fish studies conducted in other back-bay environments were

reviewed for diversity, density and biomass data for comparison to results of the current study.

A total of 20 species, represented by a combined total of 26,672 fish, was captured during the summer 2003 study. The most abundant fishes were juvenile slough and deepbody anchovy, which represented 96 percent of the total individuals caught. Other commonly captured species included California halfbeak, round stingray, queenfish, barred pipefish, bay pipefish, arrow goby, cheekspot goby, and yellowfin goby.

The SBPP discharge channel had considerably higher fish densities than Sweetwater River during each sampling event, with a mean density over seven times that of Sweetwater River. The large numbers of juvenile anchovy captured in the discharge channel were most responsible for this difference. Nearly three times as many adult anchovy were found in Sweetwater River than in the discharge channel, suggesting anchovy may move out of the channel as they mature, thus resulting in the differences in demographics between areas.

Comparison of the water quality data at the two sites shows temperature and salinity to be slightly higher in the discharge channel at the time of sampling. DO was slightly lower at the Sweetwater River site during the instantaneous sampling performed coincident with fish sampling. These parameters vary at both sites throughout each day, and these sites in general have comparable DO and salinity values. This is confirmed not only by long-term monitoring of physical parameters, but also by the similar species composition at both sites.

The discharge channel is a unique environment that shows some similarity to other back-bay environments, while also providing conditions that allow for unusual species occurrences, atypical juvenile abundances, and seasonal use patterns. The unique temperature environment of the channel may provide a warm water refuge area for several bay species during the winter, but may similarly preclude some species from full use of the area during the hottest portions of the summer months. The site was found to provide habitat for warm-water species not typically found elsewhere in California such as diamond stingray, California halfbeak, California needlefish, bonefish, and shortfin corvina.

DRAFT

1.0 Introduction and Background

1.1 Introduction

This report is an updated thermal discharge assessment for the South Bay Power Plant (SBPP) to comply with a CWC Section 13267(b) information request by the San Diego Region of the California Regional Water Quality Control Board (RWQCB). In the request, RWQCB staff concluded that some of the previous studies of the power plant's intake and discharge effects on the water quality and biological resources of south San Diego Bay (South Bay) might be outdated and may not reflect current plant operations or be representative of existing conditions. A letter dated May 24, 2002 from the Board's executive director to Duke Energy South Bay LLC describes several open issues regarding the power plant's intake and discharge (**Appendix A**). The studies described in the Board's directive are designed to address the open issues and to collect additional information on present conditions in the power plant's cooling water source and discharge areas. The updated information forms the basis of continuing the National Pollutant Discharge Elimination System (NPDES) permit renewal process for SBPP Permit Number CA0001368.

This volume addresses these questions related to potential power plant discharge impacts and includes the following:

- Updated Discharge Impact Assessment for Compliance with Section 316(a) of the Clean Water Act (CWA),
- Updated Study on the Viability and Distribution of Eelgrass in South Bay, and
- Updated Dissolved Oxygen Assessment.

A companion volume (*Volume 2: 316(b) Demonstration for the South Bay Power Plant*), addresses related RWQCB questions concerning potential impacts associated with entrainment and impingement of marine organisms by the SBPP cooling water intake system.

DRAFT

1.2 Background

The South Bay Power Plant is an electric power generating facility owned by the San Diego Unified Port District and operated by Duke Energy Power Services. It is located on the southeastern shoreline of San Diego Bay and uses bay water for once-through condenser cooling. Unit 1 began operations in 1960 followed by three additional units in 1962, 1964, and 1971. Under the California State Thermal Plan, the cooling water discharge from SBPP Units 1 through 4 is classified as an existing discharge.

In 1972 and 1973, San Diego Gas and Electric (SDG&E), the plant's previous owner and operator, conducted a thermal effects study as required by the State Water Resources Control Board. The study concluded that the existing elevated-temperature cooling water discharged from SBPP had caused no prior appreciable harm to the aquatic community of San Diego Bay or to the beneficial uses of those waters (Ford et al. 1973). However, the study also concluded that the discharge did have effects on the benthic community within the discharge channel, which, for the purpose of the study, was not considered to be part of San Diego Bay. A subsequent data review of annual summer benthic studies conducted between 1977 and 1994 concluded that no appreciable long-term upward or downward trends in species diversity or abundance had occurred within the discharge channel (Ogden Environmental and Energy Services Co., Inc. 1994). In 1996, SDG&E was required to conduct further comprehensive effluent studies on eelgrass and fishes, which were completed in 2000 and submitted to the RWQCB (Merkel & Associates, Inc. 2000a; Merkel & Associates, Inc. 2001, respectively).

Section 316(a) of the CWA requires that States impose an effluent limitation with respect to the thermal component of a discharge that will assure the protection and propagation of a balanced, indigenous population of shellfish, fish, and wildlife in the receiving water. Although the intake and discharge structures at SBPP remain unchanged since the previous studies, the RWQCB moved the point of compliance for discharge water temperature 4,000 feet closer to the discharge basin in 1996.

As part of the permit renewal process, the RWQCB requested that studies be designed to address the following questions:

1. *What are the effects of the cooling water discharge on aquatic and benthic species during the days when water temperature is the highest in the discharge channel? Are these effects permanent or temporary?*

2. *Do temperature, dissolved oxygen (DO), and/or chemical makeup (chlorine, metals, toxicity, etc.) have a combined effect on the species abundance and diversity in the discharge channel?*

3. *What portion of the discharge channel does not support beneficial uses, due to elevated temperatures? What are the affected species, and do these species exist in other parts of the discharge channel and in South Bay?*

Many factors, both natural and anthropogenic, affect the abundance and distribution of organisms in South Bay. The studies described in this report include physical and chemical measurements of the discharge water column recorded during July through September when the greatest heat stress is imposed on the biota, and concurrent measures of eelgrass distribution, benthic invertebrates and fishes. Although a variety of physical measurements were made during the course of the study, such as water temperature, turbidity, and current flow, this field investigation was not intended to ascribe biological effects to any specific environmental factors but rather to examine patterns of distribution in the biota in relation to the SBPP discharge. The present report refines existing information on the extent of effects of the SBPP discharge previously identified through various monitoring studies beginning in the early 1970s.

DRAFT

1.3 Regulatory Setting

1.3.1 Overview

Elevated temperature discharges are regulated in California through water quality objectives established by the State Water Resources Control Board (SWRCB) in the Water Quality Control Plan for Control of Temperature in the Coastal and Interstate Waters and Enclosed Bays and Estuaries of California (Thermal Plan) (SWRCB 1975). The thermal discharge at the SBPP is defined as an existing discharge in the Thermal Plan and is subject to a narrative standard which requires that the limits imposed on the discharge be sufficient to "assure protection of the beneficial uses" of the receiving water. The Thermal Plan does not provide guidance on how to make a protection of beneficial uses determination. At the federal level, the Clean Water Act (CWA) requires that any state limit be sufficient to protect a 'balanced indigenous population'.

The purpose of this section is to describe the statutory and regulatory background on the regulation of thermal discharges from both a federal and state perspective. Background is provided on how the standards were set and how they have been interpreted. The intent of this information is to provide an historical context for the standards established for thermal discharges and the tools used at both the state and federal level to assess whether an established limit meets the water quality objective.

1.3.2 Federal Regulation of Thermal Discharges

The federal regulation of thermal discharges has a complicated regulatory and legal history. Congress recognized that heat is unique in that it does not persist in the environment and does not continually degrade water quality as other substances may. Congress adopted special provisions in the CWA that allows for a variance to "any effluent limitations proposed for the thermal component of any discharge" which are "more stringent than necessary to assure the protection and propagation of a balanced, indigenous population of shellfish, fish, and wildlife in and on the body of water into which the discharge is made ...".

The EPA, Congress, and the judiciary have provided guidance as to the meaning of the statutory terms of Section 316(a). For example, the EPA drafted interagency technical guidance in 1974, 1975, and 1977 (USEPA 1977) to assist dischargers in developing the necessary studies to assess the protection of a balanced indigenous population. EPA's technical guidance, together with the legislative and judicial records on Section 316(a) help to answer the questions of what constitutes a 'balanced indigenous population', how the boundaries of the water body are determined, what degree of protection is required, and what level of 'assurance' is needed.

The EPA has recognized that the statutory term 'population', which biologists use to define the organisms of a particular species, is more properly interpreted as 'community,' which refers to assemblages of the populations of organisms occupying a body of water. To be 'balanced', EPA states that an aquatic community must not be "dominated by pollution-tolerant species whose dominance is attributable to polluted water conditions." However, species diversity at each trophic level is not required and some change to species composition and abundance is consistent with a 'balanced community.' EPA has recognized that "[e]very thermal discharge will have some impact on the biological community of the receiving water," and therefore "[t]he issue is the magnitude of the impact and its significance in terms of the short-term and long-term stability and productivity of the biological community affected". EPA's 316(a) technical guidance for existing discharges indicates that biological communities will be protected adequately if 'appreciable harm' is avoided. It is not intended that every change in flora and fauna should be considered 'appreciable harm'; rather the potential for harm requires an evaluation of whether changes in survival, growth, and reproduction put the abundance and persistence of the water body populations at risk. Thus, thermal effluent limitations will provide adequate protections unless the thermal discharge would cause biological changes so substantial that community imbalance, elimination, or replacement would result.

It is generally accepted that scientific certitude is not possible when quantifying environmental impacts. Thus, EPA looks to 'reasonable assurance' as the basic standard of proof necessary to demonstrate compliance with the federal variance standard of protecting a balanced, indigenous community.

1.3.3 California Regulation of Thermal Discharges

The SWRCB and the RWQCB are the state agencies with primary responsibilities for the coordination and control of water quality and the RWQCB, in exercising its responsibilities, must conform to and implement the policies laid out in the Porter-Cologne Act. The SWRCB meets its responsibility to coordinate California water quality through the development and issuance of a series of plans and policies. These plans and policies are then used by the nine Regional Boards to develop their basin-specific water quality control plans (Basin Plans). The plans and policies that directly relate to the regulation of thermal discharges in California are discussed in more detail below.

1.3.3.1 Thermal Plan

The Thermal Plan establishes specific water quality objectives for elevated temperature, including thermal discharges. As noted earlier, SBPP is defined in the Thermal Plan as an existing discharge. Thermal limits set for existing discharges are required "to assure protection of the beneficial uses and areas of special biological significance."

The 'general water quality provisions' section of the Thermal Plan sets out specific criteria for the use of dispersion (i.e., mixing) zones in areas of special biological significance or where necessary to protect a specific beneficial use. In addition, the Thermal Plan contains definition of numeric objectives for the mixing zone for new discharges. Review of both these Thermal Plan provisions and definition confirm the appropriateness of allowing a mixing zone in establishing thermal discharge limits.

The Thermal Plan requires existing dischargers, such as SBPP, to conduct a study to define the effect of the discharge on beneficial uses and to identify design and operating changes if the discharge is not in compliance with the Plan. Additionally, all thermal discharges must be monitored to determine compliance with permit requirements. Thermal discharges that are deemed significant by the SWRCB or RWQCB shall be required to implement expanded monitoring programs (either continuous or periodic) to determine whether the limits provide "adequate protection to beneficial uses (including the protection and propagation of a balanced indigenous community of fish, shellfish, and wildlife, in and on the body of water into which the discharge is made)." The Thermal Plan does not provide any requirements for how such a determination is made.

1.3.3.2 San Diego Region Basin Plan

The San Diego Region Basin Plan (SDRWQCB 1994) establishes the historical, present and potential beneficial uses for the Basin. For each beneficial use, the Basin Plan specifies the water quality objectives necessary to ensure protection of that use. The Basin Plan includes by reference various SWRCB and RWQCB plans and policies to protect water quality including those previously discussed. The RWQCB establishes water quality objectives that in its judgment will ensure the reasonable protection of the designated beneficial uses, considering all the demands made or to be made upon the water. The beneficial uses established by the Basin Plan for San Diego Bay are listed below.

- Industrial Service Supply
- Contact Water Recreation
- Commercial and Sport Fishing
- Wildlife Habitat
- Preservation of Biological Habitats of Special Significance
- Migration of Aquatic Organisms
- Rare, Threatened, or Endangered Species
- Navigation
- Non-Contact Water Recreation
- Estuarine Habitat
- Marine Habitat
- Spawning, Reproduction, and/or Early Development
- Shellfish Harvesting

DRAFT

1.4 Effects of Thermal Discharges: Overview

Temperature is recognized as a critical factor affecting species composition, abundance, geographic distribution, and vertical distribution (e.g., Kinne 1963; Norris 1963; Coutant and Brook 1970), and as an important physiological factor (e.g., Meldrim and Gift 1971; Lüning and Neushul 1978). Thermal discharges into enclosed bays, similar to South Bay, can affect the survival, growth, and reproduction of marine organisms, and their distribution and movements through temperature avoidance or attraction. Biological effects from the SBPP thermal discharge depend on total temperature distributions in the plume, which are the net result of:

- ambient water temperature;
- level of generation and associated amounts of cooling water flow and waste heat discharged from SBPP; and
- the spatial distribution of discharged heat in the dispersing plume.

Temporal changes and interaction among all three of these factors result in variation in temperature exposure in the receiving waters.

Temperature affects metabolic processes of organisms by influencing the kinetics of chemical reactions and the effectiveness of enzymes. Among organisms lacking the physiological mechanisms to control tissue temperature, such as marine plants, invertebrates, and fish, the rate of metabolism at rest rises nearly exponentially with temperature increase. These marine organisms can survive within a range of temperatures specific to each species, known as their thermal tolerance range. The organism can adjust to the thermal environment physiologically, thereby shifting its tolerance range, but this acclimation has limits and ultimately a temperature may be reached that is lethal. Upper temperature limits for survival are dependent on the duration of exposure. Temperature elevations produced by thermal discharges have the potential to directly exceed the metabolic limits of exposed organisms, resulting in acute or chronic mortality.

The potential for the SBPP plume to affect biological communities depends on distance from the discharge structure. The highest exposure temperatures are limited to the area in closest proximity to the point of discharge where water velocity and turbulence exclude many species from residence. Ford et al. (1970) concluded that warm late summer discharge temperatures had an adverse effect on benthic fauna over a distance of approximately 500 to 1300 m from the point of discharge. In this area the number and diversity of benthic species was reduced compared to control stations.

Mobile species, such as fish and many macroinvertebrates, have the ability to move away from potentially lethal temperatures or toward preferred temperatures. These organisms may avoid elevated discharge temperatures and move to thermal transition zones of lower

water temperatures (Stephens and Zerba 1981). These movements can result in localized changes in fish assemblages (Adams 1975; Stephens et al. 1994). The diversity of fish assemblages was increased by thermal stratification associated with the discharge from a coastal power plant in King Harbor, Redondo Beach in southern California (Stephens et al. 1994). Avoidance of areas with elevated water temperatures for mobile species are generally not a problem if the area is small and access to critical habitat, major migration, or recruitment pathways are not blocked.

Thermal plumes may also attract certain species. Attraction to thermal plumes would only present problems if the attraction caused a nuisance for recreational or commercial utilization of the resource, resulted in overwhelming dominance and simplification of the community, or contributed to other discharge effects.

Within the range of thermal tolerance, there are temperature optima for physiological functions such as growth and reproduction. As water temperatures increase above this range physiological performance degrades. As a result, the effect of temperature on metabolism and behavior may indirectly affect marine life by changing the nature of the interactions among species present in the community. Alteration of the temperature environment by a thermal discharge has the potential to alter the competitive ability of species and result in changes in community composition.

DRAFT

1.5 Study Design

The studies described in the Board's directive are designed to address open issues regarding the extent of measurable effects of the SBPP thermal discharge on water quality in South Bay and its effect on benthic faunal communities, eelgrass habitat and fish assemblages. The recent additional work completed in 2003 represents an opportunity to synthesize NPDES discharge data and to consolidate findings from separate investigations that have been completed in the intervening 20 years. For example, 14 years of receiving water monitoring data from 1977–1991 were summarized in 1994 to analyze trends in biological communities and physical parameters in the vicinity of SBPP (Ogden 1994). The present study draws on data from these earlier reports but also includes new data that allows finer delineation of the near-field transition zone.

1.5.1 Background

In 1972 and 1973, San Diego Gas and Electric (SDG&E), the plant's previous owner and operator, conducted a thermal effects study as required by the State Water Resources Control Board. The study concluded that the existing elevated-temperature wastes discharged from SBPP had caused no prior appreciable harm to the aquatic community of San Diego Bay or to the beneficial uses of those waters (Ford et al. 1973). However, the study also concluded that the discharge had adverse effects on the benthic community within the discharge channel, which, for the purpose of that study, was not considered to be part of San Diego Bay. A subsequent USEPA data review of annual summer benthic studies conducted between 1977 and 1994 concluded that no appreciable long-term upward or downward trends in species diversity or abundance had occurred within the discharge channel (Ogden 1994). In 1996, SDG&E, was required to conduct further comprehensive effluent studies on eelgrass and fishes, which were completed in 2000 and submitted to the RWQCB (Merkel & Associates, Inc. 2000a, 2001, respectively).

1.5.2 Analysis Rationale

The discharge assessment rationale assumes that effects of the SBPP discharge will be expressed among the receiving water's biological community as gradients of changes in species abundance and distribution in response to changes in temperature or associated physical parameters due to the distribution and dispersal of the thermal plume. This rationale also assumes that discharge plume temperatures are the overriding variable in affecting biological changes. However, the study rationale also recognizes the potential for secondary discharge effects from other discharge constituents or interactions of these constituents and discharge temperatures by including studies of secondary discharge effects such as turbidity, flow, and dissolved oxygen.

The analysis of the biological data from the intertidal and subtidal benthic and subtidal fish studies focuses on identifying patterns of change in the biota from the point of discharge to the west end of the discharge channel and beyond. The analyses are intended to identify any differences in the spatial pattern that exist between biota on the south (impact) and north (reference) sides of the jetty (CVWI). Multivariate analysis is used to identify changes at the community level and will also be used to identify species or taxa that are most responsive to temperature changes. These species or taxa are then examined individually to investigate their tolerance for temperature maxima and duration, when such information exists. Data on seawater temperatures recorded at the biological sampling locations are analyzed for both maximum temperature and time of exposure (dose). The spatial patterns of change in the biological data are compared with the temperature monitoring data to determine if the changes can be attributed to the discharge. Spatial gradients of change detected in the presence of the plume are compared with control areas where similar patterns would not be expected. Another analysis approach used is the application of pollution sensitivity indices to benthic assemblage data (SCCWRP 2003). This method uses the assemblage composition in a sampled habitat to describe its response to a broad range of pollutants. Details on the sampling methods, station arrays and statistical testing procedures of the data are presented in the appropriate sections of this report.

By modeling the physical environment of the South Bay we can better assess the influence of the SBPP relative to the natural environment. Because both the natural environment and the SBPP create an elevated temperature gradient from south to north during daylight hours, such modeling is essential in determining the relative contributions of the coincident thermal generation factors of the SBPP cooling water system and solar heating.

The results from previous studies are extremely valuable in determining if any major biological changes have occurred in the control areas that may be attributed to some larger scale environmental effect. The combined results are used to address the questions presented in Section A.1 of the RWQCB letter (**Appendix A**).

1.5.3 Study Limitations

In order to assess the various potential causal effects of the discharge, the thermal effects must be partitioned from the effects of the other non-thermal variables. The analysis is made difficult due to the magnitude of non-thermal variables (i.e., flow velocity, turbidity, and substrate composition) relative to temperature, and the variability of the potential responses in affected organisms. With the exception of temperature and velocity, the cooling water passes through the CWS essentially unaltered from ambient conditions. Even when chlorine is added for biofouling control, the allowable discharge limits for residual chlorine are ultra-low concentrations that are rapidly scavenged by

organic and inorganic chlorine demand in the receiving waters. Although the partial pressure of dissolved oxygen varies with water temperature, dissolved oxygen (DO) cannot come out of solution under pressure of the CWS and only escapes solution at the air–water interface beyond the discharge structure.

Discharge velocities and turbulent mixing in the discharge channel as well as circulation patterns influenced by SBPP can affect the distribution of the South Bay's natural waterborne sediments eroded by wind and tidal currents across the bay's extensive mudflats. The turbidity from this natural sediment suspension process combined with the discharge temperatures may also act in concert to affect the receiving water communities, particularly eelgrass, which is sensitive to changes in light and which may be sensitive to a combination of light and temperature. This combined potential effect of changes in non-thermal discharge factors such as turbidity and dissolved oxygen could lead to complex biological responses that would be difficult to separate and identify. Field studies are generally not sufficient to resolve the roles of individual factors due to the low level of secondary effect responses and the high variability of natural populations and environmental factors. Investigating the interaction of water quality constituents is normally reserved for a laboratory setting where each factor can be varied in a controlled manner and biological responses can be standardized.

Concentrations of other either incidental or added discharge constituents in the discharge that are close to or below detectable levels are not expected to produce any measurable changes in receiving water biota. Biological effects attributed to the SBPP discharge constituents, if there were any at such low concentrations, could only be evaluated under controlled laboratory conditions.

Further confounding the effort to distinguish the effects of individual factors are the complications introduced by variable biological tolerances and strategies that can ensure persistence of species in marginal environments, even if there are subtle ecological costs or benefits to being present in such conditions. These may include reduced fecundity, increased or decreased growth rates, altered interspecific competition or predation, etc. While these conditions certainly exist, there is no reasonable way in a large-scale field environment to evaluate all of the factors. As such, the simple ecological metrics of diversity, richness, biomass, abundance, and species presence are used as indicators of biological suitability and ultimately are used to determine whether the ecologically-based beneficial uses of the receiving waters are being protected.

1.6 Report Organization

Sections 1.0 and 2.0 provide background information and physical data relevant to the biological results presented in subsequent sections. Section 3.0 presents the biological study methods, data analysis methods, sampling results, and discussions for each subtask. Some information on power plant description and environmental setting are duplicated in the companion volume to this report *Volume 2*: *South Bay Power Plant 316(b) Entrainment and Impingement Final Report*. Section 4.0 synthesizes information from Sections 2.0 and 3.0 on the spatial and temporal extent of the changes resulting from the discharge. Literature Cited for all sections is listed in Section 5.0.

DRAFT

2.0 Description of the South Bay Power Plant and Characteristics of the Source Water Body

2.1 South Bay Power Plant

The South Bay Power Plant (SBPP) uses the waters of San Diego Bay for once-through cooling of its four electric generating units. Each unit is equipped with two circulating water pumps (CWP) that supply cooling water. CWP capacity varies between units, ranging from 148 m^3/min to 259 m^3/min (39,000 gallons per minute [gpm] to 68,400 gpm), based on the manufacturer's pump performance estimates. The quantity of cooling water circulated through the plant is dependent upon the number of pumps in operation. With all eight pumps in operation, the cooling water flow through the plant is 1,580 m^3/min (417,400 gpm) (**Table 2.2-1**) or 2,275,000 m^3/day (601 million gallons per day [mgd]).

Table 2.1-1. South Bay Power Plant, generating capacity and cooling water flow by unit.

Unit	Gross Generation (MWe)	Total Flow per Unit (2 CWPs/Unit) (m^3/min)	Total Flow per Unit (2 CWPs/Unit) (gpm)
1	152	295	78,000
2	156	295	78,000
3	183	472	124,600
4	232	518	136,800
Total	**723**	**1,580**	**417,400**

2.1.1 SBPP Intake

Cooling water is withdrawn from San Diego Bay via an intake channel that connects the SBPP with the southeast corner of the bay (**Figure 2.1-1**). The intake channel is about 180 m (600 ft) in length, has a bottom width of about 60 m (200 ft) at its widest point, and tapers to 15 m (50 ft) width near the Unit 4 screenhouse. The maximum depth of the channel is approximately 5.4 m (17.7 ft) below mean lower low water (MLLW). The channel was constructed by dredging and diking operations during plant construction in the early 1960s and removed materials formed part of the CVWI, which separates the intake and discharge channels. Variations in water level due to tidal fluctuations range from a low of –0.7 m (–2.3 ft) to a high of +2.5 m (+8.2 ft) MLLW.

The cooling water intakes at the SBPP consist of three separate screenhouse structures for its four units. Units 1 and 2 share a single screenhouse structure while Unit 3 and Unit 4 each have individual screenhouses. As shown in **Figure 2.1-1**, water flow within the intake channel first approaches the screenhouse serving Units 1 and 2. The Unit 3 screenhouse is located an additional 40 m (131 ft) downstream, and the Unit 4 screenhouse another 28 m (92 ft) downstream, near the head of the channel.

Directly behind the screenhouses are the CWPs. Cooling water from the Units 1 and 2 CWPs exits the screenhouse via four 122 cm (48 in) diameter conduits that carry the flow approximately 61 m (200 ft) to the units' condensers. Intake conduits for Units 3 and 4 (one for each CWP) are 152 cm (60 in) in diameter, and also 61 m long. At each of the condensers the cooling water is dispersed through several thousand thin-walled condenser tubes. Units 1, 2, and 3 have dual-pass condensers that direct the cooling water through the condenser twice. Unit 4's condenser is a single pass design. Tubing material in the Unit 1 condenser is AL-6X, a stainless steel alloy, the other condensers are equipped with copper-nickel tubes.

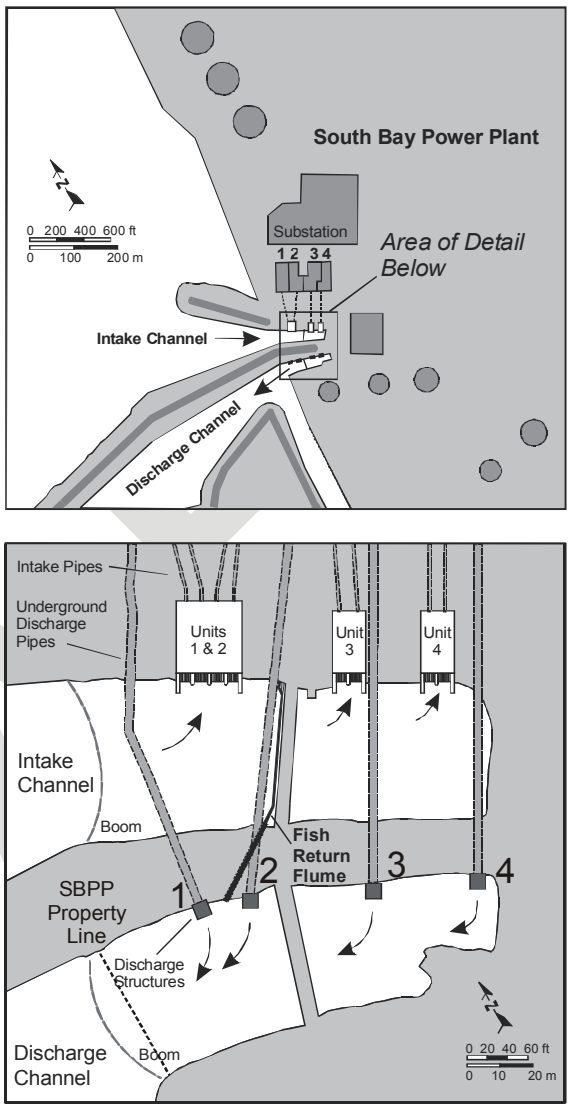

Figure 2.1-1. Diagram of SBPP circulating water intake and discharge structures.

2.1.2 SBPP Discharge

Exhaust steam, exiting the plant's turbines, passes over the exterior of the tubes in the condenser boxes where it is condensed by cool seawater water flowing through the tubes. The resulting condensate is pumped back to the plant's boilers as part of the continuing steam cycle and the cooling water exits the condenser as heated effluent. The change in cooling water temperature (delta T°) that occurs during passage through the condenser varies depending on a number of factors. Plant generating load and cooling water flow

are the main factors affecting delta T°. Flow can be reduced by condenser tube micro-fouling, tube blockage (caused by debris) and fluctuations in cooling water flow caused by tidal shifts or degradation of CWP performance.

SBPP uses chlorine injection to prevent or inhibit microfouling on the interior heat transfer surfaces of its condensers and ancillary heat exchangers. Chlorination is limited to two hours per day per unit by the plant's NPDES permit. The concentration of chlorine injected is periodically adjusted to compensate for fluctuations in chlorine demand in the cooling water but is limited to 0.2 mg/l (200 ppb) total residual chlorine (TRC) or lower depending on total cooling flow at the point of discharge. The plant is also limited to using less than 151.5 kg (334 pounds) of chlorine per day (Addendum 1 to Order No. 96-05).

Upon exiting the condensers, warmed cooling water from the four units is carried through discharge pipes about 137 m (450 ft) to the discharge basin located at the head of the discharge channel. The diameter of the discharge pipe for Units 1 & 2 is 183 cm (72 in) and 213 cm (84 in) for Units 3 & 4. The discharge channel originates on the side of the jetty, opposite the head of the intake channel. The discharge channel is defined in the SBPP NPDES permit (CA0001368, Order 96-05, Finding 23) as "…the waters bounded by the jetty, a line extending from the southwesternmost end of the jetty to the eastern side of the mouth of the Otay River, the southern shoreline of San Diego Bay, and the shoreline of the discharge basin." The same finding within the permit, defines the SBPP discharge points as the outlets of the cooling water discharge pipes.

2.1.3 CWP Flows and Point-of-Discharge Water Temperatures

The flow of cooling water discharged by SBPP is dependent upon the number of CWPs in operation at any given time. Maximum flow with all eight CWPs in continuous operation is 2,275,164 m^3/d (601.1 mgd). **Figure 2.1-2** shows the SBPP daily average discharge flow for December 1, 1998–September 30, 2003. During this time the daily CWP flow ranged from 425,056 m^3/d (112.3 mgd), the equivalent of both of the smaller Unit 1 or Unit 2 CWPs operating for 24 hours, to 2,275,164 m^3/d (601.1 mgd), the continuous operation of all eight pumps. Maximum discharge flows occurred much more frequently between December 1998 and the end of 2000. Since that time, a decline in demand for electricity from SBPP and the consequent reduction in generation have reduced the frequency of full-flow operation. Unit 4, in particular, has seen limited use in 2002 and 2003. During 2003 SBPP has, on a weekly basis, operated with all eight CWPs in service (if possible) for a period of about 24 hours to accommodate the impingement sampling conducted as part of the 316(b) studies described in Volume 2 of this report. As a result, the cooling water flows for this period are more variable than those from 1999–2002.

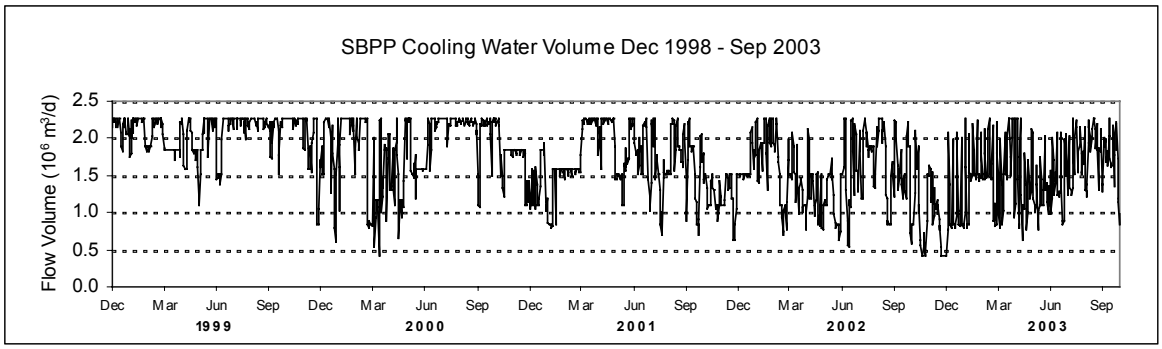

Figure 2.1.2. SBPP daily average circulating water flow from December 1, 1998 through September 30, 2003.

The SBPP discharge temperature is a function of intake water temperature, generating load, and cooling water discharge flow. During December 1, 1998–September 30, 2003, the daily average discharge temperature varied from a minimum of 13.8°C (56.8°F) to a maximum of 36.5°C (97.6°F). Major fluctuations in discharge temperature are seasonal, with the highest yearly temperatures occurring in July and August and the lowest from December through February. This is not a function related only to the power plant operation, but rather primarily the result of normal ocean temperature cycles, and atmospheric and solar heating. The influence of the power plant on the discharge temperature, expressed as the difference between intake and discharge temperatures (delta T°) ranged from –0.1 to 8.5°C (–0.2 to 15.3°F) as a daily average.

DRAFT

2.2 San Diego Bay Environmental Setting

2.2.1 Physical Description

San Diego Bay is the largest estuary between San Francisco Bay and Baja California. The bay is relatively long and narrow, 25 km (15.5 mi) in length and 1–4 km (0.6–2.4 mi) wide, and forms a crescent shape between the city of San Diego to the north and Coronado Island/Silver Strand to the south. The bay is separated into two distinct topographic regions, the outer bay, which is generally narrow and deep, and the inner bay, which is wide and shallow. Exchange with the ocean is limited to a single channel at the mouth. This north-south channel is about 1.2 km (0.7 mi) wide, with depths between 5–15 m (16.4–49.2 ft) (SPUPD 1976).

San Diego Bay, like other tidally-influenced waters in California, has a mixed (diurnal plus semidiurnal) tide with the semidiurnal tide being the larger of the two. The tides in the bay are weakly resonant, so that the tidal range is 5.6 ft (1.7 m) at the entrance and increases toward the head of the bay. It reaches 5.9 ft (1.8 m) at National City halfway down the bay. The range at SBPP is not known but may be slightly larger. The tidal prism of the bay (volume between MLLW and Mean Higher High Water [MHHW]) is approximately 7.4 x 10^7 m^3 (60,000 acre feet).

Tidal currents can be reasonably strong near the entrance of the bay at Pt. Loma, up to 1.0 m s^{-1} (meters per second) (3.3 fps), yielding an average tidal excursion (distance traveled by a parcel of water in one tide) of approximately 4.3 km (2.7 mi) (Chadwick et al. 1996). The head of the bay in the south bay ecoregion (near SBPP) is closed and without substantial tributaries. Thus, the horizontal motion of the tide near SBPP is small, with weak currents of approximately at 0.1–0.2 m s^{-1} (0.3–0.6 fps). Because of the weak tidal currents near the head of the bay, the flushing and residence time of the bay are controlled by the two-layer estuarine circulation. An absence of freshwater inflow means that this estuarine circulation is also weak much of the year, so the residence time can be quite long—several months. A detailed analysis of current velocities in the vicinity of SBPP with consideration of the plant intake and discharge flows is presented in Section 2.5 *Receiving Water Currents and Bathymetry*.

San Diego Bay is a low-inflow estuary. Rainfall averages approximately 26 cm (10 in) per year and significant freshwater inflow occurs for only a few months during the winter. In response to seasonal heating and cooling, water temperatures in San Diego Bay can exhibit a seasonal range of ~8–9ºC (14–16ºF) (Smith 1972). Because of the low freshwater inflow, considerable solar heating and weak flushing of the head of the bay, bay waters become quite warm and slightly more saline (relative to adjacent coastal

waters) in late summer and early winter. A detailed analysis of water temperatures in the vicinity of SBPP is presented in Section 2.3 *Receiving Water Temperature Monitoring*.

Currents in San Diego Bay are primarily produced by tides in the form of standing waves (Wang et al. 1998). Westerly afternoon winds occur throughout the year averaging less than 10 kt (5 $m \cdot s^{-1}$); easterly winds occur during winter evening and early mornings and are also about 5 $m \cdot s^{-1}$ or less (SDG&E 1973, Wang et al. 1998). The effect of wind driven waves on currents is generally small in San Diego Bay. Most of San Diego Bay is vertically well mixed in terms of thermal stratification. In the vicinity of SBPP, vertical density gradients can develop due to the discharge of warm surface water from the power plant. This condition can persist for several days during periods of low tidal energy (neap tides). In summer the evaporation rate in southern San Diego Bay is higher than the minimal freshwater inflow (< 10 inches annually). This can cause the south bay to become hypersaline (> 35 percent). Under these conditions a "reversed estuary" phenomenon can become established. In this case the heavier saline water flows down-estuary (north) along the bottom of the bay, while the less salty oceanic water flows up-estuary (south) near the surface (Wang et al. 1998).

2.2.2 Biological Description

SBPP is located along the southeastern shoreline of San Diego Bay, near the only remaining portions of the area's natural estuarine habitats. The shoreline and bathymetry of the bay have been altered through urbanization, waterfront development, and extensive dredging. The development of San Diego Bay and its use as a naval base and large commercial shipping hub has resulted in water quality changes as well as the alteration of benthic substrates. Modifications, including fill projects, periodic dredging, and the construction of piers, wharves, and docks have significantly altered the shoreline, as well as intertidal and subtidal habitats.

In the past 70 years the shallow expanses of San Diego Bay and littoral habitats have been largely eliminated from the northern two-thirds of the bay and greatly reduced in the south bay. Shallow submerged lands in the south bay have been reduced to 65 percent of their original area (SDUPD 1990). Less than 40 percent of the original intertidal mud flat areas in the south bay remain today, and salt mashes have been reduced to a few remnant patches (SDUPD 1990). Between 1940 and 1960 chronic pollution of the bay from sewage and industrial discharges greatly reduced the abundance and diversity of species and blanketed large areas of the bottom with sludge. Regulation of discharges into the bay initiated during the 1970s has resulted in an improvement in water quality and a gradual recovery of the abundance and diversity of species. Industrial activity in San Diego Bay still impacts water quality. The San Diego Unified Port District has many regional projects are underway to curb pollution and remediate the bay environment.

South Bay is a relatively shallow basin (<3.7 m [12 ft]) and is characterized by warm water temperatures and sluggish tidal currents. The Otay River flows into the south bay approximately one mile south of the power plant and the Sweetwater River channel enters the bay about three miles north of SBPP. While San Diego Bay is still considered an estuarine system, freshwater inflow has been nearly eliminated by water diversion, utilization of groundwater, and infrequent runoff (Browning et al. 1973). A variety of aquatic habitats are contained within the boundaries of South Bay and several important terrestrial habitats occur adjacent to its shore. Allen (1999) examined the ecological relationships of fish fauna and habitats throughout San Diego Bay in four ecological regional areas or 'ecoregions' (**Figure 2.2-1**). The south ecoregion is the area of San Diego Bay south of a line drawn in west southwesterly direction from the Sweetwater River Channel to the Silver Strand State Beach on the San Diego Peninsula. The south central ecoregion extends from the Coronado Bridge south to the boundary of the south ecoregion at the Sweetwater River Channel.

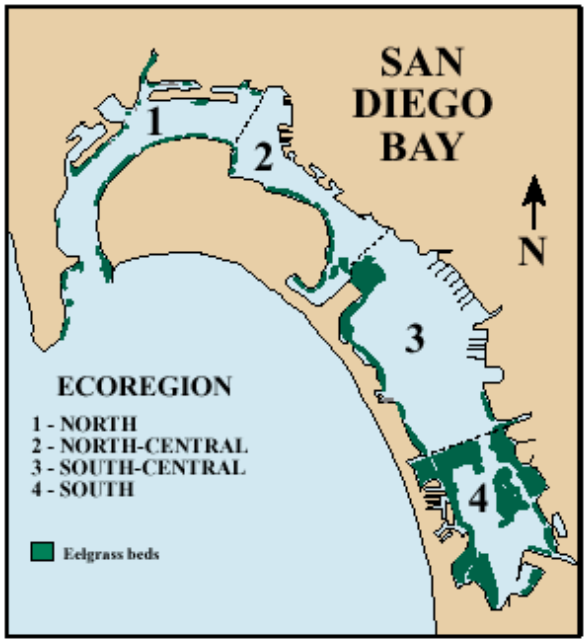

Figure 2.2-1. Map of ecoregions in San Diego Bay (from Allen 1999).

The aquatic habitats in the south ecoregion, in the vicinity of the SBPP, are characteristic of protected inshore marine environments. The flora and fauna of the region consists of communities living above, on, and within soft benthic substrates. Benthic substrates are composed mostly of alluvial sediments, including fine-grained sand, silt, and clay. Some expanses of bottom along the western shoreline of the bay, however, are dominated by larger-grained sand (Browning et al. 1973). Because of the absence of freshwater inflow, plant and animal communities are typical of marine and higher salinity estuarine environments. Aquatic habitats include submerged lands (or subtidal areas), eelgrass *Zostera marina* beds, mudflats, and salt marshes. Salt evaporation ponds located adjacent to the southernmost reach of the bay provide important habitat for shorebirds and migrating waterfowl.

The CVWI adjacent to SBPP is a constructed peninsula that separates the inflow and discharge channels of the power plant. The island itself was largely constructed from dredge spoils, and portions of the access causeway are armored with rock rip-rap to prevent erosion. Tidal inlets within the reserve form wetland areas, and adjacent areas provide seasonal habitat for several species of nesting shorebirds including endangered

California least terns *Sterna antillarum browni* and endangered western snowy plovers *Charadrius alexandrinus nivosus*.

2.2.2.1 Submerged Lands

Submerged lands encompass all subtidal and regularly submerged areas of the south bay. Eelgrass beds are spread over approximately 343 ha (848 ac) (Merkel and Associates 2000a) within the 993 ha (2,454 ac) of area in the south bay designated as submerged lands. With the exception of dredged channels, depths in the south bay do not exceed 3.7 m (12 ft), and 57 percent of the acreage is less than 1.8 m (6 ft) (USFWS 1998). Twenty-six percent of the area is reported to be less than 0.9 m (3 ft) in depth (USFWS 1998).

The submerged land area in the south bay supports nearly 300 invertebrate species (USFWS 1998) and at least 50 species of fishes, sharks and rays (Allen 1999). Common invertebrates include various types of worms, gastropod and bivalve mollusks, and crustaceans. Recreationally important fish species found in the south bay include the barred sand bass *Paralabrax nebulifer*, spotted sand bass *Paralabrax maculatofasciatus*, diamond turbot *Hypsopsetta guttulata*, California halibut *Paralichthys californicus,* black croaker *Cheilotrema saturnum*, opaleye *Girella nigricans*, striped mullet *Mugil cephalus*, and bonefish *Albula vulpes*. Northern anchovy *Engraulis mordax*, two species of bay anchovy *Anchoa* spp., and Pacific sardine *Sardinops sagax* are occasionally abundant in the area. Round stingray *Urolophus halleri* are known to be abundant in the south bay (LES 1981) as are several other species of bottom-dwelling sharks and rays.

Submerged lands in the south bay are also an important resting and feeding area for waterfowl migrating along the Pacific Flyway. Surveys by the USFWS during 1993–1994 found almost 200,000 birds at one time utilizing the habitat available in the south bay (USFWS 1998). Common waterfowl include the surf scoter *Melanitta perspicillata*, scaup *Aythya* spp., black brant *Branta bernicla nigricans*, bufflehead *Bucephala albeola*, loons *Gavia* spp., and western grebe *Aechmophorus occidentalis*. Seabirds such as gulls *Larus* spp. and cormorants *Phalacrocorax* spp. are also common in the area. Additionally, a number of listed (endangered and threatened) bird species, and species of special concern, have been observed in the south bay. Bird species in the area that are protected under state or federal law include the California least tern, western snowy plover, brown pelican *Pelecanus occidentalis*, peregrine falcon *Falco peregrinus*, and bald eagle *Haliaeetus leucocephalus*.

Three species of marine mammals have been observed in the South Bay. During waterfowl surveys in the south bay, the USFWS reported observing California sea lions *Zalophus californianus* and Pacific bottle-nosed dolphins *Tursiops truncatus* within their study area (USFWS 1998). While most of the observations occurred in the northern half of the area, three bottle-nosed dolphins were observed in the southernmost regions of the bay. Harbor seals *Phoca vitulina* were reported to have been observed near the cooling

water discharge channel of SBPP, possibly foraging for animals attracted to the heated effluent (ESA 1997). All marine mammals are federally protected.

Green sea turtles *Chelonia mydas* occur in the discharge channel and vicinity of SBPP, attracted by the warm waters of the discharge. Although green sea turtles migrate considerable distances, the SBPP discharge channel is the northernmost locale on the Pacific Coast where they reside with any regularity (Eckert 1994).

2.2.2.2 Eelgrass

San Diego Bay's remaining eelgrass beds cover over 500 ha (1,245 ac), which is the largest eelgrass habitat in California. The larger expanses of eelgrass in San Diego Bay can be attributed to the reduction of raw sewage and industrial waste discharge into the region since the 1970s (SDUPD 1990, USFWS 1998). Of this area 343 ha (68 percent) are located in the south bay ecoregion (Merkel and Associates, Inc. 2000a). The distribution and abundance of eelgrass in the south bay vary from year to year and on a seasonal basis. The general distribution patterns have remained stable over the past several years except during recent El Niño events. Eelgrass beds are the most expansive in the vicinity of the Sweetwater Marsh National Wildlife Refuge (NWR), Crown Cove, and an area to the north of Emory Cove. Several dredged navigational channels break up the area of eelgrass coverage in the south bay.

Eelgrass is a flowering marine plant that grows in the shallow, sunlit waters of protected bays and estuaries. Eelgrass forms extensive beds in soft benthic substrates. The beds provide cover and spawning substrate for many species of fish and invertebrates, and are considered important nursery areas. Eelgrass is an important food source for green sea turtles in the area and a variety of seabirds and migrating waterfowl. The black brant, a small migratory goose species, feeds heavily on eelgrass during its migrations along the coast.

Eelgrass is a wide-ranging plant species that occurs along the Pacific coast of North America from the Bering Strait south to lower Baja California and around to the Gulf of California. It typically occurs in water temperatures from 5–27°C (41–80.5°F) (Phillips 1984). Within the south bay ecoregion eelgrass grows in waters exceeding 32ºC (90ºF) (Merkel and Associates, Inc. 2000a). Eelgrass grows down to depths of 15.2 m (50ft) if ample sunlight is present, but water turbidity in an area will limit its growth and the depth to which it occurs. Within the south bay ecoregion eelgrass grows in waters up to 2.1 m (7 ft). Eelgrass is a marine species and is not tolerant of low salinities. In the south bay ecoregion salinity is not considered a significant factor affecting the distribution of eelgrass (Merkel and Associates, Inc. 2000a).

2.2.2.3 Mudflats

Mudflats are present along two-thirds of the shoreline of the south bay and are absent only along the western shore in the vicinity of the Coronado Cays (USFWS 1998). The

largest expanse of mudflat habitat in the region extends from the southern boundary of Emory Cove around the south end of the bay to the SBPP plant site. Another large expanse of mudflat habitat extends north along the eastern shoreline of the bay from the Chula Vista Boat Yards to the northern boundary of the Sweetwater Marsh NWR. Mudflat habitat occupies approximately 199 ha (492 ac) in the south bay and adjoins the salt evaporation ponds along its southern margins.

Mudflats are rich in organic matter and support a diverse assemblage of invertebrates. An extensive assortment of birds and fishes utilize this abundant invertebrate fauna as a primary food source. During low tide, shorebirds such as the western snowy plover, Belding's savannah sparrow *Passerculus sandwichensis beldingi*, western sandpiper *Calidris mauri*, dunlin *Calidris alpina pacifica*, marbled godwit *Limosa fedoa*, willet *Catoptrophorus semipalmatus*, long-billed curlew *Numenius americanus*, northern phalarope *Phalaropus lobatus*, killdeer *Charadrius vociferus*, American avocet *Recurvirostra americana* and red knot *Calidris canutus* forage the mudflats during their migrations along the Pacific Flyway. Over 26 species of shorebirds were reported to have been identified as utilizing the south bay habitats for a wintering ground (Browning et al. 1973). When mudflats are submerged, a variety of terns (including least terns), grebes, and black skimmer *Rhynchops niger* use the habitat to forage for small fishes. Sixty-seven species of birds were reported to have been observed in mudflat and salt pond habitat during bird counts by the USFWS (USFWS 1998). Several fish species are closely associated with mudflat habitats and are preyed upon by terns and a variety of probing shorebirds. These temperature and salinity-tolerant fishes include the California killifish *Fundulus parvipinnis* and two goby species; the arrow goby *Clevlandia ios* and the longjaw mudsucker *Gillichthys mirabilis.*

Mudflats in the south bay provide an important food source for a number of protected bird species. The California least tern and western snowy plover are federally protected under the Endangered Species Act and either fully protected (least tern) or listed as a Species of Special Concern (snowy plover) under California law.

2.2.2.4 Saltmarsh

Salt marshes are the driest of the habitats in the south bay that are influenced by the tides (USFWS 1998). Because they are less influenced by the tides, the loss of salt marsh habitat has been particularly extensive due to shoreline development. The 23 ha (57 ac) of salt marsh that remain in the south bay are distributed among six different locations. The largest patches of salt marsh habitat are located along the northern boundary of the Sweetwater Marsh NWR, adjacent to the J Street fill, and the in the biological study area south of Emory Cove. Small patches also occur in the Chula Vista Wildlife Reserve, the salt evaporation ponds, and along the Otay River channel. Salt marsh habitat not included in the 23 ha (57 ac) estimate, but considered critical, is also present in narrow strips along other tidally-influenced regions of the Otay River and along some portions of the salt pond dikes.

Salt marsh habitat is characterized by low-growing, salt-tolerant vegetation and is typically dominated by pickleweed (*Salicornia* spp.). Salt marshes are used by a variety of shorebirds for nesting and feeding, and as escape areas during high tide. A great variety of shorebirds, herons, egrets, rails and some waterfowl species may frequent small patches of salt marsh habitat. Fifty-seven species of birds were counted during bird surveys conducted by the USFWS in a salt marsh along the Otay River (USFWS 1998). Until recently a 91 m (300 ft) stretch of salt marsh habitat along the Otay River supported nesting pairs of the light-footed clapper rail *Rallus longirostris levipes*, which is listed as a federally endangered species (USFWS 1998). Light-footed clapper rails are found exclusively in salt marshes and the extensive loss of this habitat type has coincided with the species' decline. The Belding's savannah sparrow, listed as threatened under state law, nests in salt marsh habitats within the south bay. Over 100 nesting pairs were observed during USFWS bird surveys.

DRAFT

2.3 Receiving Water Temperature Monitoring

2.3.1 Introduction

The purpose of the receiving water temperature monitoring program was to collect data to describe the extent and dispersal of the thermal plume originating from SBPP. The heated effluent discharged by SBPP is warmer than the receiving water when the power plant is generating electricity. The warm water, which is less dense than the receiving water, generally floats to the bay surface, except in the discharge channel area where turbulent mixing and flow volumes can cause it to contact the bottom. The thermal effluent spreads outward with the momentum of the plume, increasing in surface area while becoming thinner (in depth) and cooler as it moves away from the discharge. As the plume spreads at the surface its heat dissipates into the receiving water body and ultimately the atmosphere.

The extent and distribution of the thermal plume is dependent upon a variety of factors including the temperature of the discharge relative to the receiving water, the volume of the discharge, tidal conditions, solar heating effects, and meteorological conditions. The discharge temperature is mainly dependent upon the intake water temperature, plant electrical generating load, and volume of cooling water. As the rate of power production increases, greater amounts of heat are transferred into the cooling water discharge (see Section 2.1 *Discharge Description*). The volume of water discharged varies with the number of circulating water pumps that are in service. The combination of temperature and volume can result in a warm plume with a relatively small distribution (higher discharge temperature and low discharge volume), a cooler mass of water extending over a larger surface area (lower discharge temperature and high discharge volume), or any combination of the two variables. Circulating water pumps are normally shut down as generating units are removed from service, but occasionally the pumps remain operational even though load has been reduced. For example, all of the circulating water pumps (if operable) were functioning for a period of at least 24 hr during weekly impingement sampling in 2003, regardless of plant load. During these periods, the additional flow resulted in a large volume of ambient temperature water (from units not producing heat) that diluted the heated discharge.

Tidal fluctuations also affect the distribution of the discharge plume. At slack high tide, the plume can be dispersed over a wider expanse of the discharge channel. During an outgoing spring tide, the plume may narrow, but extend further north into San Diego Bay. The receding tide can also bring water that has been heated by solar radiation in the shallows of the bay into contact with the plume. The measurements described in the following sections provide a detailed description of plume characteristics under various conditions.

2.3.2 Methods

2.3.2.1 Field Data Collection

Twenty-one subtidal and ten intertidal temperature monitoring stations were established in the vicinity of the SBPP (**Table 2.3-1** and **Figure 2.3-1**). The majority of the stations were clustered around the power plant's intake and discharge channels to record the magnitude and distribution of the discharge plume. Several far-field stations were also established further to the north beyond the influence of the plume. The proximity of the stations to the power plant's discharge ranged from approximately 65 m (328 ft) to nearly 5 km (3 mi) (**Table 2.3-2**). These distances are estimates of the shortest flow-paths between the SBPP discharge and each monitoring station, not linear measurements between the points. Eleven of the subtidal stations (those designated A, C, D, E, F, or N) were placed at locations that were part of the ongoing NPDES receiving water monthly monitoring program for SBPP (MEC 2003). All of the intertidal stations and the remaining ten subtidal stations (those designated R or T) were established at new locations that were concentrated around the intake and discharge channels. All of the temperature recorders were initially deployed on July 15–16, 2003.

Each of the subtidal stations was equipped with an array of three temperature recorders deployed below a buoy (**Figure 2.3-2**). One recorder was located just below the surface of the water, one at a depth of 1 m (about 3 ft), and one just above the sediment-water interface. The position of the upper two recorders, relative to the water's surface, remained constant regardless of tide height. The bottom recorder's position was fixed and the depth separating the recorder from the surface changed with the tides. The depth at which the bottom recorder was located also varied between stations, depending upon the position of the station within San Diego Bay. Subtidal station depth ranged from 0.4 m (1.2 ft) below MLLW (Station SR4) to 4.2 m (13.9 ft) below MLLW (Station SA3). Each of the intertidal stations was equipped with a single, fixed-position temperature recorder. The elevation of all ten intertidal recorders was approximately 0.3 m (1.0 ft) above MLLW. As such, the recorders were exposed to air during some low tide conditions. Air temperatures were deleted from the temperature database during data processing.

All of the monitoring stations were equipped with Stowaway Tidbit® temperature recorders manufactured by the Onset Computer Corporation. The units had a recording range from -5–37ºC (24–99ºF), were accurate to ± 0.2ºC (± 0.4ºF), and were programmed to synchronously record temperatures at 10-minute intervals. The recorders closest to the discharge were replaced in early September 2003 with similar instruments that had a range of -20–50ºC (-4–122ºF) and were accurate to ± 0.4ºC (± 0.8ºF). All recorders were calibrated and each was checked to verify its operability and accuracy after it was retrieved and the data were downloaded.

2.3.2.2 Analysis Methods

An analysis of the basic temperature records was accomplished by comparing mean, minimum, and maximum temperatures among stations under a variety of plant operating and environmental conditions. Other analysis methods are described in the following subsections.

Relative Temperatures (Delta T°)

In an effort to isolate the contribution of SBPP to the temperatures recorded at the discharge stations, the difference in temperature, or delta T°, between the reference stations and discharge stations was calculated for each of the synoptic data entries. For intertidal stations, the mean reference temperature was calculated from the readings taken at Stations IR1, IR2, and IR3, and was subtracted from the readings taken at the same time at each of the intertidal stations. The temperatures recorded at Stations IR4 and IR5 were not included in the calculation of the reference mean. These two stations, the eastern most stations, were in close proximity to the marina and its boat channel to the north and a considerable distance from the other three IR stations that lie along the intake channel leading to the power plant.

For subtidal stations, selecting an appropriate reference station was difficult. Ideally the reference station should be located in a physical setting that is identical to that of the discharge stations and is subjected to all of the same natural influences, but is totally removed from the influence of the power plant. The far field stations SN2 and SA3 are the furthest distance from the power plant, but are located in deeper, cooler water than the discharge stations in the shallows of the south bay. Station SF2 is located about 3 km (1.9 mi) west of the plant discharge, in shallow water, but is positioned in an area that consistently receives a southerly intrusion of cooler water from the more northerly regions of the bay. Most of the remaining stations were positioned in the potential path of the discharge plume and, as such, were unsuitable as reference stations. For the purpose of the delta T° calculations, temperature readings from Stations SR1, SR2, and SR3 were used as reference. The mean of the three stations was calculated for each of the monitoring depths (surface, -1 meter, and bottom), for each 10-min reading. For the purpose of comparison, the temperatures recorded at the selected reference stations (combined data from stations SR1, SR2, and SR3 at all three levels) were checked against the daily mean intake temperatures reported by SBPP in their monthly NPDES discharge monitoring reports. The average difference between the daily mean reference temperature and the plant's reported daily average intake temperature, over the period from mid-July through the end of September 2003, was only 0.19°C (0.34°F). A paired t-test of the daily mean reference and intake temperatures found no significant difference between the two.

To aid in visualizing the delta T° measurements a series of animations was developed (refer to accompanying CD). A set of twice-monthly AVI files were created to present delta T° in relation to distance from the discharge boom at 10-minute sample intervals for the surface, 1-m subsurface, bottom, and intertidal station locations.

Gradient Analysis

To analyze gradients in temperature as a function of distance from the discharge, three temperature gradient models (functions of distance x or x^2) were fit to stations within 2,800 m (9,186 ft) from the discharge boom (about the distance to the first reference station). The synoptic mean temperatures at the reference stations (T_{SR}) used in calculating station delta T° (*i.e.,* SR1, SR2, and SR3) were not included in regressions but were visualized in the animations.

Model 1:
$$\left(T - \frac{\sum_{i=1}^{3} T_{SRi}}{3} \right) = a + b\,x$$

Model 2:
$$\left(T - \frac{\sum_{i=1}^{3} T_{SRi}}{3} \right) = a + b\,x^2$$

Model 3:
$$\left(T - \frac{\sum_{i=1}^{3} T_{SRi}}{3} + 10 \right) = e^{a+b\,x}$$

Three linear regression models were developed and tested for a best-fit comparison of the empirical data. Two models (1 and 2) were fit by linear regression. A third model (3) was fit by linear regression using logarithms (a constant 10 degrees was added to avoid log of a negative value). Model 1 predicts that the change in relative temperature with distance is equal to a constant b. Model 2 depicts a change in relative temperature with distance as a linear function of distance. Model 3 represents relative temperature changing exponentially with distance from the discharge boom. Model 1 was used in subsequent analysis because it best fit the frequencies of empirical excursions. The x-intercept at a delta T° of 2.2°C (4°F) for each 10-minute interval set of temperatures was calculated. If the 2.2°C (4°F) delta T° excursion did not occur in any interval, a zero was recorded as an excursion distance from the discharge boom. Excursion distances greater than 3.5 km (2.2 mi) were not used in the models because they exceeded empirically derived excursion results.

Time Series Analysis

Two methods of time series analysis were used to analyze the temperature data for repeating patterns. The first, autocorrelation, multiples the time lags of temperature and distance by itself in order to look for repeating features in the data. The second, cross-correlation, uses the product of the temperature and distance to see repeating patterns.

Autocorrelation plots of the surface, 1-m subsurface and bottom excursions of the 2.2°C (4°F) distance from the discharge boom were examined to determine relationships between temperature and operation of the power plant.

Temperature Exposure: Duration and Frequency

The maximum temperatures recorded at the individual monitoring stations and the mean temperatures calculated from the body of data taken at each station describe the temperature regimes found at each station, but not the cumulative exposure or the duration of exposure to different temperatures. To accomplish this, accumulated temperature data from each station were analyzed to determine the frequency of exposure to a variety of elevated temperatures ranging from 26–38°C (79–100°F). Two threshold temperatures, 27°C and 30°C (81°F and 86°F), were analyzed to determine the duration of individual excursions above these thresholds.

The time period used in both the frequency and duration analyses runs from each station's time of deployment (July 15–17, 2003) through the end of September 2003, with the exception of Stations ST2 and SR5. Station ST2 either drifted, or was moved, from its original position shortly after its initial deployment. The station was reestablished on August 14, 2003, which was the date used as the start of its temperature record. The benthic level temperature recorder at Station SR5 malfunctioned and did not record. Comparison of the data from Station SR5 surface and 1-meter recorders with that from the Station SR4 recorders, however, indicates that these adjacent stations had very similar temperature records. The similarity would probably extend to the benthic temperatures as well. Only those data recorded at the intertidal stations and the benthic level of the subtidal stations were used in the analyses.

Frequency analysis of the temperature data does not provide insight into the actual duration of individual exposures to elevated temperatures. For this purpose, the data were analyzed to determine the length and number of individual excursions into two temperature zones; greater than or equal to 27°C (80.6°F) and greater than or equal to 30°C (86.0°F). The first temperature was selected because it was the warmest temperature recorded at the far-field Station SN2 during the study period. The second temperature was selected as approximately the warmest temperature recorded at the reference stations (SR1–SR5) during the same period. Both provide good thresholds for assessing elevated temperature exposure. An excursion was defined as two or more consecutive temperature readings at, or above, the threshold temperature. The excursion was concluded when the temperature dropped back below the threshold, and the duration was calculated from the number of consecutive readings. At the intertidal monitoring stations, the temperature excursion would also be concluded when the tide level dropped below +1.0 ft MLLW and the station was exposed to the atmosphere.

Table 2.3-1. Locations of subtidal (S series) and intertidal (I series) temperature stations. Subtidal stations consisted of a surface, 1-m (3.3 ft) subsurface, and bottom temperature recorder (see Figure 2.3-2). *Intertidal stations were at a fixed elevation of 0.3 m (1.0 ft) above MLLW.

Station	Latitude (N)	Longitude (W)	Depth below MLLW*	
			meters	feet
SUBTIDAL				
SA3	32° 37.780’	117° 07.136’	4.2	13.8
SC3	32° 37.211’	117° 07.149’	2.3	7.5
SD4	32° 37.109’	117° 06.884’	1.4	4.6
SE3	32° 36.863’	117° 07.143’	1.1	3.6
SE4	32° 36.866’	117° 06.858’	1.3	4.3
SE5	32° 36.785’	117° 06.603’	1.7	5.6
SE7	32° 36.801’	117° 05.930’	1.7	5.6
SF2	32° 36.566’	117° 07.482’	0.4	1.3
SF3	32° 36.621’	117° 06.971’	1.4	4.6
SF4	32° 36.552’	117° 06.852’	1.8	5.9
SN2	32° 38.201’	117° 07.704’	2.0	6.6
SR1	32° 36.988’	117° 06.392’	3.1	10.2
SR2	32° 37.013’	117° 06.480’	2.2	7.2
SR3	32° 37.070’	117° 06.650’	2.6	8.5
SR4	32° 37.143’	117° 06.364’	0.9	3.0
SR5	32° 37.238’	117° 06.401’	0.4	1.3
ST1	32° 36.792’	117° 06.005’	2.0	6.6
ST2	32° 36.777’	117° 06.141’	2.0	6.6
ST3	32° 36.772’	117° 06.254’	1.6	5.2
ST4	32° 36.723’	117° 06.430’	1.9	6.2
ST5	32° 36.825’	117° 06.788’	2.0	6.6
INTERTIDAL				
IR1	32° 36.955’	117° 06.438’	+0.3	+1.0
IR2	32° 36.984’	117° 06.547’	+0.3	+1.0
IR3	32° 37.018’	117° 06.683’	+0.3	+1.0
IR4	32° 37.131’	117° 06.217’	+0.3	+1.0
IR5	32° 37.223’	117° 06.257’	+0.3	+1.0
IT1	32° 36.816’	117° 06.006’	+0.3	+1.0
IT2	32° 36.799’	117° 06.144’	+0.3	+1.0
IT3	32° 36.777’	117° 06.288’	+0.3	+1.0
IT4	32° 36.741’	117° 06.403’	+0.3	+1.0
IT5	32° 36.853’	117° 06.804’	+0.3	+1.0

DRAFT

Table 2.3-2. Distance of subtidal (S series) and intertidal (I series) temperature stations from the SBPP discharge boom (property line). Distances are the shortest drift path to the station from the plant discharge. Order of stations reflects increasing distance.

	Drifter distance from discharge boom	
Station	**meters**	**feet**
SUBTIDAL		
SE7	65	213
ST1	181	594
ST2	396	1,299
ST3	572	1,877
ST4	857	2,812
SE5	1,150	3,773
ST5	1,445	4,741
SF4	1,591	5,220
SF3	1,817	5,961
SE3	2,294	7,526
SE4	2,305	7,562
SF2	2,624	8,609
SD4	2,728	8,950
SR3	2,805	9,203
SC3	2,938	9,639
SR2	3,089	10,135
SR1	3,234	10,610
SR4	3,272	10,735
SR5	3,301	10,830
SA3	4,017	13,179
SN2	4,917	16,132
INTERTIDAL		
IT1	182	597
IT2	362	1,188
IT3	621	2,037
IT4	833	2,733
IT5	1,475	4,839
IR3	3,345	10,974
IR2	3,570	11,713
IR1	3,742	12,277
IR5	3,999	13,120
IR4	4,038	13,248

DRAFT

2.3.3 Intertidal Temperature Results

Intertidal temperature data were recorded from July 15 through October 13, 2003**.** All of the recorders functioned properly and passed their post-retrieval calibration.

2.3.3.1 Absolute Temperature Comparisons

The highest water temperatures at each station were recorded during August 2003. The highest maximum temperature and monthly mean temperature, 38.1ºC (100.6ºF) and 32.3ºC (90.7ºF), respectively, were recorded at Station IT1, the intertidal station closest to the discharge. The maximum, minimum, and mean temperatures at each intertidal station during July, August, and September 2003 are presented in **Figure 2.3-3**. As expected, the maximum and mean temperatures at the five stations located in the discharge channel (IT1, IT2, IT3, IT4, and IT5) decreased with increasing distance from the discharge, with the temperature in August, for example, dropping by 3.4ºC (6.1ºF) [maximum] and 2.9ºC (5.2ºF) [mean] over a distance of 1.3 km (0.8 mi). The minimum temperatures recorded at the discharge channel stations were similar, with the minimum temperature during August 2003 for example, ranging from 26.4ºC (79.5ºF) to 26.9ºC (80.4ºF). The periods with the lowest temperature readings correspond with periods of minimal plant load and low discharge volumes, usually in the late night and early morning hours when electrical demand was lowest. These are also the intervals when solar heating effects are at a minimum. During periods of low plant load and limited solar input, no temperature difference was discernible between the discharge intertidal stations.

The reference intertidal stations, located in the vicinity of the intake channel, recorded maximum temperatures during August 2003 ranging from 29.7–31.6ºC (85.5–88.9ºF) (**Figure 2.3-3** and **Appendix B**). Mean temperatures at these stations in August ranged from 26.6–27.8ºC (79.9–82.0ºF). Mean and maximum temperatures were slightly cooler at Stations IR4 and IR5 than at Stations IR1, IR2, and IR3. The minimum intertidal water temperatures at the reference stations ranged from 23.0–25.0ºC (73.4–77.0ºF) during August.

2.3.3.2 Relative Temperatures (Delta Tº)

Delta T° calculations were made for each of the readings taken at 10-minute intervals during each recorder's period of deployment. The highest delta T° during this period was 9.9ºC (17.8ºF) and occurred at Stations IT1 and IT2 on the afternoon of September 5, 2003 (**Figure 2.3-4**). This coincided with a 1–2-hour period of 100 percent generating capacity factor (GC)(723 MWe), and was the only period of full power operation during the July–September monitoring period. The highest delta T°s calculated for Stations IT3, IT4 and IT5 were 9.0ºC (16.2ºF), 7.8ºC (14.0ºF), and 5.4ºC (9.7ºF), respectively. All three occurred on July 16, 2003 when plant load was above 600 MWe (83 percent GC) for about 6 hr. Due to daily fluctuations in electrical demand and subsequent power production, the average delta T° calculated for each discharge intertidal station is considerably lower than

the recorded maximum values. Mean monthly delta T° at the discharge stations ranged from 1.5–4.5ºC (2.7–8.1ºF) and decreased with distance from the discharge (**Figure 2.3-4)**.

The effect of the power plant on patterns of diurnal temperatures at the individual intertidal monitoring stations was examined by comparing the temperature data recorded during a multi-day period of relatively low power production with one of higher power production. The times selected were the five-day periods from September 26–30, and from September 2-6. The first period is shown in **Figure 2.3-5** and includes two days, September 27 and 28, when power production was low and averaged 77 MWe (11 percent GC) and 71 MWe (10 percent GC), respectively, and exceeded 100 MWe (14 percent GC) for a single one-hour period. During that two-day period, there was little difference (about 1–2ºC) between the reference and the discharge stations. The temperature difference between Stations IT1 and IT5 was also reduced to about 1ºC at maximum. Peak daily temperatures at each station occurred in the early afternoon and can be attributed to solar heating (reference and discharge stations) and the influence of the power plant (discharge stations only).

The second period examined (**Figure 2.3-6**) extended from September 2–6, and included the only time during the July–September monitoring period that the plant operated at 100 percent GC (723 MWe). This occurred for about two hours on September 5th. Average plant load was 350 MWe (48 percent GC) on that day. While operating at full plant load, the delta T° between the reference stations (average of IR1, IR2, and IR3) and discharge stations IT1 and IT2 reached 9.9ºC (17.8ºF), and the difference between Stations IT1 and IT5 reached a maximum span of about 8ºC (14ºF).

2.3.4 Subtidal Temperature Results

Subtidal temperature data were recorded from July 15 through October 14, 2003. Of the 63 recorders deployed, 61 functioned properly and passed their post-retrieval calibration. Two of the recorders failed to operate after deployment and did not collect data. One of the inoperative recorders was located at the far-field Station SA3 at the 1-m subsurface level (SA3B), the other was located at reference Station SR5 at the bottom position (SR5C). There is also a data gap from July 15, 2003 through August 14, 2003 for all three of the recorders from discharge station ST2 (ST2A, B, and C). The recorder array was missing and was replaced in August with a new float line and temperature recorder array. The original station line and recorders were recovered in October near reference station SR5, about 3.4 km (2 miles) from its original location. Data for this period from these recorders were not used in any of these analyses.

2.3.4.1 Absolute Temperature Comparisons

Figure 2.3-7 presents the daily mean temperatures recorded at the surface, -1 m, and at the bottom at five stations (SE7, ST4, SF4, SR2, and SN2). These stations represent the range of temperatures that were recorded between the middle of July 2003 and the end of September 2003. The warmest water was observed at the station nearest the discharge (SE7) and the coolest temperatures were recorded at Station SN2, which was the northern most station monitored. For the stations nearest to SBPP, the surface temperatures were generally warmer than the bottom temperatures. The temperatures recorded at station SN2 were generally very similar at the three depths.

As in the case of the intertidal monitoring stations, the highest temperatures recorded at the subtidal stations generally occurred in August 2003 (**Figure 2.3-7** and **Appendix B**). Since the warm water of the discharge plume tends to be less dense than the cooler receiving water, the highest temperatures at each station were usually recorded by the surface temperature unit. The highest maximum temperature and monthly mean temperature, 38.4 and 32.3ºC (101.1 and 90.7ºF), respectively, were recorded by the surface level unit at Station SE7, the station nearest to the discharge. However, at the four stations nearest discharge (SE7, ST1, ST2, and ST3), the plume often extended deep enough that identical temperatures were recorded at the surface and -1 m (-3.3 feet) positions. These four stations were located 113, 229, 444 and 620 m (371, 751, 1,457, and 2,034 ft), respectively, from the point of discharge (**Table 2.3-2**). At the next farthest station from the discharge, Station ST4 (905 m [2,969 ft]), the plume typically dispersed and thinned to a point where both the maximum and mean temperatures recorded at the -1 m level were cooler than those at the surface. The monthly minimum, mean, and maximum temperatures at the surface, -1 m, and bottom of each subtidal station during July, August, and September 2003 are displayed in **Figures 2.3-8, 2.3-9** and **2.3-10**.

The effect of the power plant on diurnal temperature cycling at the individual subtidal monitoring stations was examined by comparing the temperature data recorded during a period of relatively low power production with one during higher power production. The times selected were the same intervals in September 2003 analyzed for the intertidal stations (Section 2.3.3). The temperature data analyzed were those records taken by the surface temperature units at the eight stations that lie within 2 km of the point of discharge. During the two-day period when plant load was reduced, there was little difference between the eight stations (**Figure 2.3-11**). The maximum temperature difference between the station nearest to the discharge (SE7) and the station located 2 km from the discharge (SF4) were only about 1–2°C (1.8–3.6°F) throughout this period. On the day preceding this period (September 26th) when peak plant load reached 263 MWe (36 percent GC), the temperature difference between stations SE7 and SF4 was as great as 7°C (12.6°F).

The second period, September 2–6 (**Figure 2.3-12**), included the only time during the July–September monitoring period that the plant operated at 100 percent GC. This

occurred for two hours on September 5th. Average plant load was 350 MWe (48 percent GC) on that day. While operating at full plant load, the temperature difference between Stations SE7 and SF4 was as great as 9°C (16.2°F). It can also be seen that during the nighttime periods there was very little water temperature difference between these stations due to limited power plant output and no solar heating.

A set of animations was constructed that show a map of changing surface and bottom temperatures at all of the subtidal stations together with the variations in SBPP generating load and tide level (**Appendix C1** [CD format]). The animations include 7-day periods from July 15, 2003 through September 30, 2003. Four sample frames from the temperature animation files are shown in **Figures 2.3-13**. These frames are also from September 5, 2003, the day when SBPP load was at maximum for a short period of time. The first two frames (**Figure 2.3-13a, b**) are of the surface and bottom temperatures at 1510 PST; plant load was at its peak and the tide was flooding, approaching the maximum of a spring tide. Surface and bottom temperatures at the stations closest to the discharge reached a maximum of about 38°C (100.4°F), but due to the influence of the incoming tide, the elevated temperature of the discharge plume was restricted to the basin enclosed by the jetties. This is also the time of day when solar heating is at its greatest, as shown by the elevated temperatures at some of the stations within the intake channel (separated from the discharge plume by a mass of cooler water).

Comparison of the surface and bottom frames illustrates the thinning of the discharge plume as it moves away from the power plant. Near the point of discharge, the plume extends from the surface to the bottom; at more distant stations the warmer, less dense water occurs only at the surface. The second pair of frames (**Figure 2.3-13c, d**) depicts conditions at 2310 PST on the same day; plant load is at the minimum for that day (70 Mwe, 10 percent GC) and the tide is ebbing, approaching the low for that day. Under these conditions, the temperatures closest to the discharge are shown to have dropped below 30°C (86.0°F). The ebbing tide produces currents that flush the discharge plume from the area enclosed by the jetties. As a result, the surface temperature at Station SF4, located at the tip of the jetty about 2,000 m from the discharge, is now more than 3°C (5.4°F) warmer than the station (SE7) in closest proximity to the discharge. This example depicts a water mass that was heated hours previously by a combination of plant discharges and afternoon solar heating on the shallow receiving waters. The time lag is the result of the currents induced by the flooding and ebbing tides. Under these conditions the plume now extends to the northwestern corner of the Chula Vista Wildlife Island near the outer portions of the SBPP intake channel.

Other examples of the interactions of tide and power plant generation, and their effects on the distribution of the discharge plume, can be seen by viewing different portions of the animations (**Appendix C1**). The time lag between peak power production and the subsequent peak in temperature at a monitoring station is a function of the station's distance from the discharge and the magnitude of the tide cycle. Flooding tides at the time

of peak generation tend to extend the time lag, as can be seen on September 5th (**Figures 2.3-12** and **Appendix C1**). Ebbing tides tend to reduce the lag, as can be seen on September 26th (**Figure 2.3-11** and **Appendix C1**).

2.3.4.2 Temperature Spectral Analysis

The tidally-dominated fluctuations observed on September 5th are representative of fluctuations throughout the monitoring period. A characterization of these fluctuations as a function of frequency is presented in **Figure 2.3-14**, which shows the energy spectra (i.e., strength of the fluctuations versus frequency) for the surface level recorders from six of the temperature monitoring stations (ST1, ST4, SF4, SF2, SR1, and SA3). This analysis reveals patterns in temperature change based on the magnitude and frequency of shifting temperatures. Similar spectra are also shown for tidal level fluctuations and variations in the SBPP thermal loading.

The spectra are associated with specific processes taking place at the dominant semidiurnal tidal frequency (once every 12 hr) and also at the diurnal frequency (once every 24 hr). The diurnal frequency results from a combination of diurnal tidal fluctuations and diurnal solar heating. The smaller peaks in the spectra at periods around 8 hr, 6 hr, and <4 hr represent harmonics of the major diurnal and semidiurnal periods. Such harmonics are commonly observed in coastal settings in or near estuaries.

The SBPP thermal discharge also cycles the amount of heat output on daily time scales due to the daily cycle in demand for electric power. SBPP thermal loading fluctuations contain strong signatures at the diurnal frequency and, to lesser extent, at the semidiurnal frequency. The SBPP-driven signals were detected by comparing the intensity of the diurnal cycle peak for the stations within the discharge basin (ST1, ST4, and SF4) with those located further from the point of discharge, particularly the reference Station SR1 and the far-field Station SA3. Both of these stations have similar diurnal and semidiurnal cycle peaks. In contrast, Stations ST1, ST4 and SF4, in closer proximity to the discharge, each have diurnal peaks of much greater intensity than those for the semidiurnal period. This is indicative of the influence of the SBPP's thermal loading cycle and its interaction with the tides.

Figure 2.3-15 portrays an example of the development of the thermal plume at SBPP on August 16, 2003. Temperature is shown for the station distances from the discharge, (**Table 2.3-2**), and at the depths of those locations (**Table 2.3-1**). On that date, plant output was raised to 450 MW (62 percent GC) at 0900 PST, increased to 550 MW (76 percent GC) by 1500 PST, and reduced to 250 MW (35 percent GC) and 150 MW (21 percent GC) at 2100 PST and 2400 PST, respectively. A 1.58 m (5.2 ft) high-high tide occurred at 1207 PST just before maximum power generation, a 0.58 m (1.9 ft) high-low tide occurred at 1811 PST and a 1.43 m (4.7 ft) low-high tide occurred at 2351 PST. Cooling water flow was approximately 25 mgh (maximum output) throughout this period. By 1200 PST temperatures in the intertidal and subtidal nearfield (stations closer than Station ST4) were

above 35°C (95°F), and by 1800 PST subtidal bottom temperatures were also above 35°C. An animated portrayal of temperature at depth versus distance is presented for the period July 16–September 30, 2003 in **Appendix C1** (CD format).

2.3.4.3 Relative Temperatures (Delta T°)

The maximum instantaneous delta T° calculated for the three monitoring depths, at any station, occurred at Station SE7, the closest station to the discharge, on September 5, 2003. Maximum delta T°s of 11.0, 11.1, and 10.7°C (19.8, 20.0, and 19.3°F) were calculated for the surface, -1 meter, and bottom temperatures, respectively. As previously mentioned, the only episode of full power (723 MWe) operation that occurred during the monitoring period from July 15, 2003 through September 30, 2003, occurred on September 5, 2003. The surface temperature recorders at each of the six stations in closest proximity (less than 1,150 m) to the discharge all registered their maximum delta T°, ranging from 11.0–9.2°C (19.8–16.6°F), on this date. Stations further from the discharge had maximum values on various other dates during the monitoring period. For almost all stations, at all levels, the highest monthly mean delta T°s occurred in August. The July, August, and September 2003 mean delta T° for each level at each subtidal station are presented in **Figure 2.3-16**. The stations are arranged in ascending order of their distance from the discharge (see **Table 2.3-2** for distances). Mean delta T° decreased as a function of increasing distance from the power plant discharge. The values calculated for Stations SF2, SR4, and SR5 reflected the intrusion of cooler water from the more northerly portions of bay. The coolest water temperatures were recorded at Stations SA3 and SN2, due mainly to their more northerly position in San Diego Bay and closer proximity to cooler ocean water.

Temperatures exceeded a 2.2° (4°F) delta T° approximately 80 percent of the time at the inner discharge stations but declined rapidly past Station ST3 (a distance of 572 m [1,877 ft] from the point of discharge) (**Figure 2.3-17**). Intertidal stations were consistently warmer than their adjacent subtidal stations in the discharge channel. The 2.2° (4°F) delta T° dissipated as it moved beyond the western edge of CVWI, contacting the bottom less than 10 percent of the time at Station SE3.

A discussion of the empirical delta T° data and a model that was developed to assess and predict the extent of the thermal plume are presented in the following section. A complete presentation of the delta T° data can be found in **Appendix C2** [CD format].

2.3.5 Thermal Gradients: Delta T° Modeling and Estimation

Thermal gradients were modeled in order to describe the three-dimensional aspects of the SBPP thermal plume. Analysis of the thermal gradient during July–September 2003 showed that the temperature rarely exceeded, and never averaged above, 8.3ºC (15ºF) for any 24-hr period. This is the regulatory compliance maximum for SBPP combined

discharges at a distance of 305 m (1000 ft) (NPDES Monitoring Station S1) from the west end of the SBPP discharge basin. During 3 percent of the time the 8.3ºC delta T° excursion distance extended to 181 m (594 ft) [Station ST1] from the discharge boom on the surface and 1 percent of the time on the bottom. Rarely did the 8.3ºC delta T° excursions exceed 396 m (1,299 ft) [Station ST2] from the discharge basin at the subtidal or intertidal stations and then only for brief periods.

Thermal maxima measured during the study never exceeded an 11.1ºC (20ºF) delta T° above the mean temperature at the reference stations (see **Section 2.3.4**). There was only one temperature measurement of 11.1°C (20.0°), which was recorded on September 5, 2003, at 1620 PST. All other recordings were below this temperature.

Excursions of 2.2°C (4°F) delta T° were measured empirically from station temperatures and also estimated using a model. These modeled excursions were estimated by linear regressions of the delta T° 2.2°C versus station distances from the discharge boom. The distances, shown in **Table 2.3-2**, were measured in a straight line from the discharge boom to Station ST4, then from ST4 to SF4, SF4 to SF3, and SF3 northward (refer to **Figure 2.3-1**). Each subtidal station had three temperature sensors: surface, 1-m subsurface, and bottom (**Figure 2.3-2**). Temperature data from Station SF2 were substantially lower throughout the study than any other subtidal stations at similar distances and were therefore not included in the delta T° excursion model. Each intertidal station had a recorder at approximately the 0.3 m (1.0 ft) above MLLW level. For intertidal temperatures, only "in water" data were used in the modeling (see Section 2.3.3–*Intertidal Temperature Results*).

Examples of the intercept fit for the surface, 1-m subsurface, bottom, and intertidal temperatures for two periods when SBPP discharge temperature was high, on the afternoons of July 16, 2003 and September 5, 2003, are shown in **Figure 2.3-18**. Examples from these two days demonstrate empirical thermal conditions and excursion distances of the 2.2º C (4°F) field at the four monitored depth strata. It can be seen that the maximum distance for the 2.2°C (4°F) delta T° excursion on July 16 was between 1,400 m and 1,975 m (4,600 ft and 6,480 ft) from the discharge boom. The maximum distance was 1,554 m and 1,879 m (5,098 ft and 6,165 ft) on September 5.

Empirical excursion distances were recorded as the farthest station distance where relative temperature exceeded 2.2°C (4°F). A comparison of frequencies of empirical and modeled excursions showed a relatively good correspondence at intertidal and surface subtidal stations (**Figure 2.3-19**). The 1-m subsurface and bottom subtidal stations had greater variation between the empirical and modeled excursion distances.

The model was then used to separate this area into 100-m segments to help in understanding the distance of the 2.2°C (4°F) excursions from the discharge boom location (**Figure 2.3-20**). The percent frequency of modeled excursion distances is similar for the surface and –1 m temperatures. The excursion distance at the bottom depth is generally

closer to the discharge than at the two shallower depths. In the intertidal zone, the frequency was higher at shorter distance from the discharge than was seen at the subtidal stations. This is possibly due to the removal of air temperature records from the intertidal data set. It can also be seen that during 12–22 percent of the time the 2.2°C (4°F) excursions do not extend greater than 100 m from the discharge boom.

Table 2.3-3 presents excursion distances from the discharge boom at different percentage frequencies of the 2.2°C (4°F) delta T° recordings for modeled data less than 2,800 m (9,186 ft) from the discharge boom. The linear regression model was used to estimate excursion distances based on the empirical data. A map of the percent frequency of the modeled temperature excursions for the four depth strata is presented in **Figure 2.3-21**. It can be seen that the surface and –1-m depth temperatures extend farther away from the discharge than the bottom temperatures due to the buoyancy of the warm water.

An example of the dynamics of the thermal plume delta T° as a function of power plant operation at relatively high power generation and cooling water flows is shown in **Figure 2.3-22a, b**. The 2.2°C (4°F) delta T° excursions are not evident at 0100 PST. By 0500 PST (plant power output of 105 megawatts), the 2.2°C delta T° thermal excursion is estimated at a distance of 844 m (2,769 ft). As power generation increased to 254 MWe (35 percent GC) at 0700 PST, the thermal plume reached 1,145 m (3,757 ft). At 0900 PST power generation was 496 MWe (69 percent GC) and the excursion distance was 1,587 m (5,207 ft). Temperatures at the discharge were warming above 35°C (95°F) by 1100 PST as the excursion distance expanded to 1,856 m (6,089 ft). Cooling water flow increased with increased power generation (637 MWe [88 percent GC]) at 1300 PST but the excursion distance was similar (1,797 m [5,896 ft]) as seen two hours earlier. With the plant at 723 MWe (100 percent GC) at 1500 PST and a discharge temperature of 38°C (100.4° F), the thermal excursion was 1,673 m (5,489 ft). The excursion distance was still similar (1,756 m [5,761 ft]) at 1700 PST with power generation at 482 MWe (66.7 percent GC) and the same cooling flow. Even though the plant continued to decrease power production but not discharge flow through 2100 PST, the 2.2°C delta T° excursion distance remained at about 1,600–1,800 m (5,250–5,900 ft) due mainly to the effect of the ebbing tide. By 2300 PST, the temperature near the discharge had decreased but the excursion distance had increased to 2,353 m (7,720 ft) due to the influence of the ebbing tide.

The surface and subsurface excursion distances showed a small but significant negative correlation at 12 hours, again following the cycle of plant operations during the daytime (**Figures 2.3-23** and **2.3-24)**. The bottom excursions had a positive autocorrelation at 12 hours that may reflect both tidal cooling at the reference stations and tidal advection of thermal water accentuating the relative differences in temperature. Discharge temperatures measured at Station SE7 autocorrelated negatively at 12 hours and positively at 24 hours due to plant operations. Reference mean temperatures (average of Stations SR1, SR2 and SR3) showed high positive correlations over all lags to 24 hours. Surface and subsurface were somewhat accentuated at 12 and 24 hours. Autocorrelation analysis of the delta T° at

the discharge Station SE7 showed positive correlation at 24 hours and a significant negative correlation at 12 hours in surface, subsurface, and bottom stations. The cross-correlations of delta T° and SBPP discharge temperature at Station SE7 over excursion distance showed positive correlation developing to a peak at four hours and a negative correlation at eight hours previous. The positive correlation shows the lag in development of the thermal excursion. The difference in lag times demonstrates the cycle of plant operations.

Table 2.3-3. Distances and percent of time that the modeled 2.2ºC (4ºF) delta-Tº isotherm was exceeded. A linear model was fit to 10 min interval temperature readings relative to Stations SR1, SR2 and SR3 at stations <2,800 m from the discharge boom during July–September 2003.

	Percent of Modeled Intervals						
Depth Strata	**95%**	**90%**	**75%**	**50%**	**25%**	**10%**	**5%**
				Distance m (ft)			
Surface	0	0	**611** (2,044)	**1,372** (4,501)	**1702** (5,585)	**1,986** (6,515)	**2,230** (7,317)
1-m Subsurface	0	0	**520** (1,705)	**1,249** (4,096)	**1,602** (5,255)	**1,852** (6,075)	**2,119** (6,951)
Bottom	0	0	**145** (477)	**842** (2,763)	**1,382** (4,533)	**1,834** (6,018)	**2,294** (7,526)
Intertidal	0	0	**712** (2,337)	**1,153** (3,784)	**1,475** (4,839)	**1,672** (5,484)	**1,929** (6,330)

2.3.6 Temperature Exposure: Frequency and Duration

The results of the frequency analysis are found in **Table 2.3-4**. The table provides the percentage of time each station spent above 26°C, 28°C, 30°C, 32°C, 34°C, 36°C, and 38°C (78.8°F, 82.4°F, 86.0°F, 89.6°F, 93.2°F, 96.8°F, and 100.4°F). The stations are listed in order of increasing distance from the SBPP discharge. As expected, the frequency of exposure to the warmer temperatures is greatest for those stations closest to the plant discharge. Subtidal Stations SE7, ST1, ST2, ST3, and ST4 each had temperatures above 28°C (82.4°F) more than 50 percent of the time and intertidal Stations IT1, IT2, and IT3 each had temperatures above 30°C (86.0°F) more than 50 percent of the time. The shallow depth of the intertidal stations relative to the subtidal stations contributes to the increased exposure to higher temperature. Eliminating data acquired during the lower tides (less than one foot above MLLW) affected the differences between the intertidal and subtidal temperature distributions since the lower tides occurred at night during that time of the year

and the subtidal temperatures recorded at these times were, on average, cooler than daytime temperatures. Elimination of the subtidal temperature data from these same periods would tend to skew the distribution towards the higher temperatures.

The results of the duration analysis for excursions to 27°C (80.6°F) or above are shown in **Table 2.3-5**. The table lists the number of excursions that occurred at each monitoring station with a duration of >10 min–6 hrs, >6–12 hrs, >12–24 hrs, >24–48 hrs, >48–72 hrs, >72–96 hrs, and >96 hrs. The table also displays the longest exposure that occurred at each station. The results of the duration analysis for excursions to 30°C (86.0°F) or above are shown in **Table 2.3-6**.

DRAFT

Table 2.3-4. Percentage of time spent above 26°C, 28°C, 30°C, 32°C, 34°C, 36°C, and 38°C at each of the subtidal (benthic level only) and intertidal temperature monitoring stations from the time of deployment (July 15–17, 2003) through the end of September 2003. Stations are listed in order of increasing distance from the discharge.

	Distance from discharge	Percentage of time spent above threshold temperature						
Station	**meters**	**>26ºC**	**>28ºC**	**>30ºC**	**>32ºC**	**>34ºC**	**>36ºC**	**>38ºC**
SUBTIDAL								
SE7	113	95%	68%	32%	17%	8%	1%	0%
ST1	229	94%	71%	32%	13%	5%	1%	0%
ST2	444	90%	64%	32%	15%	5%	0%	
ST3	620	94%	67%	28%	11%	4%	1%	0%
ST4	905	93%	57%	16%	2%	1%	0%	
SE5	1,198	92%	49%	11%	1%	0%		
ST5	1,493	92%	45%	13%	1%	0%		
SF4	2,007	91%	46%	10%	1%	0%		
SF3	2,233	86%	40%	8%	1%	0%		
SE4	2,587	85%	30%	3%	0%			
SE3	2,704	64%	21%	3%	0%			
SF2	2,992	31%	2%	0%				
SD4	3,039	69%	20%	2%	0%			
SR3	3,412	61%	9%	0%				
SC3	3,490	40%	9%	1%	0%			
SR2	3,695	66%	14%	0%				
SR5	3,831	No data	No data	No data	No data	No data	No data	No data
SR1	3,841	59%	6%	0%				
SR4	3,855	49%	5%	0%				
SA3	4,334	14%	0%					
SN2	5,439	3%	0%					
INTERTIDAL								
IT1	230	96%	82%	55%	34%	18%	5%	0%
IT2	410	96%	81%	54%	32%	15%	3%	0%
IT3	669	96%	83%	52%	26%	11%	2%	0%
IT4	881	95%	76%	37%	13%	3%	0%	
IT5	1,523	93%	56%	17%	4%	0%		
IR3	3,393	70%	19%	2%	0%			
IR2	3,618	73%	21%	1%	0%			
IR1	3,790	71%	21%	1%	0%			
IR5	4,047	49%	6%	0%				
IR4	4,086	45%	6%	0%				

DRAFT

Table 2.3-5. The number and duration of temperature excursions to 27°C or above, at each of the subtidal (benthic level only) and intertidal temperature monitoring stations from the time of deployment (July 15–17, 2003) through the end of September 2003.

	Distance from discharge	Number of temperature excursions to 27°C or above for the specified durations							Longest duration
Station	meters	>10 min to 6 hrs	>6 hrs to 12 hrs	>12 hrs to 24 hrs	>24 hrs to 48 hrs	>48 hrs to 72 hrs	>72 hrs to 96 hrs	>96 hrs	hours
SUBTIDAL									
SE7	113	14	2	15	4	2	1	2	471.2
ST1	229	14	1	8	4	1	2	2	956.6
ST2	444	12	2	8	3	0	0	2	433.3
ST3	620	7	4	12	3	2	2	1	959.2
ST4	905	38	7	16	1	2	0	3	523.0
SE5	1,198	31	5	11	3	1	1	4	379.2
ST5	1,493	31	5	17	2	1	2	3	378.3
SF4	2,007	64	24	16	2	1	0	3	408.3
SF3	2,233	83	38	7	1	2	0	2	268.5
SE4	2,587	56	26	13	0	2	0	1	390.7
SE3	2,704	81	27	7	1	1	1	0	81.(
SF2	2,992	23	7	5	0	0	0	0	23.(
SD4	3,039	78	25	1	2	0	0	1	252.8
SR3	3,412	88	14	2	1	0	0	1	199.0
SC3	3,490	66	23	0	0	0	0	0	8.
SR2	3,695	81	11	4	1	1	0	1	254.3
SR5	3,831		No data	No data	No data	No data	No data	No data	No data
SR1	3,841	48	6	2	1	1	0	1	174.3
SR4	3,855	24	7	5	0	0	1	0	86.(
SA3	4,334	33	0	0	0	0	0	0	5.
SN2	5,439	1	0	0	0	0	0	0	0.
INTERTIDAL									
IT1	230	24	9	50	0	1	2	1	136.5
IT2	410	24	10	51	2	1	1	1	136.5
IT3	669	6	10	48	0	1	0	3	136.5
IT4	881	21	9	48	0	1	1	2	136.5
IT5	1,523	20	15	43	0	2	1	1	136.5
IR3	3,393	81	24	19	0	0	0	0	23.1
IR2	3,618	47	20	18	0	0	0	1	136.3
IR1	3,790	100	22	19	1	0	0	0	39.(
IR5	4,047	38	11	6	1	0	0	0	36.1
IR4	4,086	30	13	11	0	0	0	0	21.2

DRAFT

Table 2.3-6. The number and duration of temperature excursions to 30°C or above, at each of the subtidal (benthic level only) and intertidal temperature monitoring stations from the time of deployment (July 15–17, 2003) through the end of September 2003.

	Distance from discharge	Number of temperature excursions to 30°C or above for the specified durations							Longest duration
Station	meters	>10 min to 6 hrs	>6 hrs to 12 hrs	>12 hrs to 24 hrs	>24 hrs to 48 hrs	>48 hrs to 72 hrs	>72 hrs to 96 hrs	>96 hrs	hours
SUBTIDAL									
SE7	113	57	18	11	0	1	1	0	90.3
ST1	229	59	16	13	0	0	1	1	111.0
ST2	444	25	15	7	0	0	0	1	101.8
ST3	620	58	15	10	0	0	1	0	94.3
ST4	905	58	5	3	0	0	1	0	82.5
SE5	1,198	49	3	3	0	0	1	0	88.3
ST5	1,493	31	4	4	0	0	1	0	92.0
SF4	2,007	51	6	1	1	0	0	0	38.7
SF3	2,233	67	6	0	0	0	0	0	9.2
SE4	2,587	28	1	0	0	0	0	0	6.8
SE3	2,704	32	0	0	0	0	0	0	5.3
SF2	2,992	0	0	0	0	0	0	0	0.0
SD4	3,039	17	0	0	0	0	0	0	3.3
SR3	3,412	0	0	0	0	0	0	0	0.0
SC3	3,490	10	0	0	0	0	0	0	3.3
SR2	3,695	1	0	0	0	0	0	0	1.2
SR5	3,831		No data	No data	No data	No data	No data	No data	No data
SR1	3,841	0	0	0	0	0	0	0	0.0
SR4	3,855	0	0	0	0	0	0	0	0.0
SA3	4,334	0	0	0	0	0	0	0	0.0
SN2	5,439	0	0	0	0	0	0	0	0.0
INTERTIDAL									
IT1	230	27	34	27	0	0	1	0	87.8
IT2	410	40	30	26	0	0	1	0	87.5
IT3	669	41	31	21	0	0	0	1	119.2
IT4	881	53	22	13	0	1	0	0	70.0
IT5	1,523	30	10	3	0	0	1	0	72.2
IR3	3,393	9	1	0	0	0	0	0	6.5
IR2	3,618	4	0	0	0	0	0	0	5.3
IR1	3,790	4	0	0	0	0	0	0	5.0
IR5	4,047	0	0	0	0	0	0	0	0.0
IR4	4,086	0	0	0	0	0	0	0	0.0

DRAFT

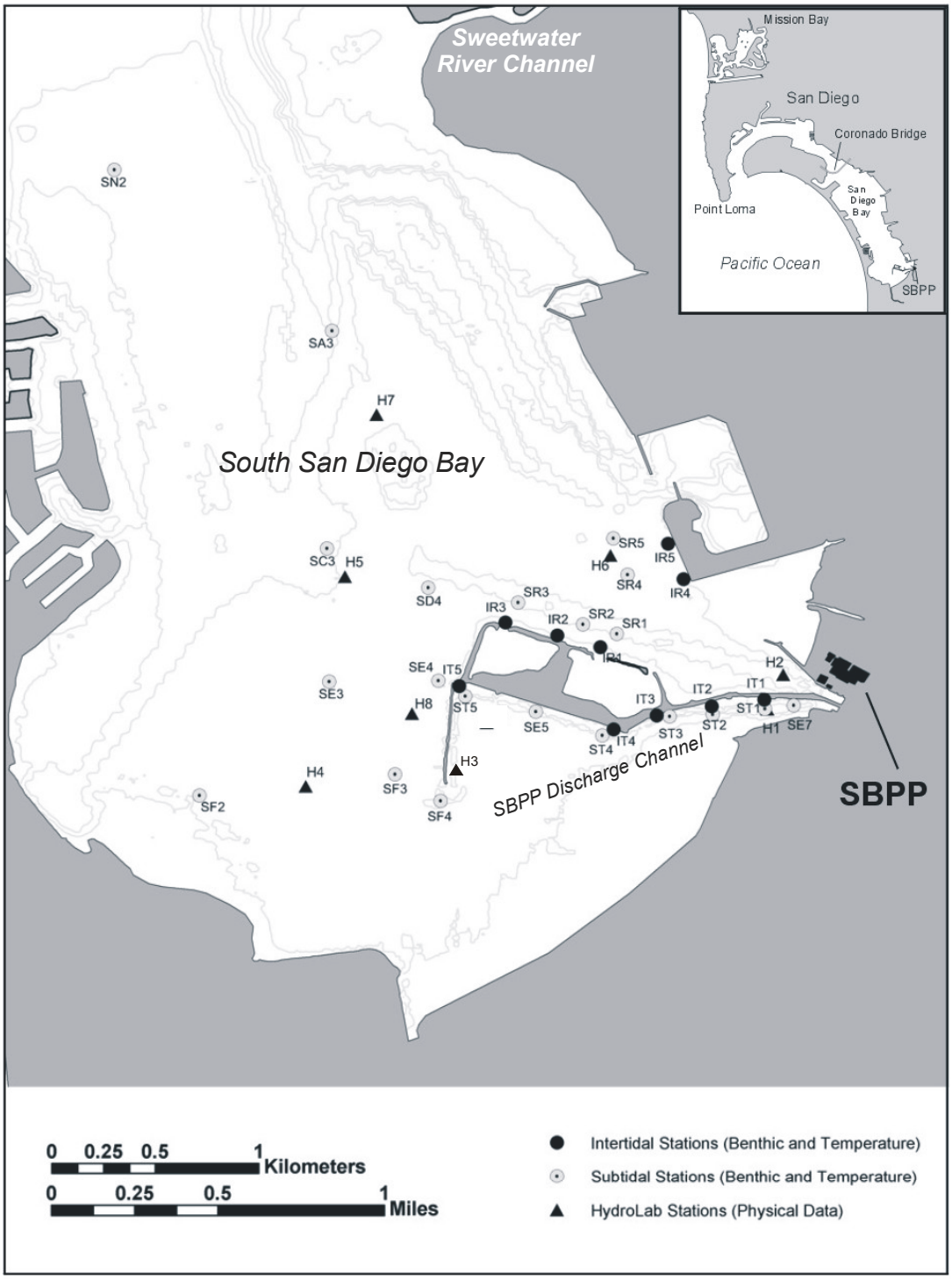

Figure 2.3-1a. Station location map of *in situ* temperature recorders, sediment grain size samples, and benthic biological samples: all stations shown.

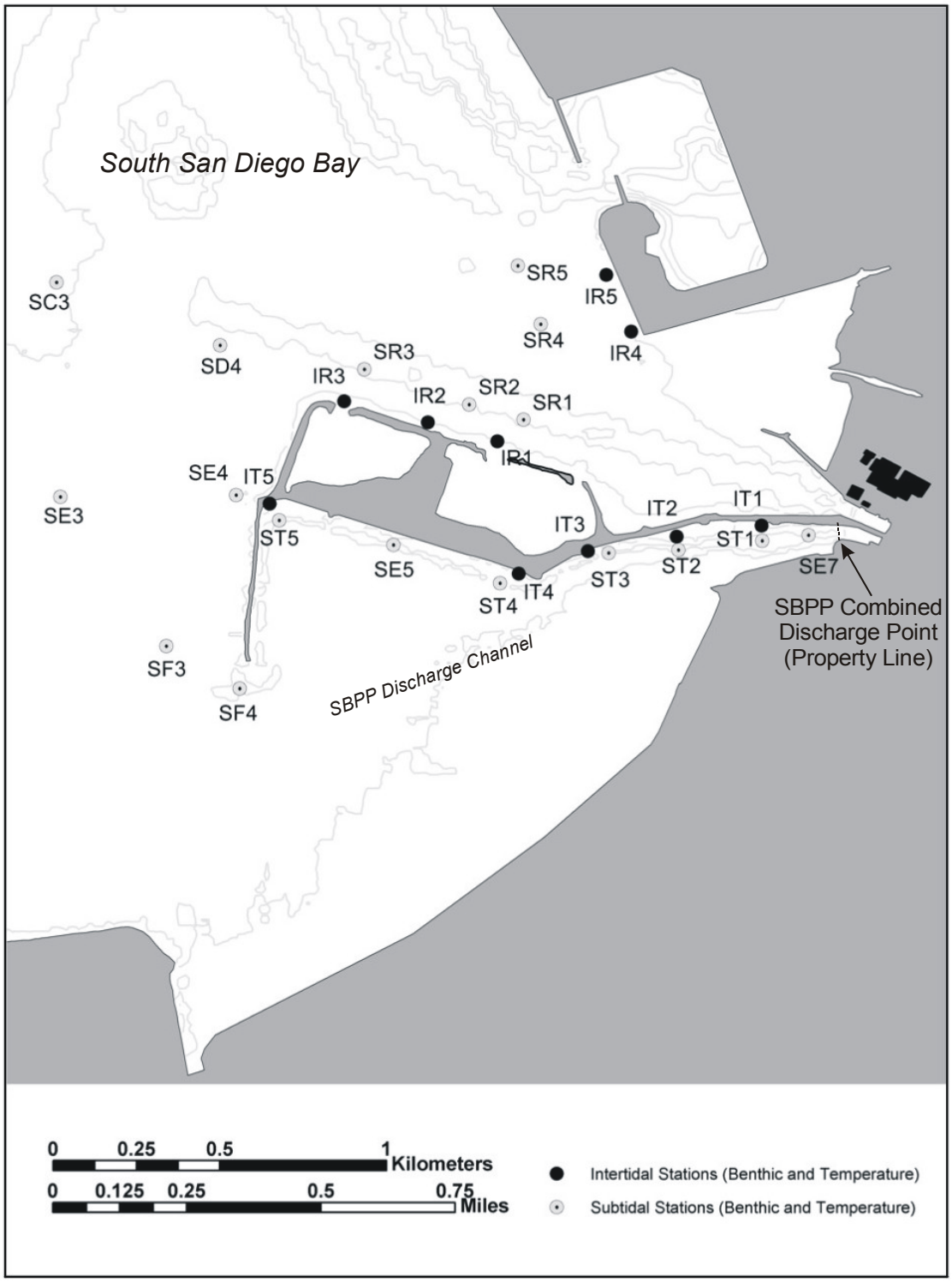

Figure 2.3-1b. Station location map of *in situ* temperature recorders, sediment grain size samples, and benthic biological samples: detail of intake channel and near-field stations.

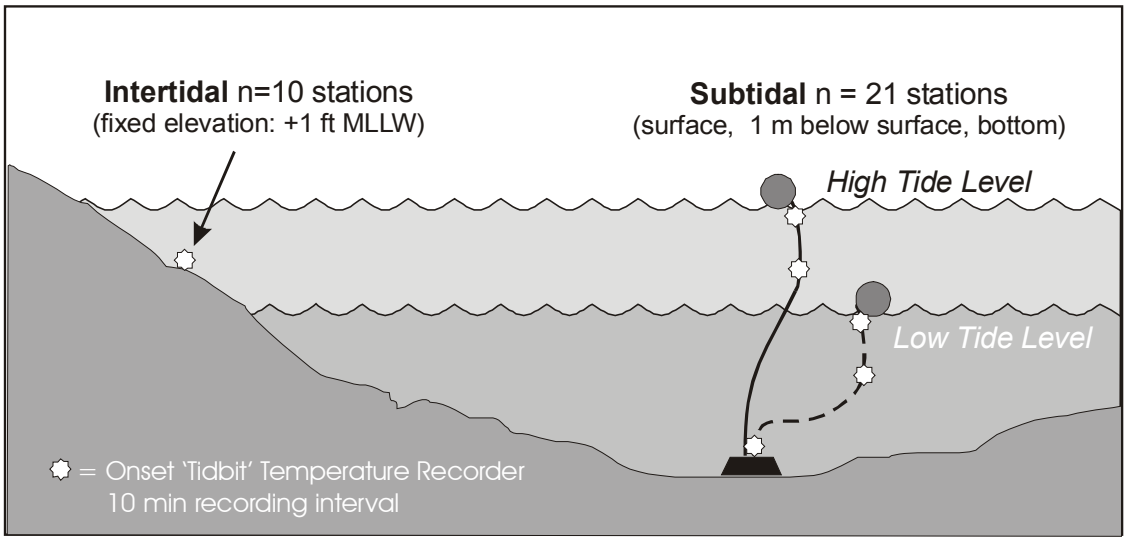

Figure 2.3-2. Diagram of intertidal and subtidal temperature arrays in relation to tidal elevation and channel morphology.

DRAFT

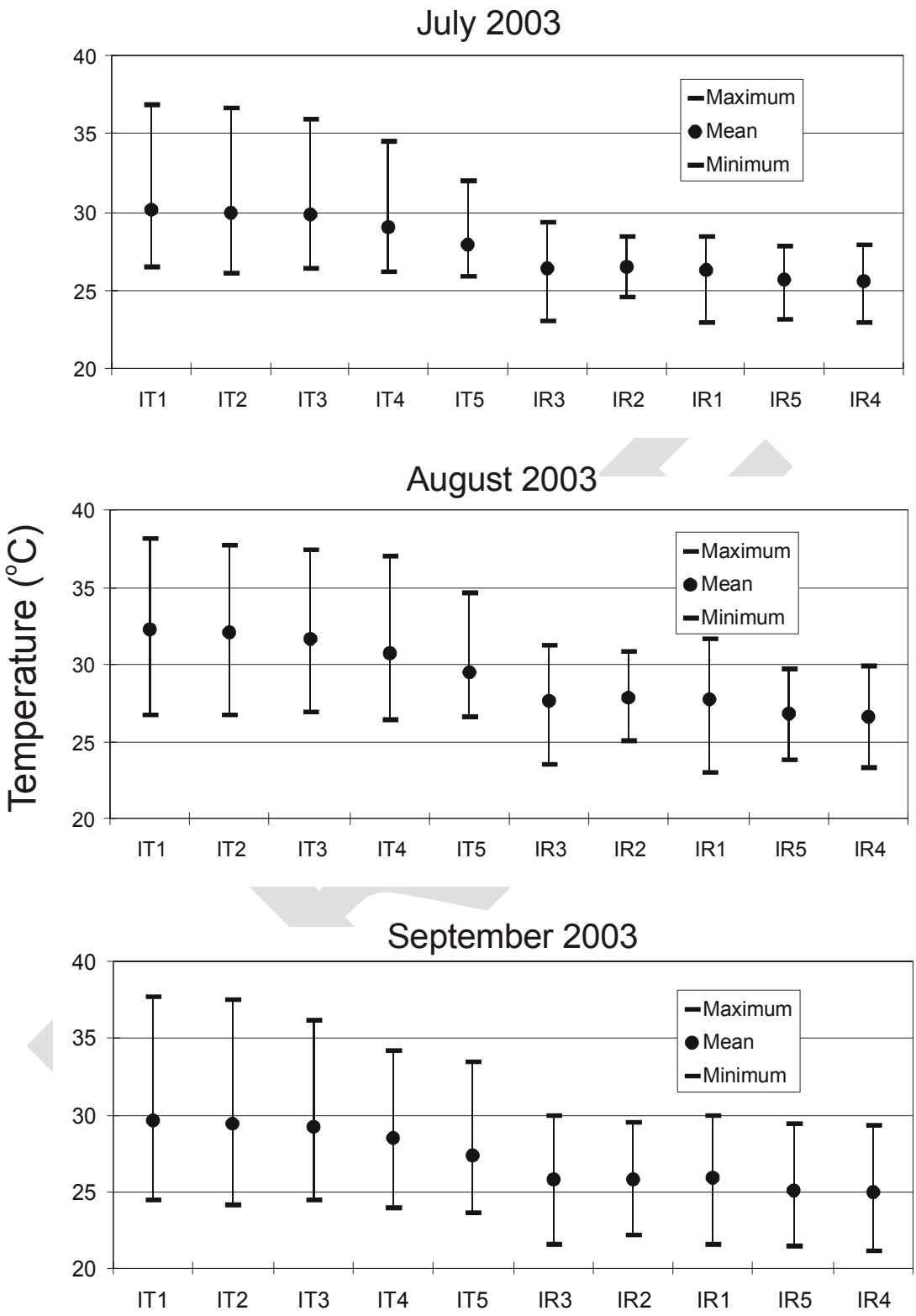

Figure 2.3-3. Intertidal station temperatures (minimum, mean and maximum) in July, August, and September 2003. Stations are arranged in increasing distance from the discharge.

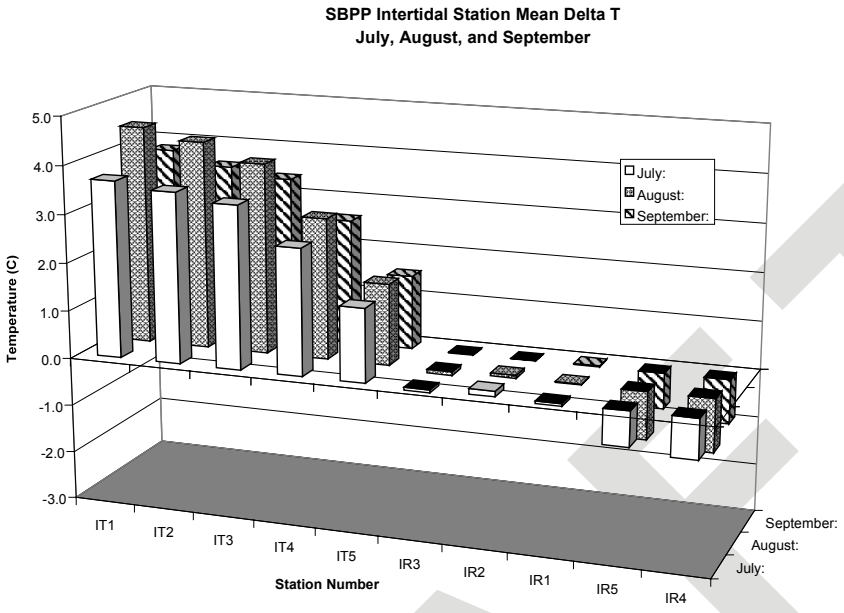

Figure 2.3-4. Intertidal station mean delta T° in July, August, and September 2003. The average temperatures of Stations IR1, IR2 and IR3 in the intake channel defined the reference temperatures.

DRAFT

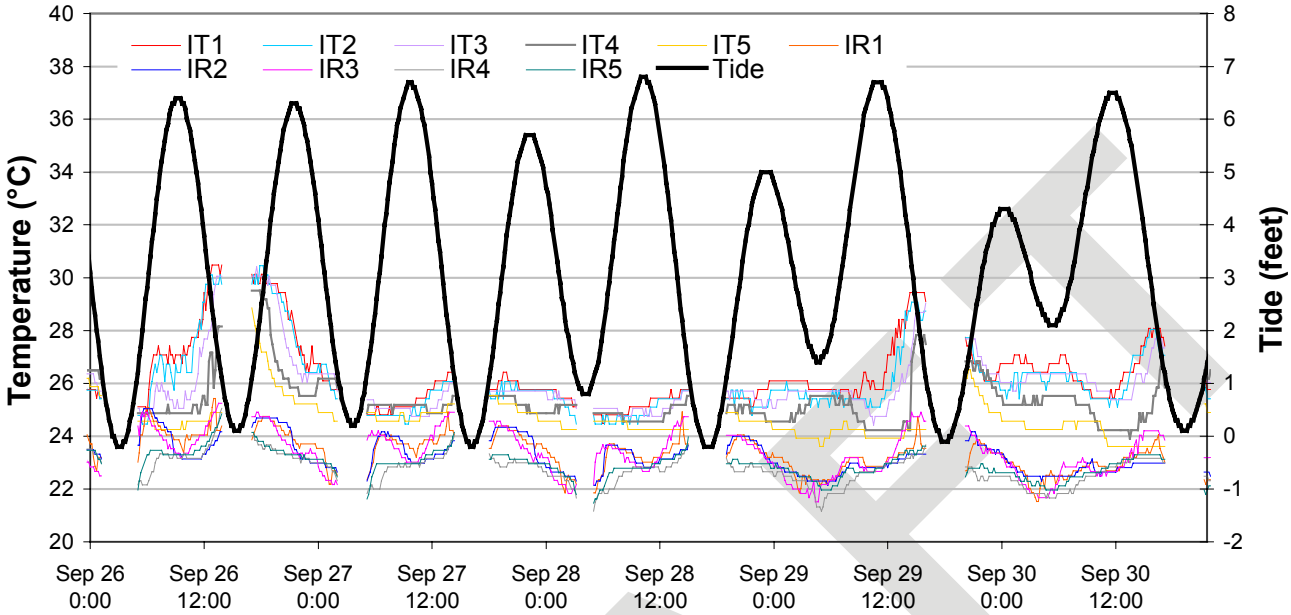

Figure 2.3-5. Intertidal station water temperatures and tidal curve from September 26–30, 2003. Temperatures removed at tides below +1 ft MLLW when recorder was exposed to air.

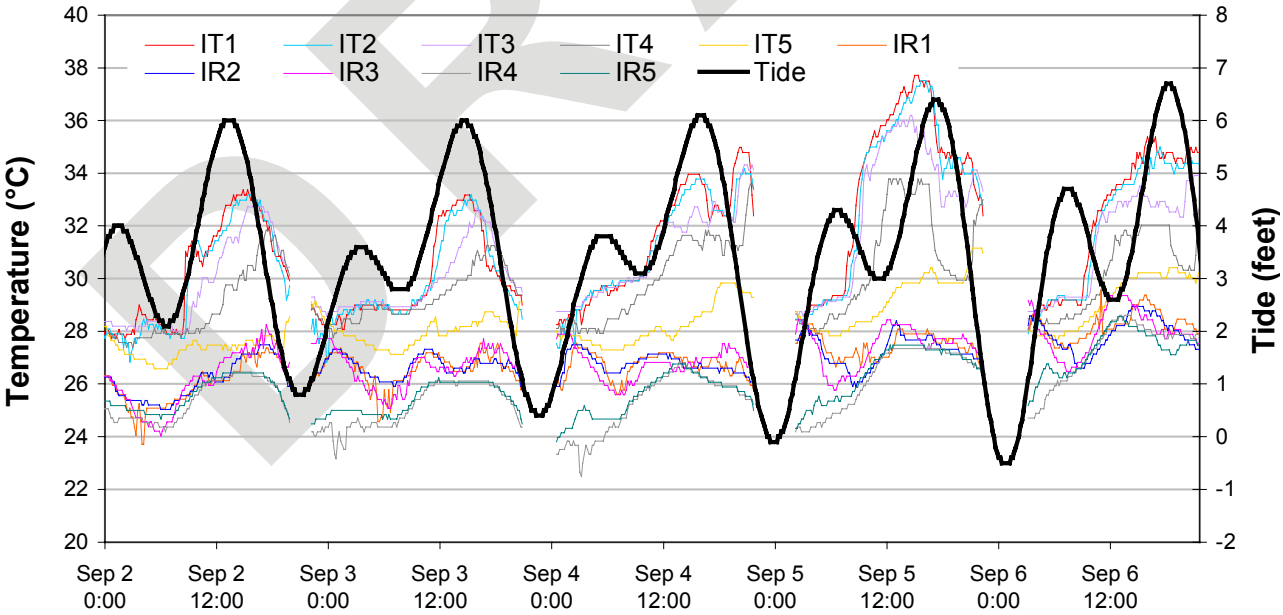

Figure 2.3-6. Intertidal station water temperatures and tidal curve from September 2–6, 2003. Temperatures removed at tides below +1 ft MLLW when recorder was exposed to air.

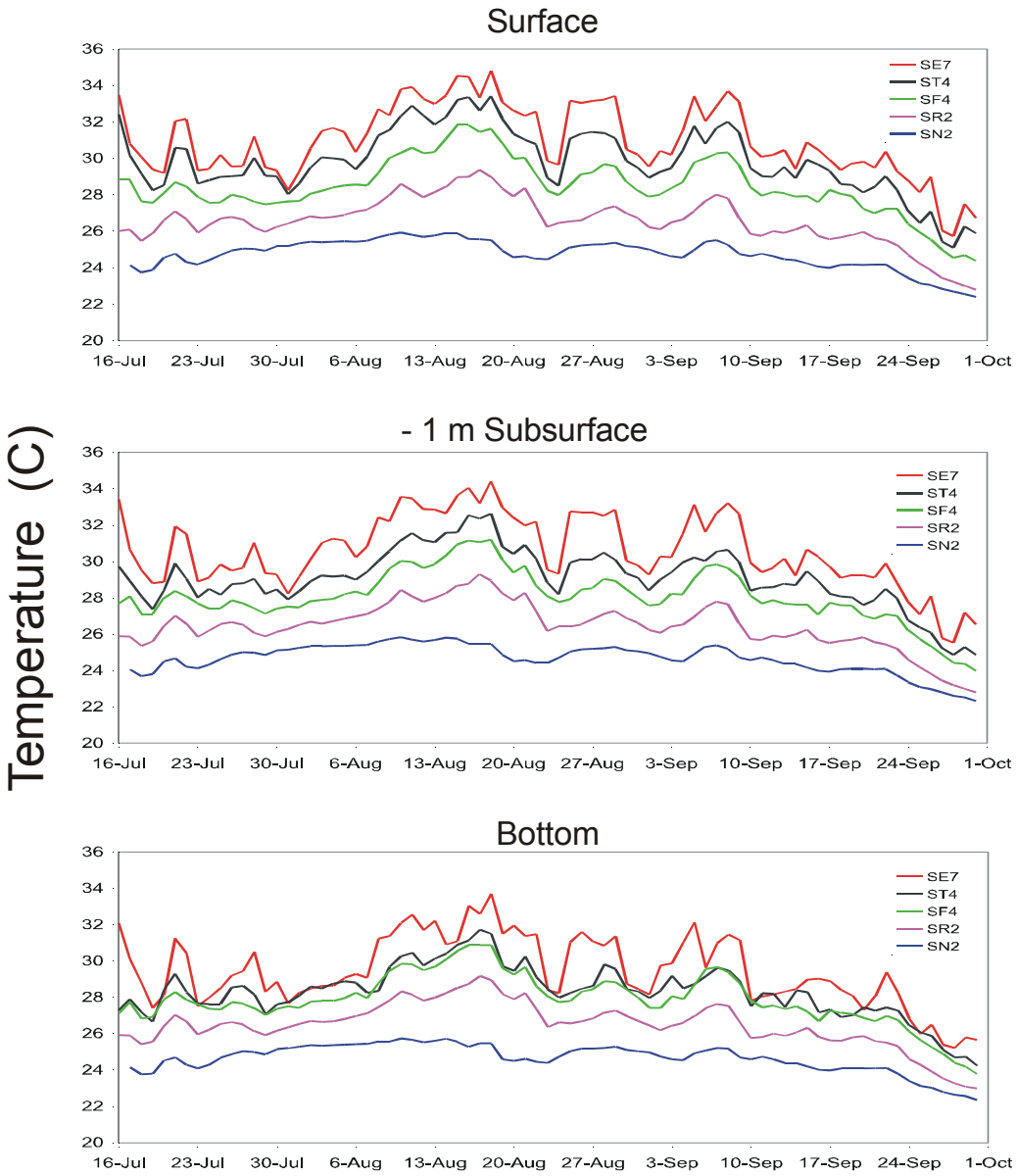

Figure 2.3-7. Surface, -1 m subsurface, and bottom mean temperatures recorded at five stations from mid-July through September 30, 2003.

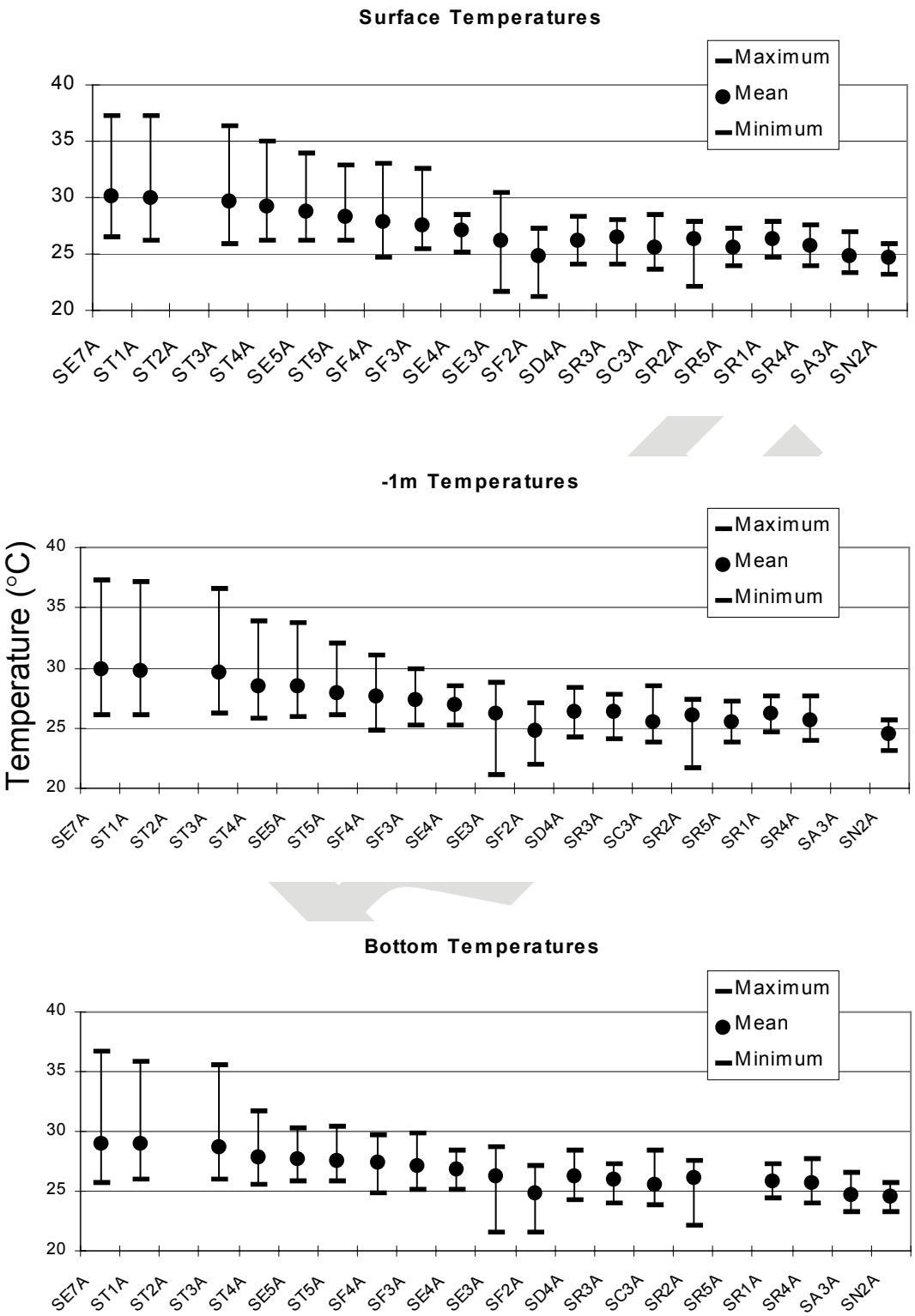

Figure 2.3-8. Maximum, mean, and minimum temperatures at the surface, 1 m subsurface, and bottom levels at the subtidal stations in July 2003. Station numbers arranged in increasing distance from the discharge boom.

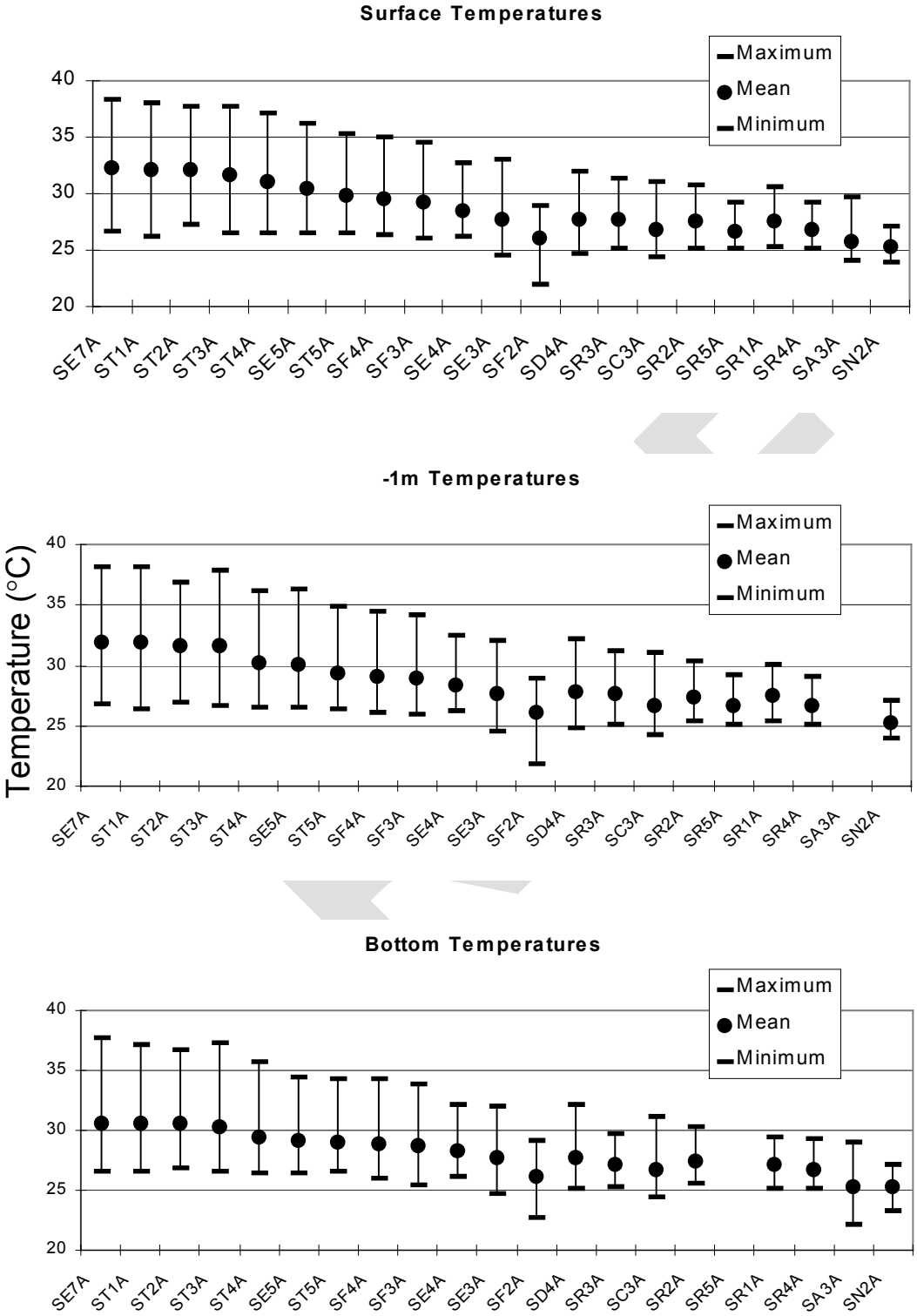

Figure 2.3-9. Maximum, mean, and minimum temperatures at the surface, 1 m subsurface, and bottom levels at the subtidal stations in August 2003. Station numbers arranged in increasing distance from the discharge boom.

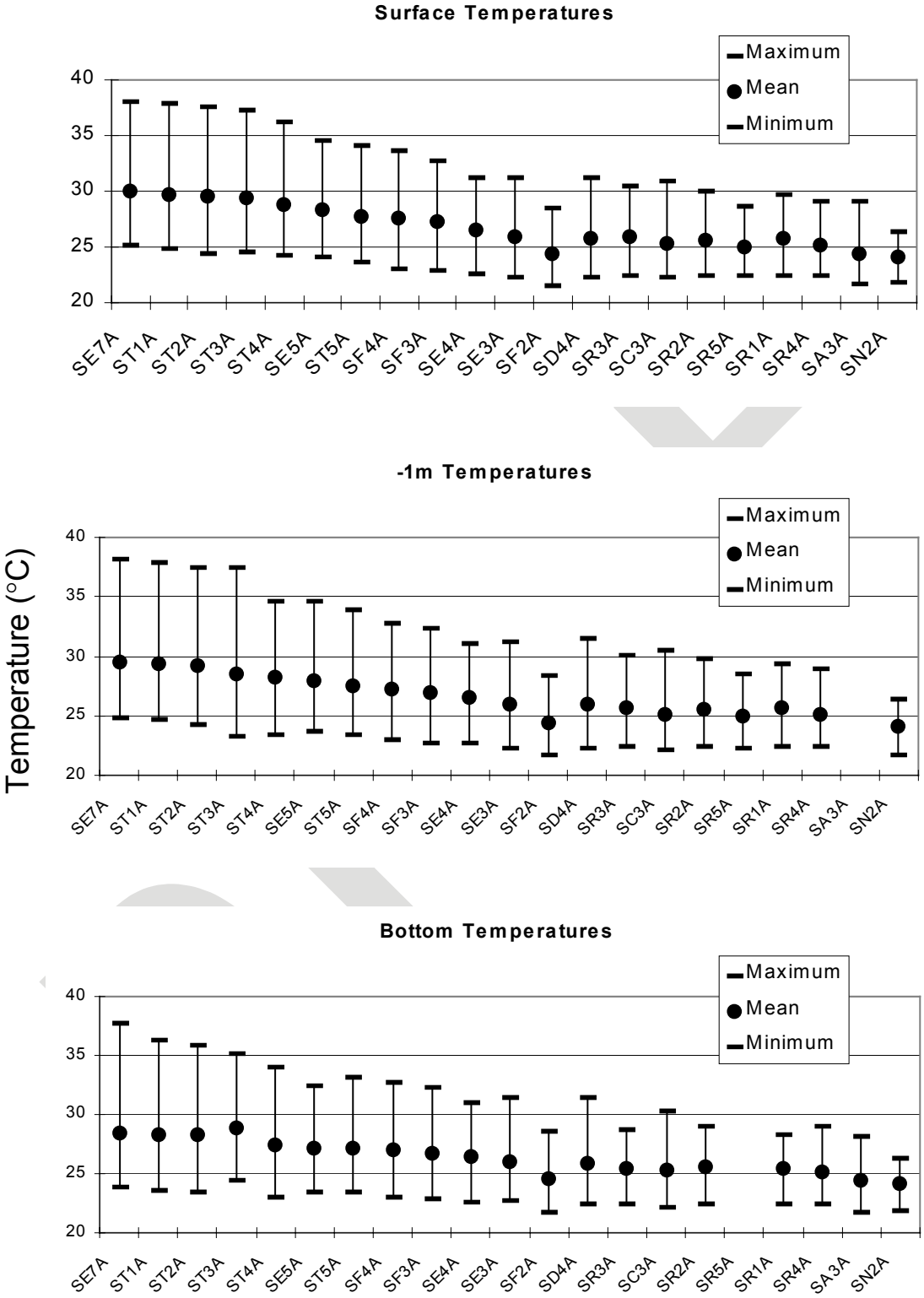

Figure 2.3-10. Maximum, mean, and minimum temperatures at the surface, 1-m subsurface, and bottom levels at the subtidal stations in September 2003. Station numbers arranged in increasing distance from the discharge boom.

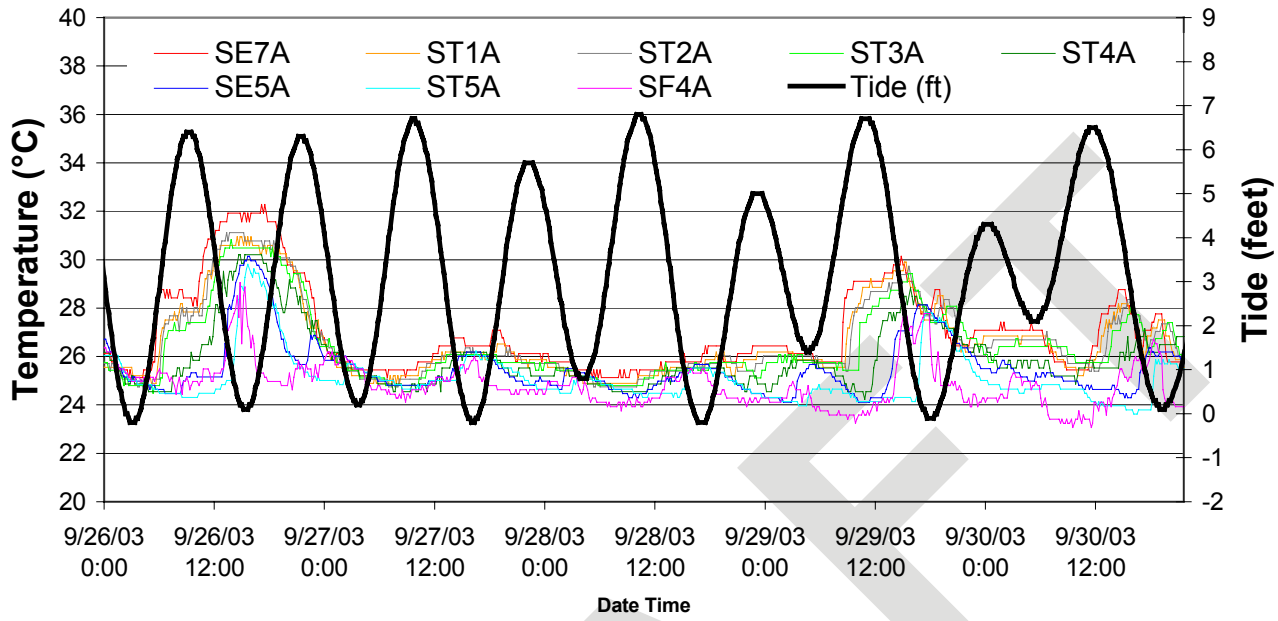

Figure 2.3-11. Surface station water temperatures recorded at the eight subtidal stations located within 2,000 meters of the SBPP discharge boom, September 26–30, 2003.

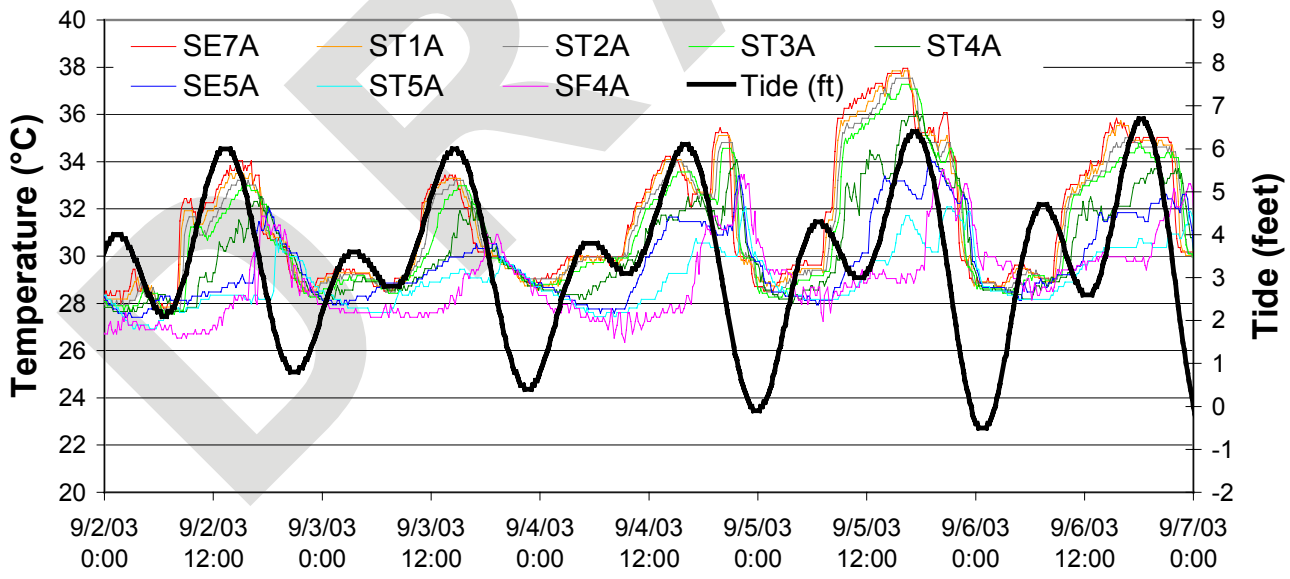

Figure 2.3-12. Surface station water temperatures recorded at the eight subtidal stations located within 2,000 meters of the SBPP discharge boom, September 2–6, 2003.

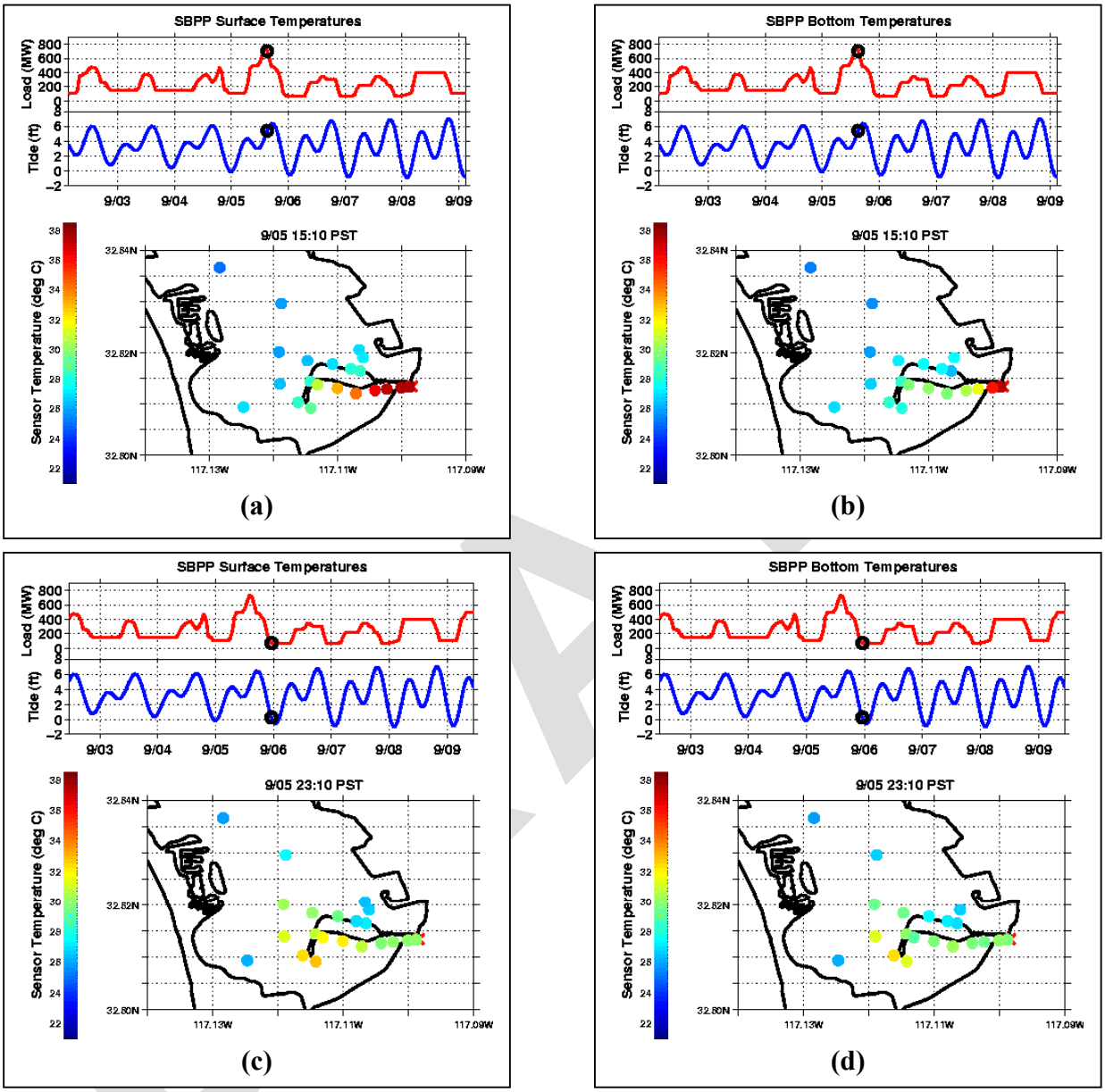

Figure 2.3-13. Frames copied from animations showing plant load, tide level, and surface or bottom temperatures at all 21 subtidal monitoring stations on September 5, 2003 at 1510 PST (a and b) and 2310 PST (c and d).

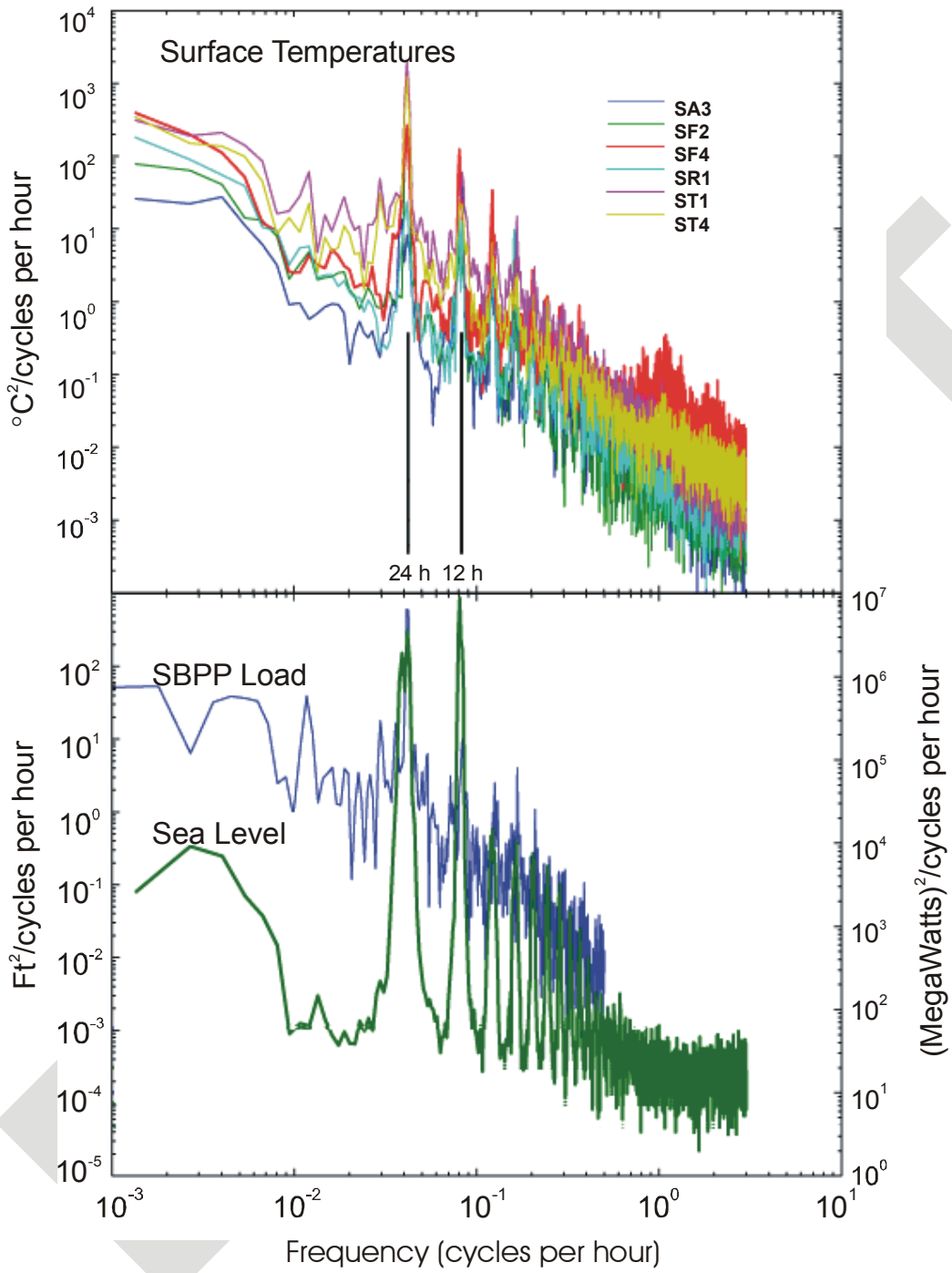

Figure 2.3-14. Power spectra for selected surface level temperature recorders (upper) and for SBPP load (MWe) and sea level (lower).

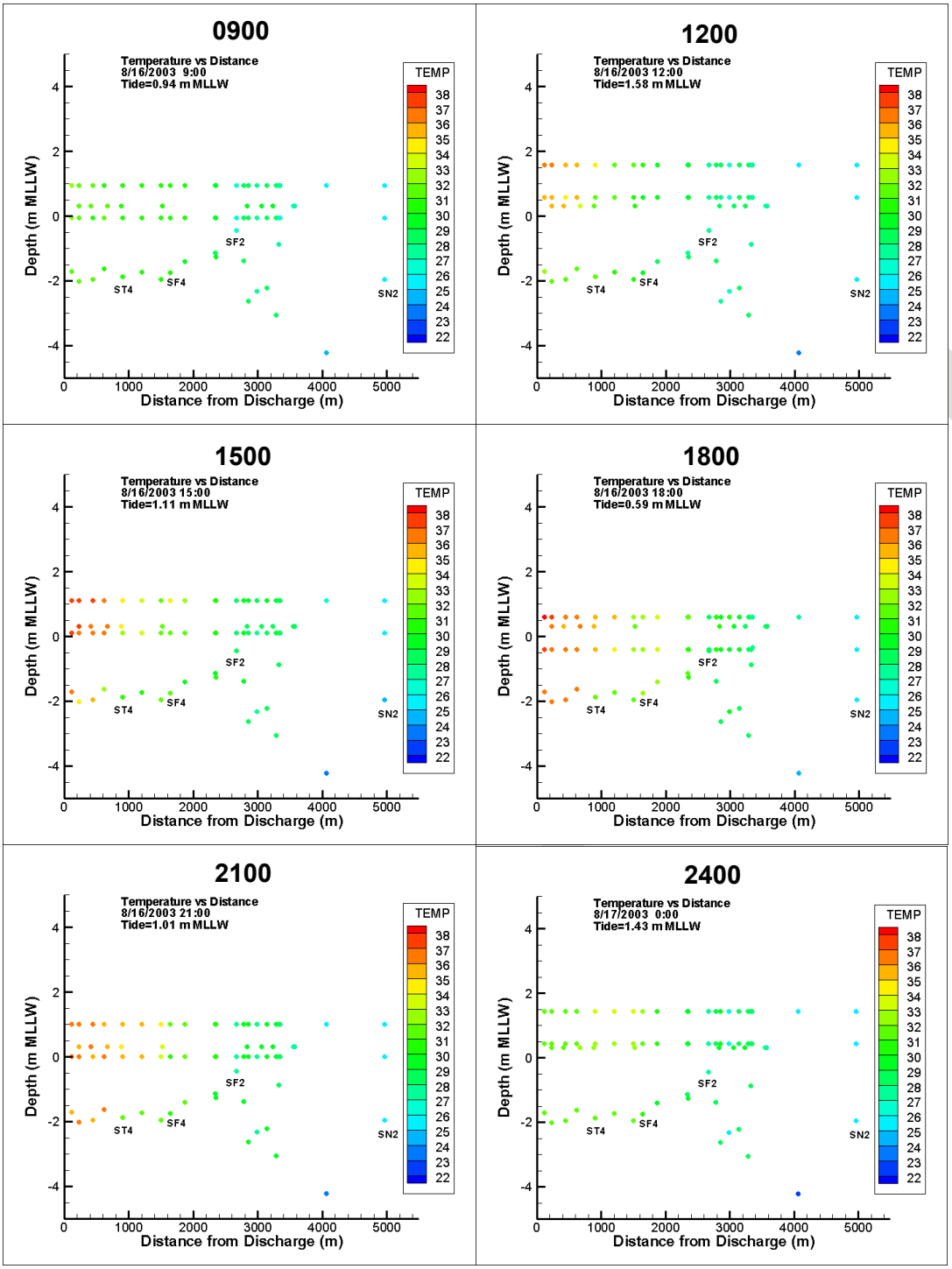

Figure 2.3-15. Example of the development of the thermal plume at SBPP on August 16, 2003 showing temperature at depth as a function of distance from the discharge boom. Plant output was raised to 450 MWe at 0900 PST, increased to 550 MWe by 1500 PST, and reduced to 250 MWe and 150 MWe at 2100 PST and 2400 PST, respectively. A 1.58 m high high tide occurred at 1207 PST, a 0.58 m high-low tide occurred at 1811 PST and a 1.43 low-high tide occurred at 2351 PST.

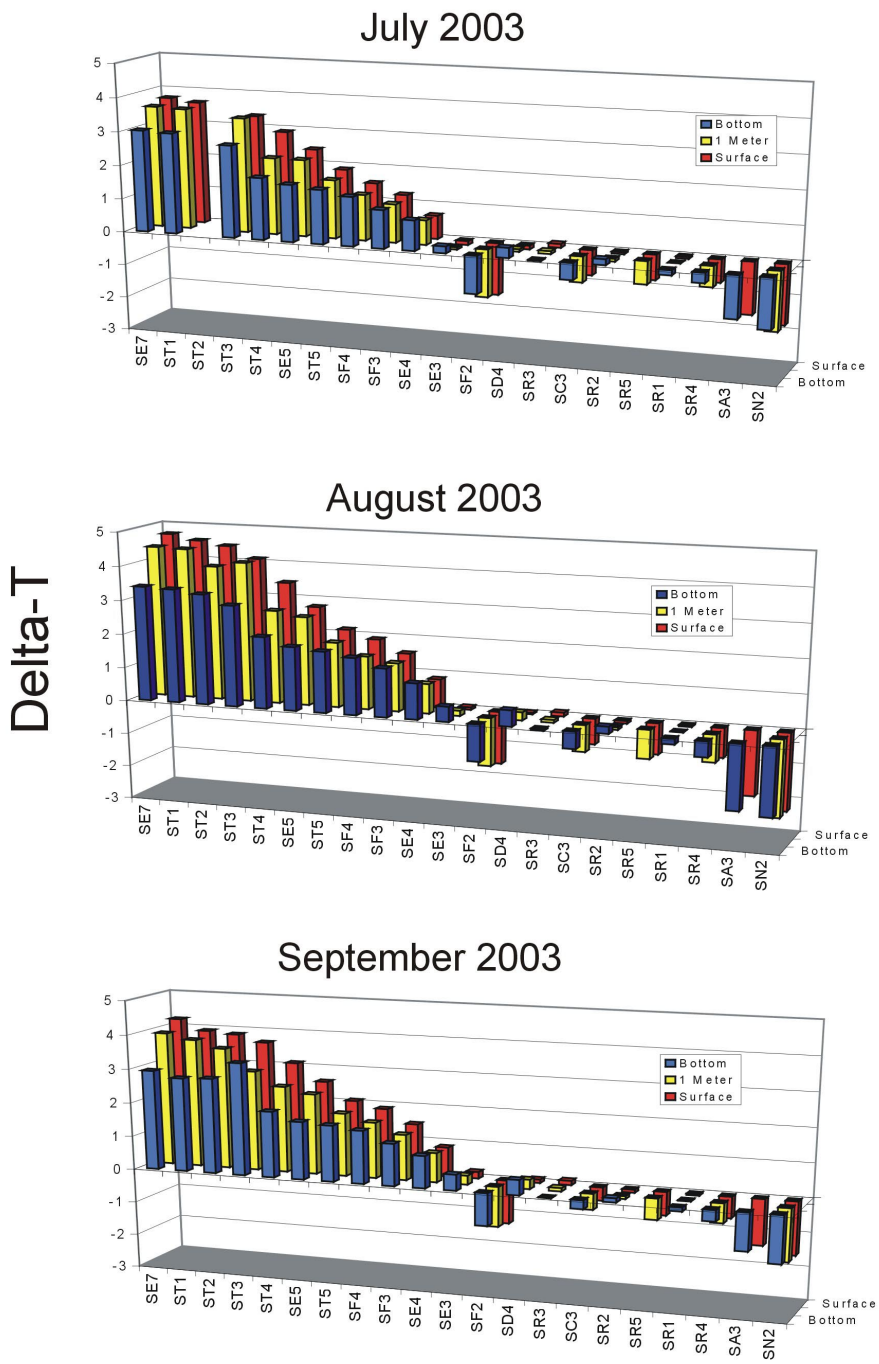

Figure 2.3-16. Subtidal station mean delta-T° in August 2003 at surface, 1-m subsurface, and bottom levels. The average temperatures of Stations SR1, SR2 and SIR3 in the intake channel defined the reference temperatures. Station numbers arranged in increasing distance from the discharge boom.

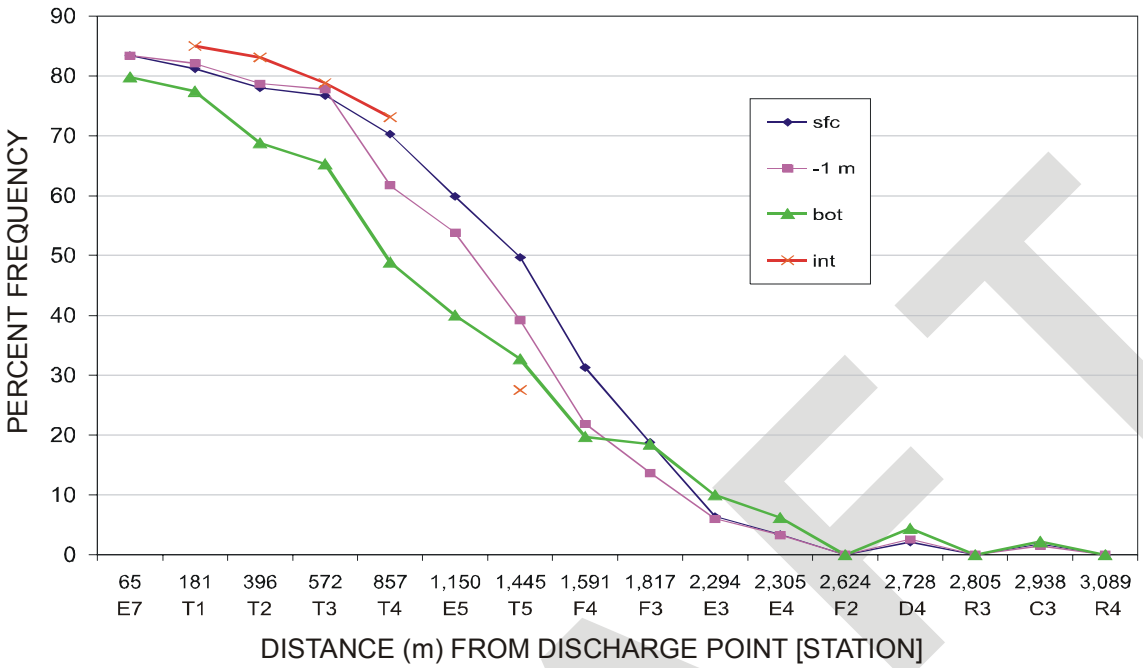

Figure 2.3-17. Percent frequency that the delta-T° exceeded 2.2°C (4°F) at various distances from the SBPP discharge boom. Empirical values are shown for surface, -1 m below surface, and bottom for each subtidal station to an excursion distance of 3,089 m (10,135 ft) [Station SR4] and for each intertidal station in the SBPP discharge channel. Refer to Figure 2.3-1b for station locations.

DRAFT

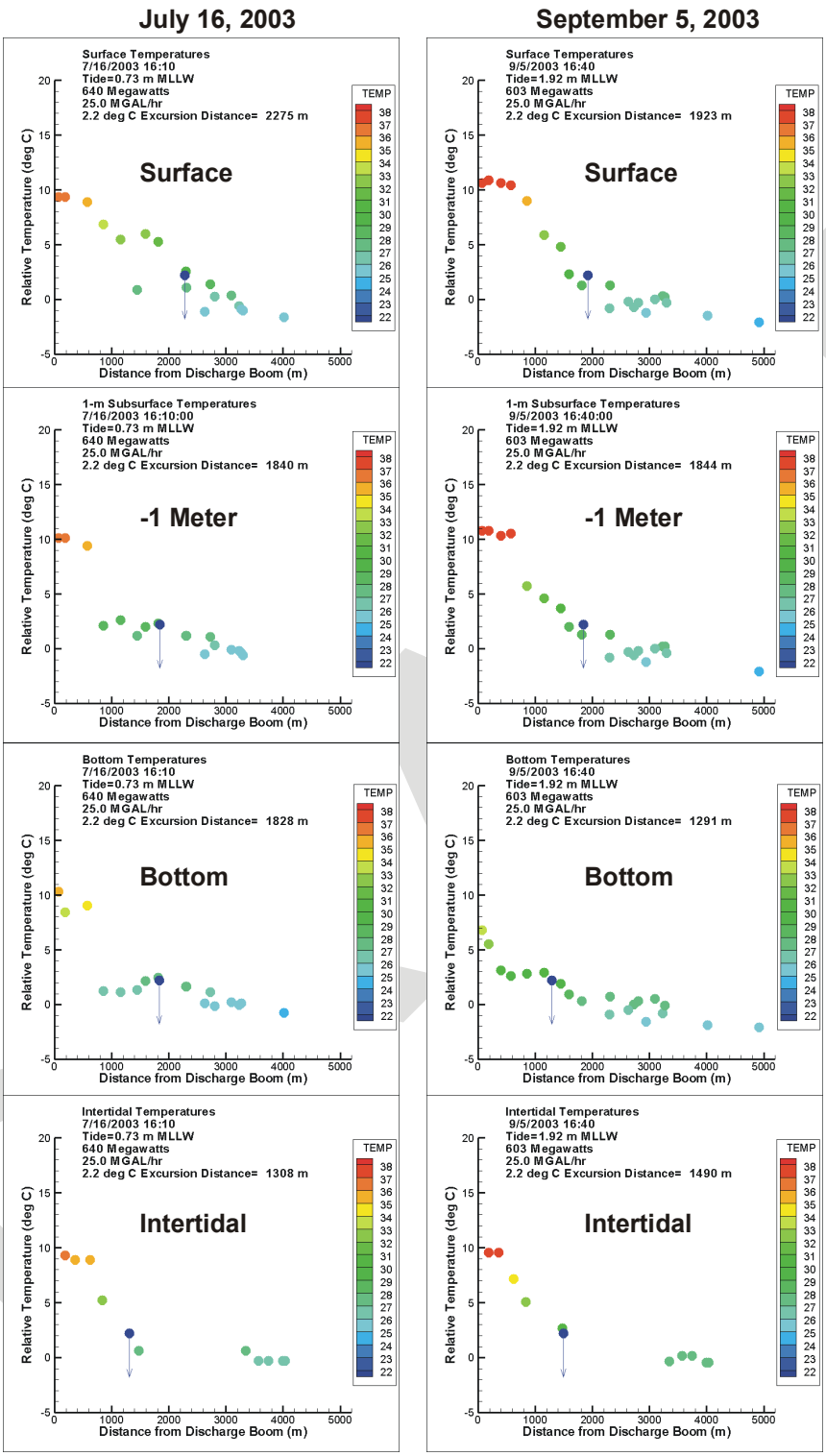

Figure 2.3-18. Example temperatures, 2.2°C (4°F) relative delta T° and excursion distances (ball and arrow) modeled by linear regressions of station temperatures <2.8 km from the discharge boom. Plots show surface, 1-m subsurface, bottom and intertidal strata (top to bottom) on two dates, July 16 and September 5, 2003 (left, right) when excursions were largest at high plant output.

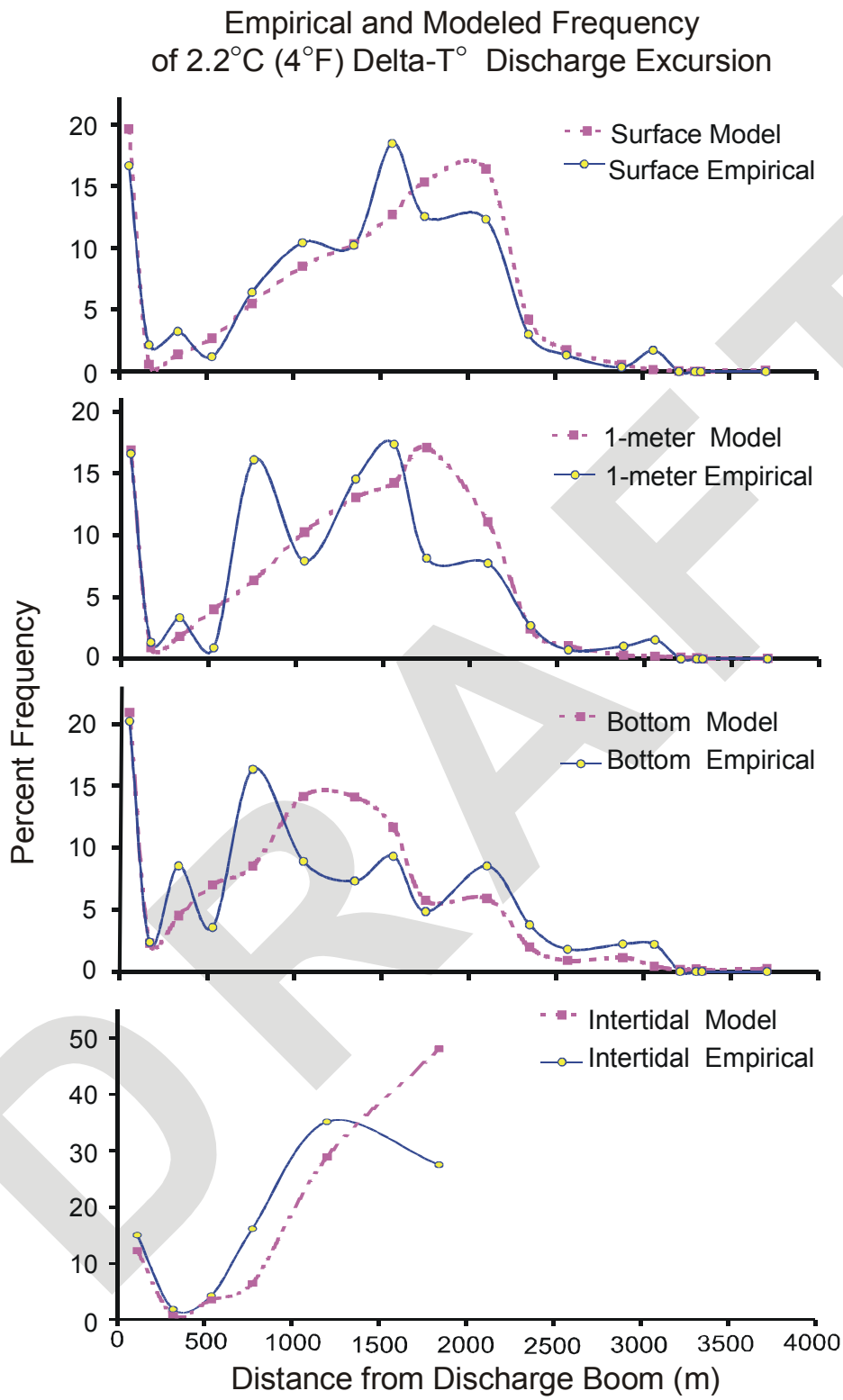

Figure 2.3-19. Comparison of empirical and model linear regressions of percent frequencies of 2.2°C (4°F) discharge delta T° excursion distances at four depths. Excursions were modeled from conditions in July–September 2003. Note larger frequency scale in intertidal graphic.

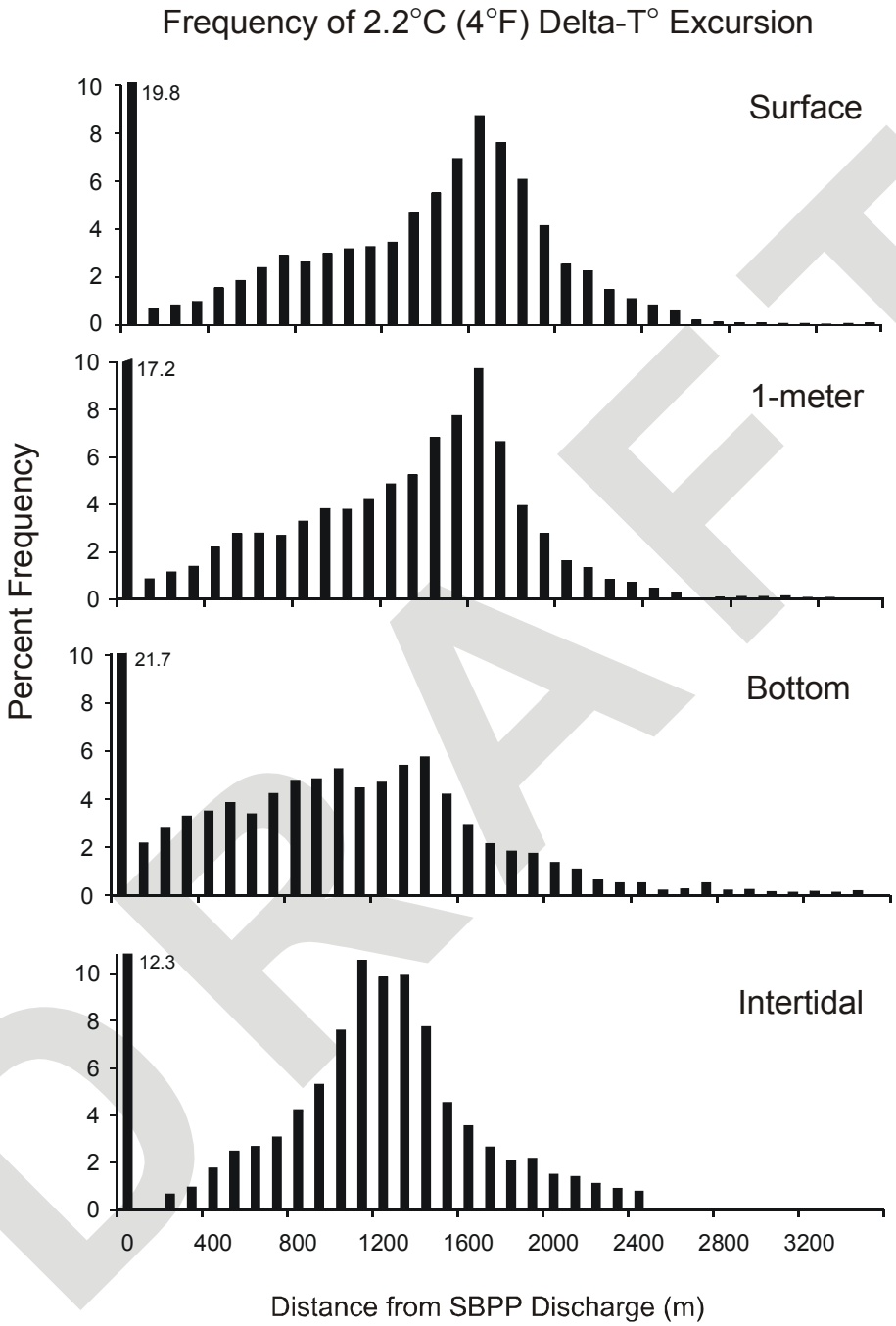

Figure 2.3-20. Percent frequencies of 2.2°C (4°F) discharge delta T° excursion distances at four depths modeled by linear regressions of station temperatures <2.8 km from the discharge boom. Excursions were modeled from conditions in July–September 2003.

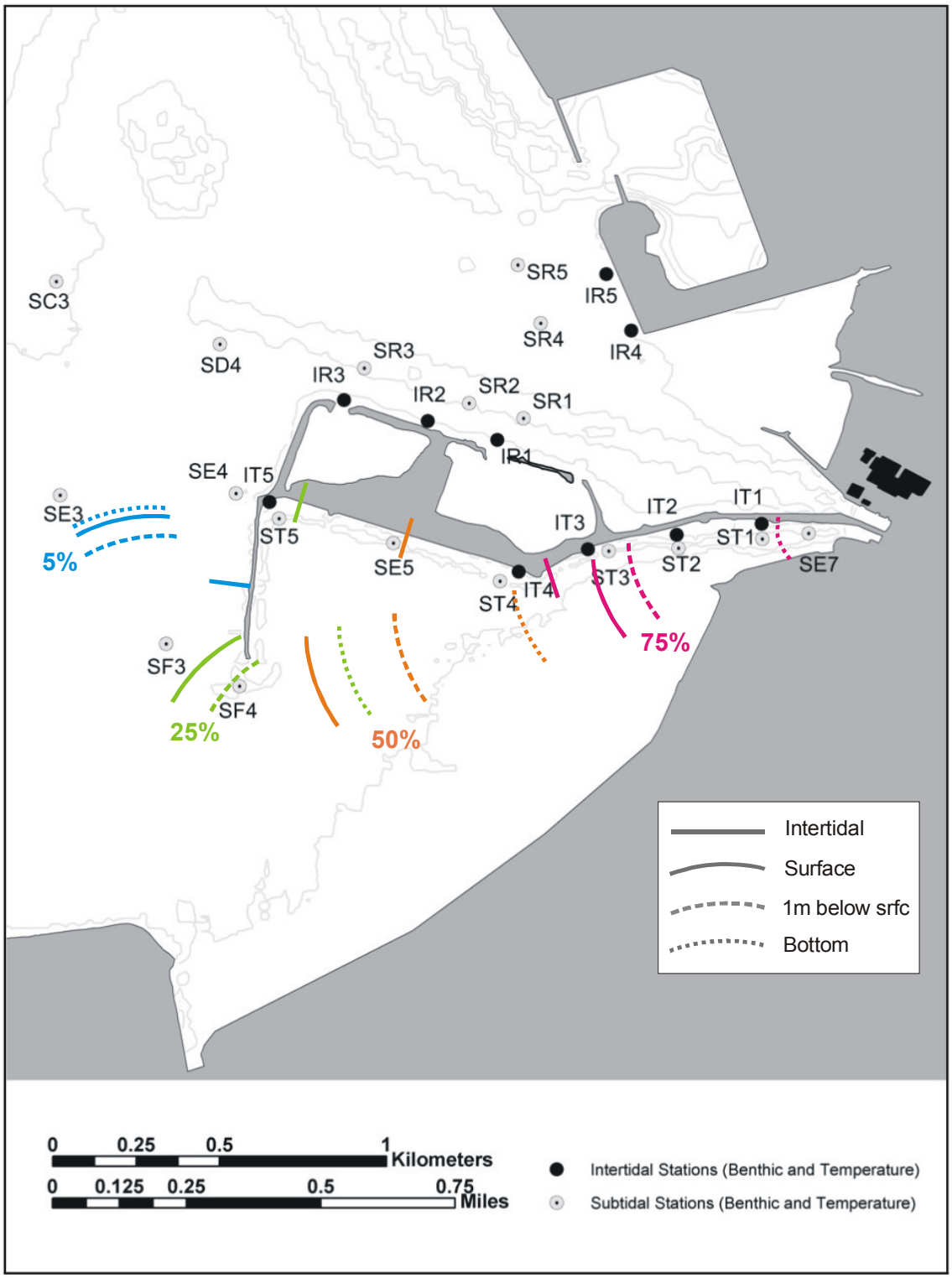

Figure 2.3-21. Map of percent frequencies of 2.2°C (4°F) discharge delta T° excursion distances at four depths modeled by linear regressions of station temperatures <2.8 km from the discharge boom. Excursions were modeled from conditions in July–September 2003.

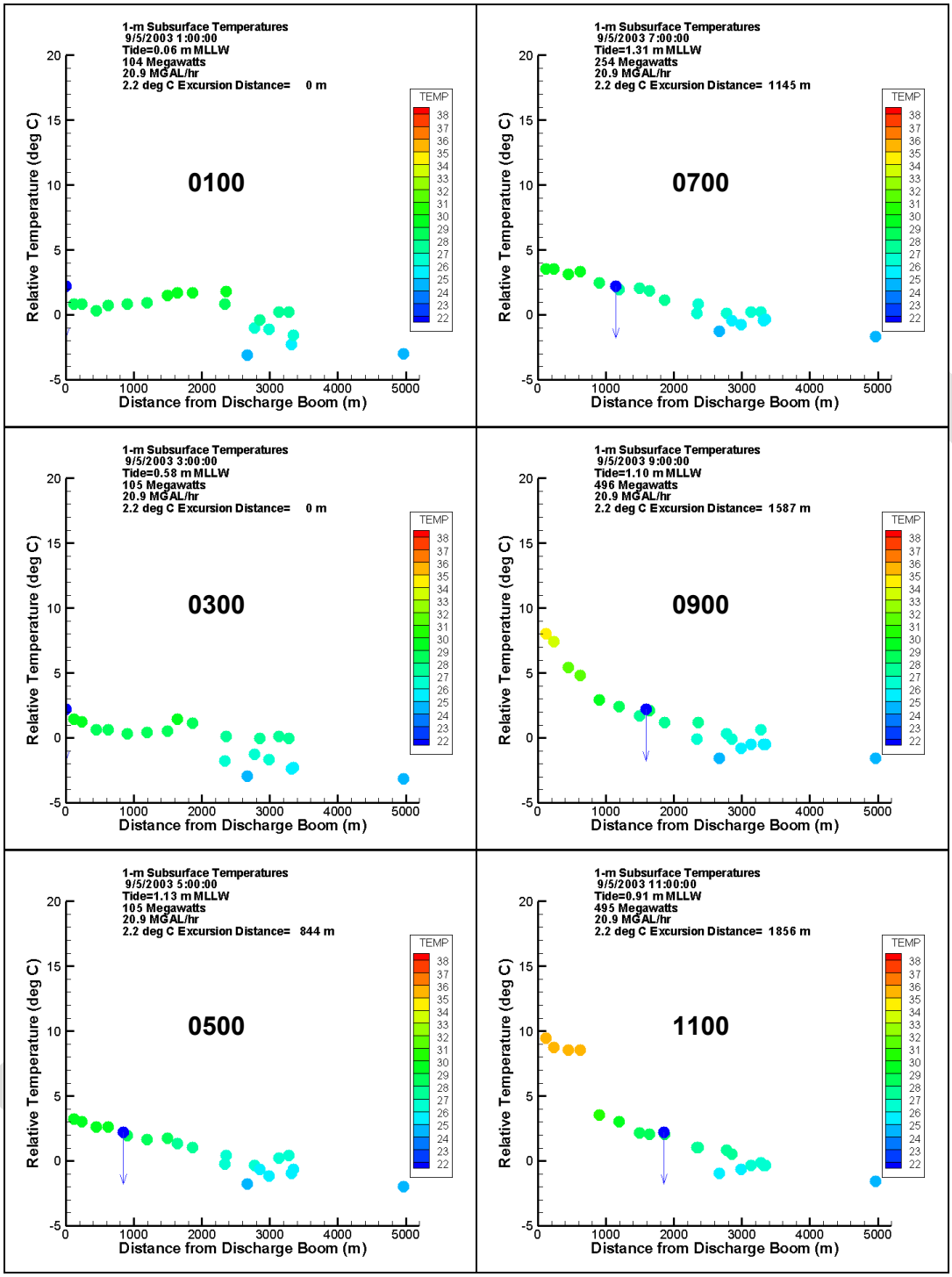

Figure 2.3-22a. Dynamics of the thermal plume on September 5, 2003; 0100–1100 PST. Graphics depict thermal conditions in South Bay at 1-meter subsurface monitoring stations. Graphics coordinate with tide height and SBPP generation output (at top in each graphic) and show temperatures, 2.2°C (4°F) relative delta T° and excursion distances (ball and arrow modeled by linear regressions of station temperatures <2.8 km from the discharge boom).

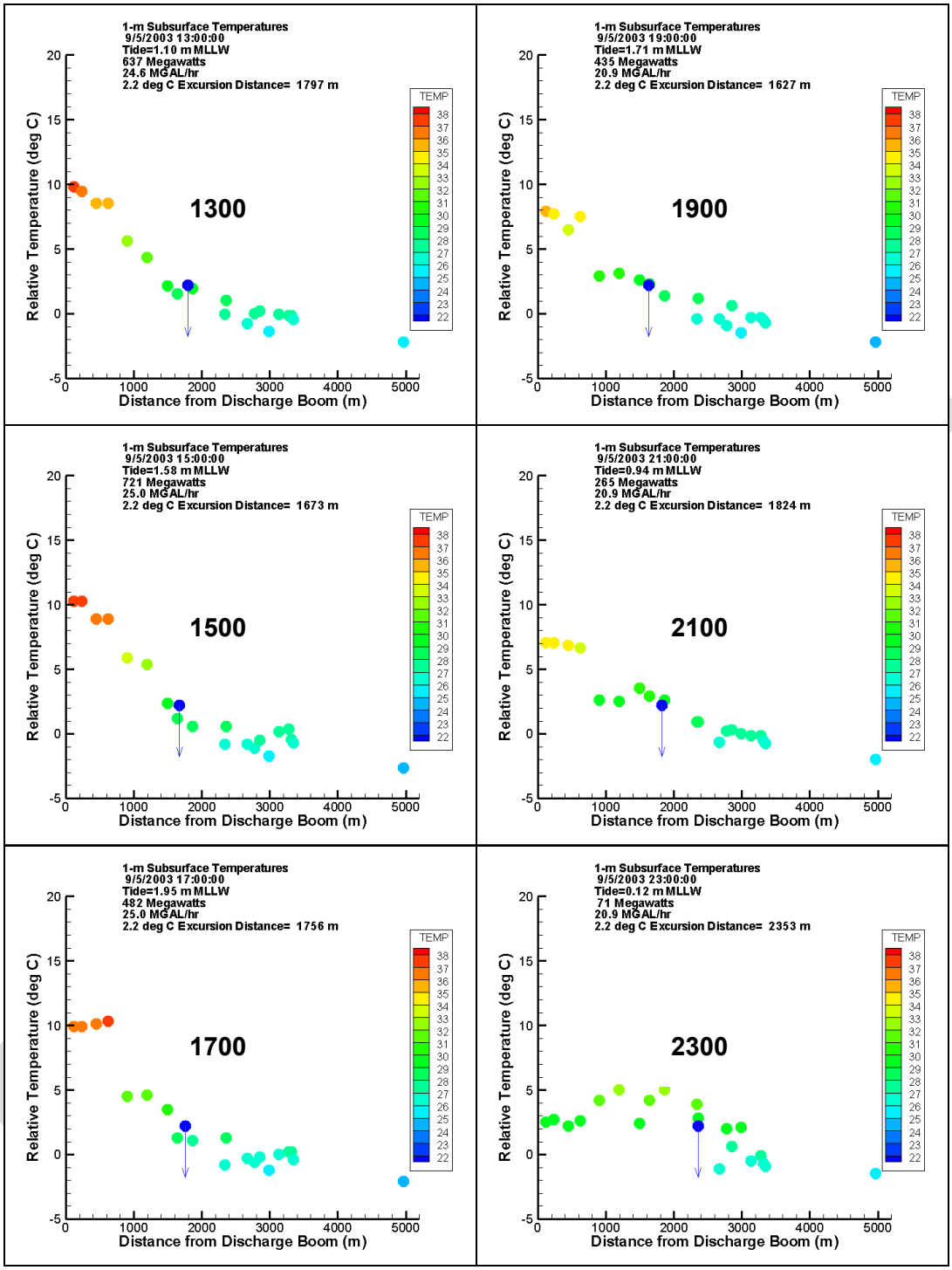

Figure 2.3-22b. Dynamics of the thermal plume on September 5, 2003; 1300–2300 PST. Graphics depict thermal conditions in South Bay at surface stations (left) and 1-m subsurface monitoring stations (right). Graphics coordinate with tide height and SBPP generation output (at top in each graphic) and show temperatures, 2.2°C (4°F) relative delta T° and excursion distances (ball and arrow modeled by linear regressions of station temperatures <2.8 km from the discharge boom).

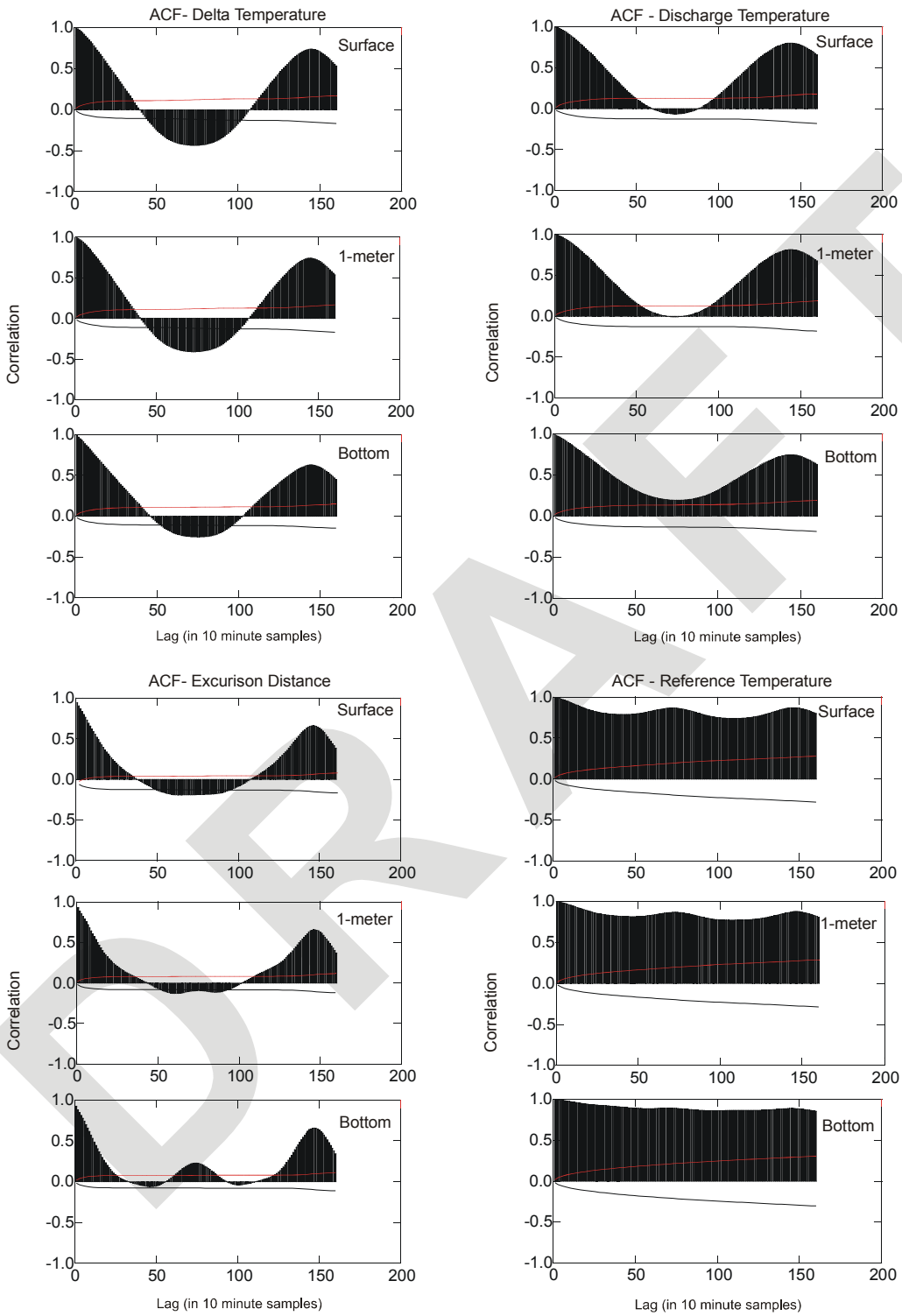

Figure 2.3-23. Autocorrelation functions (ACF) and lines of significance for delta T°, discharge temperature (SE7), delta T° excursion distance and reference (average temperatures of SR1, SR2, and SR3).

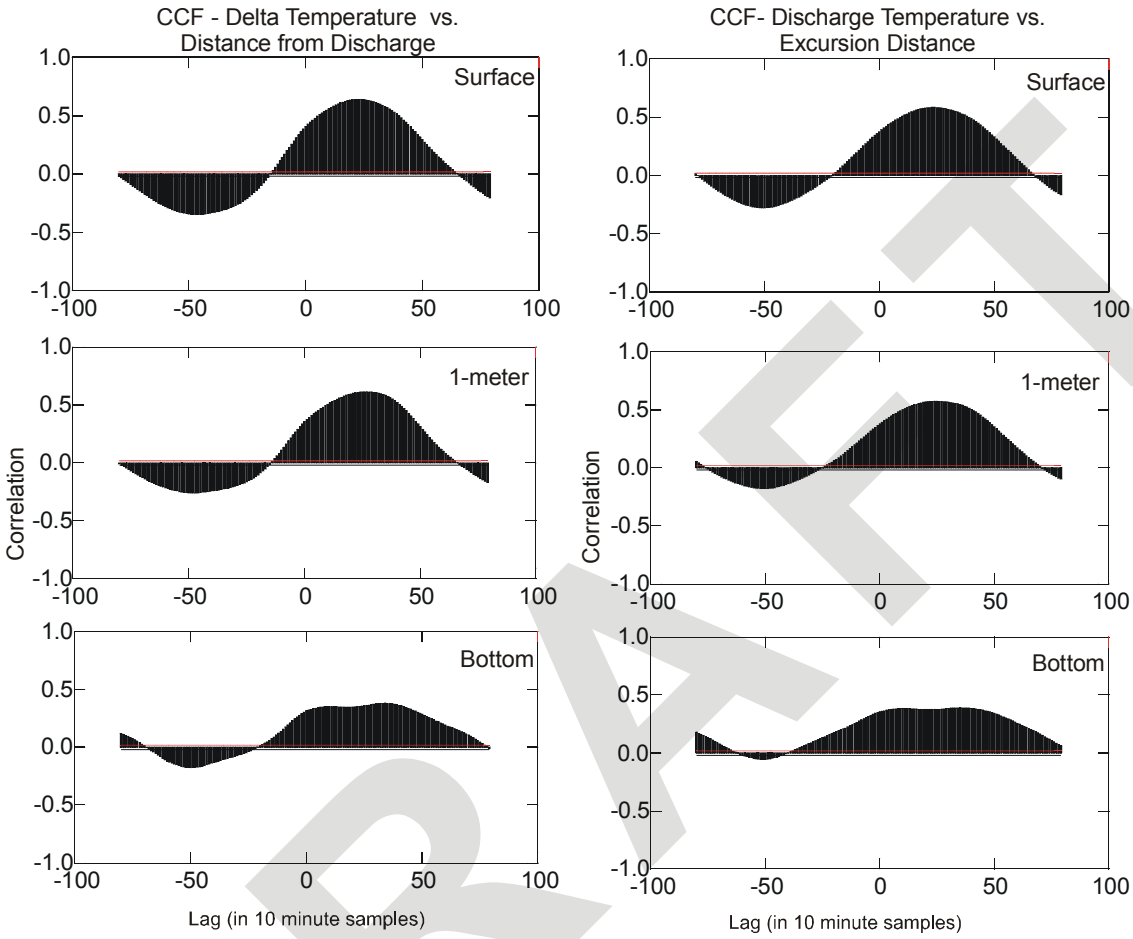

Figure 2.3-24. Cross-correlation functions (CCF) and lines of significance for delta T° vs. distance from the discharge and discharge temperature (SE7) vs. 2.2ºC delta T° excursion distance.

DRAFT

2.4 Receiving Water Dissolved Oxygen Monitoring

2.4.1 Introduction

Oxygen is vital to the process of cellular respiration in all species except for the anaerobic bacteria. As the DO level decreases so does the partial pressure of oxygen. Thus, diffusion across the gas exchange membranes of oxygen-requiring species becomes less efficient when DO levels are depressed. Environments where DO levels are significantly or regularly depressed will tend not to support the same biological communities as similar environments with persistently higher oxygen levels.

The purpose of receiving water dissolved oxygen (DO) monitoring was to:

1. Evaluate whether the SBPP causes a decrease in the concentration of DO in South Bay to levels below naturally occurring conditions; and,

2. Determine if any observed declines in DO result in altered biological communities from what might be expected as a balanced indigenous community under natural environmental conditions.

To accomplish these objectives it was necessary to evaluate how the DO environment of South Bay influenced by the SBPP differs or is similar to comparable back bay environments in the region. It was also necessary to compare biological communities found within the influence of the SBPP and those found at reference areas existing outside of the SBPP influence. Biological aspects of this monitoring are addressed in Section 3.0.

Dissolved oxygen is a measure of the amount of oxygen dissolved in a given quantity of water. Dissolved oxygen is commonly reported as milligrams of oxygen per liter of water (mg/l). This measurement is synonymous with parts per million (ppm) where the number of oxygen molecules are reported in relation to one million water molecules.

Oxygen enters water by diffusion from the atmosphere and as a waste product of plant and algal photosynthesis. The saturation capacity of oxygen in water is dependent upon water temperature, salinity, and atmospheric pressure (Weiss 1970). At saturation, DO concentration is inversely proportional to both water temperature and salinity, and is directly proportional to pressure. At sea level, DO saturation levels at various salinities are expressed by the relationships illustrated in **Figure 2.4-1**. The graph demonstrates that DO saturation capacity differs significantly between marine and freshwater systems and that saturation capacity decreases with increasing water temperature.

Although saturation equilibrium is dictated by the physical and chemical properties of water and the overlying atmosphere, oxygen levels in natural waterbodies are rarely at saturation levels. This is because the properties that influence oxygen levels often change more rapidly than oxygen can diffuse across the air-water interface. Physical, chemical, and biological processes within natural aquatic systems result in daily cycles where DO is produced and consumed at rates that are dictated by such factors as photosynthetic activity, biological and chemical oxygen demands (BOD and COD), and atmospheric diffusion. Dissolved oxygen levels are often elevated above the saturation capacity during daylight hours when photosynthesis is producing more oxygen than is consumed by BOD and COD. At night, DO is consumed by BOD and COD while being replenished only through the relatively inefficient mechanisms of atmospheric diffusion. As a result, it is common for DO to dip below saturation levels at night.

The differential rates at which factors add or consume oxygen from water establish a dynamic equilibrium in which diffusion across the air-water interface is only one factor that can affect DO levels. Diffusion is aided by physical aeration such as that caused by breaking waves or surface wind turbulence. While other factors such as respiration, COD, and photosynthesis are directional, either always adding or always depleting oxygen from the water, diffusion processes act only to nullify the difference between the oxygen saturation level and the saturation capacity of the water. Thus diffusion can act to increase or decrease the amount of oxygen dissolved in the water. Further, the strength of the diffusion gradient is proportional to the deviation of oxygen levels from a saturated state.

2.4.2 Methods

2.4.2.1 Study Sites

Dissolved oxygen monitoring was conducted at eight monitoring stations within the South Bay ecoregion (**Figure 2.4-2**). Station locations were chosen to encompass a range of habitat conditions in South Bay and to provide a characterization of areas potentially subject to influences of the SBPP thermal plume. To accomplish this, sampling was conducted at both the intake (Station 2) and discharge (Station 1) immediately adjacent to the SBPP, as well as in the surrounding waters of the open portions of South Bay (Stations 3–7).

The objectives of DO monitoring required placement of the DO regime of South Bay in relation to an expected regime for similar environments not under the influence of cooling water discharge. To this end, three external (Batiquitos Lagoon, Agua Hedionda, and Seal Beach National Wildlife Refuge) reference sites and one internal reference site (Sweetwater River Channel) were chosen (**Figure 2.4-3**). The reference stations were established in areas that physically resembled the environment of the southern end of San

Diego Bay. South Bay and the reference areas share the same physical characteristics of being shallow soft-bottom back-bay environments with low water turnover. A priori determination of DO ranges were not a consideration in reference site selection. In addition, the fish communities at all of the external reference areas have been characterized through extensive sampling programs conducted within the past ten years (MEC 1995a, b, Merkel & Associates 2002). The fish community of the San Diego Bay reference site, Sweetwater River Channel, has not previously been sampled and, as such, this area was evaluated during the present study (see Section 3.4– *Fishes*). Although no two sampling locations can ever be considered the same, the selection of multiple reference sites allowed the DO regime of the SBPP discharge channel to be evaluated within a broad context that included similar habitats that supported balanced indigenous fish communities (see Section 4.4– *Integrated Discussion: Fishes)*.

2.4.2.2 Data Collection

At each of the monitoring stations, untended monitoring was carried out by deployed Hydrolab® Datasonde 4 and Datasonde 4a multiprobe water quality meters. Water quality probes were set approximately 10 cm (3.9 in) from the bay bottom. Standard Datasonde probes used for this investigation included temperature, salinity, and DO probes. To minimize interference with probe sensors, all bottom vegetation was cleared from a 0.75-meter (2.5 ft) radius around the station. Data for all measured parameters were logged every 15 minutes during station logging runs.

Data collection for the eight South Bay sampling stations and four reference stations was performed during the period of July 3 through September 25, 2003 (**Appendix E**). Data were not collected continuously and simultaneously at all eight South Bay sampling stations because the number of Datasonde units was limited and required that units be rotated periodically among the sampling stations. Datasonde rotation among sites did not affect data quality for comparative purposes because variation of measurements within stations was lower than that observed among stations. External reference stations had one sampling point each and were monitored on a nearly continuous basis.

2.4.2.3 Equipment Servicing

Throughout the length of the study, Datasonde multi-probe maintenance was performed frequently due to limited data storage capacity and battery life, as well as to the high sedimentation and biological fouling rates that could interfere with data logging. Routine and frequent maintenance decreased the potential for gaps in data and minimized instrument fouling and subsequent measurement drift or decay. Over the course of the study, instrument maintenance was conducted at intervals ranging from 3 to 15 days. Datasonde units were removed from the water and replaced with recently calibrated units. Routine maintenance included complete cleaning and instrument calibration; data were also downloaded during routine maintenance.

All instruments were calibrated in the laboratory prior to deployment in the field. To confirm and improve the accuracy of data, a data validation and post-deployment calibration technique was used during the study. During routine maintenance at each station, a laboratory-calibrated Hydrolab® Quanta Multiprobe unit was lowered into the water and the on-site parameters were recorded in the field notes, providing a starting and ending reference reading for each sampling interval. To further gauge the accuracy of collected data, retrieved Datasonde units were tested in calibration standards prior to data download to detect deviation from the original calibration. For an in-depth discussion on Hydrolab® Datasonde data management and correction procedures refer to Merkel & Associates (2000a).

2.4.2.4 Condition and Validity of Collected Data

During the course of the field investigations, a total of 42,961, fifteen-minute sampling intervals were recorded for the combined South Bay and reference monitoring stations. These intervals returned valid data the majority of the time; however, no station returned valid data for all sampling intervals. In addition, data from the deployed instruments could at times contain a substantial amount of spurious information. This included data taken by the instruments prior to their being put into the water, data from probes that collected drifting algae or debris thus providing blatantly erroneous readings, and data that showed erratic response or decay without apparent cause. To make use of the data sets, it was essential to use only the valid data from the instruments. Because the units were deployed, the data collected could be corrupted, lost, or could return erroneous values that did not reflect true environmental conditions. Some losses were of a short or intermediate duration (e.g. algal fouling of probes, signal decay from sediment loading or biotic activities), while other problems eliminated data for an entire station for the monitoring interval (e.g. power failures, failed logging files).

Data collected from monitoring stations were reviewed for the quality of data records. This review focused on identification of the amount of good data (e.g. within normal ranges, calibrated between stations, reflecting consistent records) that was ultimately used in the study analyses. Integral in this process was the use of the on-site measurements from tended units described in the maintenance section above. These data were compared to the data retrieved from the deployed unit, allowing for the evaluation of data accuracy. When considered in conjunction with the measurements recorded when the units were placed in calibration standards upon retrieval, it was determined whether removal or correction of the data set was required.

To ensure that data being evaluated were reflective of true conditions, it was necessary to trim the data records to remove spurious data prior to conducting analyses. To accomplish this a standard set of protocols was used to ensure that the remaining data portrayed a true and accurate representation of the monitored environment. The rules employed to clip data included:

- No data are to be used which precede deployment of instruments or which are collected within the first twenty minute period immediately following deployment;
- No data are to be used which are either out of sensor range or are the preceding or following data points around a sensor range violation;
- No data are to be used where instrument diagnostic reports indicate sensor or calibration failures;
- No data are to be used where human error or instrument failures resulted in no data being collected for the time period (i.e. null values will not be used in developing trendlines or means);
- No data are to be used from that portion of a record in which data trends and patterns suggest that units were under the influence of abnormal conditions or were not functioning properly. Data trimming for these purposes should also be backed by observed instrument problems or conditions from field log notes where possible (e.g. sensors in mud, flooding of sensors, animals in or on sensors).

Additional data acceptance standards are discussed below by individual parameter.

Temperature

Temperature data consistently matched the on-site data check within 0.04%. The only cause for data to not be accepted during this study was if the unit had fallen off of its station. Indications that a unit had fallen into the mud included data that showed little response to tidal flow (due to mud in the pressure sensor), and deterioration of data recorded by other probes. During the present study, 99.81% of the temperature data collected were accepted.

Dissolved Oxygen

Collected DO data were examined after each monitoring interval. An instrument working correctly would collect DO data that reflected the daily cycling of light and tide. Initial inspection of the retrieved data was required to reveal that general pattern. If the data instead revealed a flat line or an erratic line (for example oscillating between 2 and 12 mg/l with each reading), the data were considered suspicious. The probe itself was then examined for damage, the circulator was tested to confirm that it was still able to turn, and the post-deployment readings were reviewed for problems. If the probe was found to be broken, the data were not accepted.

If the data appeared to not reflect any equipment damage, it was then compared to on-site data readings from the time of deployment and retrieval. If data were within ±5% of the DO measured simultaneously by another calibrated unit on-site, the data were accepted. During the present study, 99.64% of the DO data collected were accepted.

Salinity

Salinity data were conditionally accepted if they did not deviate by more than ±2% from the on-site data check taken by another calibrated unit. Units were then placed in a known salinity standard when they were retrieved and the reported value was recorded. If the retrieved unit also did not deviate from the known calibration standard by more than ±2%, the data were not accepted.

2.4.2.5 Data Analysis

The accepted data sets were transferred and graphed using Statistica® Version 5.5 statistical analysis software for Windows®. Graphical analysis of data includes presentation of plots of mean parameter values for each 15-minute data-logging period. Although the 15-minute interval data are retained in calculations and graphics, they are simply referred to as hourly data. In text and graphics, these data have been referred to as mean hourly curves for the parameter data (e.g., mean hourly curve of DO). When these data are averaged to give a single daily value, they are referred to as the mean daily value for the parameter (e.g., mean daily DO concentration). Wherever ranges are associated with a statistic, the range represents ±1 standard deviation of the presented statistic (e.g., mean ± 1 s.d.).

2.4.3 Results

Dissolved oxygen, temperature, and salinity data for the South Bay open water, SBPP discharge channel, and reference stations are presented in this section. Additional data are included in **Appendix E**. Data interpretation in this section is limited to a discussion of normal ranges, controlling factors, and similarities and differences between sites. The relationships between DO and biotic communities are discussed in Section 4.0 – *Integrated Discussion*.

2.4.3.1 Dissolved Oxygen

South Bay Dissolved Oxygen

Comparison of the curves of mean hourly DO concentrations indicates that the south bay open water monitoring stations had consistently higher DO concentrations than those observed for the SBPP discharge channel monitoring stations (**Figure 2.4-4**). On average, the mean hourly DO for the south bay open water monitoring stations was 0.54 ± 0.14 mg/l higher than that observed for the discharge channel. The open water stations had a mean daily DO concentration of 5.52 ± 0.35 mg/l while the discharge channel had a mean daily DO concentration of 4.99 ± 0.32 mg/l. The minimum and maximum observed differences between the mean hourly DO concentrations between the south bay open water and discharge sites was 0.27 mg/l at 0345 and 0.83 mg/l at 1700, respectively.

Mean hourly DO concentrations with error bars for each 15-minute sampling interval are presented in **Appendix E**.

Reference Station Dissolved Oxygen

The four reference stations chosen for study displayed typical curves of mean hourly DO concentrations with daily maxima between 1500 and 1700, and minima between 0600 and 0800 (**Figure 2.4-5**). The Seal Beach NWR site had both the highest mean daily oxygen concentration (6.12 ± 1.40 mg/l), and the greatest peak concentration (8.55 ± 1.33 mg/l at 1615) of the four sites. Batiquitos Lagoon had the lowest mean daily oxygen concentration (4.08 ± 0.81 mg/l) and the lowest observed minimum mean hourly oxygen concentration (2.91 ± 0.88 mg/l at 0645). Agua Hedionda and Sweetwater River Channel had DO concentrations intermediate between the other two sites.

The combined mean hourly DO curve for the reference stations is plotted in **Figure 2.4-6**. The error bars (± 1 s.d.) for the combined plot completely encompass all of the individual site curves plotted in **Figure 2.4-5**. The combined mean daily DO concentration for the reference sites was 5.38 ± 1.01 mg/l with a mean hourly peak of 7.06 ± 1.86 mg/l at 1645 hours and minimum of 4.02 ± 1.06 mg/l at 0645 hours.

Appendix E includes charts of mean hourly DO with error bars for each of the reference stations**.** The South Bay discharge channel and open water DO curves are included with the reference station figures for comparison. The mean hourly DO curves for the discharge channel and open water sites always fell within range of values observed for each of the reference sites.

South Bay and Reference Station Comparisons

The mean hourly DO concentrations for both the south bay open water stations and the discharge channel fall within ±1 standard deviation of the mean hourly DO concentration of the reference stations (**Figure 2.4-7**). The curves of mean hourly DO for the south bay open water and discharge channel monitoring stations show muted daily trends compared to the reference stations. In comparison to the mean condition of the combined reference stations, all south bay stations had greater levels of DO in the morning and lower levels of DO in the afternoon. The mean daily DO concentrations of 5.38 ± 1.01 mg/l (reference sites), 5.52 ± 0.35 mg/l (open San Diego Bay), and 4.99 ± 0.32 mg/l (SBPP discharge channel) do not substantially differ.

While the average DO of the reference and south bay stations was similar, of note in the results is the frequency of time each site was subjected to the higher and lower extremes of the DO ranges detected. The mean hourly reference station DO concentration fell below 4.50 mg/l for greater than 28 percent of the time, while the south bay open water and discharge channel stations fell below 4.50 mg/l for only 3 percent and 0 percent of the time respectively. Alternately, the reference stations maintained DO concentrations above 6.00 mg/l for greater than 31 percent of the time, while the south bay open water

sites exceeded 6.00 mg/l only 10 percent of the time, and the discharge channel never exceeded a DO concentration of greater than 6.00 mg/l during the course of the study.

Wide diurnal ranges of DO such as observed within reference stations are typical of systems supporting high primary productivity (Lerberg et al. 2000). Photosynthesis during daylight hours generates DO levels that can be supersaturated, while the unbalanced respiratory demand combined with factors such as COD can significantly deplete oxygen at night. The dampened conditions observed within both the San Diego Bay open water and discharge channel stations are generally reflective of systems with lower primary productivity, larger water volumes, and/or greater aeration or water turn-over. It is notable that for reference stations as well as both San Diego Bay open water and discharge channel stations the mean daily DO curves were consistently below the saturation levels for the mean temperatures experienced at the stations. This suggests that DO consumption was typically higher than production at all locations throughout the study.

2.4.3.2 Temperature

Temperature data were collected coincidentally with DO data and are presented here to allow a comparison between the reference and discharge station conditions. A complete analysis of changes in receiving water temperatures in South Bay in relation to SBPP operation is presented in Section 2.3 – *Receiving Water Temperature Monitoring*.

South Bay Temperature

Mean daily temperature measurements within the open waters of south bay ranged between 25.8 and 26.3°C while the mean daily temperature within the discharge channel ranged from 27.5 to 30.0°C (**Figure 2.4-8**). The relatively narrow temperature range observed in the open water stations was somewhat surprising considering the wide range of factors influencing temperature in the south bay. These factors include solar heating, power plant cooling system discharges, wind waves, and tidal circulation.

Reference Station Temperature

As with the discharge channel, the daily temperature profiles observed at reference stations exhibited a typical pattern of daytime warming and nighttime cooling. The mean thermal ranges exhibited by reference stations varied across stations. Batiquitos Lagoon exhibited the greatest mean diurnal temperature range with a 3.5°C variation from 24.2 to 27.7°C (**Figure 2.4-9**). This mean daily temperature range exceeded that observed within the discharge channel where a 2.5°C range occurred. The mean daily temperature range at Agua Hedionda Lagoon was 22.6 to 25.0°C. Seal Beach NWR ranged from 23.1 to 25.1°C. Finally, the narrowest mean daily temperature range observed at reference stations was detected at the Sweetwater River Channel where temperatures ranged from 25.1° to 26.8°C, a thermal range of 1.7°C over the course of the day.

South Bay and Reference Station Comparisons

As with the results of the DO monitoring, the San Diego Bay open water and discharge channel stations exhibited overlap in thermal range with the reference areas. While the open bay sites were well within the range of temperatures observed at reference areas, the mean maximum discharge channel temperatures exceeded the mean maximum temperature at a reference area (Batiquitos Lagoon) by 2.4°C. The mean daily temperature of all reference sites combined was 24.88 ± 0.70°C. This is lower than the mean temperatures of 26.30 ± 0.26°C at the open water stations in South Bay and 28.54 ± 0.80°C in the SBPP discharge channel.

The patterns of diurnal temperature change were consistent between reference stations and the discharge channel stations. Similarly, the magnitude of the daily temperature change was comparable between the discharge channel and the reference stations. These patterns were not reflected in the open water stations of South Bay.

2.4.3.3 Salinity

South Bay Salinity

Mean salinity conditions present during the course of the survey did not vary significantly between San Diego Bay study stations, and daily salinity curves exhibited no detectable pattern that would suggest a temporal effect on salinity levels (**Figure 2.4-10**). Mean daily salinities values varied between 35.4 and 35.8 parts per thousand (ppt) for both the discharge channel and the open water stations. The mean salinity of the discharge channel stations was 35.6 ± 1.1 ppt with that of open water South Bay stations being 35.5 ± 1.7 ppt. These differences in means are indistinguishable in the context of the variation in salinity data (**Appendix E**).

Reference Station Salinity

As with the South Bay stations, mean daily salinities at reference stations varied little (**Figure 2.4-11**). The maximum range of mean daily salinity was observed at the Sweetwater River and the mean salinity varied by only 1.4 ppt (33.0 to 34.4 ppt). The entire range of mean salinities across all reference sites was bracketed by 31.4 to 34.6 ppt. The overall combined mean salinity of reference stations was 32.8 ± 0.2 ppt.

South Bay and Reference Station Comparisons

The South Bay stations were statistically identical and tracked closely with each other. The South Bay stations maintained salinities that were approximately 2.5 ppt higher than the combined average of the reference stations. The diurnal variation of salinity was not consistent across stations, although the extent of variability would have a negligible effect on DO saturation capacity at any particular station since a 10 ppt range at sea level and study area and reference stations' temperatures would result in DO saturation capacities that vary by only 0.1 ppt.

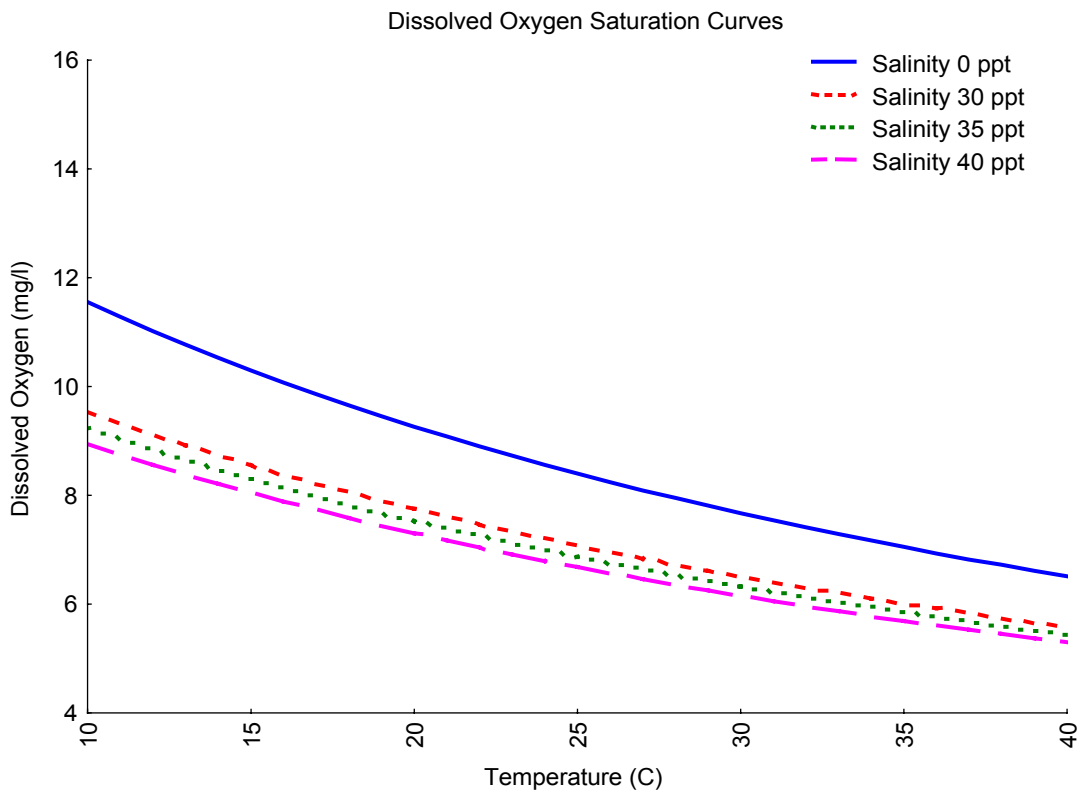

Figure 2.4-1. Temperature and salinity effects on dissolved oxygen saturation curves at sea level pressure.

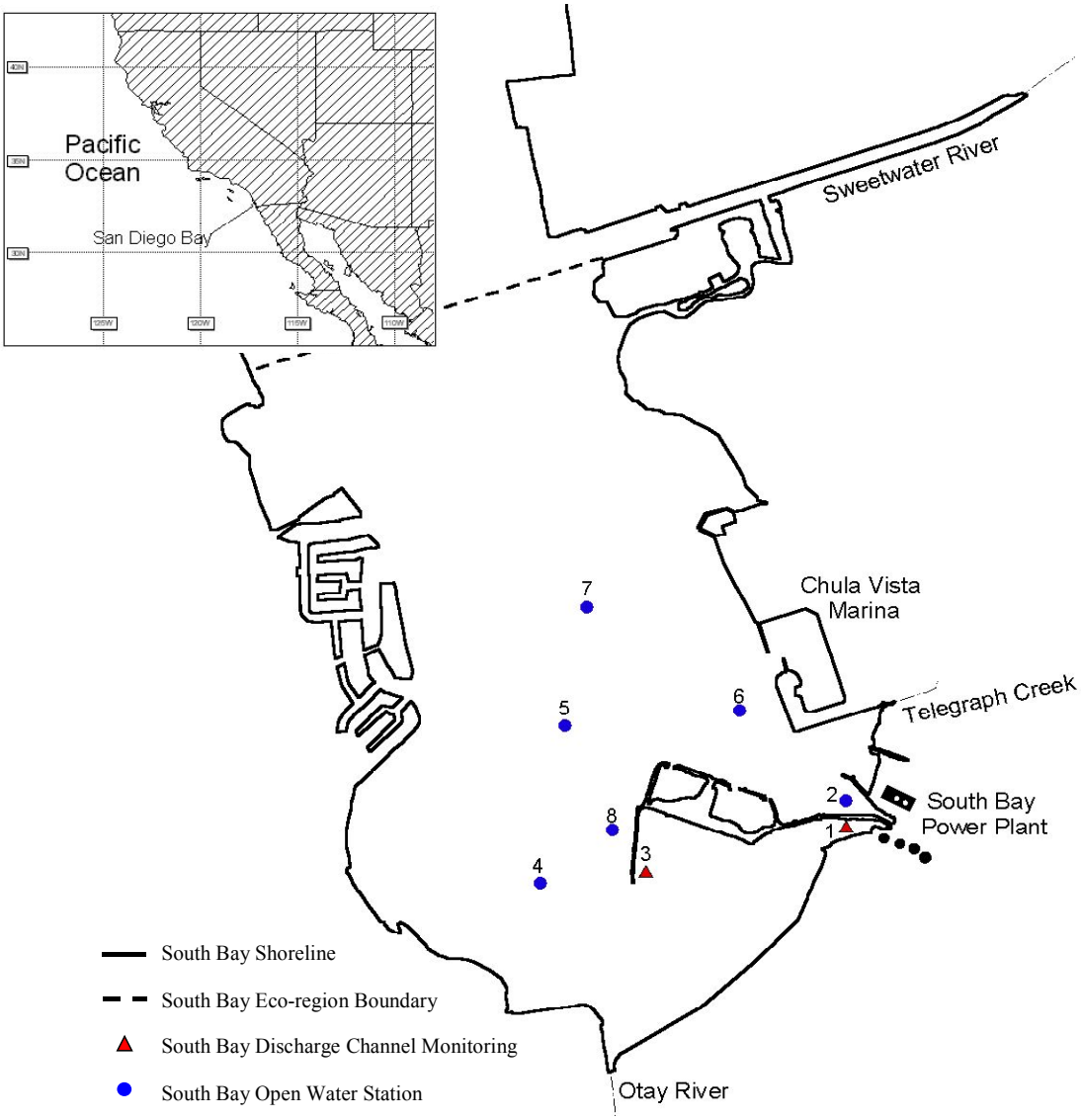

Figure 2.4-2. Hydrolab Datasonde monitoring station locations in south San Diego Bay, Summer 2003.

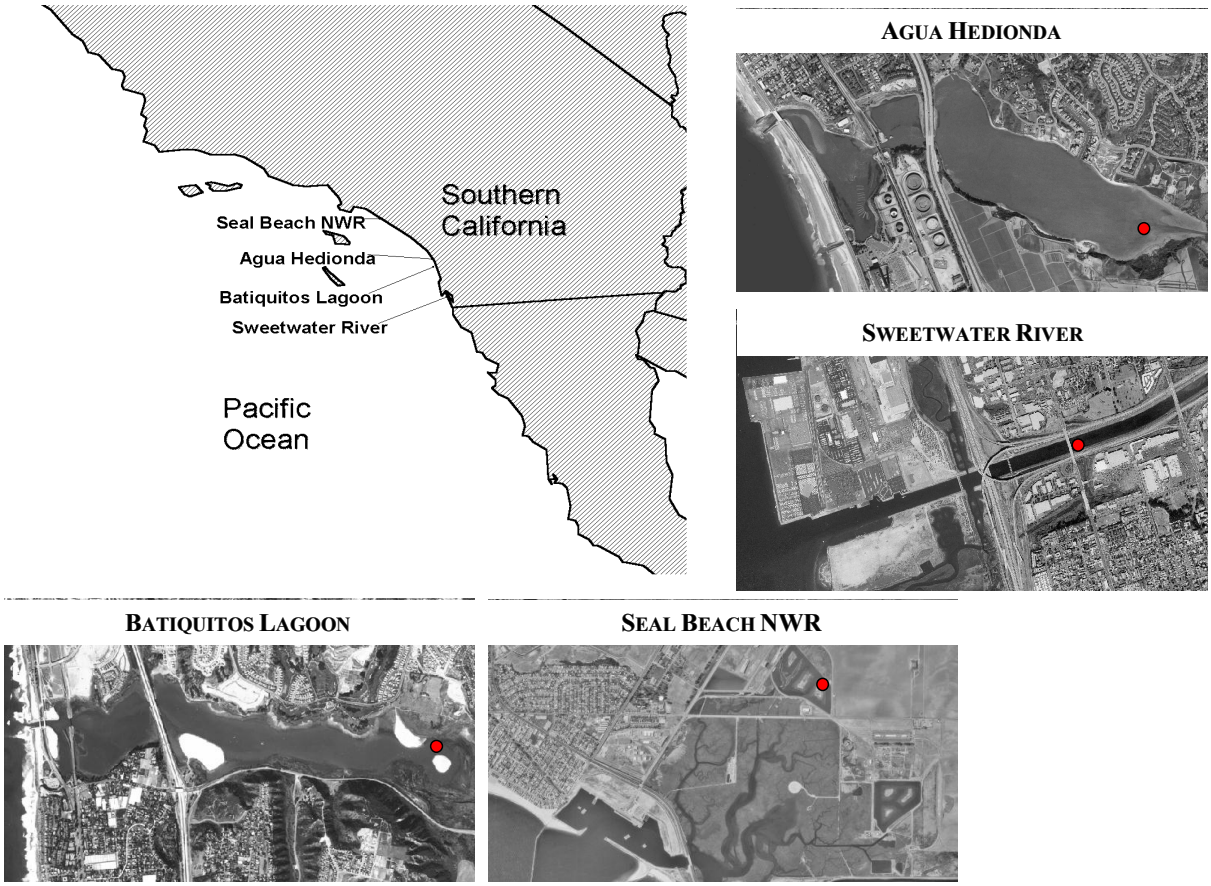

Figure 2.4-3. Hydrolab Datasonde dissolved oxygen reference monitoring station locations, Summer 2003. Dots denote station positions.

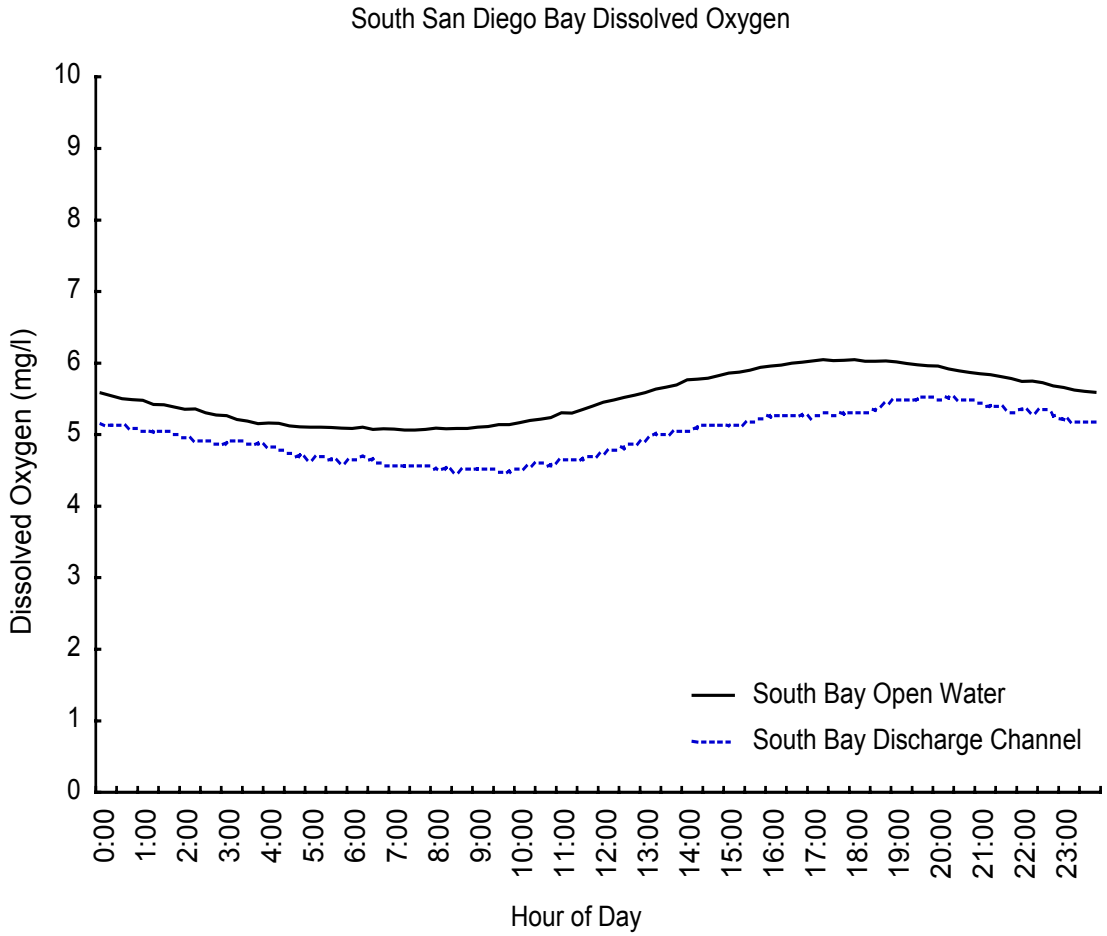

Figure 2.4-4. Mean hourly dissolved oxygen curve for south San Diego Bay open water and discharge channel monitoring stations.

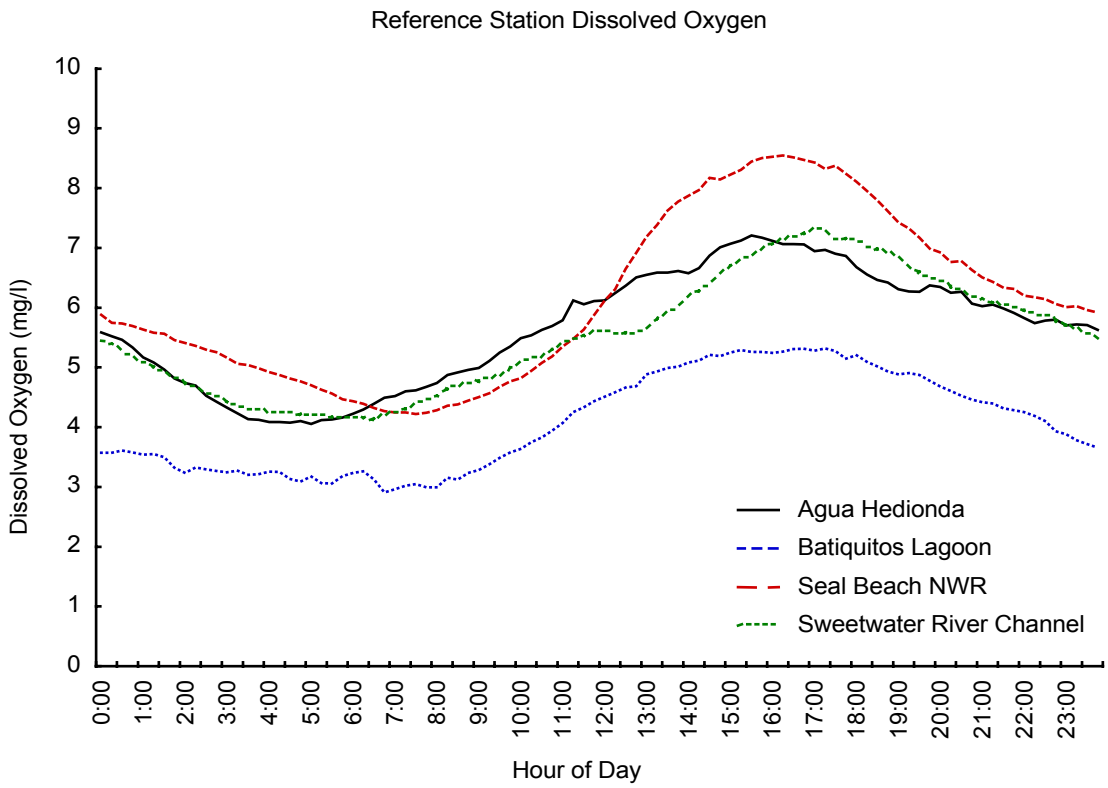

Figure 2.4-5. Mean hourly dissolved oxygen curves for each of the study reference stations.

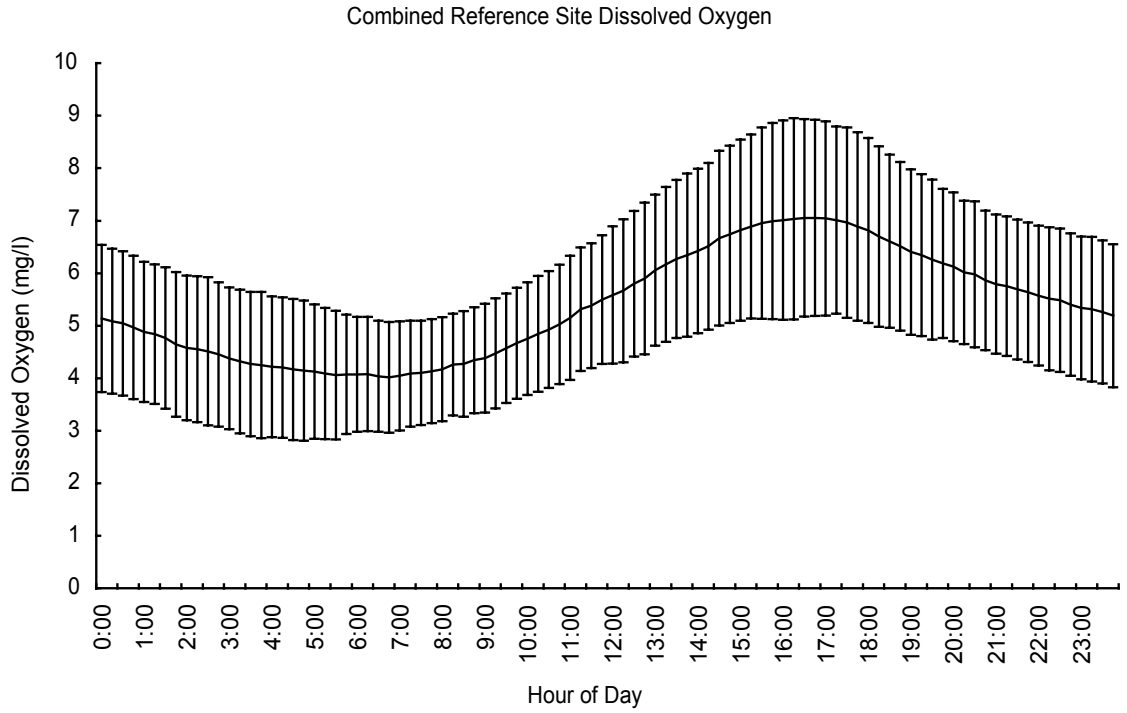

Figure 2.4-6. Mean hourly dissolved oxygen curve for the combined average of the study reference stations. Error bars are ± 1 standard deviation.

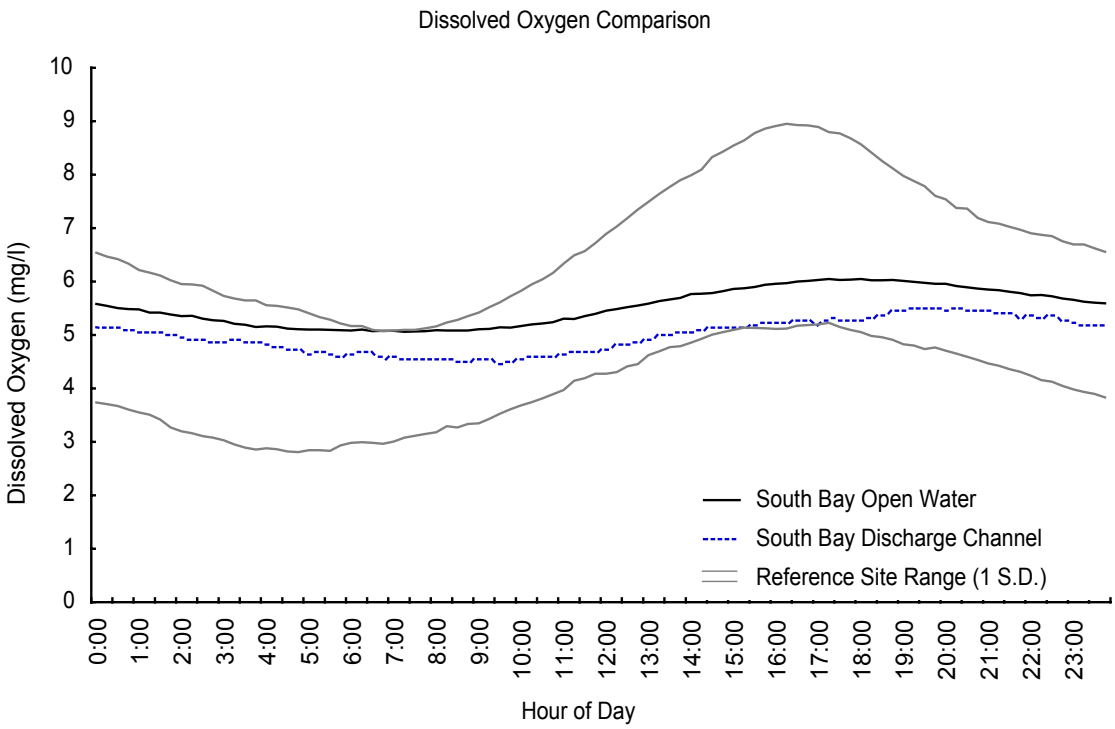

Figure 2.4-7. Mean hourly dissolved oxygen curves for south San Diego Bay open water and SBPP discharge channel monitoring stations plotted over the standard deviation of the mean hourly dissolved oxygen for the reference stations.

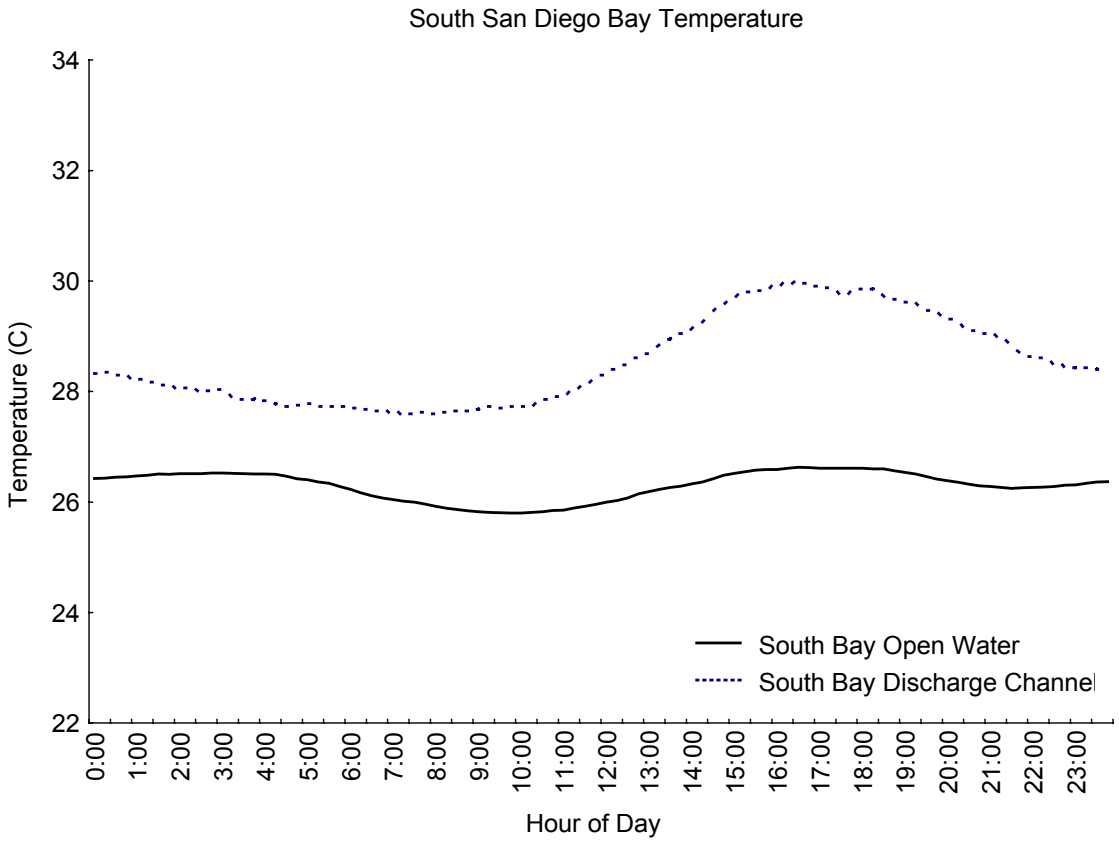

Figure 2.4-8. Mean hourly temperature curves for south San Diego Bay open water and discharge channel monitoring stations.

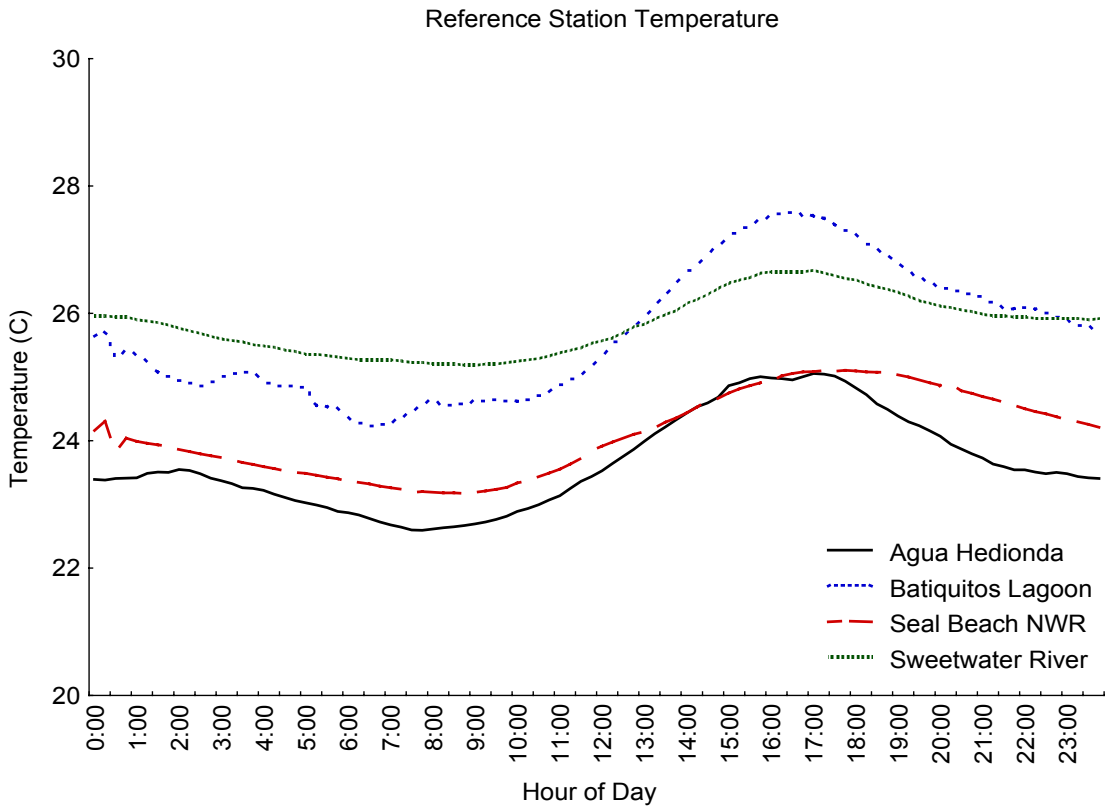

Figure 2.4-9. Mean hourly temperature curves for reference monitoring stations.

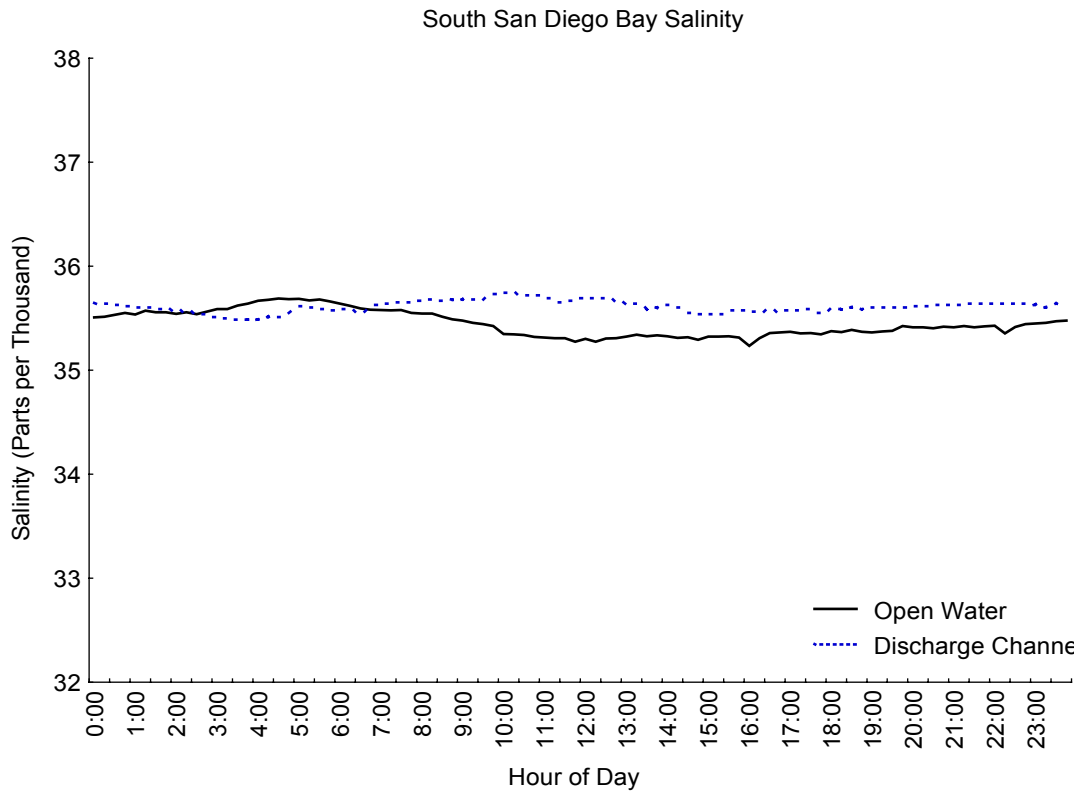

Figure 2.4-10. Mean hourly salinity curves for south San Diego Bay monitoring stations.

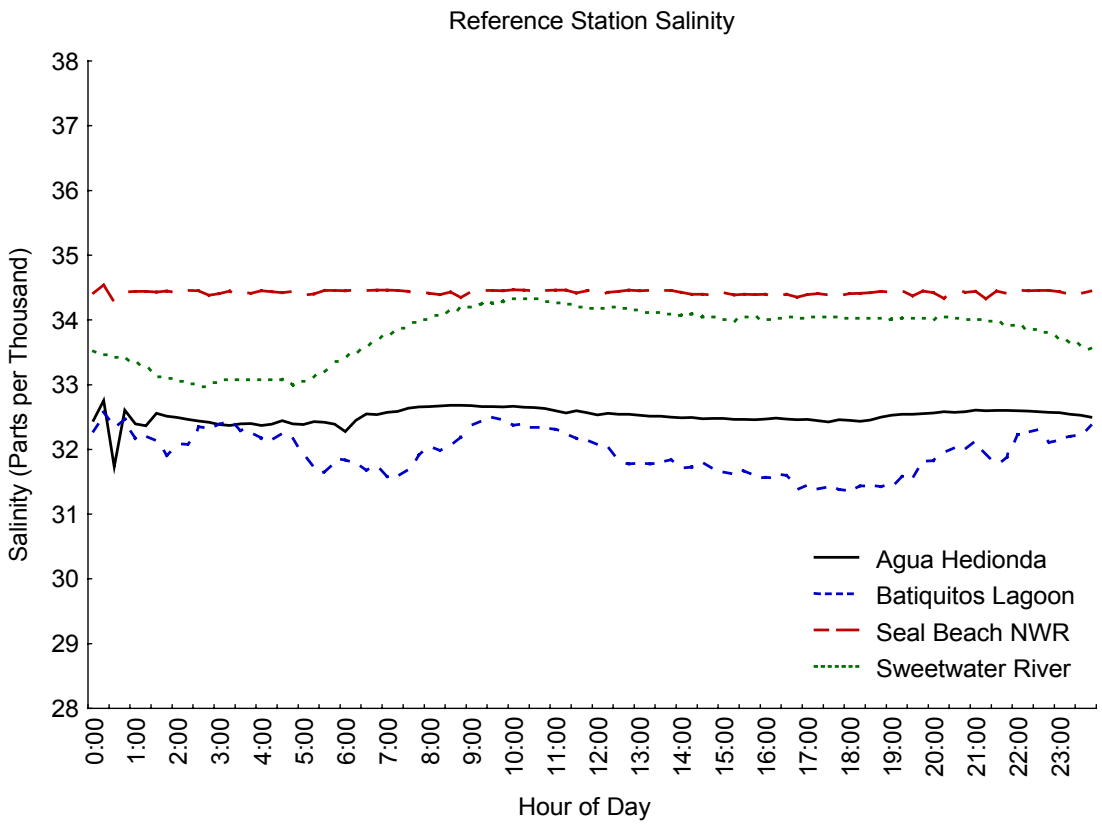

Figure 2.4-11. Mean hourly salinity curves for reference monitoring stations.

2.5 Receiving Water Currents and Bathymetry

2.5.1 Introduction

The purpose of describing current regimes and bathymetry is to provide a more detailed understanding of SBPP discharge plume behavior under a variety of power plant operating conditions and oceanographic conditions in South Bay. The information is used to interpret water temperature (Section 2.3) and turbidity patterns (Section 2.6) in the bay. A general description of San Diego Bay climate and oceanographic processes is presented in Section 2.2–*San Diego Bay Environmental Setting*.

Currents in San Diego Bay are mainly generated by a mixed semi-diurnal tidal exchange with oceanic waters through the bay entrance at Point Loma. The tidal range averages approximately 1.7 m (5.6 ft) with extremes up to 3 m (9.8 ft) (Wang et al. 1998). Tidal currents near the entrance of the bay at Point Loma can be up to 1.0 m s^{-1} (3.3 fps), yielding an average tidal excursion (distance traveled by a parcel of water from high to low tide) of approximately 4.3 km (2.7 mi) (Chadwick et al. 1996). The head of the bay in the south bay region near SBPP is closed and without substantial tributaries. Thus, the horizontal motion of the tide near SBPP is small resulting in weak currents of approximately at 0.1–0.2 m s^{-1} (0.3-0.7 ft s^{-1}).

Wang et al. (1998) calculated the maximum and minimum tidal prisms for seven cross-sections of San Diego Bay. At each position they estimated the change in water volume passing the area during a flooding tide. The tidal prism varied at each area due the bay's configuration and bathymetry. The mean area and volume of the bay were estimated at 4,300 ha (10,625 ac) and 2.79 x 10^8 m^3 (9.85 x 10^9 ft^3), respectively. Most of the tidal prism, 1.20 x 10^8 m^3 (43 percent of the mean bay volume), occurs at the mouth of the bay during spring tides. During neap tides, only about 8 x 10^6 m^3 (about 3 percent of the mean bay volume) is replaced. In the south bay the tidal prism represents about 10 percent of the mean bay volume during spring tides, while it is less than 1 percent during neap tides.

Differences in water densities due to variations in temperature and salinity between bay and ocean water contribute to complex circulation patterns in the bay (Chadwick et al. 1996). Thermal stratification influences the structure of the outflow and inflows during tidal exchanges. For example, as ebb flow weakens, a period of two-way exchange occurs, with the surface layer flowing seaward, and the deep layer flowing into the bay. Circulation can also be influenced by hypersaline conditions that occur in the south bay, particularly in summer. With negligible freshwater inflow the average residence time for a parcel of water in the head of the bay increases markedly. Residence times in summer

1993 were estimated at greater than 40 days for South Bay (Largier et al. 1996). Solar heating and evaporation with prolonged residence times can also cause hypersaline-related inverse circulation near the head of the bay. Under these conditions a 'reversed estuary' phenomenon can occur in which the heavier saline water flows northward along the bottom of the bay and less salty oceanic water flows southward near the surface (Wang et al. 1998).

The overall effect of wind driven waves on currents is generally small in San Diego Bay because the winds are typically mild, ranging between 7–14 kph (4–9 mph) and the distance traveled is short (SDG&E 1973, Wang et al. 1998). Higher velocity afternoon winds ranging between 19–22 kph (12–14 mph) can have dramatic localized impacts particularly in shallow waters where they cause bottom scouring and re-suspension of sediments (Merkel 2000a) (see Section 2.6–*Receiving Water Turbidity Monitoring*).

2.5.2 Methods

Our study of current patterns in the SBPP vicinity consisted of three elements:

1. Bathymetry mapping of the south bay area for modeling circulation patterns;
2. Measurements of current speed and direction at fixed locations during various tide conditions and discharge flow volumes; and
3. Determination of discharge flow contribution to current speeds based on the cross-width area of the receiving water body.

2.5.2.1 Bathymetry Surveys and Mapping

Accurate bathymetry was needed for the TRIM-2D numeric model (see Section 2.6–*Turbidity*) and for other modeling purposes, and was constructed using three data sets. A large portion of the bathymetric data was available from the US Navy (1994). These data were augmented from other previous surveys and from additional surveys completed in this study to provide better resolution for the south bay area from Sweetwater River to the bay's head.

Merkel and Associates collected data for this study throughout most of South Bay using a Furuno FCV-600L single-beam fathometer operating at a frequency of 200 kHz. The Furuno echosounder was mounted on the port side of the vessel, with the 15º beam-width transducer located approximately 0.15 m (0.5 ft) below the water surface. Transects were spaced 38 m apart and vessel speed for surveying was approximately 3.5 kt. Positional data were collected with a Leica MX400 differential GPS and integrated with bathymetry every 1 sec. The area surveyed covered almost the entire southern end of San Diego Bay south of the Sweetwater River channel for a total area of 934 ha (2,309 ac). Corrections

to tidal elevations were made using a gauge located on the Navy Pier (Broadway Pier, Naval Supply Center).

Tenera Environmental surveyed about 218 ha (539 ac) adjacent to the discharge of the SBPP. This bathymetric survey provided bottom depths of the discharge area with centimeter horizontal and vertical accuracy using a BioSonics 200 kHz digital echosounder (8º beam-width transducer) with survey-quality base and roving GPS units. The base GPS was positioned on a San Diego Port Authority benchmark (J-Street Marina, Chula Vista, CA) for referencing soundings to MLLW.

During the Tenera survey of the discharge area, vessel speed was approximately 2 kt (1 m s^{-1}), and the area surveyed was transected approximately every 30 m (98 ft) nearest the discharge and to approximately 50 m (164 ft) over the mudflats and outside the breakwater (**Figure 2.5-1**). Two sets of tracks were made (right angles to each other) to provide a check on the quality of the soundings and to improve coverage. A channel adjacent to the CVWI and dikes was sampled more intensively. The transducer sounded at a rate of 5 pings per second. The pulse width was 0.2 msec. As a result, bottom contours from the depth data along transects were very detailed and with high resolution.

Vertical and horizontal positions in geographical coordinates (latitude and longitude) of the transducer were measured using base and rover GPS and Waypoint Consulting (Calgary, Alberta Canada) software. Base and rover systems consisted of a Canadian Marconi Corporation L1 GPS operating at 5 Hz, Novatel Pinwheel antenna, and Compaq iPaq datalogger that collected the GPS data including carrier phase. The base and rover systems were initialized for 20 minutes with two antennas mounted on tripods. The base GPS remained at a predetermined benchmark (at SBPP), and the rover was transferred to the vessel for the survey. A second 20-min set of static data was collected after the survey to provide redundancy in an event that a lock was lost on the GPS satellites and to increase position accuracy of the survey. The post-processed positions were very vertically accurate to centimeter-level precision. Vertical resolution of the echosounder was 1.9 cm (0.75 in) and its offset was measured using a 'barcheck' (13 cm disk) set at several depths.

In mapping, corrected soundings were referenced to mean lower low water (MLLW) by applying the vertical corrections supplied from Waypoint Consulting software. Coastline positions and respective elevation values were set to + 0.9 m (3 ft) MLLW for the analysis. Bathymetry elevation data from three sources were merged into one data set of elevation points. The survey areas and sources were: 1) 218 ha discharge embayment area (Tenera survey), 2) south bay, south of the Sweetwater River (Merkel & Associates, Inc.), and 3) Sweetwater River to Coronado Island narrows and the periphery of south bay unmapped by Tenera and Merkel & Associates, Inc. (US Navy 1994, from Merkel & Associates, Inc.). The Navy (1994) data, as provided, was evenly spaced on 15 m (49 ft) cells across the bay. This resolution became the base cell size used for a final surface

grid and Triangulated Integrated Network (TIN) creation, including subsequent bathymetry calculations. However, higher resolution spacing from the GIS was used for display and calculations.

A bottom grid (cell size of 15 m) was created from the merged data set in ArcGIS (ESRI, Inc.) using Inverse Distance Weighted (IDW) interpolation with a search radius of 12 points and power of two (2). Bottom contours in 0.3 m (1 ft) intervals were then derived from the resultant bottom grid and plotted in the GIS with a coastline theme that delineated reference breakwaters, piers and other recognizable features.

The bottom grid was also used to create a TIN layer in the GIS from which volume of the basin was calculated for current modeling purposes. TIN routines are of particular use in volume determinations for configurations that are not a simple straight layout, such as turning basins, settling basins, widening sections, and curved channels. The grid was used to determine water volume of the south bay (SBPP up to the Coronado Narrows). Volume determinations were made for various depth regimes: -10 ft to -5 ft, -5 ft to -2 ft, and remaining areas at 1 ft intervals, using the assumption that the shoreline is a vertical barrier, dike, or rip-rap. (see companion report *Volume 2: Compliance with Section 316(b) of the Clean Water Act (CWA); Section 2.3 – Source Water Volume*).

2.5.2.2 Current Surveys

In general, currents are a function of tides, wind, and localized flow inputs. Data on wind speed and direction were recorded by Merkel & Associates during May–September 2003. These data were collected from a temporary weather station on the Chula Vista Wildlife Island (CVWI) access dike near Station T2.

Water currents were measured in the discharge area using Acoustic Current Doppler Profilers (ADCP). ADCPs have become a preferred method for measuring currents. An ADCP measures the velocity of water using the physical principal called the Doppler shift. Sound is broadcast and received in three piezo-ceramic transducers, each measuring a Doppler shift in frequency. As particles in the water move away, the frequency of the reflected sound wave decreases. By comparing the three measurements, direction and speed can be estimated. By measuring the return signal at different times, the ADCP measures the water velocity at different distances from the transducer.

The bathymetric survey (above) provided bottom depths of the discharge embayment with centimeter horizontal and vertical accuracy. The discharge embayment was defined as the portion of South Bay east of a line from the Otay River mouth to the breakwater extending south from the CVWI (**Figure 2.5-1**). This area of approximately 131 ha (324 ac) at the +3 ft mean MLLW was surveyed using transects spaced at 10–15 m (33–49 ft). Water currents and bathymetry were also measured in an 87 ha (215 ac) area immediately outside the breakwater separating the discharge embayment from the greater South Bay area.

A survey of 19 stations sampled flood and ebb tide conditions in the discharge vicinity (**Figure 2.5-1**). A 2 MHz Nortek ADCP was used to sample the 19 stations two to three times each on August 4–6, 2003. The current meter, designed for measuring discharge current velocity, was mounted to a small floating platform called the 'BoogieDopp', which was secured to an anchored 4.5 m (14.8 ft) survey boat (**Figure 2.5-2**). The sensor recorded current speeds in 0.20 m (0.66 ft) depth increments from the surface to the bottom relative to the fixed direction of the survey boat. Two readings at each position were required to obtain current direction and to estimate current velocity. The first reading was taken with the axis of the BoogieDopp parallel to the anchored boat. The second reading was taken with the axis of the BoogieDopp set at nearly right angles to the survey boat. The paired speed and heading recordings were combined using the deviation θ from the ideal right angle relation between paired speed samples *S1* and *S2*. The equations for estimating speed *S* and relative heading ψ from the two measurements at each station were:

$$S = \sqrt{S_1^{\,2} + \left(S_2\left(\cos\theta + \sin\theta\tan\theta\right) - S_1\tan\theta\right)^2}$$

$$\psi = \cos^{-1}\left(\frac{S_1}{S}\right)$$

A second current study was done between July 17 and August 14, 2003 in the discharge channel at a location approximately 1 km (0.6 mi) from the discharge. Velocities were measured with a 1 MHz Sontek Acoustic Doppler Profiler (ADP, to distinguish from the Nortec ADCP) that was permanently fixed near the bottom (**Figure 2.5-3**) at an elevation of -2.40 m (-7.87 ft) relative to MLLW in the discharge channel (**Figure 2.3-1b**). The elevation of the ADP's head and piezo-ceramics was at -2.0 m (-6.6 ft) MLLW. The ADP was oriented pointing upward and recorded current vectors (east, north, and up) for five minutes each hour at a ping rate of 5 times per second. Current directions were stratified into 0.40 m (1.31 ft) elevation bins (the instrument's narrowest bin width capability). A 13.5° counter-clockwise rotation was required to move the reference frame from magnetic to true north (ºT).

The ADP had an instrument blanking range of 0.7 m (2.3 ft) from the transducer where data could not be taken due to the nature of the acoustic transmitter. At each measurement, the average, standard deviation, significant amplitude, and signal to noise ratio of the velocity vectors were recorded over 600 seconds. Significant amplitude of the acoustic return signal was monitored in each elevation bin to determine if the surface interfered with the measurements. Water surface detection was determined where the amplitude of the acoustic return increased, relative to the adjacent elevation bin. Tidal data used for graphical analysis of current measurements were based on predictions at National City by the computer program Tides and Currents (Nobeltec Corp., Portland, OR).

2.5.2.3 Current Speeds Determined From Discharge Embayment and Intake Channel Bathymetry

The plant flow contribution to current speed was approximated using cross-sectional areas in the discharge embayment and intake approach channel. Simplistically, current speed was estimated as flow divided by area. North-south bathymetry transects (**Figure 2.5-1**) provided detailed cross-section profiles of the discharge embayment and intake channel relative to MLLW to estimate water speeds influenced by power plant operation. The discharge transects were 325 m, 830 m, 1260 m, and 1,680 m (1,066, 2,723, 4,134, and 5,512 ft) from the discharge boom. The intake transects were approximately 40 m, 135 m, 260 m, and 450 m (131, 443, 853, and 1,476 ft) from the intake channel. The points of latitude and longitude were projected onto a straight-line and the cross-sectional areas below fixed tide levels were calculated. The cross-sectional areas were calculated for three tidal regimes: 1) mean water level (MWL, +0.93 m, 3.05 ft for south bay); 2) mean lower low water (MLLW, 0 m); and 3) extreme low water (ELW, -0.64 m, -2.1 ft). For the intake estimates, further projections (ψ) were necessary to depict the cross-section areas at right angles to the flow direction.

We estimated flow speeds (V) in the discharge and intake areas assuming full operation of the power plant (Q) (1,580 m^3 min^{-1} [417,400 gpm or 25 mgh]) and dividing that value by the projected cross-sectional area (A) for various tide conditions.

2.5.3 Results

2.5.3.1 Bathymetry

The bathymetry of the south bay area is characterized by gently sloping mudflat areas transected by dredged and natural channels (**Figure 2.5-5**). The SBPP withdraws water from a dredged intake channel (2.7 m, 9 ft MLLW) along the northern side of the CVWI and discharges the water along the southern edge of the Refuge, initially through a 15 m (50 ft) wide discharge channel. The depth of the 183 m (600 ft) long discharge channel is -3.8 m (-12.5 ft) MLLW. The channel continues along the southern edge of the CVWI and turns south along the CVWI breakwater. Much of the remaining area in the discharge embayment is shallower and bounded along the southern edge by a wide mudflat. Much of the mudflat lies below the mean water level (+0.8 m, +2.6 ft). Consequently, discharge water flows over the whole embayment mainly when tidal levels are above the mean water level.

The channel alongside the breakwater wraps around the breakwater tip and enters South Bay where the channel (-1.2 to -1.8 m, -4 to -6ft MLLW) widens and continues about 0.4 km (0.25 mi) in a northwest direction beyond the breakwater tip. Further west and north, the channel loses definition from the surrounding areas and the bathymetry becomes shallower (-0.6 to 0.9 m, -2 to +3 ft MLLW), but further away the area again deepens (-1.2 to -1.8 m, -4 to -6 ft).

2.5.3.2 Currents

Acoustic Doppler Current Profiler Surveys

Acoustic Doppler Current Profiler (ADCP) data were plotted to show the current vectors relative to the down-looking (BoggieDopp) survey locations for various tidal levels and cooling water discharge flows (**Figures 2.5-6a-d**). Data were collected from 0800 PDT August 4, 2003 to 0800 PDT August 6, 2003. The current velocities and average direction at each station during ebb, low, flood, and high tide conditions are listed in **Table 2.5-1**. The ADCP sampling occurred during two power plant operating conditions, on August 4 and 5 with five circulating water pumps (CWPs 1-2, 2-1, 2-2, 3-1 and 3-2) in service, and later on August 5 with an additional sixth CWP (4-1) in operation. The complete data set for all depth bins is presented in **Appendix F**.

Ebb Tide: Nineteen locations were sampled during ebb tide conditions: at six locations when five CWPs were operating and discharge flow was 54,870 m^3 h^{-1} (14.5 mgh); and at 13 locations when six CWPs were operating and the discharge flow was 70,410 m^3 h^{-1} (18.6 mgh). As expected during ebb tide, the general flow was out of the discharge embayment (back bay) towards deeper water to the north. Differing power plant discharge volumes did not appear to greatly change current velocities at the locations monitored (**Figure 2.5-6a**). For example, at Station F4 near the breakwater, current velocities were similar under the two discharge flow conditions. The current velocities at Station F4 were also among the highest 26 cm s^{-1} (0.9 fps). Station T4 at southernmost point of the CVWI was unique in measuring slightly different current patterns under the two discharge flows. This may be related to slight differences in the position of this station between the two sampling periods, differences in tidal flows between the two ebb tide conditions, and differential effects of the two discharge flow volumes, including effects of counter-eddies in the area of the point. Currents also followed the channel that runs along the southern edge of the CVWI (e.g., at Station E5). Lowest current velocities were recorded at Stations CP5 and CP9 where the water recedes off the mud flats during ebb tide.

Low Tide: Current sampling during low tide conditions (at or near slack tide) was restricted to only our deeper stations (**Figure 2.5-6b**). Six stations were sampled when the discharge flow was 18.6 mgh, three of which were also sampled when the SBPP discharge flow was 14.5 mgh. Different levels of discharge volume at or near slack low tide did not result in large differences in current velocities and direction at Stations E3 and E4 located farthest from the SBPP. In contrast, the onset of flooding tide and its effect on currents was measured at Station F3 near the breakwater of the Wildlife Refuge. There, currents flowed toward the power plant with the onset of flood tide, but at slack low tide and with greater discharge volume, currents flowed away from the power plant. Current direction and velocity measurements at Stations CP11, CP12, and CP13 during slack low tide were variable.

Flood Tide: Currents during flood tide were measured at eleven stations when the SBPP discharge flow was 14.5 mgh (**Figure 2.5-6c**). Currents at stations in the channel along the southern side of the CVWI (Stations E5 and T5) flowed in a westerly direction, influence by the discharge flow. This is similar to the current patterns observed at the same stations during ebb tide (**Figure 2.5-6a**). In contrast to outward flowing currents during ebb tide, currents at all stations (excluding T4) during flood tide flowed in an easterly direction towards the power plant (**Figure 2.5-6c**). Station T4 again showed a low (1 cm s^{-1}, 0.03 fps) velocity current in variable directions. This may have been the result of a counter-eddy effect similar to that observed during ebb tide at that location (**Figure 2.5-6a**).

In general, it appears that flooding tides may direct the discharge flow towards the southern edge of the Wildlife Refuge, whereas ebbing tides may allow the discharge flows to be more dispersed across the discharge embayment. Also, our flood tide sampling did not detect any water exiting the discharge embayment. This indicates that discharge water may not fully exit the discharge embayment during strong rising tides, particularly when discharge volumes are reduced. The currents during flood tide sampling may have been influenced slightly by the wind, because wind velocities were highest during this period and coming from the northwest (**Table 2.5-1**). This would have reduced the westerly current flows and enhanced the easterly flows.

High Tide: Five stations were sampled just prior to the peak of the high tide when the SBPP discharge flow was 54,870 m^3 h^{1} (14.5 mgh) (**Figure 2.5-6d**). In general, Stations M18, T2, and T3 showed marked decreases in bayward current velocities as the high tide peaked compared to the velocities recorded at the same locations during the ebb tide (**Figure 2.5-6a**). In contrast, Stations E7 and CP6 did not appear to be influenced in the same manner by the incoming tide.

Acoustic Doppler Profiler (ADP) Monitoring

The acoustic doppler profiler was located at an elevation of -2.4 m (-7.9 ft MLLW (**Figure 2.5-1**). The first data bin was centered at -1.1 m (-3.6 ft) MLLW with bins above every 0.4 m (1.3 ft). A time series graph of average speed, tide, and SBPP cooling water flow from July 17 through August 14 (**Figure 2.5-7**) showed that the highest current speeds are generally associated with the largest changes from high to low tide. Time series analysis showed that the autocorrelation functions of current speed and direction had highest correlations at 24–25-hour intervals with significant correlations at 12-hour intervals, typical of the mixed tidal cycle (**Figure 2.5-8**). The cross-correlation functions of current speed versus tide showed a one-hour lag to the lowest correlation indicating that the lowest speeds occurred an hour after high tides and that the highest speeds occurred at low tides (**Figure 2.5-8**).

The strongest currents near the south bank of the CVWI flowed in the direction 239°T (southwest) and occurred at low tide (**Figure 2.5-9**). The figure shows all vectors in depth bins and indicates that the largest vectors (strongest currents) were at the seafloor and the smallest at the surface.

Table 2.5-1. Current measurements at ADCP stations during different tidal levels and discharge volume conditions.

Date	Time PST	Station Location	Tide Level (ft MLLW)	Discharge Volume (mgh)	Avg. Current Velocity (cm s^{-1})	Avg. Current Heading (°T)	Water Depth (m)	Wind Speed (kph)	Wind Direction (°Mag)
8/4/03	17:28	E3	ebb 3.7	14.5	14	5	1.99	18.9	290
“	17:55	E4	“ 3.3	“	6	27	1.83	20.6	284
“	18:28	CP6	“ 2.8	“	8	274	0.85	21.2	292
“	19:06	T3	“ 2.2	“	14	256	1.49	16.2	287
“	19:25	T4	“ 2.0	“	2	245	1.17	17.3	281
“	19:50	F4	“ 1.8	“	26	252	1.84	15.4	296
8/5/03	9:03	E4	low 2.0	“	2	58	1.62	14.1	280
“	9:24	E3	“ 2.2	“	3	149	1.75	11.9	244
“	9:49	F3	“ 2.4	“	3	151	2.03	13.5	271
“	10:05	F4	flood 2.5	“	7	115	2.30	16.1	273
“	10:21	CP12	“ 2.7	“	6	140	1.18	17.0	266
“	10:34	CP13	“ 2.9	“	6	131	1.39	17.2	264
“	10:49	CP11	“ 3.0	“	2	138	1.20	16.5	245
“	11:04	CP3	“ 3.3	“	5	144	1.16	17.3	274
“	11:29	CP9	“ 3.6	“	3	98	0.82	20.6	288
“	11:47	CP8	“ 3.9	“	4	40	1.35	20.1	280
“	12:08	T5	“ 4.2	“	5	282	2.61	18.9	281
“	12:24	E5	“ 4.5	“	7	299	3.26	21.5	274
“	12:47	T4	“ 4.8	“	1	292	1.90	23.5	290
“	13:06	CP5	“ 5.1	“	3	38	1.21	22.0	258
“	13:27	T3	high 5.4	“	5	262	2.01	21.8	284
“	13:44	M18	“ 5.5	“	2	318	1.38	21.5	260
“	14:03	T2	“ 5.7	“	5	284	3.91	23.3	281
“	14:22	E7	“ 5.9	“	11	260	3.42	21.8	280
“	14:38	CP6	“ 5.9	“	6	292	1.44	25.1	285
“	17:59	CP3	ebb 4.4	18.6	6	334	1.30	17.2	264
“	18:16	CP9	“ 4.1	“	2	89	0.84	18.0	276
“	18:33	CP5	“ 3.8	“	2	290	0.79	17.0	278
“	18:50	M18	“ 3.5	“	7	213	0.65	15.7	285
“	19:06	CP6	“ 3.2	“	4	273	0.63	14.1	287
“	19:22	E7	“ 2.9	“	13	266	2.44	14.3	291
“	19:43	T2	“ 2.6	“	18	267	2.05	13.0	291
“	19:59	T3	“ 2.3	“	25	253	2.13	14.8	295
“	20:17	T4	“ 2.0	“	4	170	1.69	12.3	281
“	20:40	CP8	“ 1.7	“	14	254	0.61	14.0	290
“	20:57	E5	“ 1.5	“	13	288	1.63	13.5	295
“	21:19	T5	“ 1.2	“	3	260	2.97	12.3	290
“	21:38	F4	“ 1.1	“	26	264	1.86	10.4	283
“	21:56	CP12	low 0.9	“	2	288	0.59	6.4	271
“	22:15	CP13	“ 0.9	“	6	153	0.78	2.7	6
“	22:33	CP11	“ 0.8	“	5	301	0.58	5.0	281
“	22:54	F3	“ 0.8	“	7	291	1.59	6.4	45
“	23:15	E3	“ 0.9	“	6	129	1.37	1.6	64
“	23:31	E4	“ 0.9	“	3	55	1.35	0.6	79

DRAFT

The month long current time series data (**Appendix G**) were visualized with temperatures for Stations ST3, ST4 and SE5 using animation software. The animation shows a strong relationship between tides, currents, and temperature stratification, especially when power plant operation is high. Interestingly, bottom and surface vectors are often directed in different directions, mainly at times of lower high water and near high tide when the tidal shift is generally smallest and when currents are slowest overall. It is important to note that the standard error (standard deviation of the east and north vector magnitude components) was 2.8 cm s^{-1} (0.09 fps), indicating that slower speeds have less confidence of value. The direction components from slower current speeds will also have less confidence.

We plotted temperature, current speed, and direction associated with conditions 2 hours in advance of the two high and low tides (**Figure 2.5-10)**, during slack tides (**Figure 2.5-11)**, and 2 hours after each of the four tides (**Figure 2.5-12)**. Closest correspondence for current direction and speed occurred with the two low tide conditions. The maximum current speed flowed to the southwest (away from the SBPP) before, during, and after the low low tide conditions. Similar current directions occurred but with slower speeds during the high low tide conditions. Current directions were most variable and reversed over the time spanning two hours before and after the low high and high tide conditions.

2.5.3.3 ADCP and ADP Results Compared to the TRIM-2D Model

Although the ADCP measurements and modeling results were not identical in tidal levels, in general, the 'BoogieDopp' ADCP measurements reveal similar current patterns constructed by the TRIM-2D models (**Figures 2.5-13** and **14**). Slight differences between the field and modeling results may also be due, in part, to the TRIM-2D simulations being based on a SBPP cooling flow of 25 mgh, while cooling water flow during the ADCP measurements was lower (14.5 to 18.6 mgh).

Ebb Tide: The ADCP current vectors for ebb tide (**Figure 2.5-6a**) show the same general pattern as the TRIM-2D current model (**Figure 2.5-13**). Currents are relatively well defined near the tip of the CVWI breakwater and in other areas where the general movement of currents follow the outgoing tidal direction. The ADCP station vectors measured at slow current areas (Stations CP5 and CP9, **Figure 2.5-6a**) are consistent with the reduced current speeds of the model.

Low Tide: The ADCP current vectors for low tide (**Figure 2.5-6b**) also show the same general trend as the TRIM-2D current model (**Figure 2.5-13**). The currents were mixed in direction outside the breakwater (Stations E3 and E4, **Figure 2.5-6b**). The TRIM-2D model shows this area to also be low in current velocities and with poorly defined direction (**Figure 2.5-13**). The low current speeds in the areas of ADCP Stations CP11, CP12, and CP13 (**Figure 2.5-6b**) are also reflected in the model. The mixed current

directions at Station F4 (**Figure 2.5-6b**) may be the result of the field data being collected on both sides of the low tide.

Flood Tide: Flood tide measurements of the TRIM-2D model show weak currents inside the discharge embayment (**Figure2.5-14**). Stations CP5, CP8, and CP9 were within the central portion of the discharge embayment (**Figure 2.5-6c**) where current velocities were slow, ranging between 3 and 4 cm s^{-1} (0.10 - 0.13 fps) (**Table 2.5-1**). The TRIM-2D model also shows no large movement of water out from the discharge embayment into the greater San Diego Bay. Similar results were revealed in the ADCP measurements (**Figure 2.5-6c**). The ADCP field measurements differed from the TRIM-2D model in revealing a slow westerly current flow along the southern edge of the Wildlife Refuge. The TRIM-2D model showed this area to be poorly defined in current direction and velocities.

High Tide: Only the near discharge area can be compared between the ADCP measurements (**Figure 2.5-6d**) and the modeled vectors (**Figure 2.5-14**). At high tide, ADCP currents near the discharge were generally similar to the modeled vectors. However, Stations T2, CP6, and M18 had a north component not evident in the model. The model reveals the change from relatively quiescent water in the discharge embayment during flood tide (**Figure 2.5-14**) to the onset of outward (westerly) flows at peak high tide, influenced by the discharge.

2.5.3.4 Current Speeds Determined From Discharge Embayment and Intake Channel Bathymetry

The seafloor topography of the discharge embayment and intake channel is used here as another source to determine the contribution of power plant flows to current velocities. The bathymetry profiles at the intake and discharge transects are presented in **Figure 2.5-15**. We use these data for calculating current velocities attributed to SBPP cooling flow for various tidal levels (**Table 2.5-2**).

In the discharge embayment, the cross-section analysis (**Figure 2.5-15**) shows the details of the broad plain and gentle sloping bottom (+0.6 to -0.3 m, +2 to -1 ft MLLW) over the majority of the embayment to within about 30 m (100 ft) of the Wildlife Refuge. The embayment is completely covered at MWL. A deep trench (-7 ft MLLW) is close to the southern edge of the CVWI shore and breakwater.

At tide levels above MLLW, the volume of water leaving the power plant adds to gentle flowing waters (2–15 cm s^{-1}, 0.06–0.49 fps) over the most of the area (**Table 2.5-2**). As the tide level drops, the speed of the discharge water increases from the increasingly smaller confines of the embayment. At extreme low tides the flow is concentrated near the trench area, and estimated current speeds exceed 1.5 knots (88 cm s^{-1}) at the lowest tides (-0.5 to -0.6 m, -1.7 to -2.1 ft MLLW).

The estimated high current speeds through the cross-sections correspond well with the ADP measurements collected near Station T4 (**Figure 2.5-7**, **Table 2.5-1**). The ADP measured current speeds in excess of 50 cm s^{-1} during full discharge flow (25 mgh) and low tides (-0.2 to -0.4 m, -0.6 to -1.3 ft MLLW) on August 8–13, 2003. The estimates of current speed at ELW exceed any measured by the BoogieDopp ADCP because the lowest tides (+0.24 m, +0.8 ft) never dropped below MLLW during the field survey.

Table 2.5-2. Cross-section areas and estimated current speeds at locations in the SBPP discharge embayment and intake channel with cooling water flow of 1,580 m^3 min^{-1} (25 mgh). (ELW, -2.1 ft MLLW; MLLW, 0 ft; MWL, +3 ft MLLW).

	Estimated Area (m^2)			Flow Rate (cm s^{-1})		
	ELW	MLLW	MWL	ELW	MLLW	MWL
Intake*						
I - 1	158	206	-	17	13	-
I - 2	177	238	-	15	11	-
I - 3	172	237	-	15	11	-
I - 4	168	256	-	16	10	-
Discharge						
D - 1	48	76	176	54	35	15
D - 2	40	79	452	66	33	6
D - 3	30	140	1053	88	19	3
D - 4	105	317	1195	25	8	2

* Estimated areas are projected to the right angle of flow
\- No bathymetry data reaching MWL

The intake channel is much deeper than the discharge channel (**Figure 2.5-15**). Because of the deeper bathymetry, the cross-sectional areas are greater and current speeds are much slower during any tide level compared to discharge bay speeds (**Table 2.5-2**). The greatest estimated current speed in the intake channel at ELW is 17 cm s^{-1} (0.56 fps) or less. No comparative real-time (ADP or BoogieDopp® ADCP) intake channel current speed measurements were collected because current monitoring focused on the discharge area.

2.5.3.5 SBPP Discharge and Tidal Prism Volumes

It is useful to put the water volume used by the SBPP in context with tidal exchanges and water volumes of San Diego Bay. The volume of the discharge embayment was determined for several tidal levels in ArcGIS (**Table 2-5.3**). The tidal layers provided a means to estimate the tidal volume or tidal prism. Typically, the tidal prism is defined as the volume of water between the MLLW (0 m) and MHHW (+1.8 m) levels. The tidal levels used for the prism were presented as part of the Source Water description for Region 4 (South Bay) in the companion report *Volume 2 – 316(b) Demonstration Study* (see *Appendix A, Table 2d*). The tidal prism for the discharge embayment was calculated to be 1,958,394 m^3 (69,160,006 ft^3). The SBPP cooling water flow at full operation (2,275,200 m^3 d^{-1}, 601 mgd) represents 116 percent of the tidal prism.

The maximum volume of water drawn and discharged by the SBPP with all eight circulating water pumps in operation is 0.8 percent of mean total bay volume and 3 percent of the bay's daily tidal prism (see *Volume 2 – 316(b) Demonstration Study Appendix A, Section 2.5*). The tidal prism for Region 4 (south bay) is 16,562,246 m^3 (584,975,209 ft^3) (*Volume 2 – Appendix A, Table 12d*). Full cooling water volume in the Region 4 represents 14 percent of its volume.

Table 2.5-3. Area and volume of SBPP discharge embayment for various tidal heights. (MHHW, mean higher high water; MHW, mean high water; MTL, mean tide level; MWL, mean water level; MLW, mean low water; MLLW, mean lower low water)

Tide	Elevation (MLLW)		Embayment 2-D Area		Embayment Volume	
Level	ft	m	ft^2	m^2	ft^3	m^3
	6.00	1.83	13,208,934	1,227,150	78,461,894	2,221,794
MHHW	5.91	1.80	13,208,934	1,227,150	77,273,090	2,188,131
MHW	5.19	1.58	13,208,934	1,227,150	67,762,658	1,918,825
MTL	3.06	0.93	12,855,321	1,194,298	39,675,785	1,123,493
MWL	3.05	0.93	12,845,799	1,193,414	39,547,419	1,119,858
MLW	0.94	0.29	9,172,876	852,188	15,450,084	437,498
MLLW	0.00	0.00	6,250,318	580,673	8,113,084	229,737
	-5.00	-1.52	360,712	33,511	287,887	8,152
	-10.00	-3.05	4	0	0	0

DRAFT

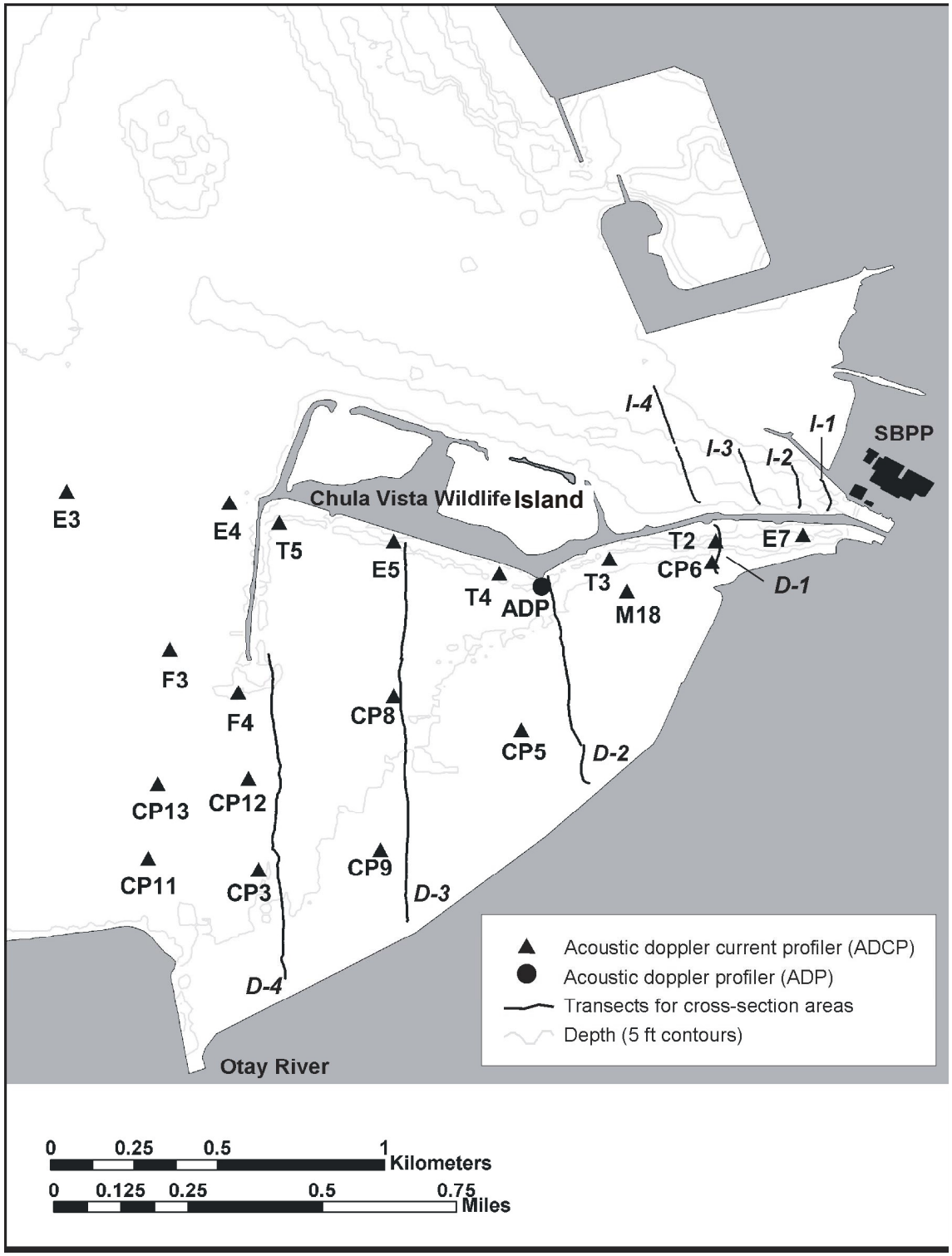

Figure 2.5-1. Locations of the ADCP and ADP sampling stations and transects for cross-section bathymetry profiles of the discharge embayment and intake channel.

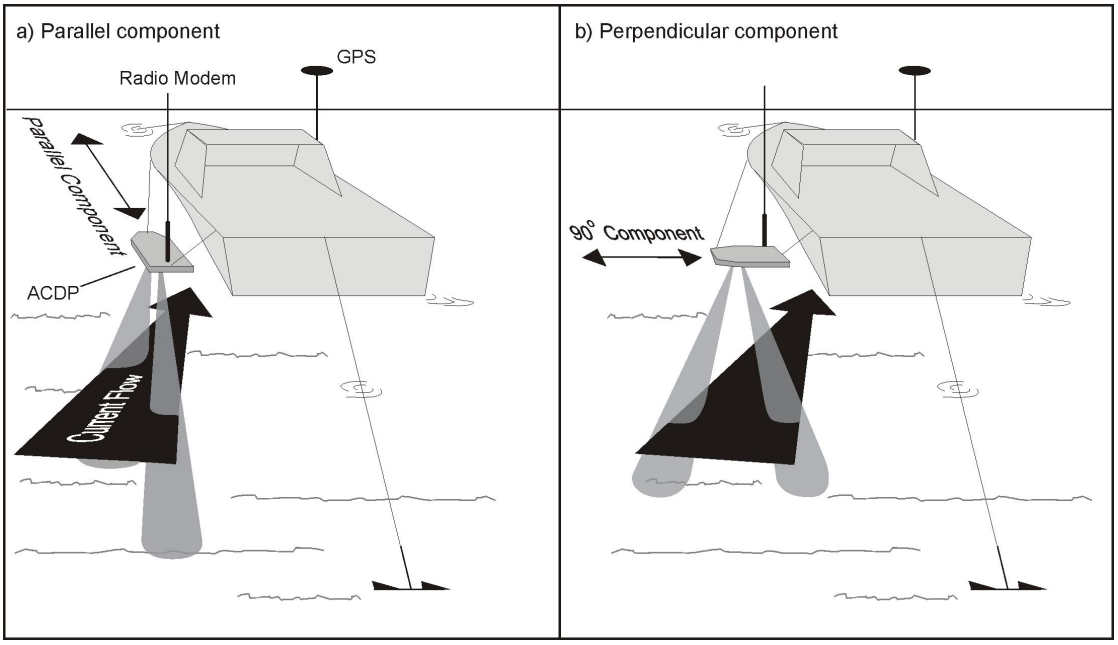

Figure 2.5-2. Acoustic doppler current profiler (ADCP) tethered to anchored survey boat. The two orientations of the ACDP shown in 'a' and 'b' were used to obtain current direction and velocity at various depth increments for each anchored position.

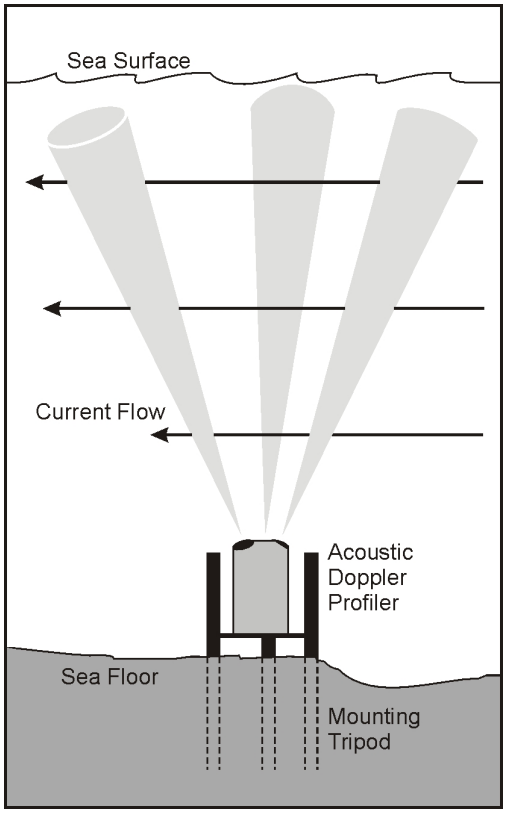

Figure 2.5-3. Acoustic Doppler profiler mounted at fixed position.

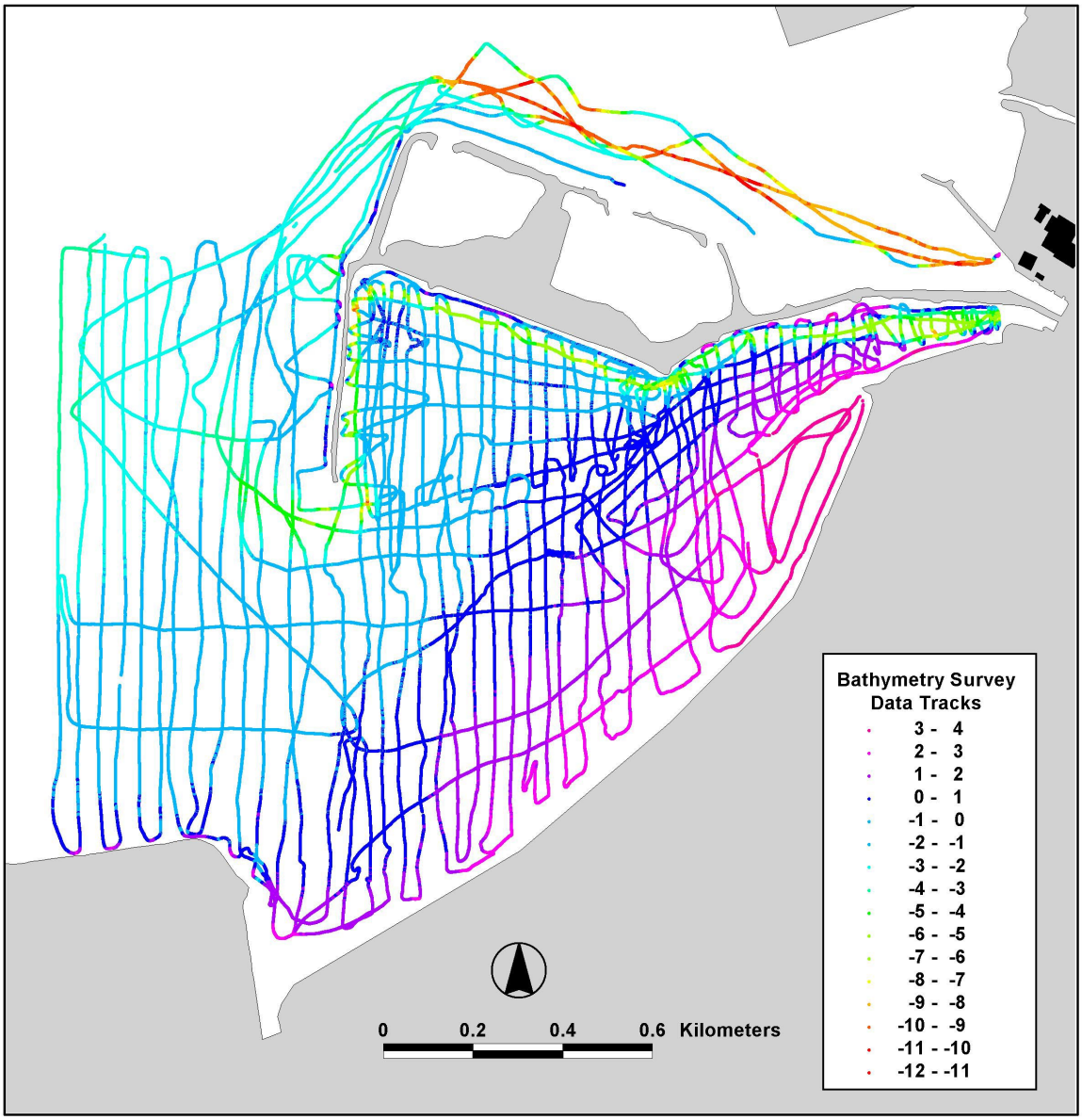

Figure 2.5-4. Tenera bathymetry survey tracks in the SBPP vicinity, July 16–17, 2003.

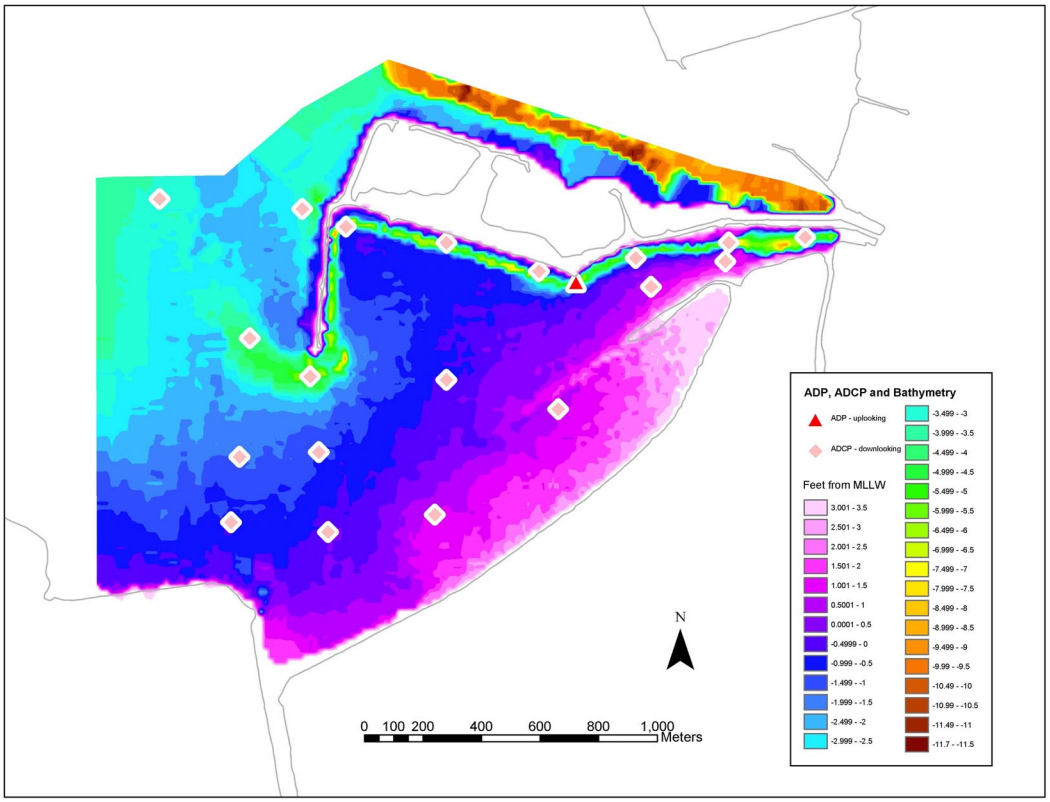

Figure 2.5-5. Bathymetry in the SBPP vicinity and locations of current sampling. Red triangle, up-looking Acoustic Doppler Profiler station; Diamonds, down-looking Acoustic Doppler Profiler stations.

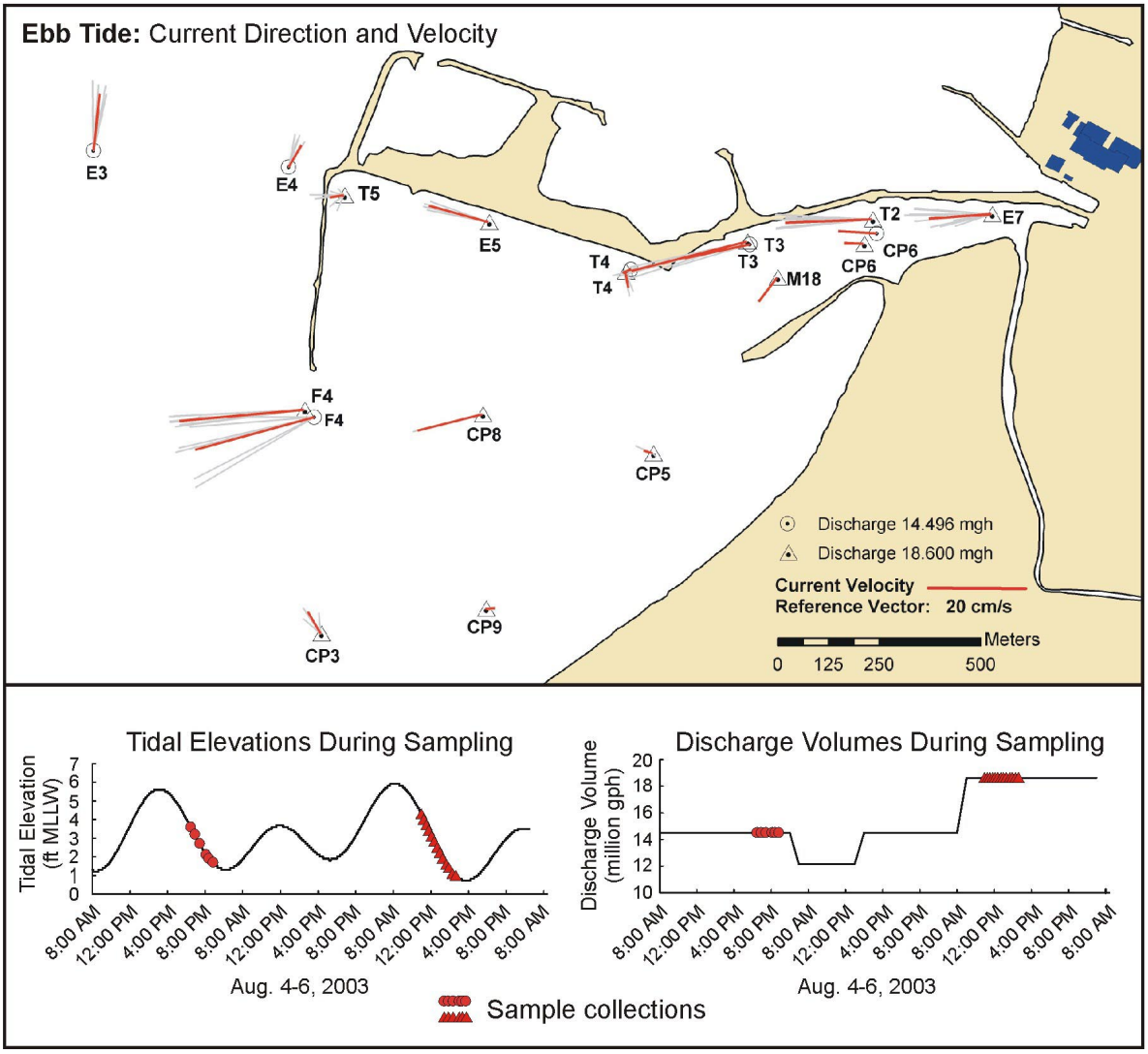

Figure 2.5-6a. Current direction and velocity during ebb tide sampling.

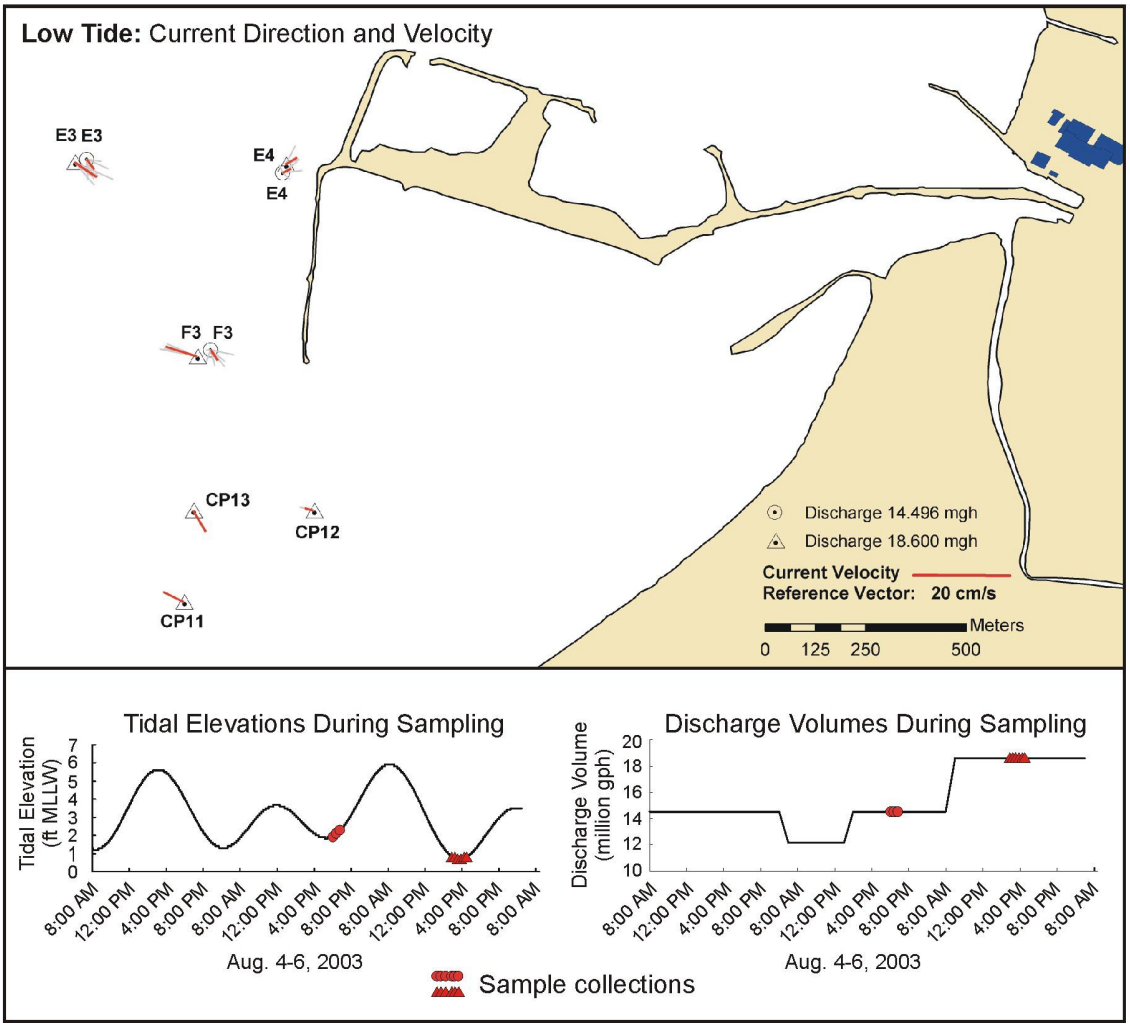

Figure 2.5-6b. Current direction and velocity during low tide sampling.

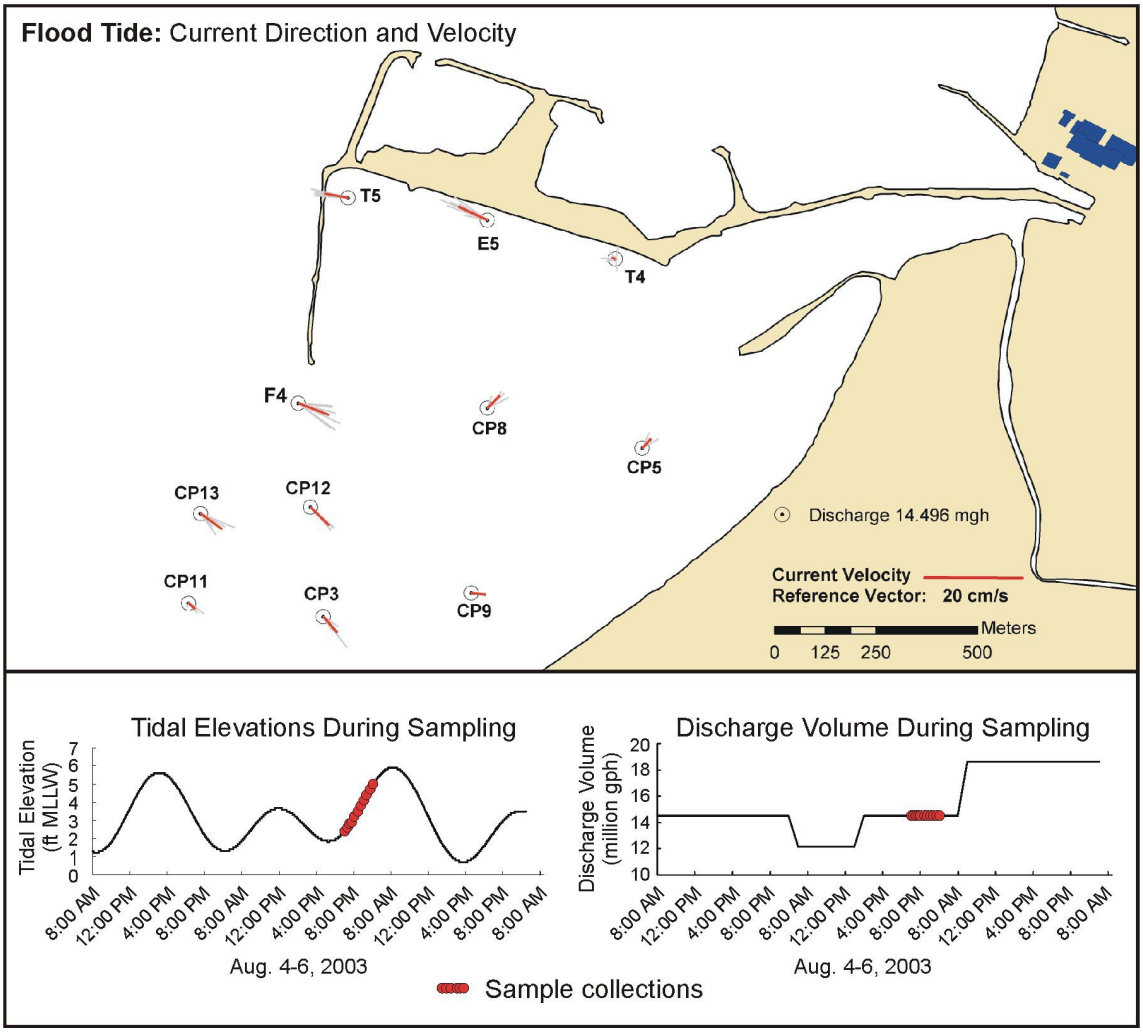

Figure 2.5-6c. Current direction and velocity during flood tide sampling.

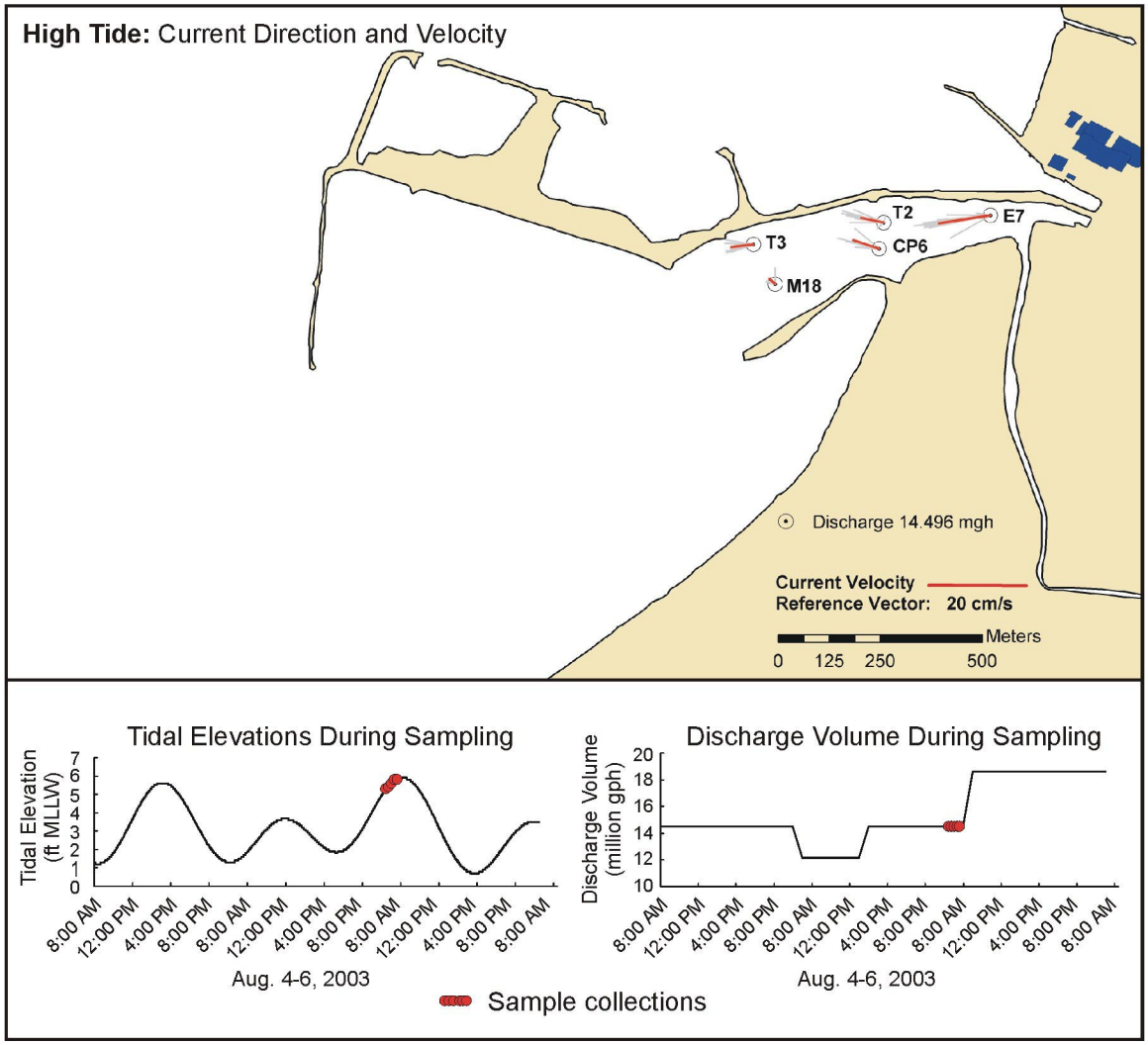

Figure 2.5-6d. Current direction and velocity during high tide sampling.

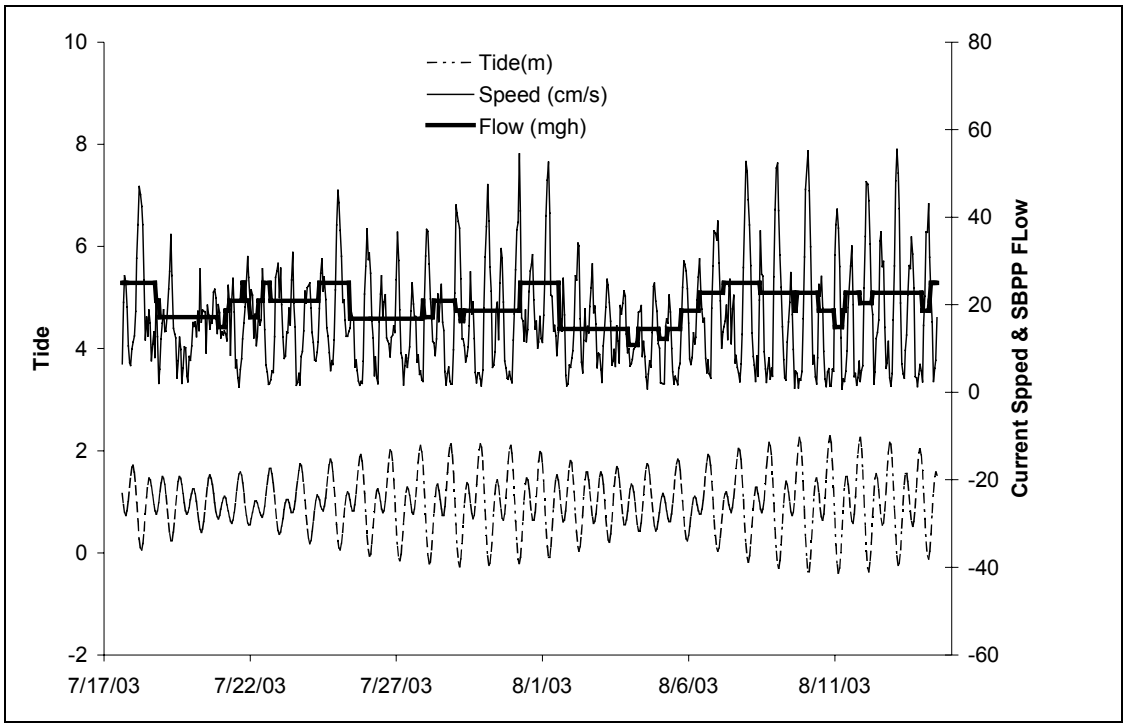

Figure 2.5-7. Time series of tide changes, hourly water column average speeds measured by the Acoustic Doppler Profiler, and discharge flow.

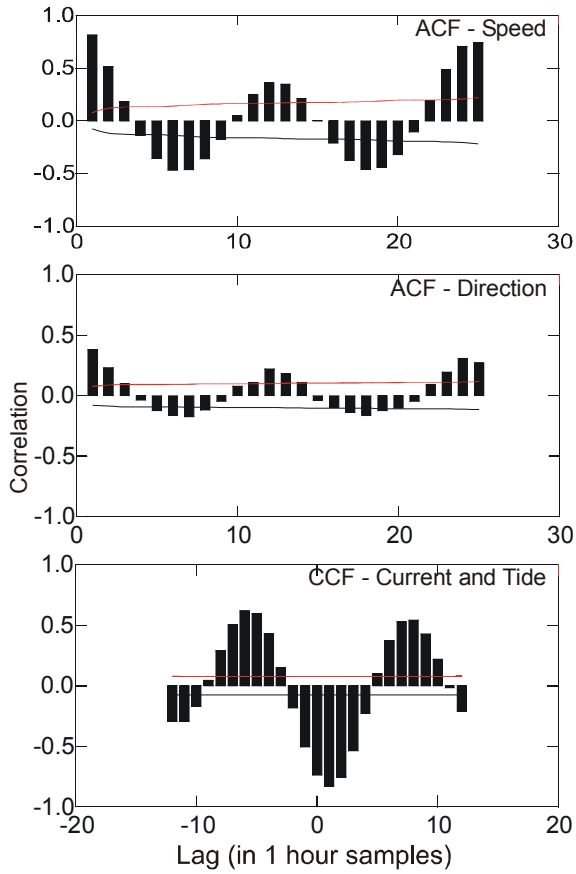

Figure 2.5-8. Autocorrelation functions (ACF) for current speed (top graph) and direction (middle graph), and cross-correlation functions (CCF) for current speed versus tide (bottom graph).

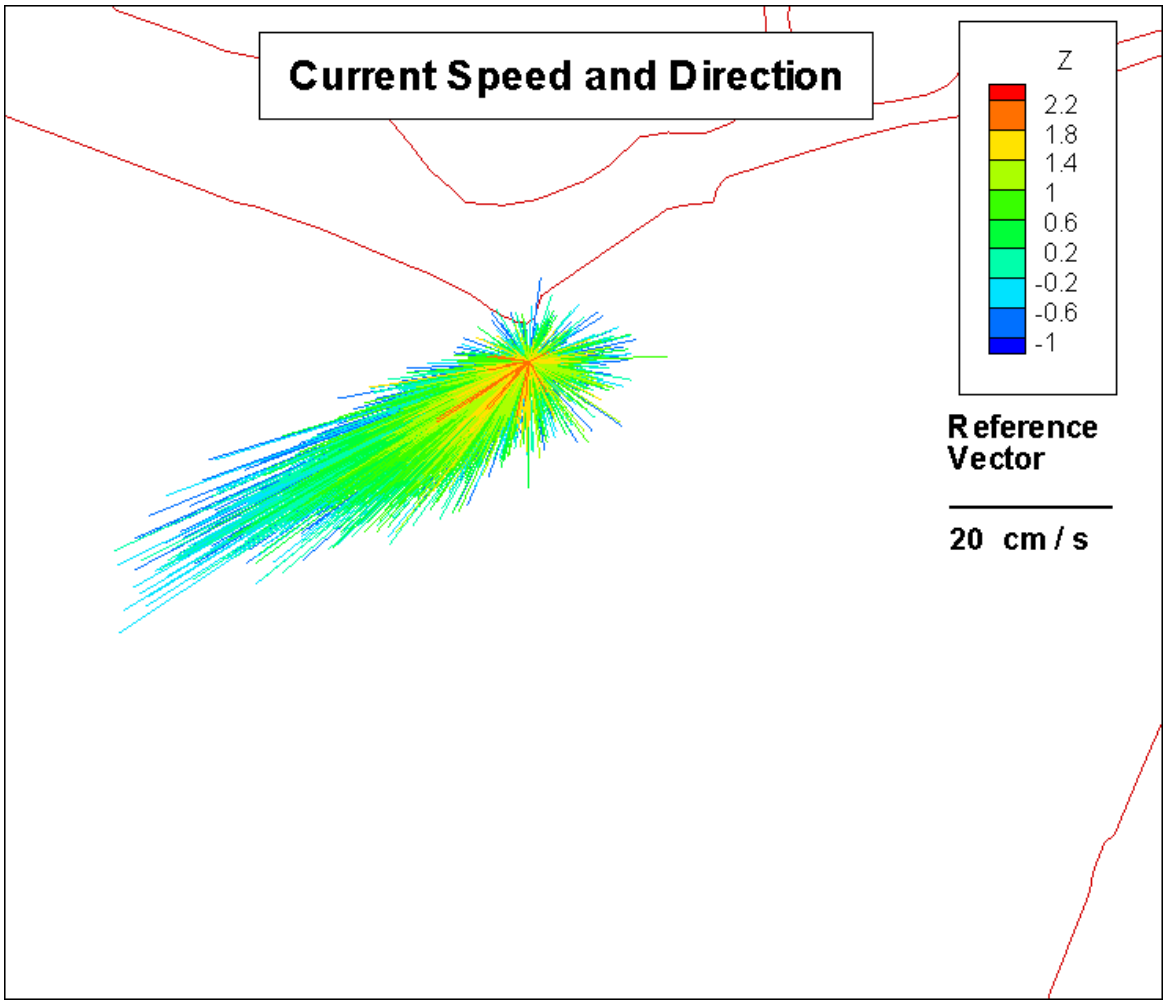

Figure 2.5-9. Current speed and direction at several depths at the ADP current meter station located approximately 0.82 km (0.51 mi) downstream from the SBPP discharge boom. Vectors represent hourly measurements, July 17 through August 14, 2003. Elevation (Z) is in meters relative to MLLW.

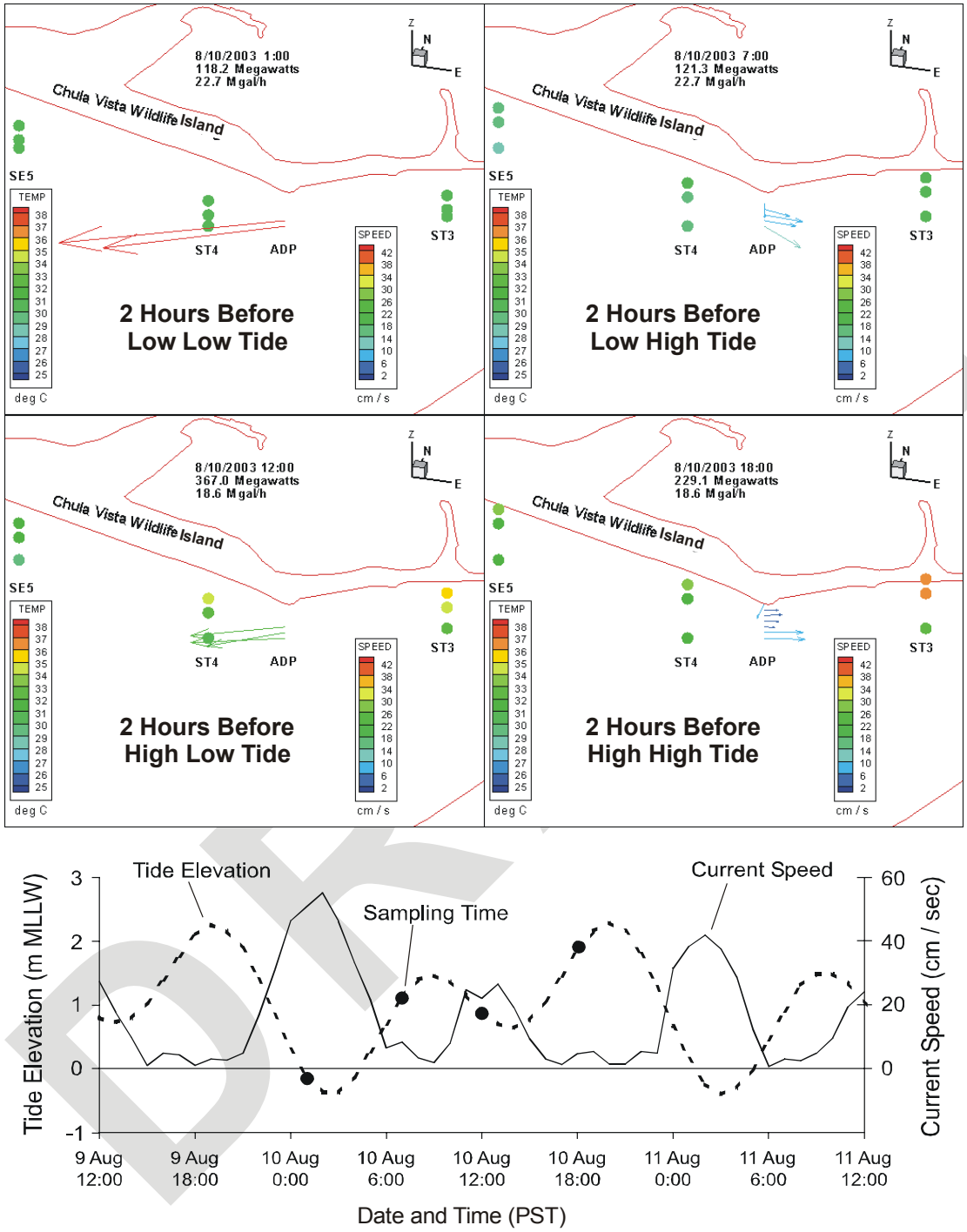

Figure 2.5-10. Current speeds and directions (Acoustic Doppler Profiler station) and temperatures (Stations ST3, ST4 and SE5) two hours before the two high and two low tides. Black circles on the tidal curve depict the sampling times. Colored balls depict temperatures at surface, -1 m, and bottom. Arrows indicate current directions and speed from the surface to bottom.

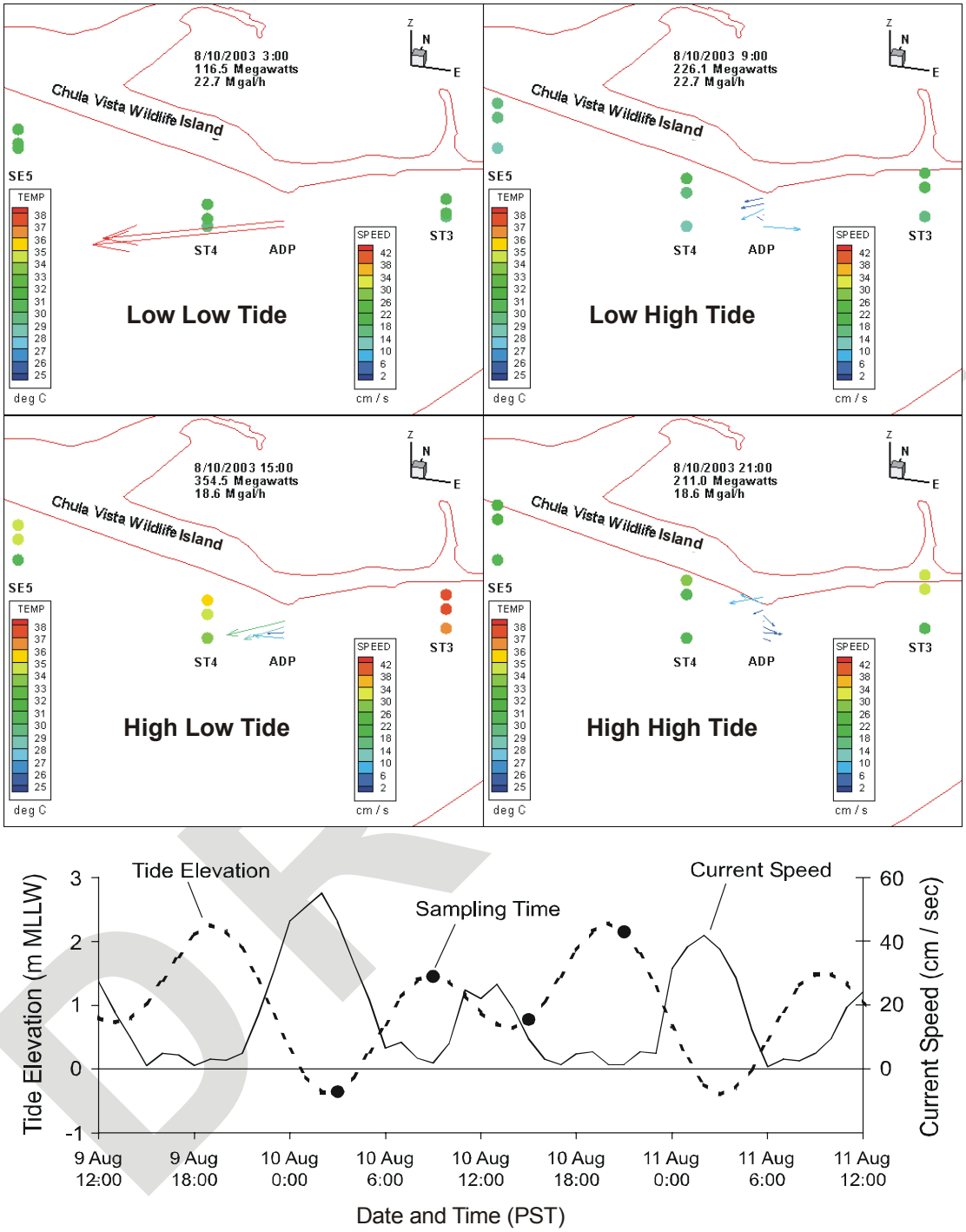

Figure 2.5-11. Current speeds and directions (Acoustic Doppler Profiler station) and temperatures (Stations ST3, ST4 and SE5) during the four slack tides. Black circles on the tidal curve depict the sampling times. Colored balls depict temperatures at surface, -1 m, and bottom. Arrows indicate current directions and speed from the surface to bottom.

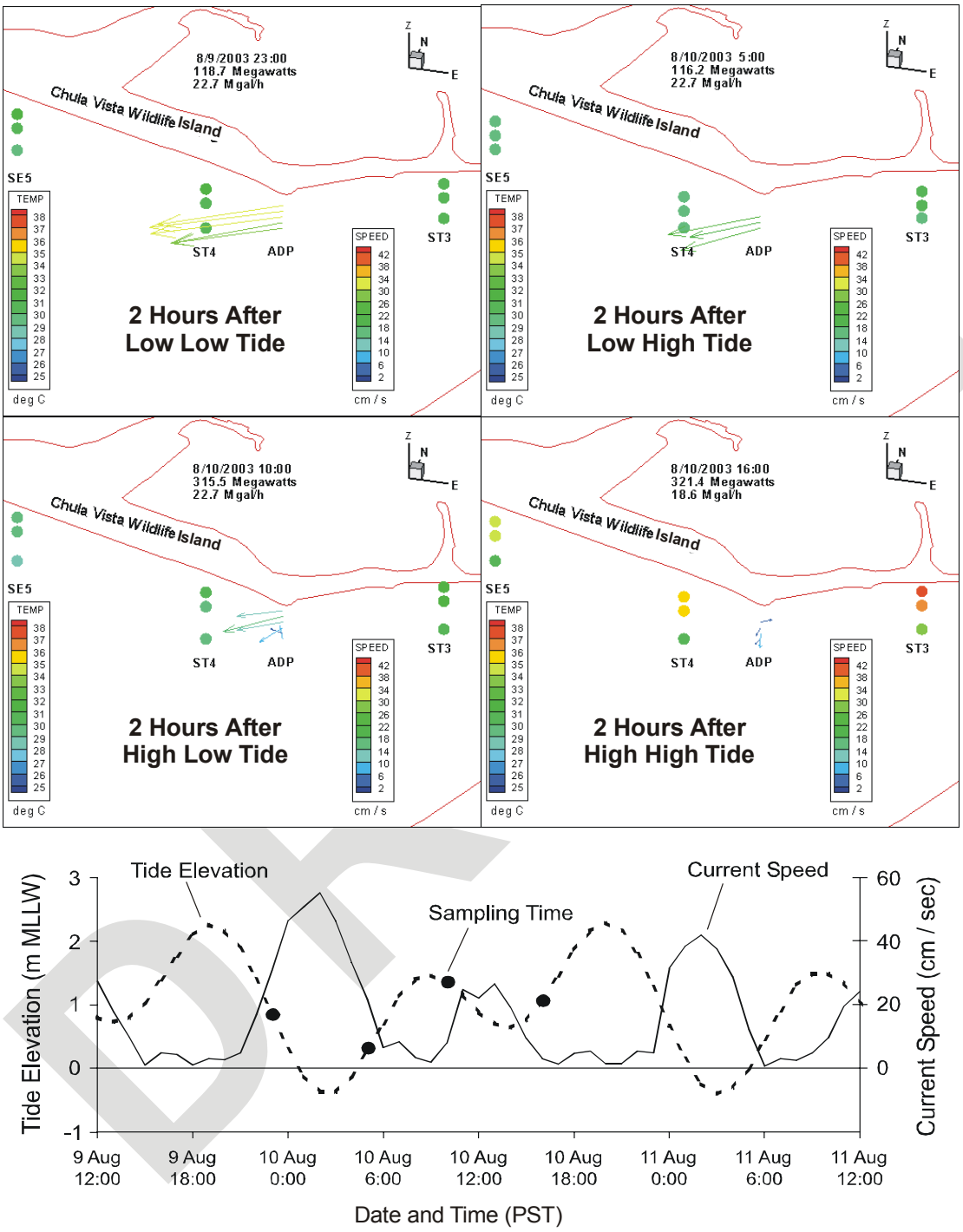

Figure 2.5-12. Current speeds and directions (Acoustic Doppler Profiler station) and temperatures (Stations ST3, ST4 and SE5) two hours after the two high and two low tides. Black circles on the tidal curve depict the sampling times. Colored balls depict temperatures at surface, -1 m, and bottom. Arrows indicate current directions and speed from the surface to bottom.

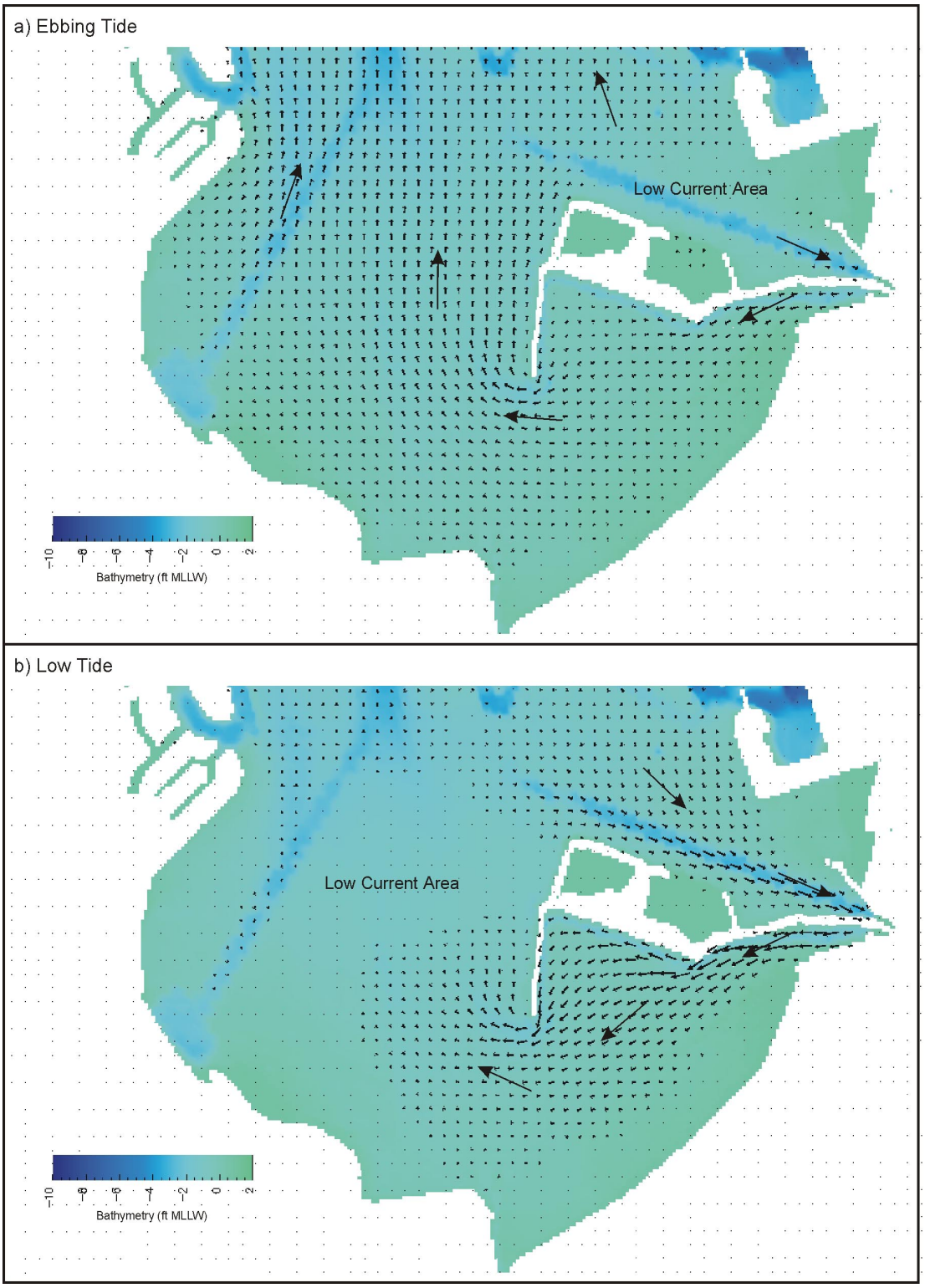

Figure 2.5-13. General current directions during: a) ebbing tide; b) low tide, superimposed on the TRIM-2D computational model.

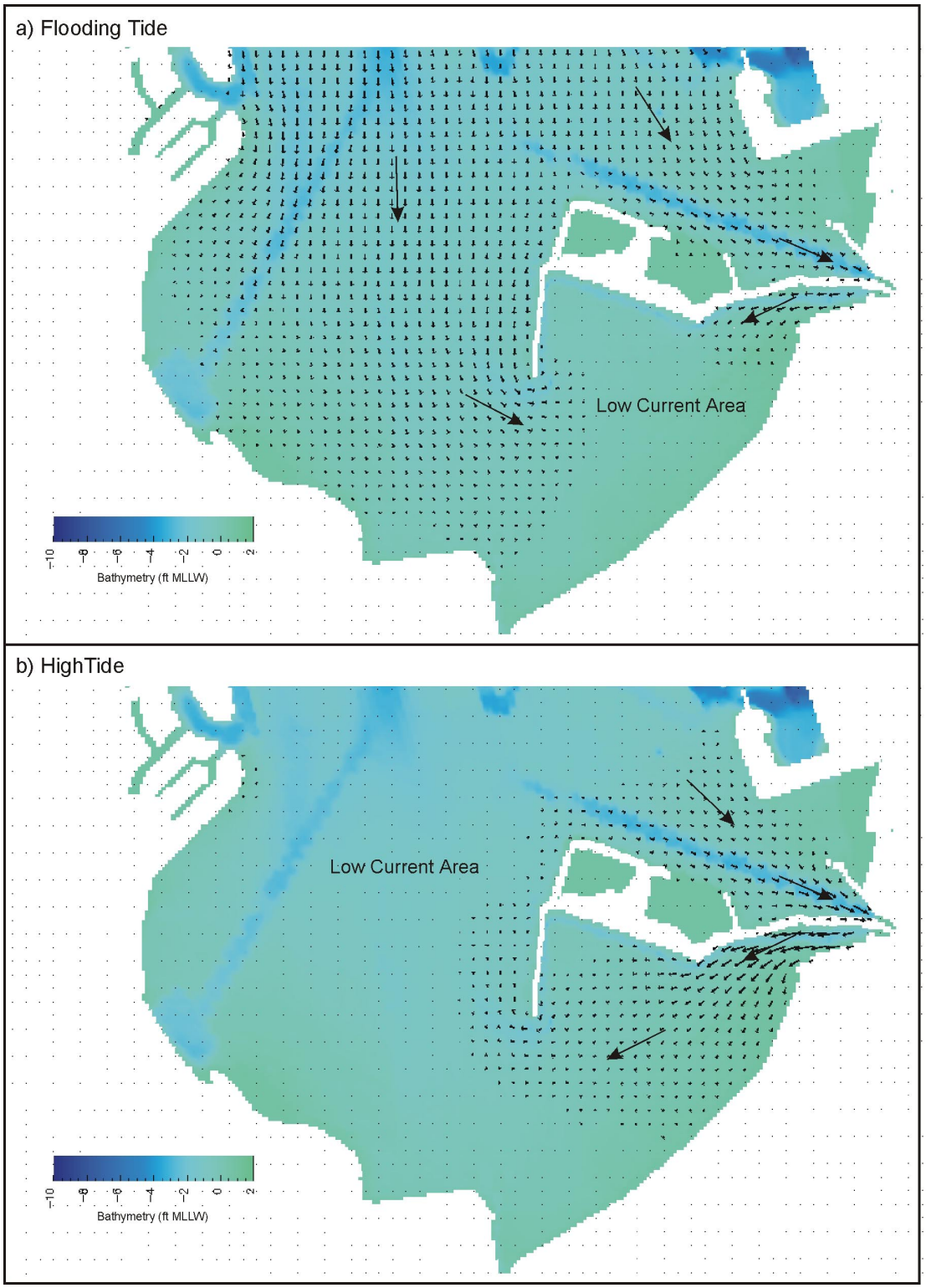

Figure 2.5-14. General current directions during: a) flooding tide; b) high tide, superimposed on the TRIM-2D computational model

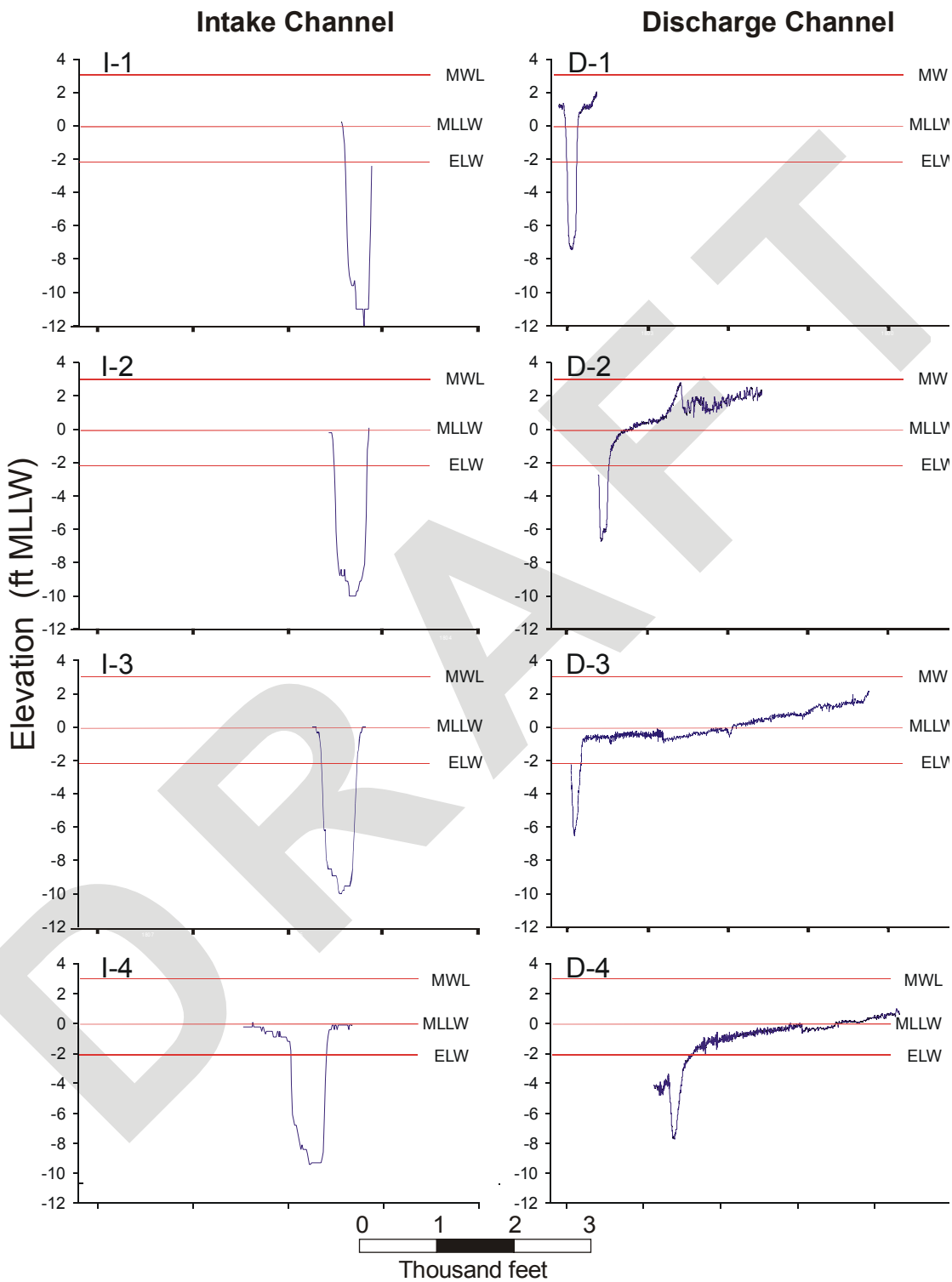

Figure 2.5-15. Bathymetric cross-sections along transects in the SBPP intake and discharge channels. The cross-sections were used to estimate current speed at different tide elevations.

2.6 Receiving Water Turbidity Monitoring

2.6.1 Introduction

Turbidity is measured as the amount of light that is scattered or absorbed by suspended particles. A turbidity meter or nephelometer is a device used to measure turbidity. A turbidity meter consists of a light source and a photoelectric cell. The photoelectric cell measures the amount of light that has been scattered 90° from the source light. The turbidity meter returns a value in nephelometric turbidity units (NTU). One NTU is equal to the scattering effect of 1 mg/l of silicon dioxide (SiO_2) in water.

For this study, the objectives of receiving water turbidity monitoring were to:

1. Map any observed spatial trends in light attenuation and turbidity in south San Diego Bay; and,

2. Collect data to support a modeling approach to evaluating the role of the SBPP on turbidity in south San Diego Bay.

Turbidity is a measure of the opacity or, alternately, transparency of water. The transparency of water determines the amount of light energy that is available at each depth for photosynthesis and its magnitude has implications for the entire aquatic community. Decreased light penetration (quality and quantity) in turbid waters reduces photosynthetically active radiation (PAR) resulting in reduced growth or even exclusion of bottom vegetation (Kenworthy and Fonseca 1996). Lowered primary productivity reduces food availability for herbivorous and detrital food webs, as well as decreasing DO. Additional biological implications of increased turbidity include clogging of fish gills, smothering of benthic organisms through associated sedimentation, clogged filter-feeding systems in various animals, and reduced feeding efficiency of visual predators.

Turbidity has numerous physical and biological causes. Physical causes of turbidity include suspension of silt, clay, and sand particles due to natural and anthropogenic sources of runoff, as well as waves, dredging and shoreline construction, and boating activity that re-suspend bottom sediments or erode shoreline (Iannuzzi et al. 1996). Biological sources of turbidity include planktonic organisms suspended in the water column, as well as small fragments of organic material derived from plants and animals. In addition, activities of marine fauna such as burrowing, feeding, and swimming can cause increased turbidity via re-suspension of bottom sediments.

Increased levels of turbidity can have numerous physical and biological effects. Turbid waters interfere with light penetration by scattering, reflecting, and attenuating light.

Suspended material can cause a change in water color due to varying effects of the material on different wavelengths of the incident light. Turbid waters are generally darker and the dark suspended particles absorb heat energy from solar radiation, resulting in increased water temperature and decreased levels of dissolved oxygen (DO).

2.6.2 Methods

To explore the spatial and temporal patterns of turbidity in south San Diego Bay, two methodologies were employed. The first method involved the use of permanent monitoring stations with deployed monitoring equipment. The second method utilized towed turbidity and photosynthetically active radiation (PAR) sensors that were towed throughout south San Diego Bay.

2.6.2.1 Monitoring Station Data Collection

Turbidity monitoring was conducted at eight monitoring stations within the South Bay ecoregion (see **Figure 2.4-1**). Station locations were chosen to encompass the potential range of turbidity values in south San Diego Bay. To accomplish this, sampling was conducted in both the intake and discharge waters immediately adjacent to SBPP, as well as in the surrounding waters within south San Diego Bay.

At each of the monitoring stations, Hydrolab® Datasonde 4 and Datasonde 4a multiprobe water quality meters were equipped with standard Datasonde primary PAR, secondary PAR, and turbidity probes (**Figure 2.6-1**). Primary and secondary PAR values were taken approximately 55cm (21.6 in) and 20 cm (7.9 in) from the bottom, respectively. Turbidity values were recorded approximately 15 cm (5.9 in) from the bottom. To minimize interference with probe sensors, all bottom vegetation was cleared within a 0.75-meter (2.5 ft) radius around the station. Data for all measured parameters were logged every 15 minutes during a station logging run.

Data collection for the eight south San Diego Bay sampling stations was conducted between July 3, 2003 and September 9, 2003. Data were not collected continuously at each station because only four Datasonde units were available for the study. Datasonde units were sequentially rotated among the eight south San Diego Bay monitoring stations during the sampling period. Refer to *Appendix E - Dissolved Oxygen Data, Table 1a* for the station deployment schedule.

2.6.2.2 Towed Data Collection

A series of transects was established in south San Diego Bay for the collection of surface turbidity and light attenuation data throughout the bay (**Figure 2.6-2)**. Transects were navigated while water was pumped to an onboard Hydrolab® Datasonde 4a outfitted with a 4-beam turbidity probe. The probe end of the Datasonde was attached to a 1.3-l (1.4-qt)

plastic tank that received water from a 15-l / min pump and released water back into the bay. Two PAR sensors were also attached to the Datasonde to collect light attenuation data. The PAR sensors were towed off the port side of the research vessel and were vertically spaced 0.3 m (1 ft) to allow for the calculation of light attenuation. The Datasonde and a Leica® MX Marine differential global positioning system were integrated via Windmill® software for Windows®. The integrated devices produced a single spreadsheet that included a timestamp, turbidity, primary PAR, secondary PAR, and a geographic position with sub-meter accuracy (**Figure 2.6-3)**. Data were recorded every 2 seconds during four 36-hr data collection events. The towed sampling events occurred in September 2003 (September 4–5, 8–9, 17–18, and 24–25).

2.6.2.3 PAR as a Surrogate for Turbidity

Turbidity meters are difficult to maintain *in situ* because their optical surfaces quickly accumulate particulates and biological films that interfere with valid measurements. Typically, a turbidity probe experiences significant signal decay within 24 hr after being deployed. However, the use of two PAR sensors can be used as a surrogate for direct turbidity measurements. Although the PAR sensors are also optical instruments and also experience signal decay through time, the difference in readings between two sensors at different depths can be used to calculate a measure of turbidity . Within a station, the two sensors foul at approximately the same rate and therefore can provide accurate data for up to 7 days.

The amount of light scattered by particulate matter manifests itself as a loss of light intensity that is exponentially proportional to depth in a homogeneously turbid water body. The drop in light intensity through the water column can be calculated using Beer's Law and is known as the diffuse attenuation coefficient (DAC) (Zimmerman et al. 1990). DAC can be calculated using the following formula adapted from Zimmerman et al. (1990);

$$DAC = \frac{\ln(I_z) - \ln(I_o)}{Z}$$

Where I_z is equal to the irradiance at the bottom PAR sensor, I_o is equal to the irradiance at the top PAR sensor, and Z is the vertical distance between the two sensors.

To determine the relationship between the PAR and turbidity readings from the monitoring stations, PAR and turbidity data needed to be collected in a way that simulates the deployed data without the turbidity probe becoming fouled. Non-deployed point data were collected on November 17, 2003, between 1000 and 1400 PDT. A Datasonde multiprobe unit with dual PAR meters and a turbidity probe were lowered over the side of a survey vessel and allowed to log data every 5 sec, for 2-min intervals. Numerous sampling sites were chosen throughout the South Bay in an attempt to capture

the range of previously observed turbidity values in the South Bay. The DAC values were aligned with their corresponding turbidity values and used to develop a mathematical correlation between DAC and turbidity.

2.6.2.4 Data Analysis

The turbidity and PAR data collected from the eight South Bay monitoring stations were collected concurrently with the data reported in Section 2.4–*Receiving Water Dissolved Oxygen*, and managed using the same criteria as described in the procedures related to the DO measurements.

All monitoring station data were transferred from Microsoft Excel® to Statistica® Version 5.5 statistical analysis software for Windows®. Statistica was used for all graphical and statistical presentation of monitoring station data. Graphical analysis of monitoring data includes presentation of example PAR data, as well as average DAC values among monitoring stations. Error bars presented with the average DAC are ± 1 standard deviation. Statistical analysis of the turbidity monitoring station data is limited to regression analysis of the relationship between turbidity and DAC.

The towed turbidity data were used to populate a 15-m turbidity grid throughout the sampled region of the South Bay. The grid was created by first interpolating the individual towed transects for turbidity. Interpolation was performed using ArcView 3.2® with Spatial Analyst® using the inverted distance weighted average (IDW) with a 750-m radius and a power of 2. The individually interpolated grid points were then averaged together and a final interpolation performed using the same IDW interpolation techniques.

The towed dual PAR data were used to calculate DAC values for all sampling points occurring between 0900 and 1600 PDT. PAR data collected before and after this time range are not included in the analysis because the associated low angle of incidence for sunlight results in spurious data. The trimmed data set resulted in six transect cycles being retained from each of the four towed data collection events.

DAC was mapped for the South Bay by individually gridding results of each of the 24 towed data collection events. The individual towed events were gridded using the same procedures applied to the towed turbidity data. The resulting individual DAC grids were averaged and re-interpolated using the same IDW techniques applied to the turbidity data.

The gridded results of the DAC mapping were aligned with the similarly gridded bathymetry data to model the light environment at eelgrass canopy height (-0.46 ft MSL) within the sampled area of the South Bay. From Beer's Law, the irradiance at any depth in a body of water can be calculated as:

$$I_Z = 2.718^{\ln I_O - (DAC*Z)}$$

Where I_z is the irradiance at some depth (Z), and I_o is the irradiance just below the water surface (refer to Zimmerman et al. 1990). For the model, the value for below water surface irradiance (I_o) was the mean surface irradiance from the towed PAR data collected at mid-day (between 1150 and 1210 PST) during each of the towed transect cycles underway during the selected time period. Results from calculations of irradiance at canopy depth were aligned with corresponding coordinates of the DAC and bathymetry values used to calculate I_z, and were plotted using ArcView 3.2®.

A hydrodynamic modeling approach was used to explain patterns in observed turbidity distribution within the south San Diego Bay to calculate the potential influence of the SBPP discharge on turbidity formation and distribution. A computer program (TRIM-2D) used the physical parameters of tidal currents, bay bathymetry, and surface wind stress, and empirical turbidity data to model turbidity with and without the operation of the SBPP cooling water intake and discharge. Based on the difference between natural and altered conditions, conclusions could be drawn regarding potential effects of SBPP on physical parameters affecting eelgrass distribution in south San Diego Bay. The modeling methods and results are presented in detail in Section 2.6.5–*Numeric Modeling of Turbidity Patterns*.

2.6.3 Results

The results from the turbidity monitoring data collection are presented first as examples of the types of data and associated values collected during sampling. These are followed by the modeling results. Discussion of associations between turbidity patterns and eelgrass distribution is presented in Section 4.0–*Integrated Discussion*.

2.6.3.1 Stationary Monitoring Data

An example of dual par data collected between September 11, 2003 and September 14, 2003 for one of the South Bay monitoring stations is shown in **Figure 2.6-4**. The influence of turbidity on dual PAR data resulted in lower daytime PAR values for the secondary (bottom) PAR sensor compared to the primary (top) PAR sensor.

Regression analysis of the supplemental dual PAR and turbidity data collected on November 17, 2003, show a significant relationship between the variables ($R = 0.74$; $p < 0.001$) **Figure 2.6-5**. The dependence of DAC on turbidity is explained by the formula:

$$DAC = 0.755 + (0.055 \times Turbidity)$$

The turbidity monitoring station data were deemed inadequate for analysis. The rapid fouling rate of the turbidity probes meant that there were not enough data for each of the

sites for meaningful comparisons. However, given the significant relationship between turbidity and DAC, the monitoring station DAC data were used as a surrogate measure for turbidity.

The average calculated DAC values for the eight South Bay monitoring stations did not indicate the presence of any SBPP associated trends with DAC (**Figure 2.6-6**). Additionally, grouped monitoring station DAC averages for the SBPP discharge channel and the South Bay open water stations show a marginally increased DAC for the discharge channel stations (**Figure 2.6-7**). In all cases, site variability obscures any potential trends in the data. These observations are in contrast with the data collected from the towed dual PAR array.

2.6.3.2 Towed Monitoring Data

A total of ten transect cycles was completed during each of the four towed data collection events. Each data collection event occurred within a 36-hr timeline that began at 0600 PDT and was completed at 1800 the following day. It took approximately 2.5 hr to complete one transect cycle and 0.5 hr to prepare the equipment for the next cycle. Remaining time was consumed for mobilization, demobilization, shift changes, and instrument calibration during the event timeline. Resulting data were spatially mapped within each transect cycle for quality assurance purposes and are presented in **Appendix H**.

An example of towed turbidity data is shown in **Figure 2.6-8**. Data for the presented figure were collected on September 17, 2003 between 1045 and 1345 PDT. The tide was a rising neap tide with tidal elevations of 1.25 m (4.1 ft) and 1.56 m (5.1 ft) at the beginning and end of the transect cycle, respectively. Wind conditions were typical on September 16th and 17th, with calm mornings and light to moderate afternoon winds (**Appendix H**).

The data for the presented transect cycle show somewhat typical turbidity conditions in south San Diego Bay with generally clear water in the northern portion of the bay, and increased turbidity in the southeast portion of the bay. The average turbidity during the run was 6.3 ± 4.8 NTU with a minimum of 2.0 NTU and a maximum 56.4 NTU. Although the water was generally more turbid in the southeast portion of the bay, the maximum observed turbidity occurred near a shallow water construction site that was being filled for shallow-water habitat restoration (32° 37' 26" N; 117° 06' 57" W).

The towed turbidity data from the September survey shows that turbidity increases moving from north to south through the South Bay (**Figure 2.6-9**). The highest average turbidity was observed in the southeast portion of the bay south of the CVWI. Turbidity is positively correlated with areas containing shallow non-vegetated mud bottoms. The east west trends in turbidity are reversed in the northern and southern portions of the South Bay. In the general water is less turbid towards the west.

The towed DAC data from September sampling shows that light attenuation increased moving from north to south in the South Bay (**Figure 2.6-10**). The greatest attenuation occurred south of the CVWI and to the east of the breakwater extending to the south of the CVWI. The increased DAC in the south was correlated with areas containing shallow-bottom unvegetated mudflats. Additionally, in the relatively clear waters in the north, there were slightly higher levels of light attenuation near the Sweetwater River mouth and other shallow-water areas.

The results of DAC mapping generally agreed with the mapped turbidity results. Both results indicated that turbidity and associated light attenuation increased moving south through the South Bay with the greatest turbidity associated with waters to the southeast of the CVWI. However, there were discrepancies in the northern portion of the South Bay. The results of turbidity mapping indicate that the waters adjacent to the Sweetwater River were slightly less turbid than waters immediately to the west, whereas the results of the DAC mapping indicate the opposite trend. This discrepancy is relatively minor in terms of absolute differences in water clarity.

The calculated in-water surface PAR average at mid-day was 1,849 $\mu E/m^2/s$. Applying the in-water surface PAR combined with the DAC and bathymetry data resulted in the map of eelgrass canopy level PAR for the South Bay (**Figure 2.6-11**). The figure illustrates the interaction of both DAC and depth in determining the amount of light available to eelgrass at canopy depth. Areas with similar depths but with increased DAC (high turbidity) had lower peak PAR levels. Similarly, areas with similar DAC values but different depths had lower PAR levels at depth.

The maximum average peak irradiance at eelgrass canopy depth was 499 $\mu E/m^2/s$, and the minimum was < 1 $\mu E/m^2/s$. The maximum as well as numerous near maximal values occurred in the shallow, clear waters in the northwest portions of the South Bay study area. Other near maximal values occurred in the southwestern portions of South Bay with slightly higher DAC values but shallow water. Additionally, the relatively turbid waters southeast of the wildlife island received high levels of irradiance due to the shallow water. The lowest irradiance values were observed in the deepest portions of the navigational channels along the northeast portions of the South Bay.

2.6.4 Numerical Modeling

2.6.4.1 Background

A long-term monitoring program of physical characteristics within south San Diego Bay was previously performed to determine the environmental parameters that control the distribution of subtidal eelgrass in the South Bay ecoregion. Results of this monitoring program established that light is the proximate factor limiting the distribution of eelgrass

within the South Bay (Merkel & Associates 2000). In addition, the field studies provided insight into the factors dictating the light environment within the South Bay through identification of significant differences in daily turbidity environments between stations supporting and stations lacking eelgrass. Correlations between turbidity patterns and wind speed and duration were also observed. These relationships support the possibility of developing a numerically-based spatial model focusing on physical parameters that can aid in explaining the observed distribution patterns of eelgrass in south San Diego Bay. The following sections present such a model, and identify the assumptions and data sources used to construct the model. In addition, pertinent outputs and interpretation of outputs is presented. This model is a further evolution of a model developed previously to investigate the physical environmental effects limiting the distribution of eelgrass in south San Diego Bay (Merkel and Sutton 2000).

2.6.4.2 Numerical Model Development

The model is based on a numerical hydrodynamic model constructed and calibrated for San Diego Bay (Wang et al. 1997). The model is structured on the depth-averaged tidal and residual circulation model known as TRIM-2D (Cheng et al. 1993) with modifications made to improve model stability and accuracy (Casulli and Cattani, 1994). The mathematical theory underpinning the TRIM-2D hydrodynamic model is described in detail in Cheng et al. (1993) while the San Diego Bay adaptations and calibrations for hydrodynamic components have been previously presented in Wang et al. (1997). Because these prior treatments have been comprehensive in their discussion of the model, this section addresses only the pertinent elements, strengths and weaknesses, model inputs, and adaptations that are considered essential for evaluation of the outputs in the current application. To fully evaluate the model, the reader is referred to the prior references.

The TRIM-2D model output is based on a computational mesh of 92,272 grid nodes equidistant from each other on 15 m spacing covering the southern portion of the San Diego Bay. The boundary for the model wetted field is set by the shoreline interface (+3 ft MLLW) throughout the south San Diego Bay limited by a east-west transect at about 32º 38.5’ Latitude.

Bathymetric data for the model was derived from National Oceanographic and Atmospheric Administration (NOAA) navigational data for San Diego Bay approach areas. Bay bathymetry is derived from U.S. Navy, Southwest Division, Nat. Resources 1993 field surveys (U.S. Navy 1994). For the South Bay region of interest in this investigation, a more recent and refined resolution bathymetric data set was created for using data collected for this project by Merkel & Associates, Inc. and Tenera Environmental.

The model was also loaded with wind direction and velocity data derived from a Weatherport® weather station located on the CVWI from May through September 2003.

Wind speed and direction data consisted of logged 15-minute running averages using data collected every 2 seconds. The collected wind data were used to calculate hourly and daily prevailing wind conditions. Prevailing wind direction was determined by assigning each logged wind direction to one of 12 directional categories composed of 30-degree intervals (e.g. N, NNE, ENE, E, etc.). The prevailing wind direction was the directional category that contained the greatest frequency of observations for the duration of the study. The prevailing wind speeds were calculated as the mean of the logged wind speeds associated with the prevailing direction for each hourly period. The model was loaded with the prevailing wind direction and average velocity for each hour. Wind vectors were combined with fetch and velocity algorithms to model the effects of wind wave height and period on bottom shear within the South Bay.

In addition to tide and wind driven circulation, data on cooling water flows into and out of the South Bay Power Plant (SBPP) were collected during summer 2003. These data were provided by the power plant and used to populate the model with a power plant sink and source. The discharge flows could range up to 601 million gallons per day (mgd), but averaged 441 mgd during the study period. For model runs, the maximum operating limit of 601 mgd was used to test SBPP effects unless otherwise stated.

Bottom sediment conditions in the model were based on particulate size loading from field data collections. To increase accuracy in the assessment of sediment re-suspendability, the surface sediments throughout south San Diego Bay were characterized over a 500-m by 500-m square grid at 60 points. This grid established ambient conditions of the bay bottom that had greater or lesser susceptibility to shear stress suspendability based on sediment grain-size, cohesion, and density properties (Merkel & Associates 2000). The sediment characteristics were interpolated between grid data points using the same IDW techniques used for other field data parameters.

Using wind data, bathymetry, and tides, the model was constructed to calculate bottom shear stress using current velocities generated either through current flow or wave-generated orbital velocities. Within the model, the Manning's roughness coefficient (n) for friction is an assignable parameter based on the roughness of the bottom environment. For the present model, n was set as a variable function of local water depth at each node, as is recommended in the initial model form and has been applied to prior San Diego Bay applications (Cheng *et al.* 1993 and Wang *et al.* 1997). The Manning's n values applied to the San Diego Bay model are provided in **Table 2.6-1**.

Table 2.6-1. Manning's roughness coefficients (n) applied to San Diego Bay TRIM-2D model.

Water Depth (m)	Manning's n Values
0.6 > Depth	0.024
2.0 > Depth > 0.6	0.022
6.5 > Depth > 2.0	0.020
12.5 > Depth > 6.5	0.018
Depth > 12.5	0.015

The modeled shear was allowed to generate suspended sediment by acting on the bottom substrate. The results of bottom shear on differential sediment conditions results in predicted sediment resuspension. To analyze the effects of the SBPP on turbidity generation, the model was run with the SBPP at maximum flow of 601mgd and without any flow. The net effects of the power plant were then calculated as the difference between with and without plant flows.

To evaluate the effects of the power plant on turbidity distribution, the suspended sediment was allowed to settle and be re-suspended by varying shear stress through the day while also being influenced by current patterns. The model was allowed to run to a point of equilibrium conditions. Outputs were reviewed for three parameters. These were currents, bottom shear stress, and turbidity environments. These model outputs, as well as the important limitations on their interpretations, are discussed below relative to their significance to the subtidal light environment. The model outputs a continuous time sequence of conditions over the course of any given run-time and is powered by the prevailing modeled tide and wind environments. The net effects of the SBPP on turbidity distribution were determined by subtracting the equilibrium turbidity states with and without the power plant flows.

2.6.4.3 Results

Weather Data

Results of summer 2003 wind monitoring showed the prevailing wind direction for south San Diego Bay was out of the west (**Figure 2.6-12**). In the South Bay, the wind blew out of the west 28 percent of the time with the wind blowing between SSW and WNW 76 percent of the time. The average daily wind speed out of the west was 12.4 ± 6.1 kph (7.7 ± 3.8 mph). Figures showing hourly prevailing wind direction and average wind speeds are included in **Appendix H**.

Currents

Current velocities were modeled for the South Bay to determine the distribution of high and low current fields and general form of the current circulation patterns. In addition, an evaluation of current conditions with and without the influence of the SBPP cooling water system was made. **Figures 2.6-13 - 16** present the current conditions (indicated by black vectors) with and without the influence of the SBPP during maximum-spring low, flood, high, and ebb tides overlaid on bathymetry in feet (indicated by color) for the South Bay study area. Maximum-spring tidal conditions were selected because they provide the greatest range of tidal current velocities and tidal levels. Thus, the greatest opportunity to view the effects of the power plant discharges is afforded.

The effects of the SBPP on current velocities and the water area affected are most pronounced during low tidal levels and are somewhat independent of the tide cycle. Model results indicate greater current velocities and a greater water area affected by maximum cooling water flows during low tides and rising tides. Thus absolute tidal level appears to be the most important influence on cooling water induced current patterns. During all modeled tidal conditions, the influence of the SBPP on South Bay currents extended around the western margin of the CVWI. Net-modeled SBPP circulation patterns suggest that SBPP discharge currents flow around CVWI and are partially entrained within the intake channel. This pattern is most pronounced during low tidal levels. For additional descriptions of current flows in the discharge channel and receiving waters of south San Diego Bay refer to Section 2.5–*Receiving Water Currents and Bathymetry*.

Bottom Shear

Bottom shear stress was modeled for the South Bay to determine the relative contributions of wind driven waves, tides, and the SBPP on bottom shear (**Figure 2.6-17**). Bottom shear model runs were performed assuming maximum spring tide conditions for 72 hr and then converted to cumulative hourly averages of bottom shear (dynes/hr). Results indicate that wind driven waves in shallow water are the greatest contributor to bottom shear in the South Bay. Shallow waters along the southern and eastern shoreline of the South Bay exhibited the greatest bottom shear stresses. Westerly winds drive this result causing maximum bottom shear in shallow areas with the greatest wind fetch.

The South Bay experienced an opposite and minimal pattern of bottom shear due to tidally driven currents compared to the effects of wind driven currents. Shore-adjacent regions of the South Bay experienced 2 orders of magnitude less bottom shear stress from tidal currents as compared to wind driven waves. Tidally driven bottom shear was greatest in the northeastern navigational channel (**Figure 2.6-17**), where currents funnel into and out of the South Bay (**Figure 2.6-14** and **Figure 2.6-16**). Overall, tidally driven

sources of bottom shear stress were minimal and not notable when mapped at the same scale as wind driven wave stresses (**Figure 2.6-17**).

To discern the effects of the SBPP on bottom shear, the wind wave and tidal driven currents were input into the Trim 2D model, and the SBPP added as a source and sink of 601 mgd at the discharge and intake channels, respectively. The maps of total bottom shear with and without the SBPP were then used to calculate the net effect of the SBPP on bottom shear stresses in the South Bay (**Figure 2.6-18**).

Results of SBPP modeled effects on bottom shear indicate that the SBPP has a negligible impact on bottom shear in the South Bay. The mapped model results with and without the SBPP are virtually indistinguishable from one another (**Figure 2.6-18**). Observation of the net effects of the SBPP supports this observation. Net SBPP impacts show minimal, localized increases in bottom shear in the shallow waters adjacent to the SBPP. Interestingly, the model predicted that the SBPP reduced bottom shear stresses in much of the area southeast of the CVWI. The negative results stem from the fact that the SBPP has minimal impacts on bottom shear combined with model error and simplicity. The two-dimensional nature of the model means that opposing wind and tidal circulation patterns can cancel each other out whereas in reality stratification of currents may occur. However, such stratification is not likely to lead to SBPP impacts on bottom shear because the warm water produced by the SBPP is less dense than the receiving water.

Turbidity

Sediment-characteristic data from Merkel & Associates (2000) were used to produce a relative index of suspendability for the South Bay (**Figure 2.6-19**). Sediment data collected by Merkel & Associates (2000) were sediment ranks throughout the South Bay based on sediment characteristics such as grain size and cohesiveness. A map of predicted sediment re-suspension was then created by spatially aligning and multiplying bottom shear stress and sediment rank within the study area and then dividing by the highest observed value from the pooled with SBPP and without SBPP data sets. The resulting data, as well as a map of the net difference with and without SBPP, were plotted with ArcView® 3.2.

Results of the predicted sediment re-suspension modeling show that the SBPP has a minimal effect on the level of turbidity (**Figure 2.6-20**). The model predicts that sources of turbidity are in areas with both high bottom shear stress and highly suspendable fine grain sediments. The model suggests that wind-wave bottom stresses dominate in the production of turbidity in shallow waters with fine-grained-non-plastic sediments.

Although the SBPP is not likely to cause increases in the amount of suspended material in the South Bay, it can influence the distribution of turbid water within the South Bay. There is a significant source of natural turbidity found within the discharge waters to the southeast of CVWI where sediments are re-suspended by wind waves (**Figure 2.6-20).**

Turbidity in the South Bay is a function of sediment re-suspension, deposition, transport, and residence time. The numeric model predicts a turbidity environment that is a result of all of these factors. The turbidity in the model has been calibrated to observational data collected during summer 2003 and then evaluated against long-term monitoring data from the ten deployed monitoring stations used in the prior South Bay eelgrass study (Merkel & Associates 2000). The model was found to realistically predict the trends and ranges of turbidity detected through the South Bay using deployed instruments.

With the allowance for the SBPP influence on this natural turbidity source, the SBPP affects the transport of turbidity in the near field of the CVWI (**Figure 2.6-21**). This effect, although minor in the context of natural circulation effects on turbidity distribution, greatly surpasses the SBPP's effect on turbidity production. In addition, the flow field of the power plant also limits the tidal bore and penetration of clearer waters from the south-central portion of the Bay southward. **Figure 2.6-21** illustrates the differences in turbidity resulting under conditions of no cooling water flows as well as the 2003 average summer flows of 441 mgd and the maximum permitted flows of 601 mgd. The most readily apparent differences between the model's turbidity plots are found in the near field region of the power plant discharge channel and the waters adjacent to the western edge of the CVWI. To better illuminate the effects of SBPP cooling water flows on turbidity levels in the South Bay, net effects were calculated between the SBPP cooling water flows at 441 mgd and 601 mgd and no cooling water flows (**Figure 2.6-22**).

As discussed previously, suspended solids generate turbidity that has significant implications to the penetration of light through the water column and thus the capacity for photosynthesis to occur within eelgrass beds in the South Bay. The role of turbidity on light, and light on eelgrass growth and distribution, is discussed in Section 4.2–*Eelgrass Integrated Discussion*.

DRAFT

Hydrolab Datasonde Multiprobe

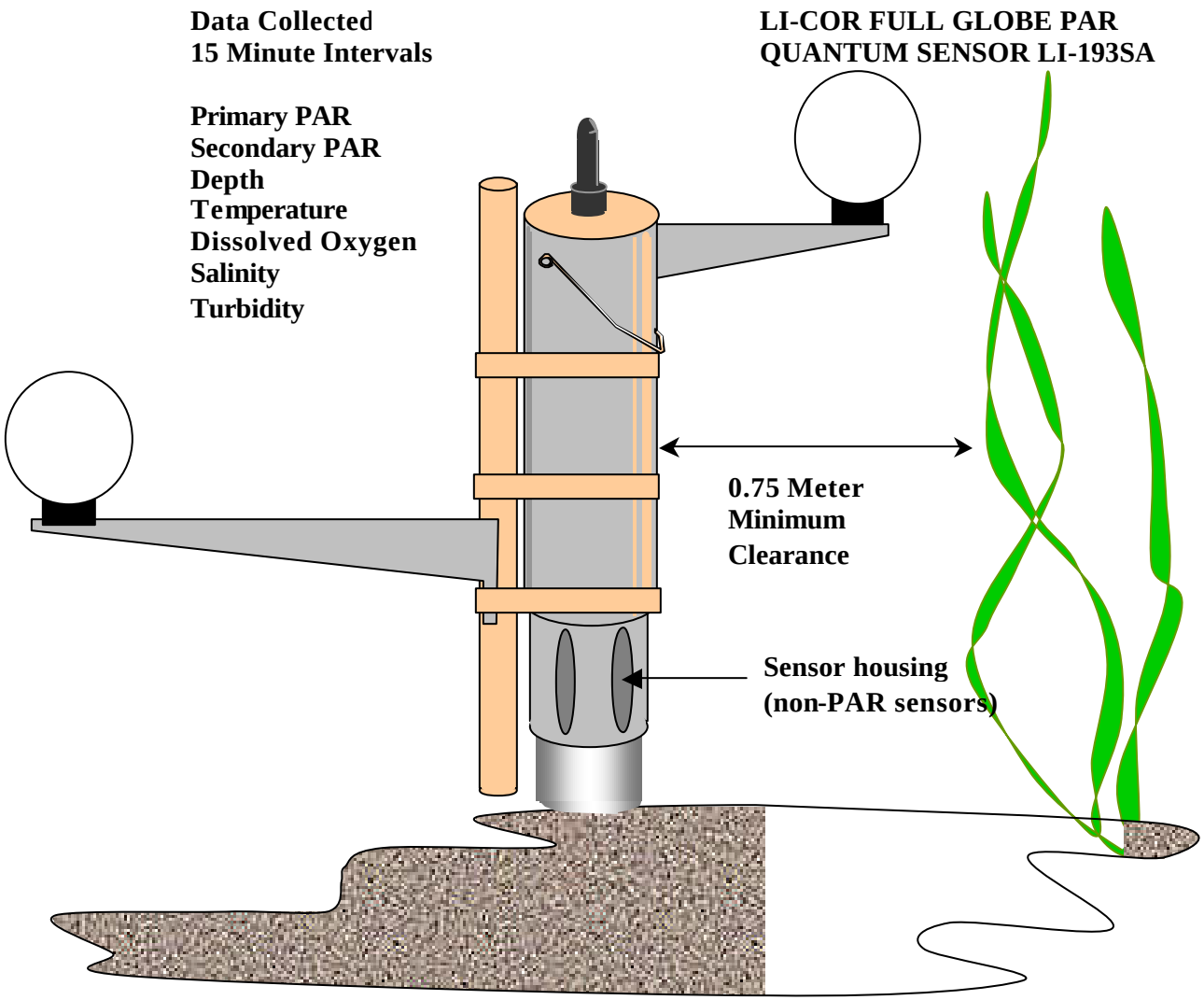

Figure 2.6-1. Hydrolab Datasonde Multiprobe, deployed station arrangement.

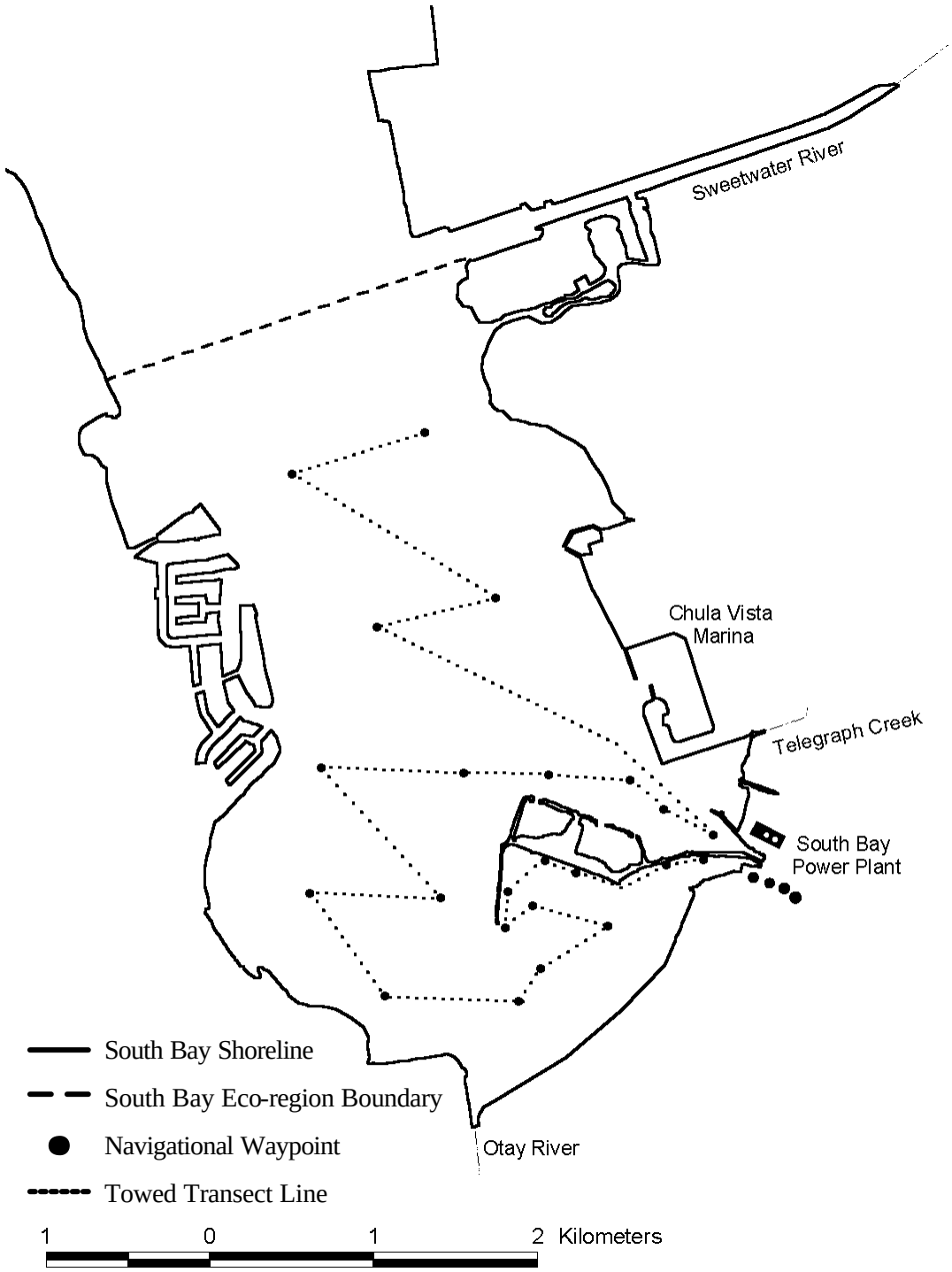

Figure 2.6-2. Transects used for towed turbidity data collection. South San Diego Bay September 2003.

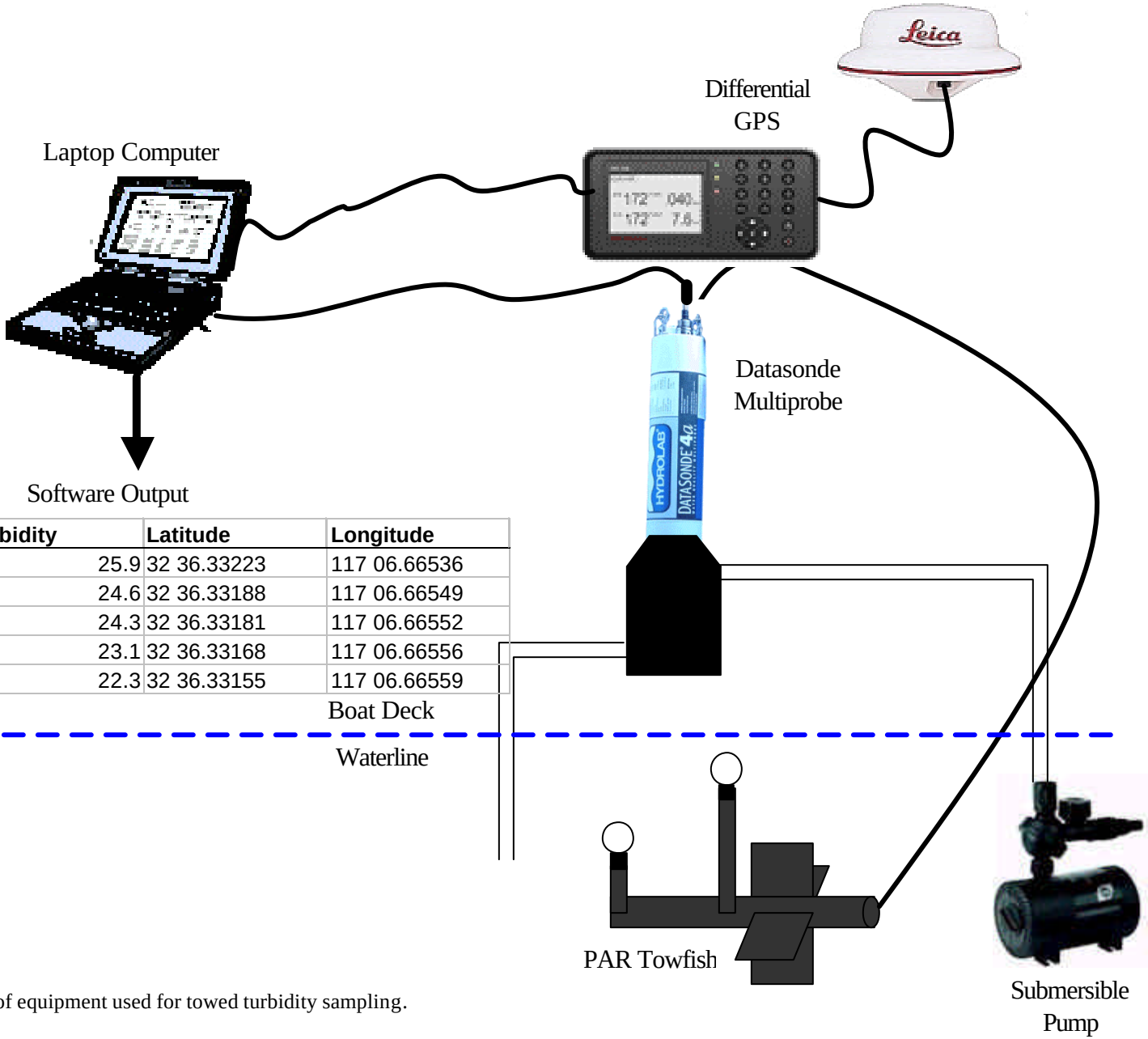

Time	Turbidity	Latitude	Longitude
11:57:02	25.9	32 36.33223	117 06.66536
11:57:17	24.6	32 36.33188	117 06.66549
11:57:22	24.3	32 36.33181	117 06.66552
11:57:31	23.1	32 36.33168	117 06.66556
11:57:37	22.3	32 36.33155	117 06.66559

Figure 2.6-3. Schematic of equipment used for towed turbidity sampling.

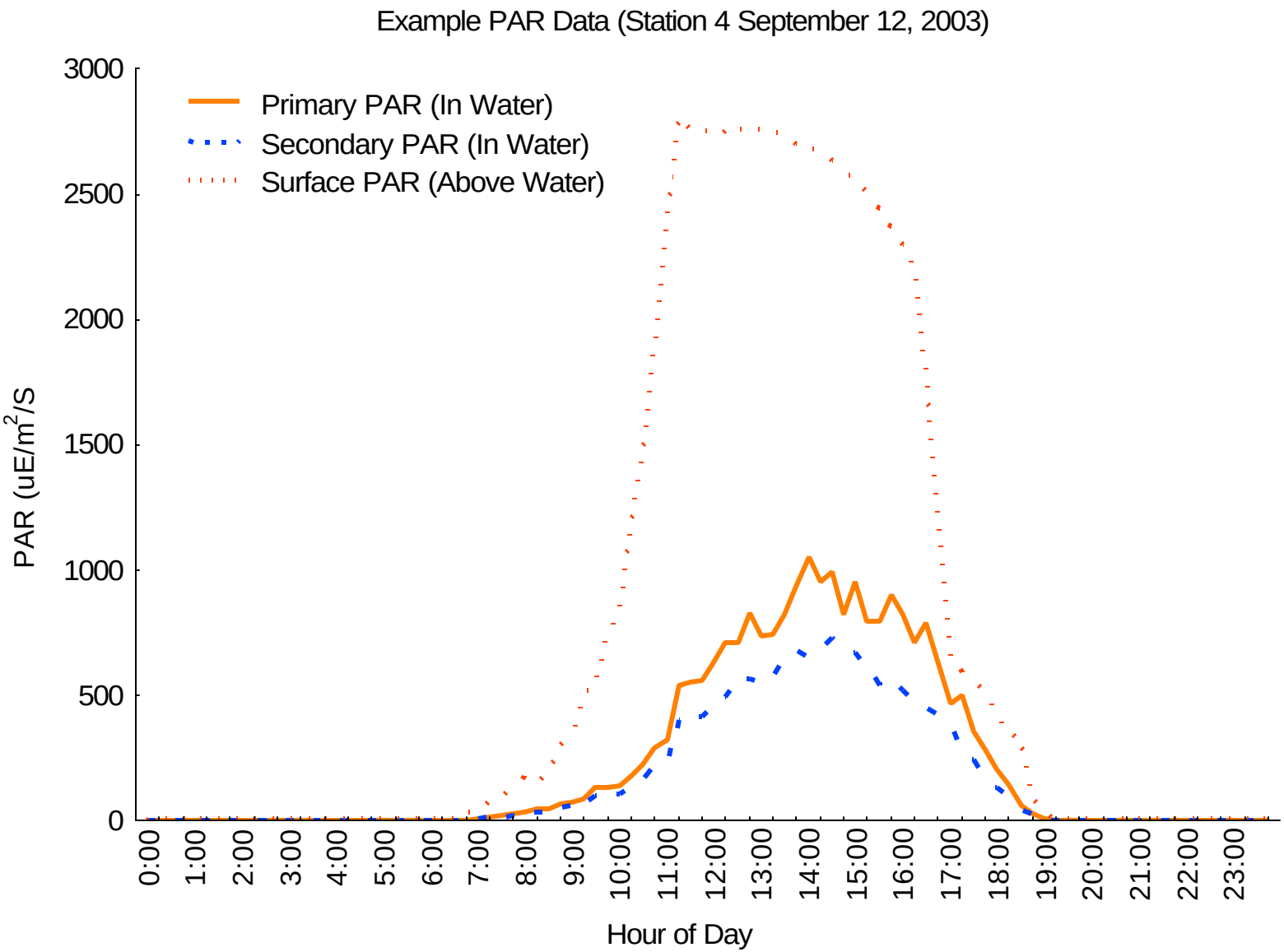

Figure 2.6-4. Example of Datasonde PAR data. Data collected at South Bay monitoring station 4 on September 12, 2003.

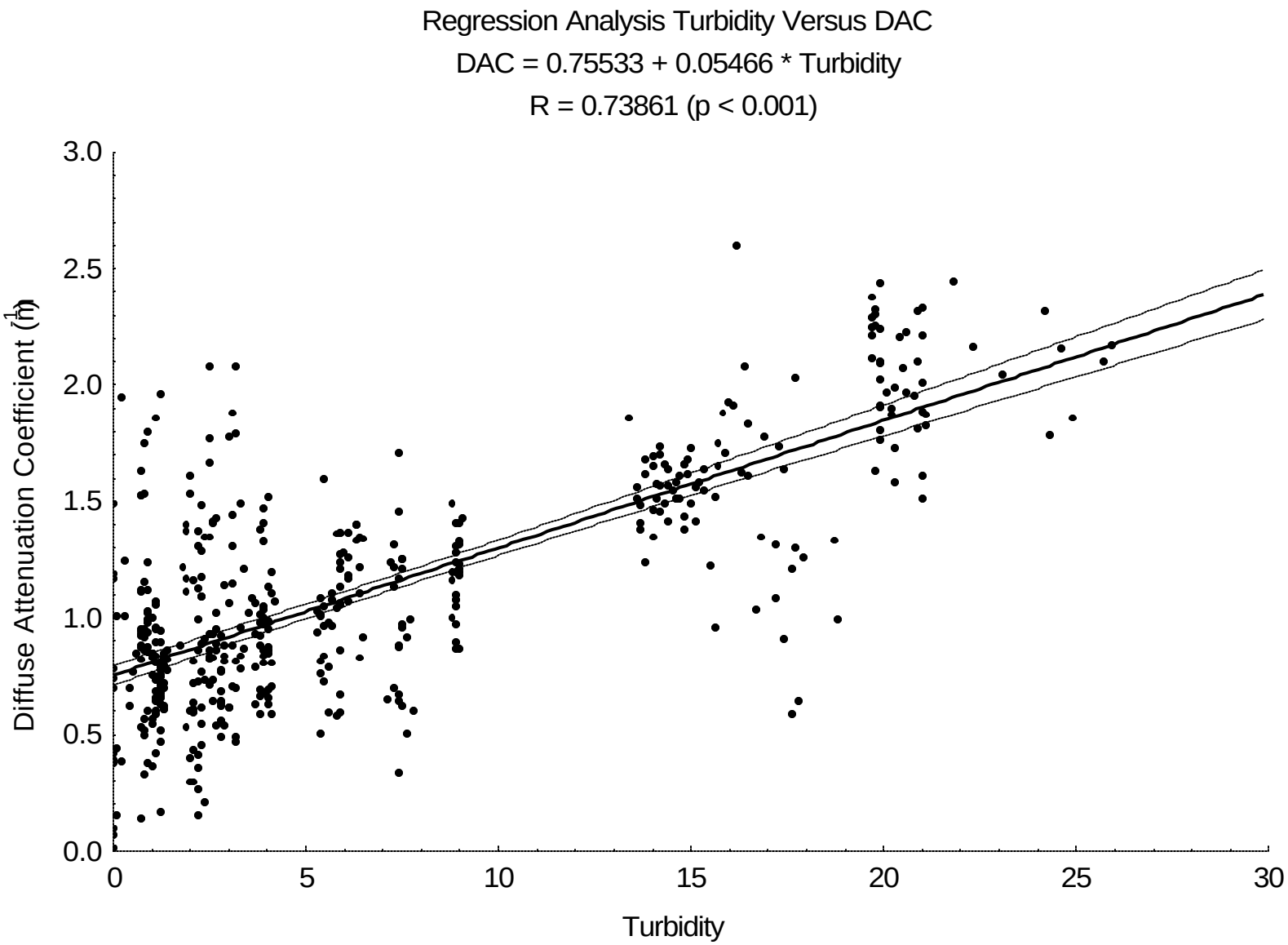

Figure 2.6-5. Relationship between the diffuse attenuation coefficient (DAC) and turbidity for South San Diego Bay. Data collected November 2003**.**

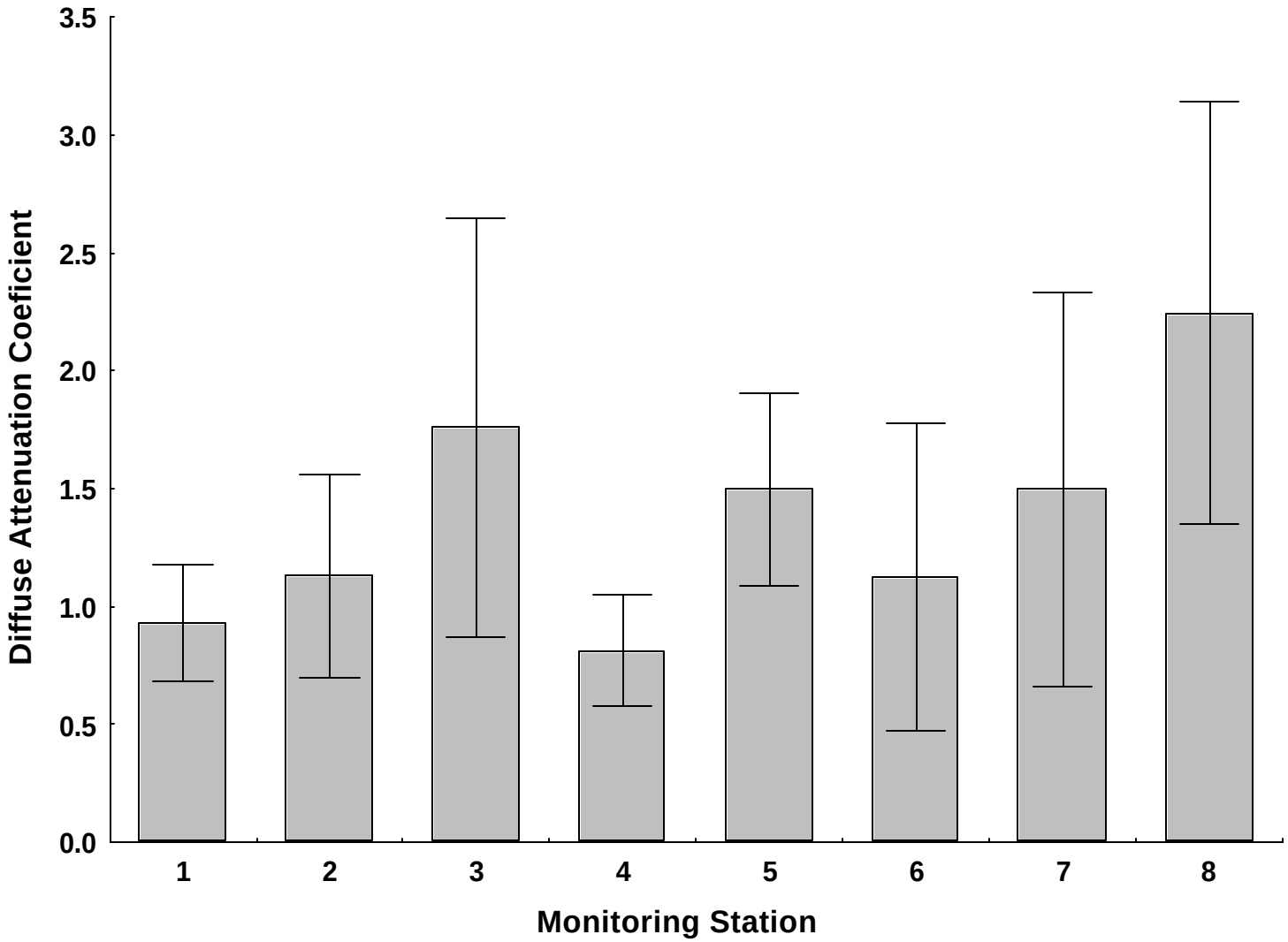

Figure 2.6-6. Average calculated DAC for the South Bay deployed equipment monitoring stations. Bars represent ± 1 standard deviation.

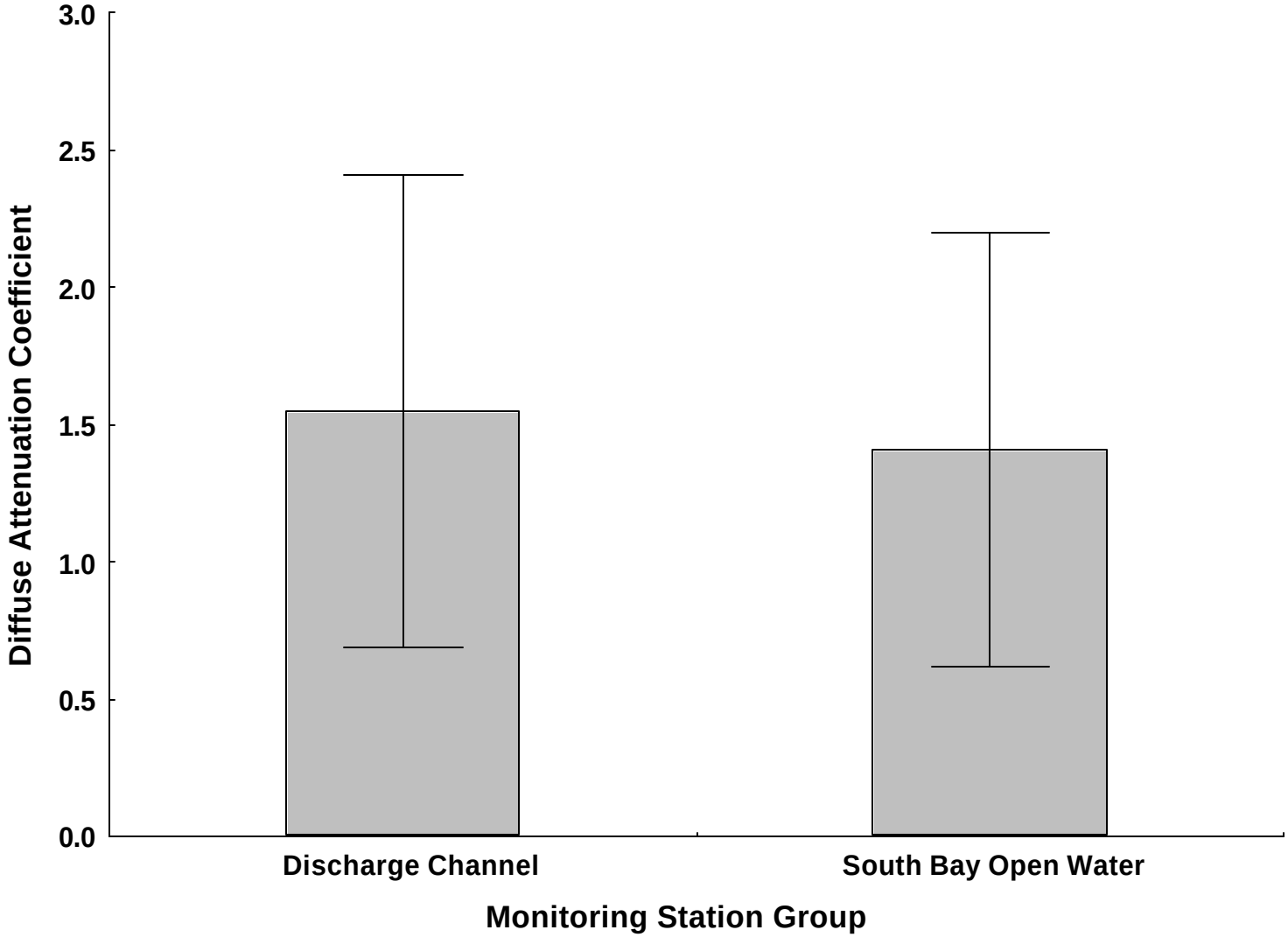

Figure 2.6-7. Average calculated DAC for SBPP discharge channel and South Bay open water monitoring station groups. Bars represent ± 1 standard deviation.

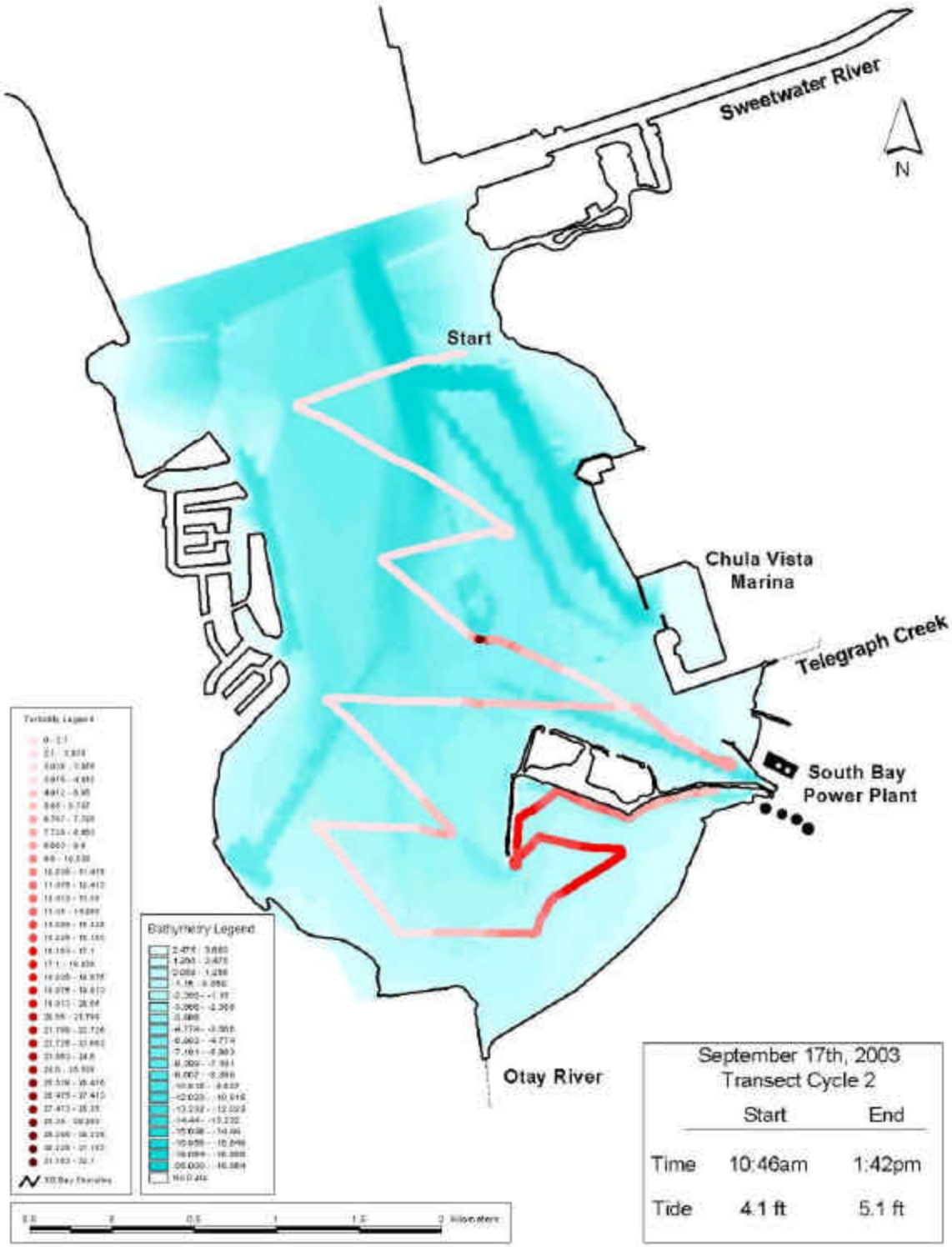

Figure 2.6-8. Example towed turbidity data. Data collected September 17, 2003 (10:46am to 1:42pm).

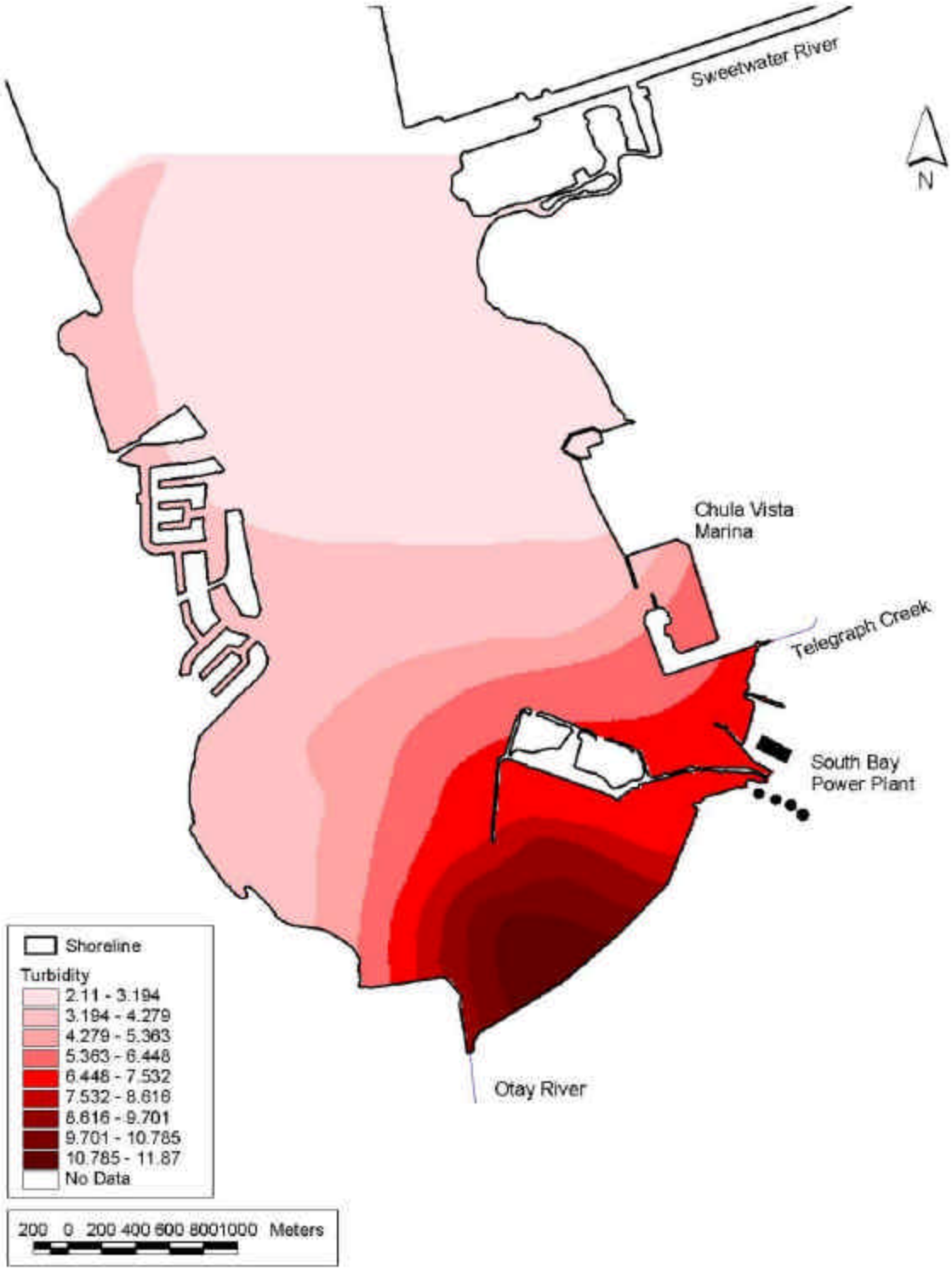

Figure 2.6-9. Interpolated map of average observed turbidity in South San Diego Bay, summer 2003**.**

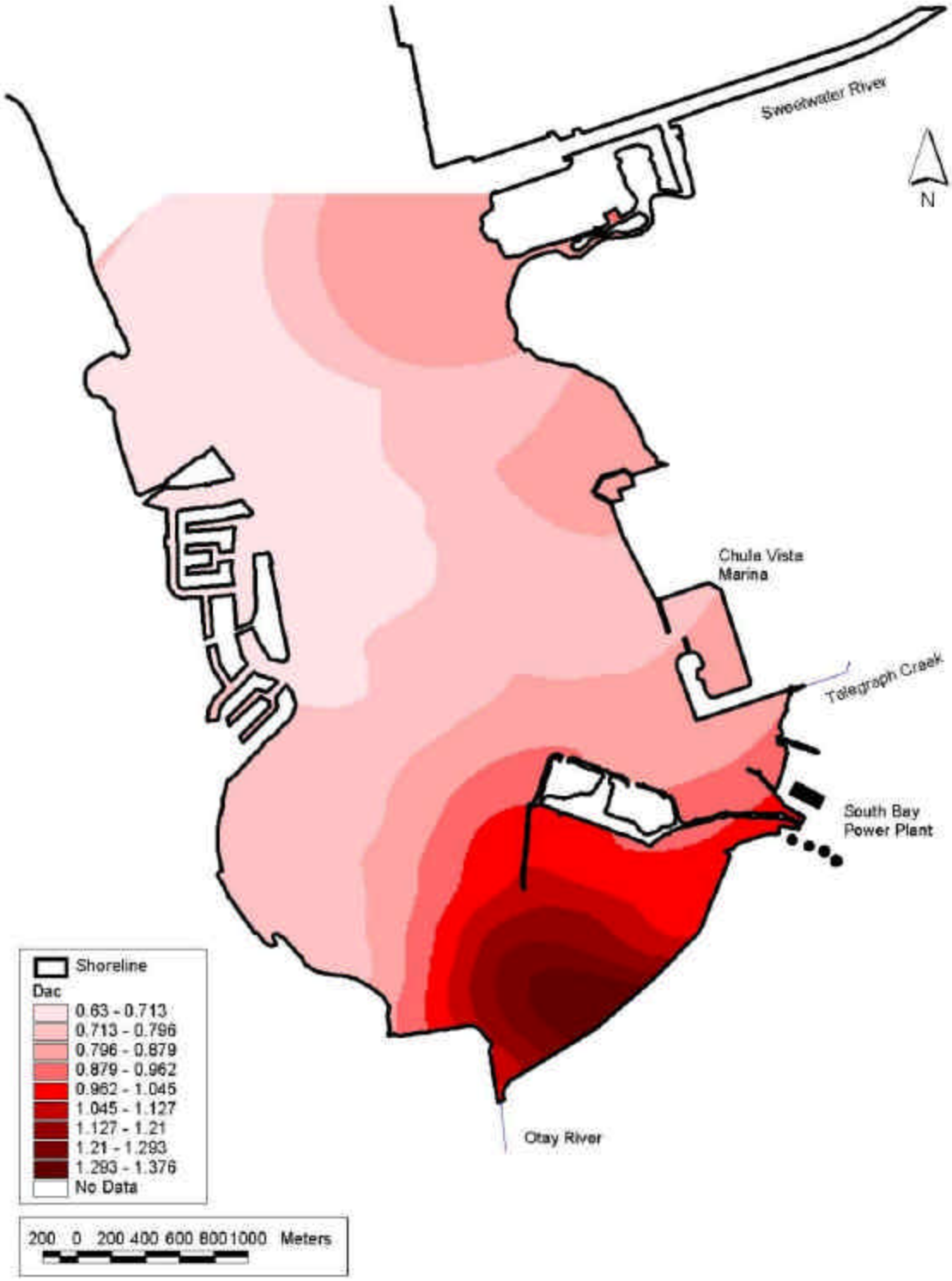

Figure 2.6-10. Interpolated map of average DAC between 9am and 4pm (PDT) for South San Diego Bay, summer 2003.

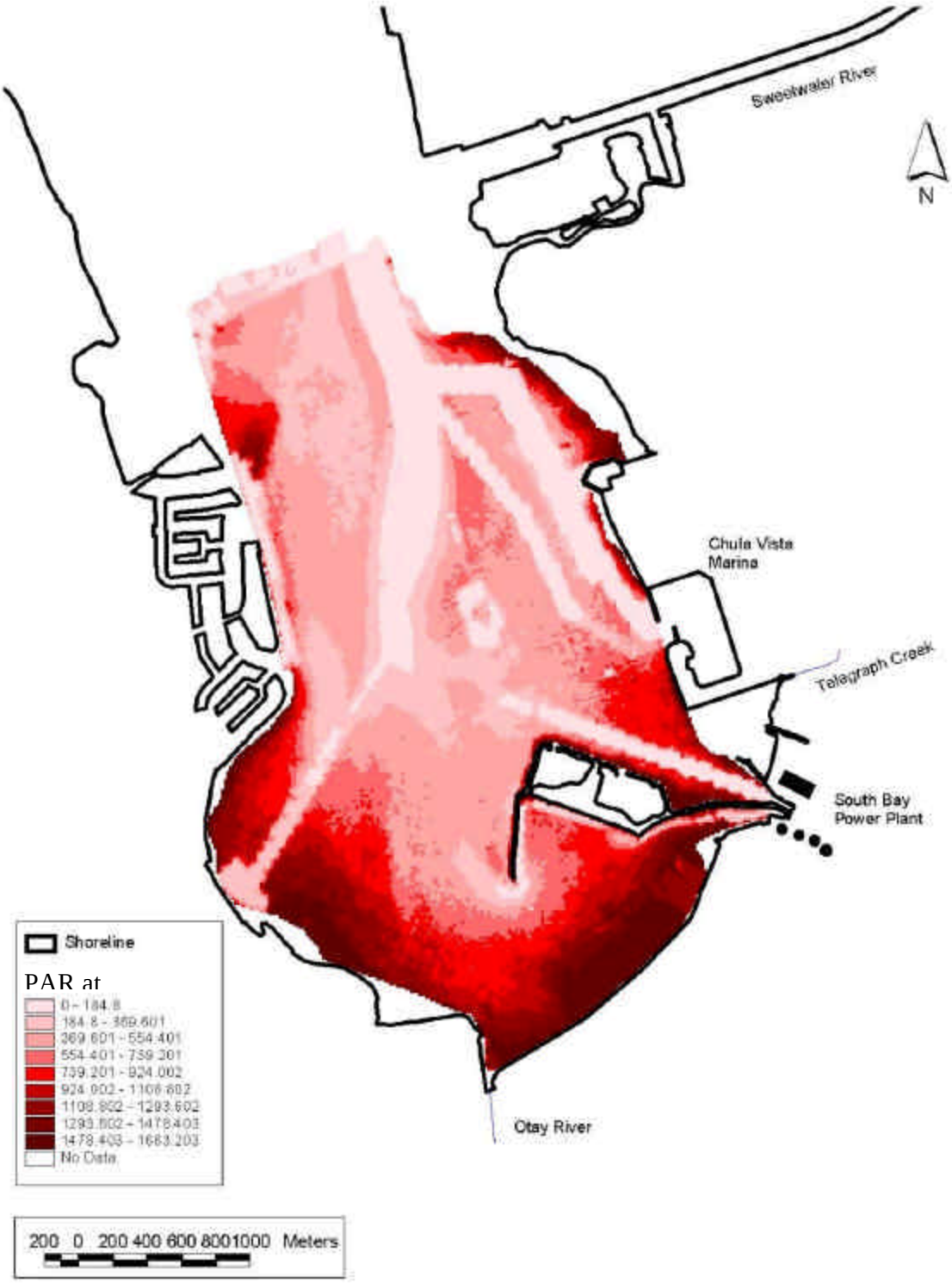

Figure 2.6-11. Interpolated map of the calculated PAR reaching eelgrass canopy elevation at mean sea level at 12pm

South San Diego Bay Wind Monitoring

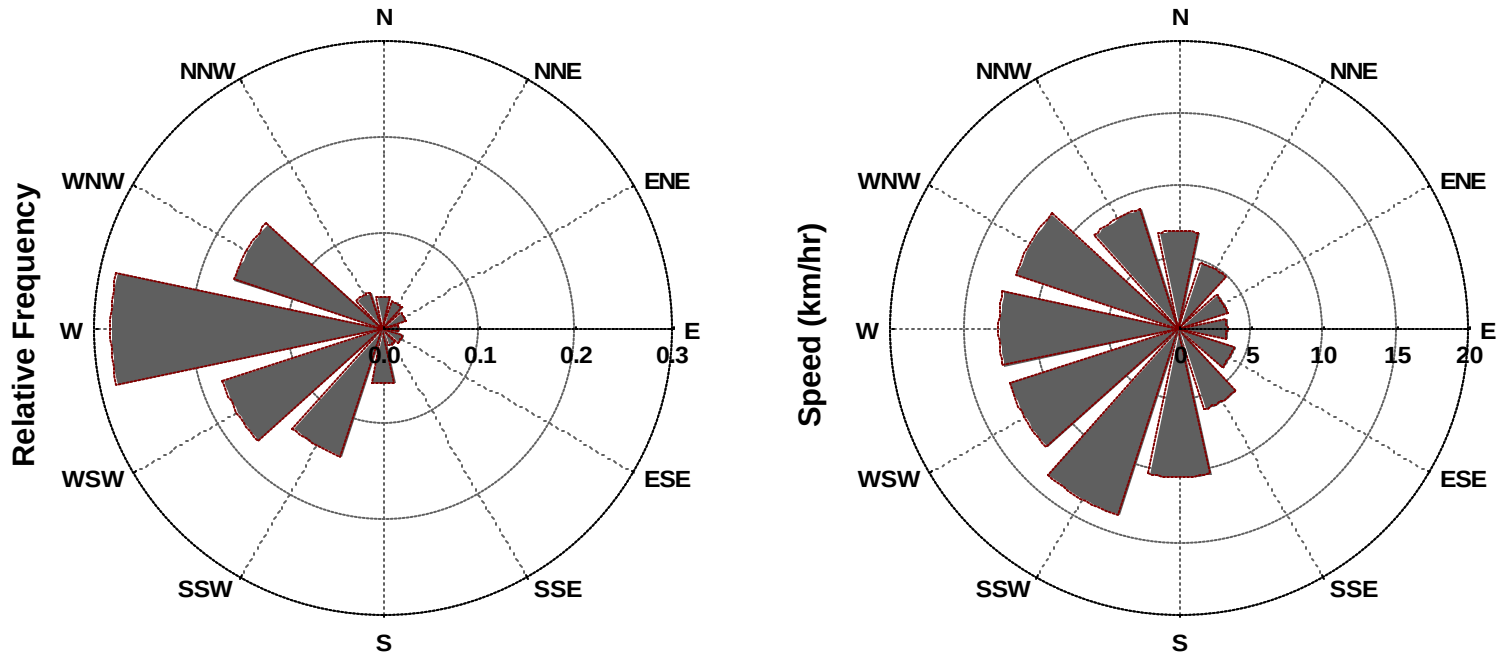

Figure 2.6-12. Wind roses showing the prevailing daily wind direction (left) and average daily wind speed for all wind directions (right). Data collected between May 25, 2003 and September 30, 2003

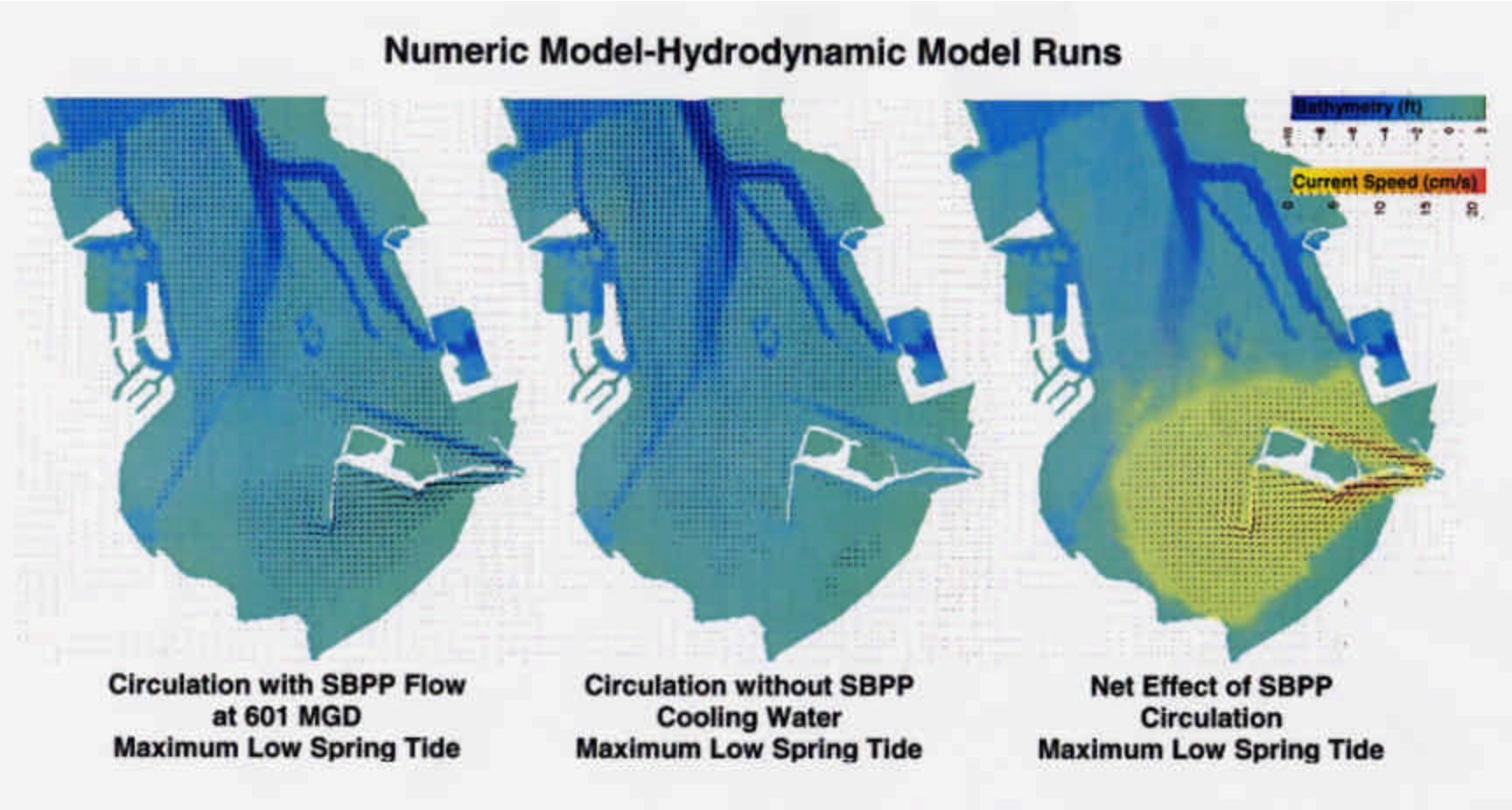

Figure 2.6-13. Spring low tide circulation effects of the SBPP as predicted by Trim 2D hydrodynamic modeling. Arrows represent current vector direction with arrow length proportional to relative current velocity. The map of net SBPP effect on current patterns (right) includes color-coded current speeds to show extent and change in current speeds associated with the SBPP.

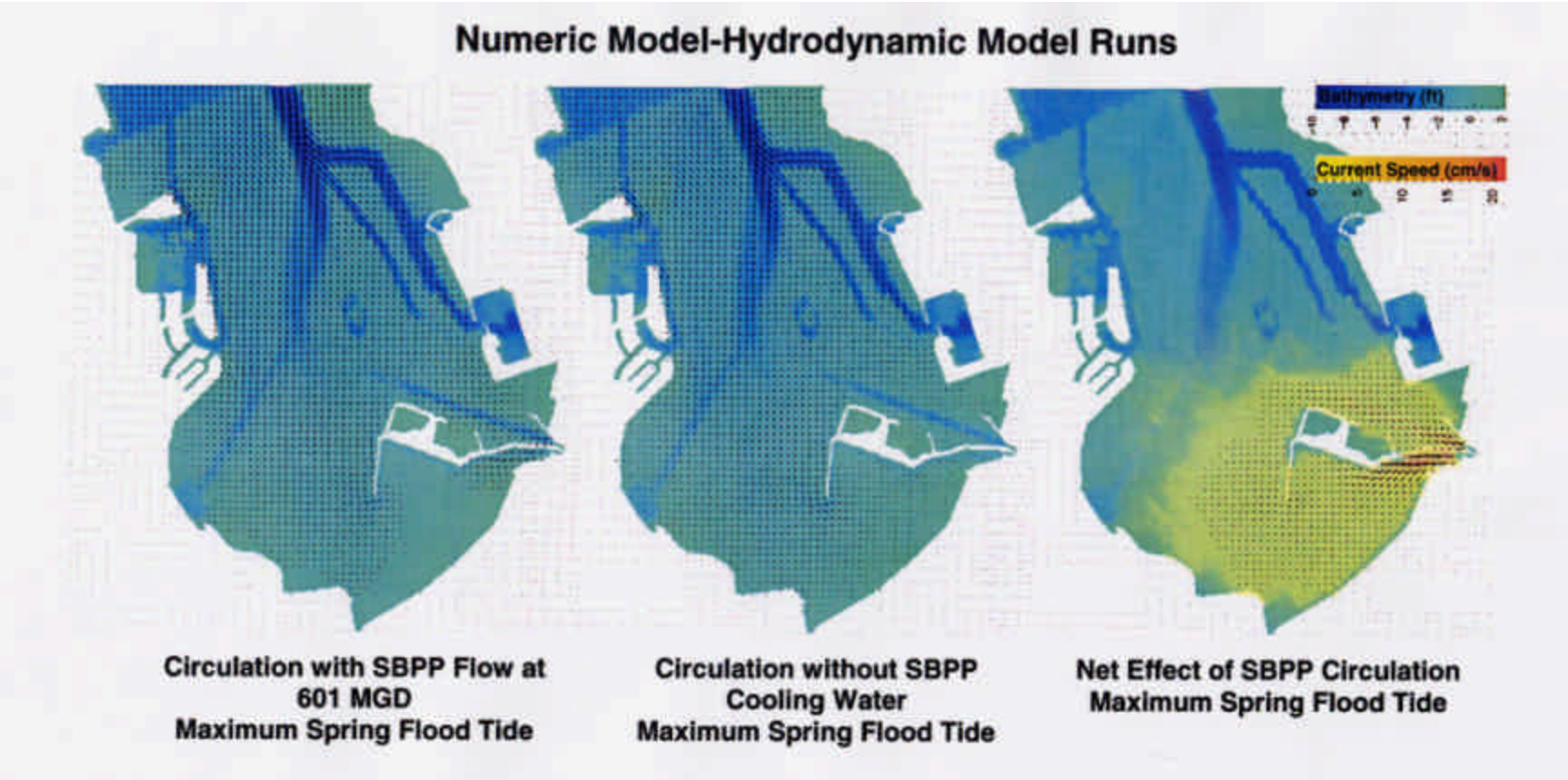

Figure 2.6-14. Spring flood tide circulation effects of the SBPP as predicted by Trim 2D hydrodynamic modeling. Arrows represent current vector direction with arrow length proportional to relative current velocity. The map of net SBPP effect on current patterns (right) includes color-coded current speeds to show extent and change in current speeds associated with the SBPP.

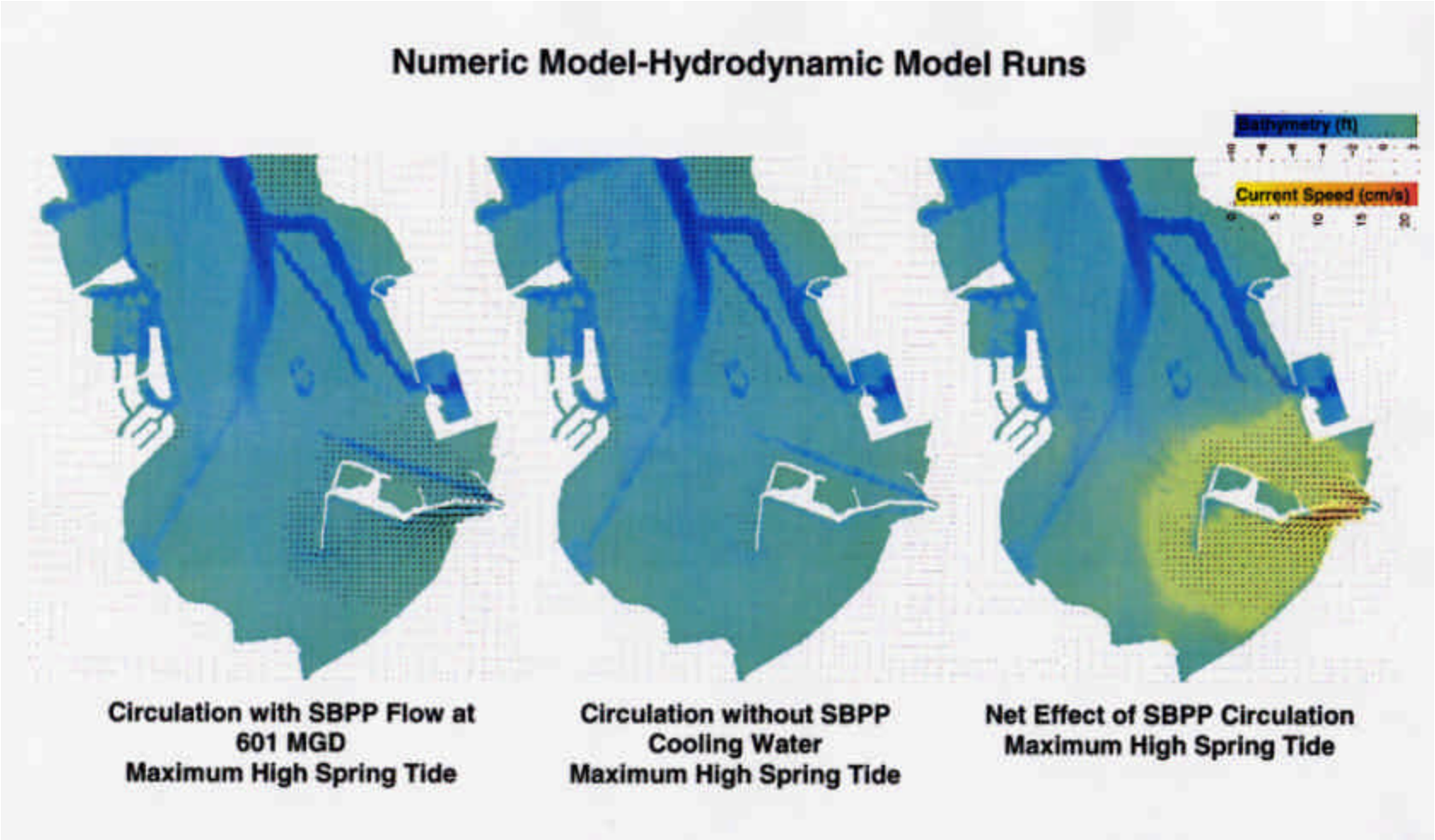

Figure 2.6-15. Spring high tide circulation effects of the SBPP as predicted by Trim 2D hydrodynamic modeling. Arrows represent current vector direction with arrow length proportional to relative current velocity. The map of net SBPP effect on current patterns (right) includes color-coded current speeds to show extent and change in current speeds associated with the SBPP.

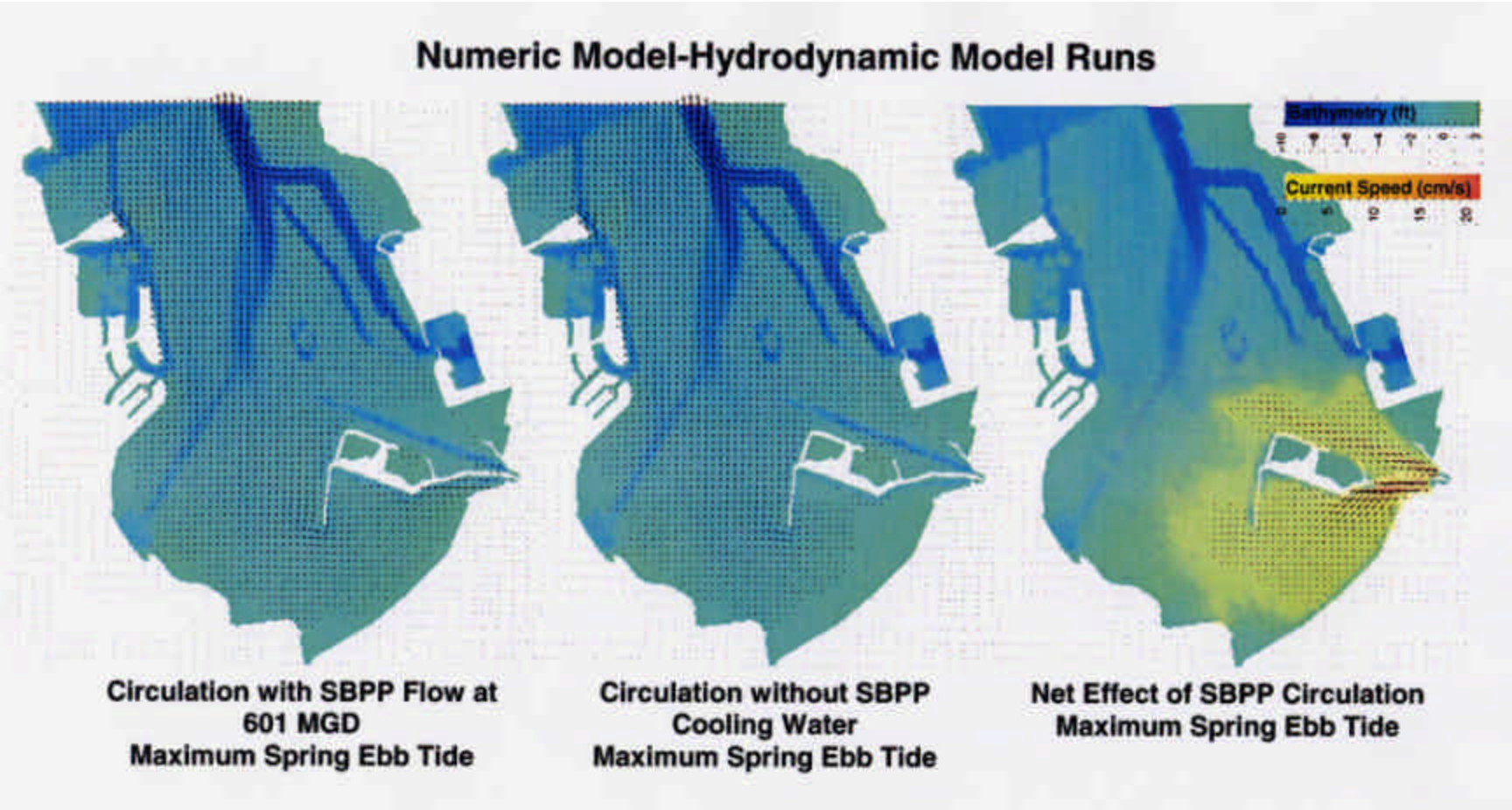

Figure 2.6-16. Spring ebb tide circulation effects of the SBPP as predicted by Trim 2D hydrodynamic modeling. Arrows represent current vector direction with arrow length proportional to relative current velocity. The map of net SBPP effect on current patterns (right) includes color-coded current speeds to show extent and change in current speeds associated with the SBPP.

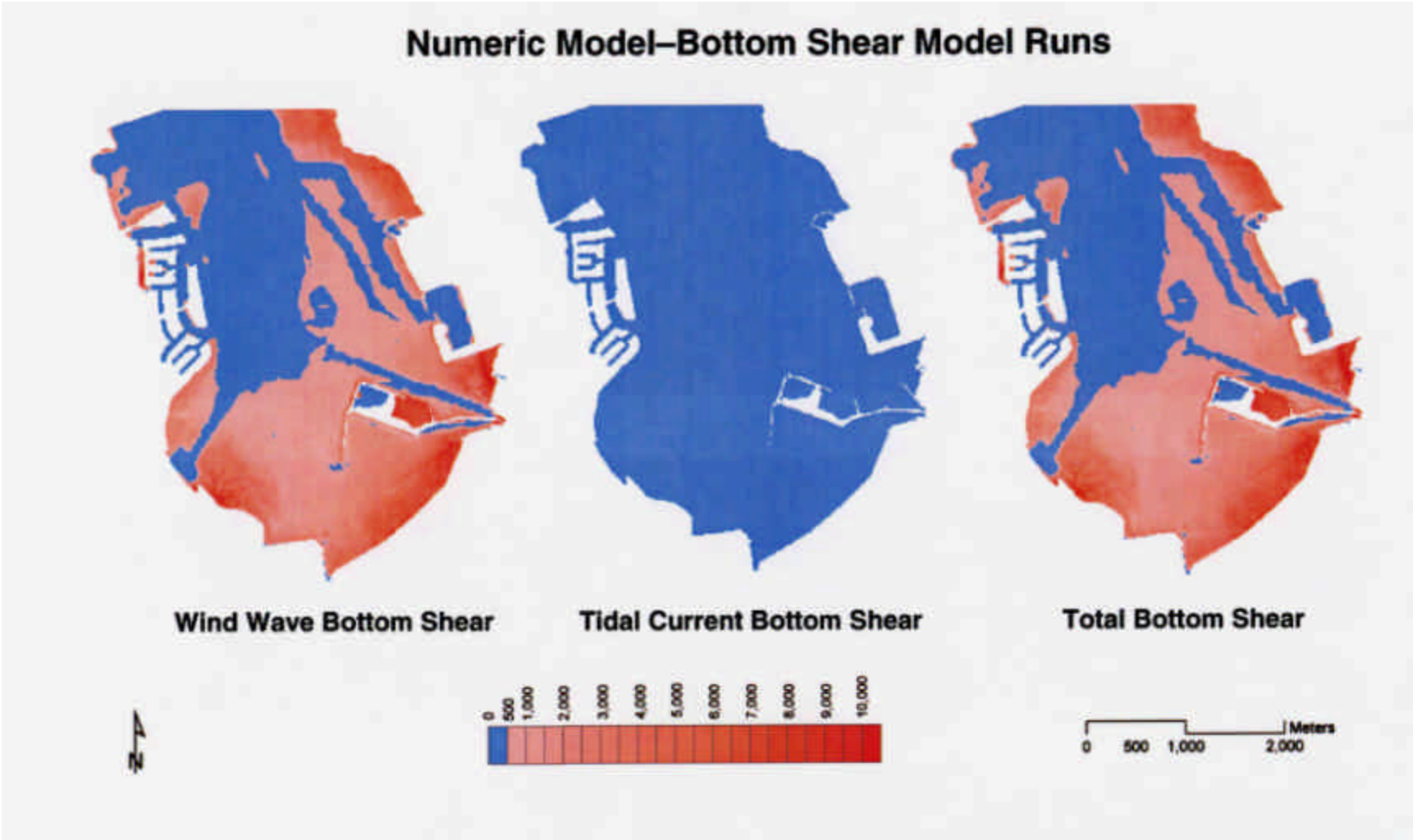

Figure 2.6-17. Numeric modeled bottom shear stress for south San Diego Bay resulting from wind driven waves (left), tides (middle), and the total of waves and tides (right). Model runs are without SBPP cooling water and reflect average cumulative dynes per hour for a 72-hour spring tidal cycle.

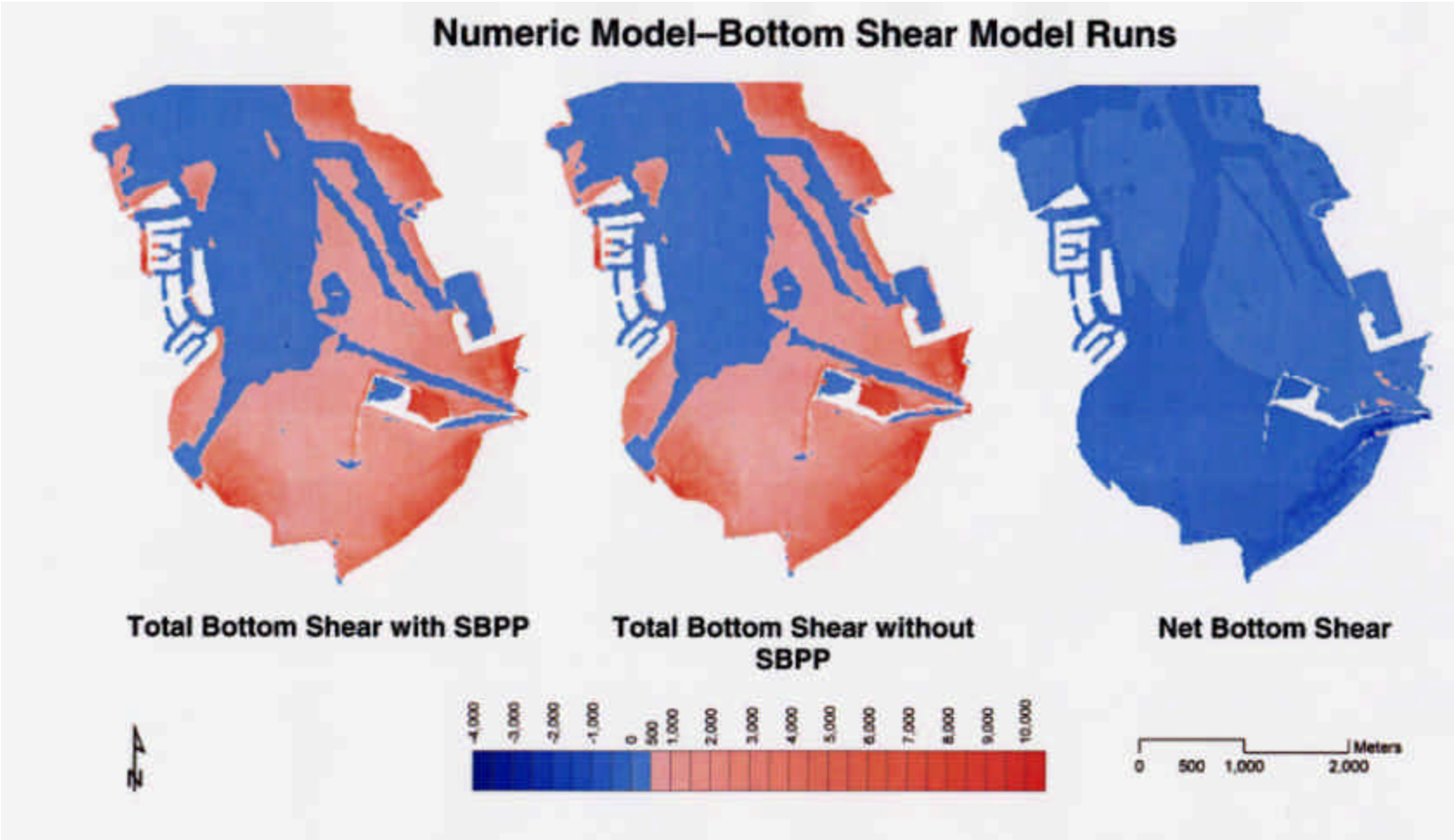

Figure 2.6-18. Numeric modeled bottom shear stress for total bottom shear with (left) and without (middle) the effects of the SBPP. The net effect of the SBPP on bottom shear is shown on the right. Model runs reflect average cumulative dynes per hour for a 72-hour spring tidal cycle.

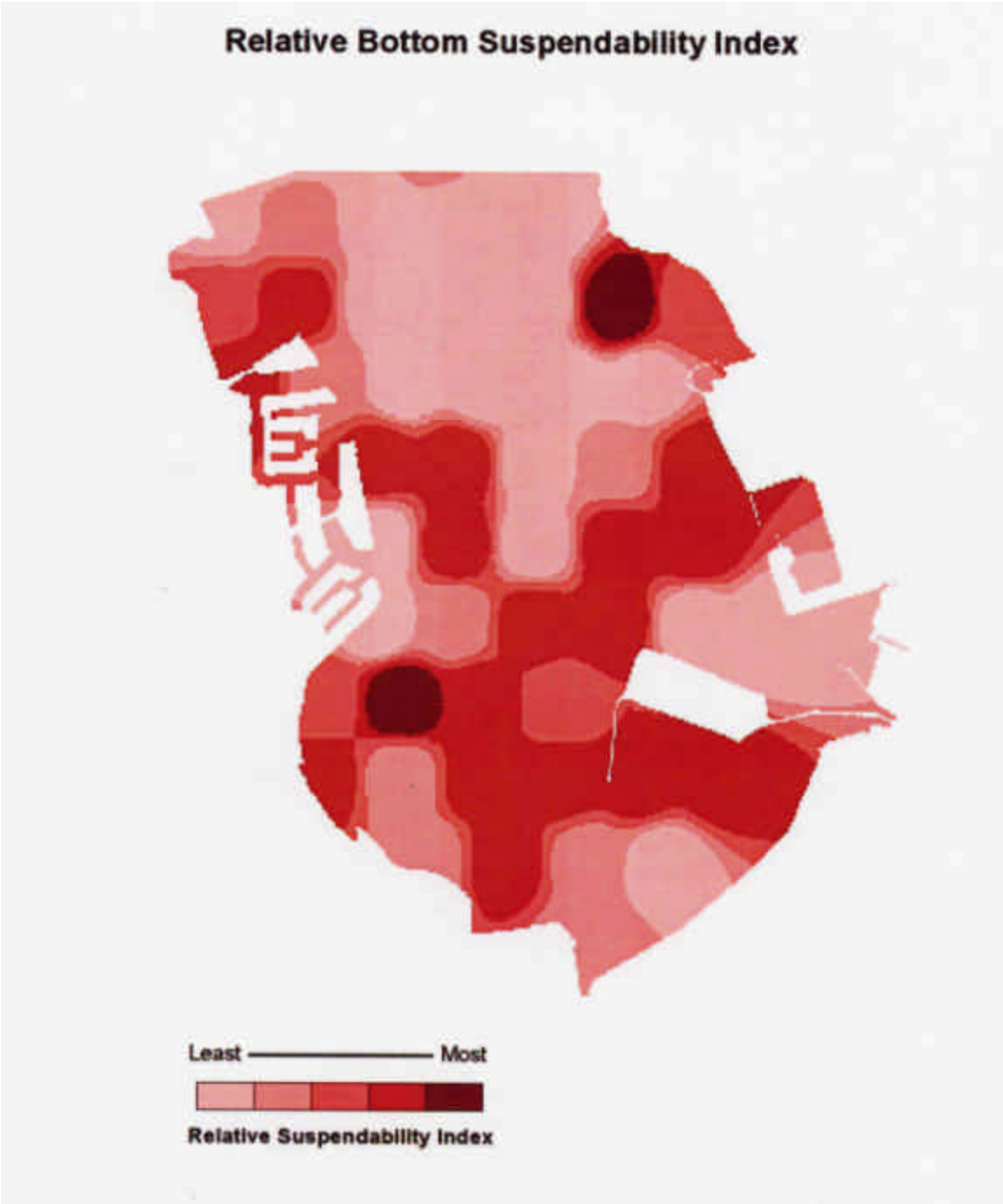

Figure 2.6-19. Relative bottom suspendability index applied to bottom sediments in South San Diego Bay. Based on data from Merkel & Associates (2000).

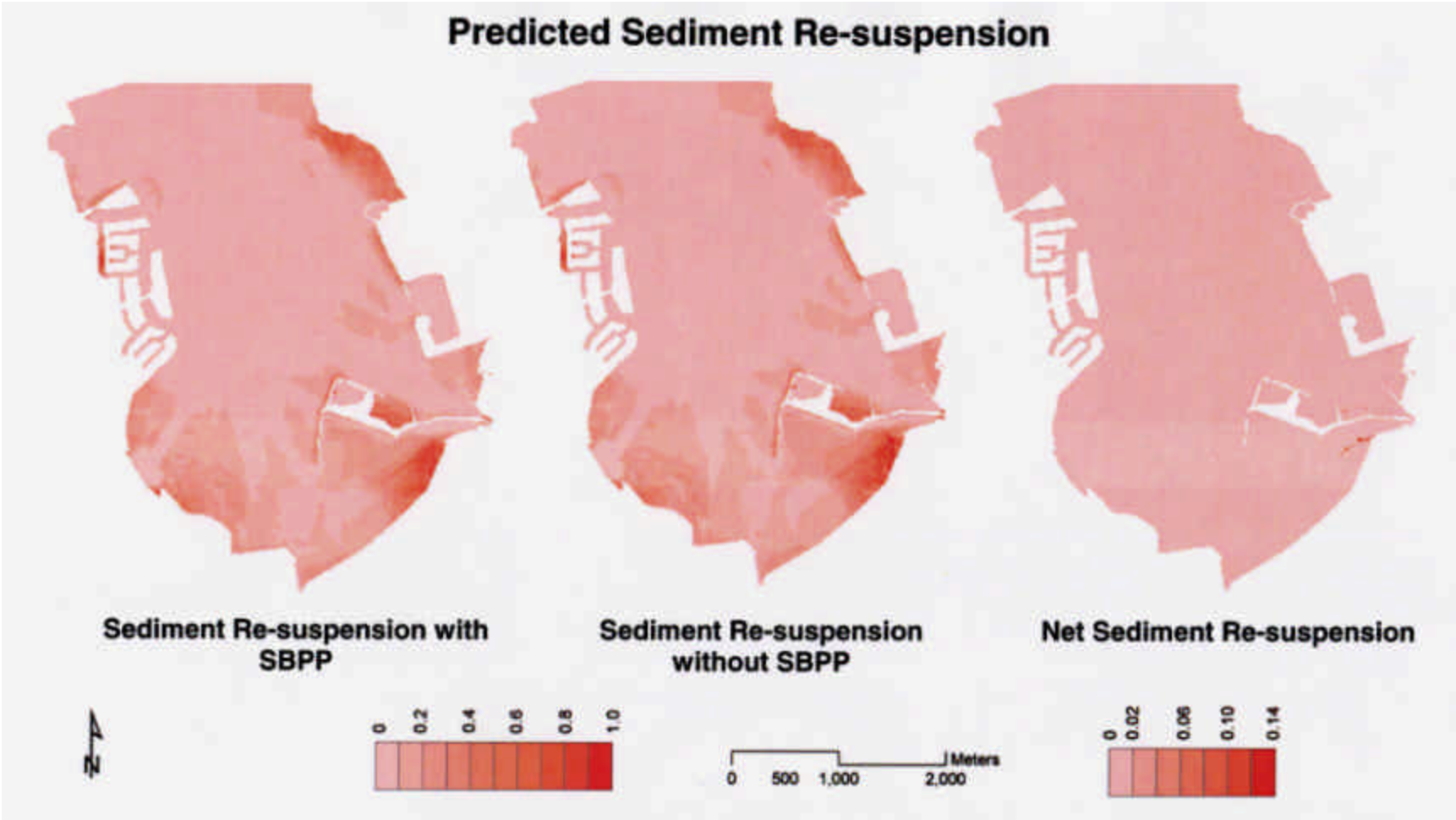

Figure 2.6-20. Predicted sediment re-suspension from combined numeric modeled bottom shear and relative bottom suspendability index. Model uses sediment characteristic data and bottom shear modeling to determine the relative probability of suspension of sediments with (left) and without (middle) the influence of the SBPP. The map on the right is of the net effect of the SBPP on suspendability of bottom sediments in South San Diego Bay. Note the different scale bar for net suspendability

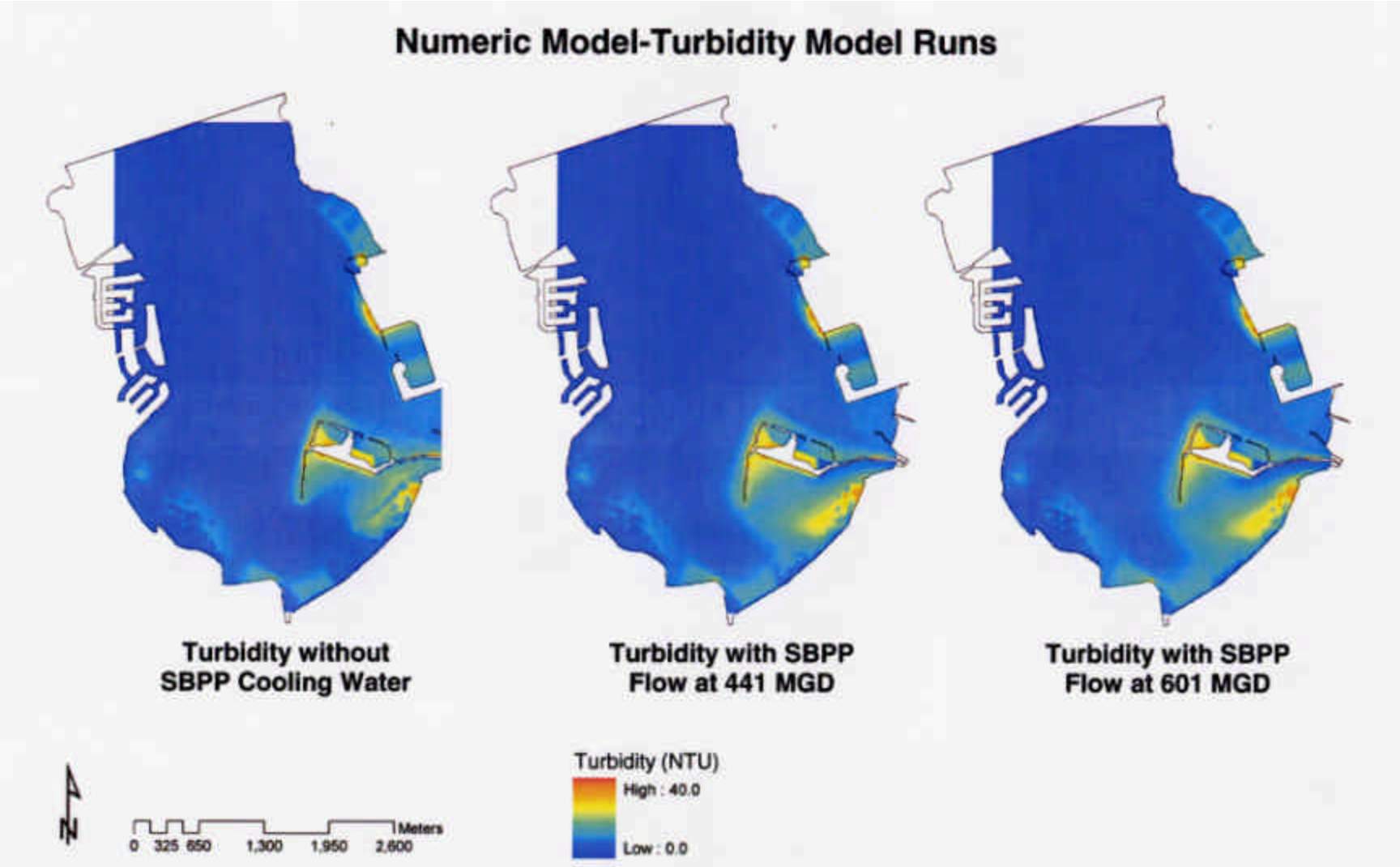

Figure 2.6-21. Numeric model predicted patterns of turbidity without SBPP cooling water flow (left), with SBPP cooling water flow at 441 mgd (middle), and with SBPP cooling water flow at 601 mgd (right). Model runs are average turbidity (NTUs) during a 72-hour spring tidal cycle.

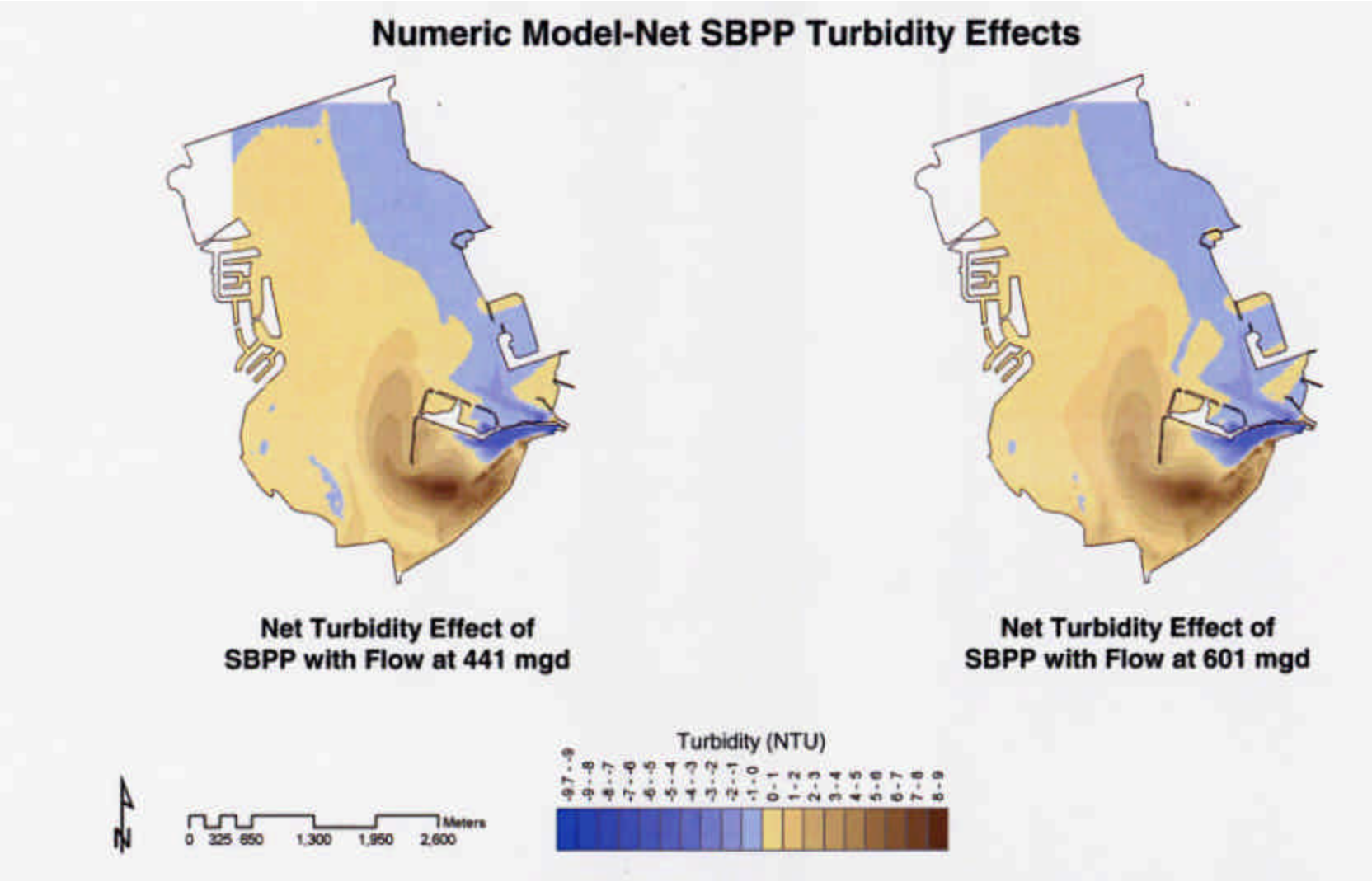

Figure 2.6-22. Numeric model of net predicted turbidity for the SBPP with cooling water flow of 441 mgd versus no cooling water flow (left) and SBPP with cooling water flow of 601 versus no cooling water flow (right). Model runs are average difference in turbidity (NTUs) during a 72-hour spring tidal cycle.

2.7 Receiving Water Sediments

2.7.1 Introduction

The distribution of particle sizes within soft sediment marine environments is a significant factor affecting the composition of infaunal assemblages (Bergen et al. 2001). A high proportion of silt and clay is often correlated with high organic matter concentrations used by deposit feeding organisms such as capitellid polychaetes and nematodes. Sandy substrates can be a more favorable habitat for certain bivalve mollusks or amphipod crustaceans or may allow certain tube-building taxa (e.g., phoronids) to predominate.

Grain size distribution is a function of the depositional and erosional patterns within an area and is influenced by the ambient current regime. In a shallow bay environment, currents result from tidal effects, wind stress, or fresh water inflows. Because of the significant contribution of sediment parameters to faunal composition, sediment samples were collected and analyzed for grain size composition from all subtidal and intertidal stations. The grain-size data along with water temperature data were used in a multivariate analysis to identify trends in the abundance and distribution of organisms in relation to the SBPP discharge.

Earlier studies in south San Diego Bay sampled sediment characteristics at 11 subtidal monitoring stations annually from 1977–1993 (see Ogden Environmental 1994 for review). Clay fractions were highest at Station E5 in the SBPP discharge channel and lowest at 'control' stations N2, A3, C3 farthest from the discharge and in the central portion of the bay (see **Figure 2.3-1**). Conversely, the larger-size fractions were in the lowest proportions at the discharge channel and in highest proportions at the control stations. Station F4 at the tip of the Chula Vista Wildlife Island (CVWI) breakwater had the greatest proportion of gravel and shell debris.

Within the south bay study area results of these earlier studies identified a sedimentation gradient that was attributed to decreasing tidal flushing in the back bay and accumulated sediments from the Otay River Basin (LES 1981). Consequently, larger particles predominated in the northwestern portion of the study area while finer-size fractions accumulated in areas of less water motion in the southeastern portion of the bay.

DRAFT

2.7.2 Methods

Sediment core samples were collected by hand at 10 intertidal and 21 subtidal stations (**Figure 2.3-1**) and analyzed for grain size composition. The core size was 5 cm in diameter by 15 cm deep. Sediment grain size of each sample was determined by using a dry weight size fraction analysis. Samples were dried and then passed through a series of standard sieves to calculate the percentage distribution of particle sizes using Procedures ASTM D 117-95 and ASTM D 1136-96a. Twelve fractions were separated ranging from gravel-sized particles and shell debris (> 6.3 mm) to a silt and clay fraction (<0.075 mm). Particle distributions were plotted as a function of cumulative percent weight passing through each screen size. The size fraction for silt-clay was arbitrarily set at 0.01 mm for the purposes of charting the cumulative passing fractions by weight.

2.7.3 Results

Samples were collected at all benthic stations on September 9–10, 2003. The 31 sampling stations were grouped into seven areas according to their tidal elevations and proximity to the SBPP discharge to facilitate comparisons of particle size distributions, as follows:

Area	Stations
Subtidal inner discharge	SE7, ST1, ST2, ST3
Subtidal outer discharge	SE5, SF4, ST4, ST5
Intertidal discharge	IT1, IT2, IT3, IT4, IT5
Intertidal reference	IR1, IR2, IR3, IR4, IR5
Subtidal north reference	SA3, SC3, SD4, SN2
Subtidal south reference	SE3, SE4, SF2, SF3
Subtidal intake reference	SR1, SR2, SR3, SR4, SR5

Most samples were comprised of coarse to fine sands with varying proportions of shell fragments and silt-clay. There was substantial variation in particle size distribution among stations, even those that were generally in close proximity. For example, in the subtidal inner discharge zone, Station ST01 had approximately 60 percent silt-clay fraction, but Station ST03 which was 400 m further west in the discharge channel had less than 5 percent silt-clay fraction with a much larger proportion of medium sands (**Figure 2.7-1a**).

The intertidal reference stations generally had a high degree of similarity in sediment composition but the corresponding intertidal stations in the discharge channel had greater variation. The intertidal reference stations (all at the +1.0 ft MLLW elevation) on the north side of CVWI and off the Chula Vista marina had the greatest aggregate percentage of sand and the least percentage of silt-clay of all zones sampled (**Figure 2.7-1d**). The two outermost intertidal discharge stations (IT5 and IT4) had comparable proportions of these size fractions, but the three inner stations had substantially higher percentages of silt-clay (**Figure 2.7-1c**). Most of the large-size particle fractions in all samples were comprised of shell debris from locally occurring mollusk populations and shell fragments originating from dredged material used to construct berms of the adjacent CVWI.

Subtidal intake reference stations generally had the greatest percentage of silt-clay, averaging over 60 percent (**Figure 2.7-1c**). Other zones had average percentages of silt-clay ranging from about 30 to 50 percent. There was not an obvious directional gradient in particle size distributions within the south bay region sampled, although there was a trend toward greater proportions of sand at the more northwesterly stations (SN02 and SA03) in the subtidal north reference zone (**Figure 2.7-1e**). A detailed comparison of the sediment size composition for each station is shown in the sediment gradation curves (**Figures 2.7-2–2.7-8**).

DRAFT

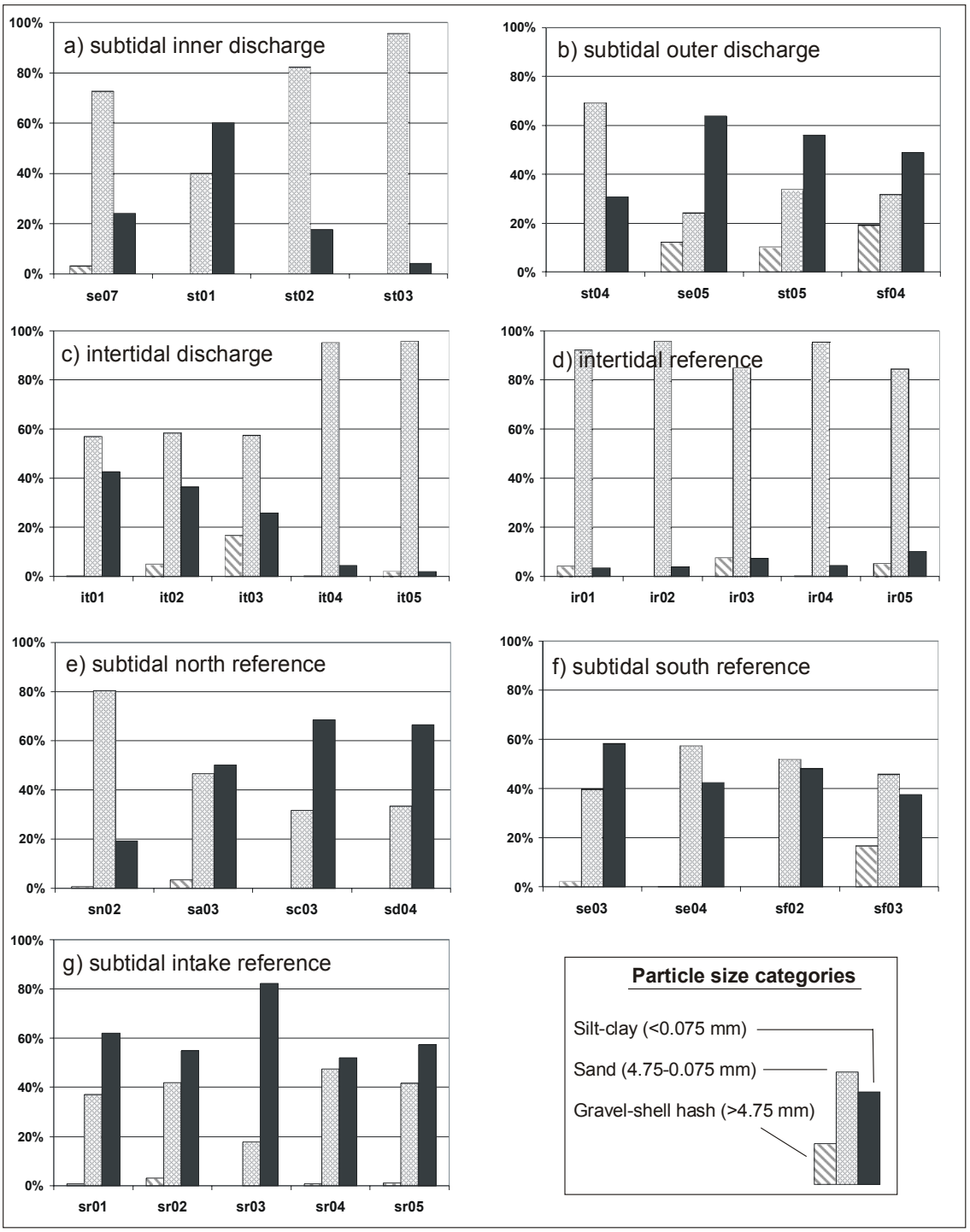

Figure 2.7-1. Percentages of gravel, sand, and silt-clay size fractions in sediment samples.

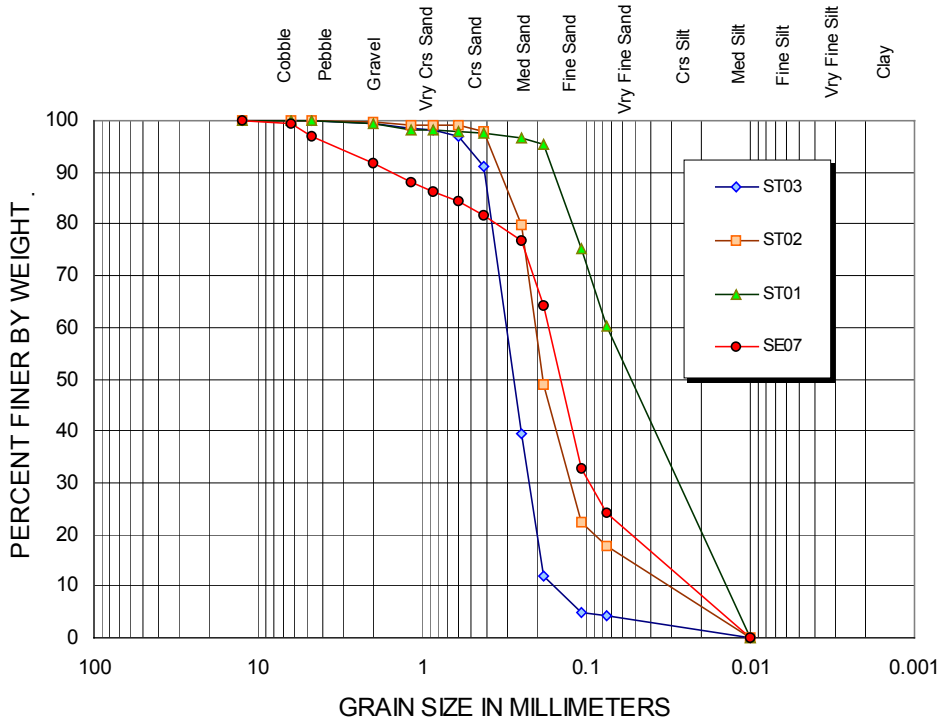

Figure 2.7-2. Sediment gradation curves for subtidal inner discharge stations.

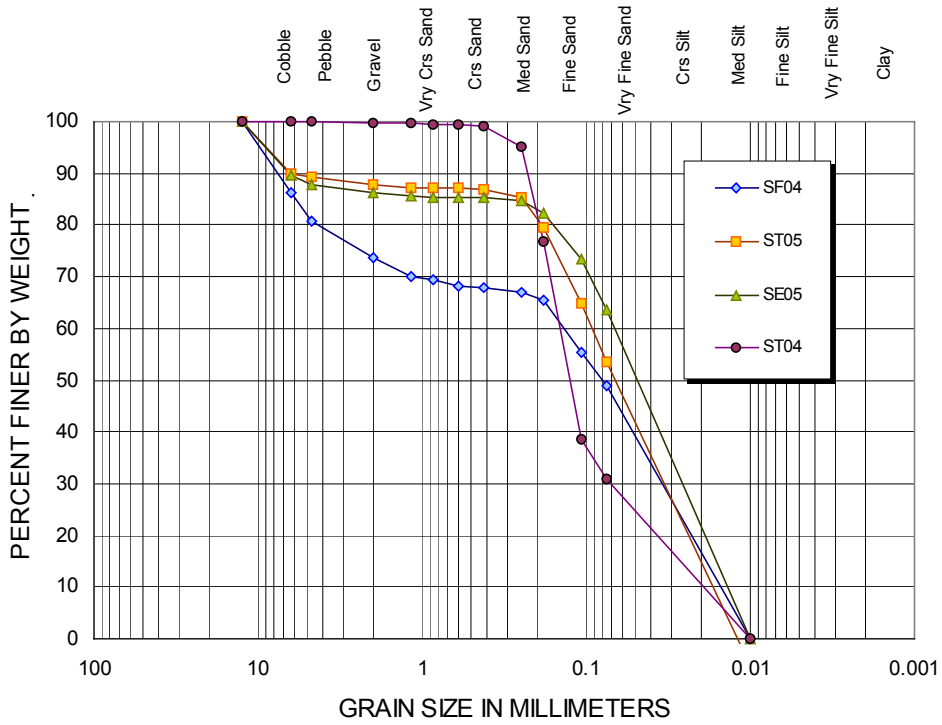

Figure 2.7-3. Sediment gradation curves for subtidal outer discharge stations.

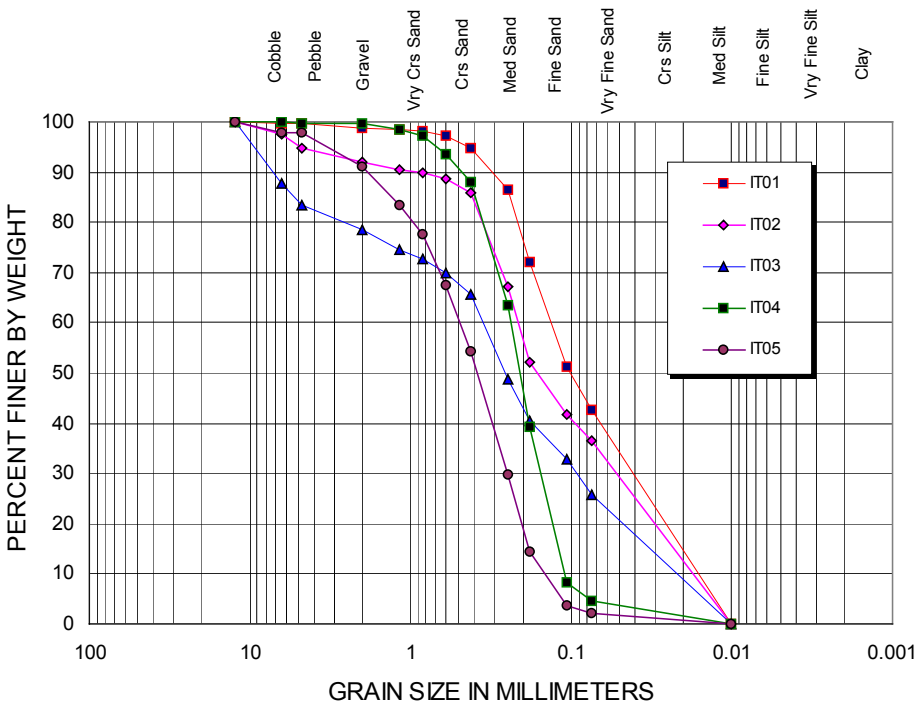

Figure 2.7-4. Sediment gradation curves for intertidal discharge stations.

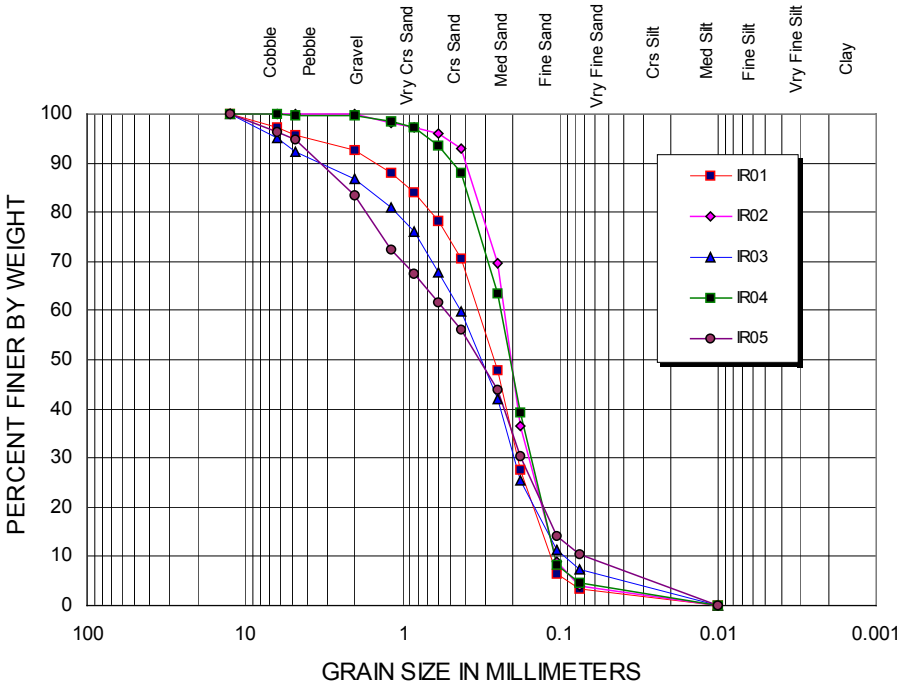

Figure 2.7-5. Sediment gradation curves for intertidal reference stations.

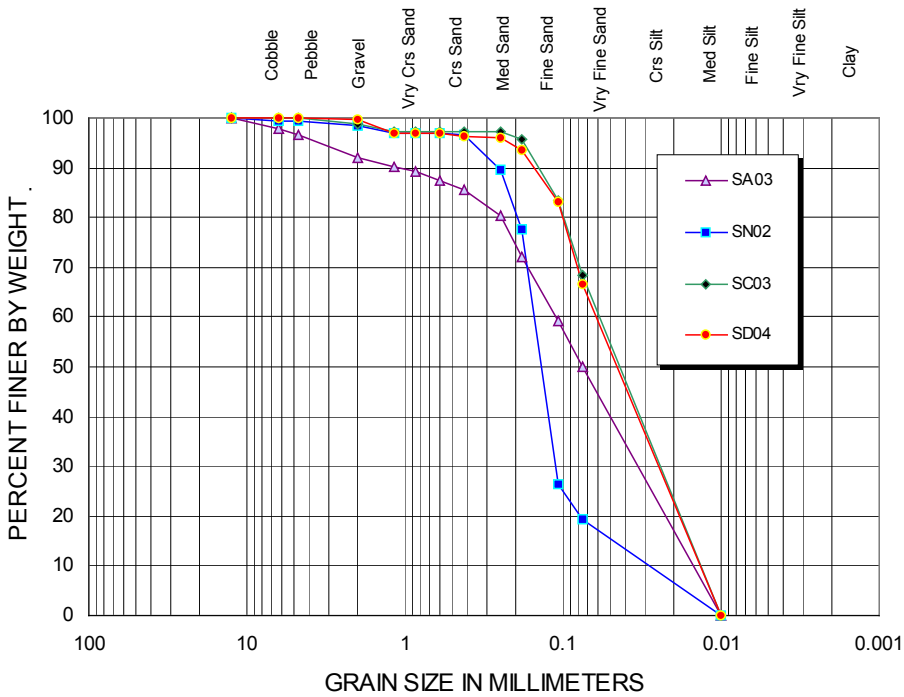

Figure 2.7-6. Sediment gradation curves for subtidal north reference stations.

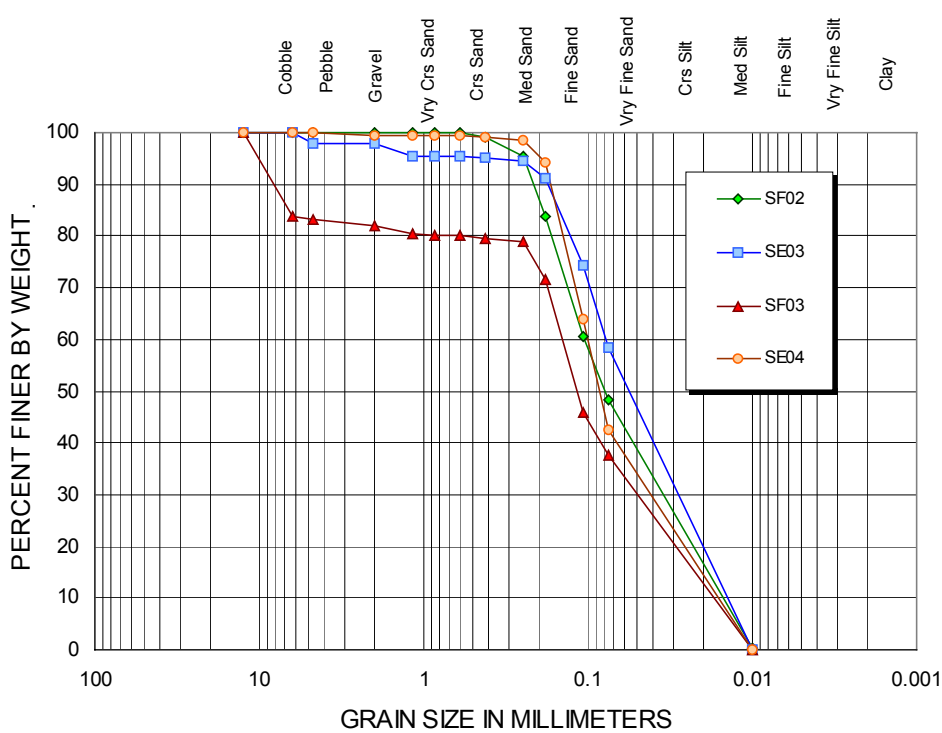

Figure 2.7-7. Sediment gradation curves for subtidal south reference stations.

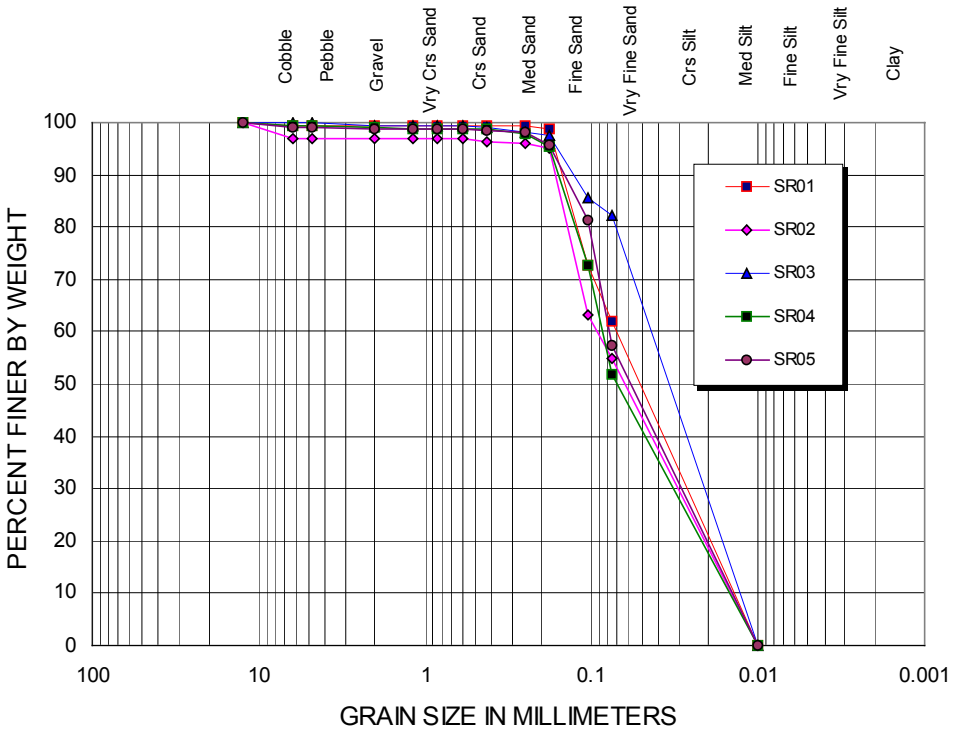

Figure 2.7-8. Sediment gradation curves for subtidal intake reference stations.

DRAFT

2.8 Receiving Water Chlorine Monitoring

2.8.1 Introduction

The SBPP currently uses chlorine injections to prevent microfouling of the cooling water condensers, piping, and associated cooling water equipment. Chlorination of the cooling system is permitted under NPDES permit 96-05. Chlorine is a broad-spectrum biocide that is effective due to strong oxidant properties. Since bacterial slimes and other microfouling organisms that foul the condenser tubes are highly susceptible to chlorine, only weak concentrations are necessary for efficient biofouling control. These small quantities combined with the chemical and biological reactions within the cooling system result in small amounts of total residual chlorine (TRC) in the discharged water.

At the SBPP, each electrical generating unit is serviced by a pair of cooling water pumps and a condenser that are an essential part of the generating cycle. The current discharge limits for total residual chlorine at the point of discharge are variable depending on the number of power generating units that are in operation. The NPDES limits for chlorine are a water-quality based standard developed from the results numerous bioassay experiments using a variety of test species and life stages. The allowable discharge levels decrease as more cooling pumps are operated due to the increase in flow volume added to the discharge. If the cooling pumps for one unit are in operation, the allowable discharge is 144 parts per billion (ppb) of TRC. If two, three, or four units are in operation, the allowable discharge concentration is reduced to 111 ppb, 95 ppb, or 85 ppb TRC, respectively. For comparison, the maximum residual disinfectant level goal (MRDLG) for chlorine in drinking water allowed by the Environmental Protection Agency (EPA), is 4,000 parts per billion (ppb). This is the level below which there is no known or expected risk to public health. The MRDLG for chlorine in drinking water is 28 times greater than the maximum TRC allowed in the SBPP discharge.

Chlorination of the cooling water system is intermittent rather than continuous. Treatments occur for a duration of 20 minutes, six times per day. Injection cycles are evenly spaced, occurring every four hours. During each cycle, half of the cooling water system of each generating unit is treated. This allows the SBPP to maintain chlorination levels that are adequate to effectively control microfouling organisms, but still remain within permissible discharge levels due to dilution and mixing with the water from the untreated half of each unit's cooling water system. The actual amount of chlorine added to each unit's cooling water system is unique because the systems have different flow capacities. Generating Units 1 and 2 have cooling water pumps that deliver 147,600 liters per minute (lpm) (39,000 gallons per minute (gpm)). Generating Unit 3 is cooled by pumps that supply 236,200 lpm (62,400 gpm), and generating Unit 4 has a cooling

water flow of 258,900 lpm (68,400 gpm). Reported values are per pump, and each generating unit is cooled by two cooling water pumps. To remain within the limits of its NPDES permit, the SBPP currently uses 0.68 lpm (0.18 gpm) of chlorine for Units 1 & 2, 0.76 lpm (0.20 gpm) for Unit 3, and 1.02 lpm (0.27 gpm) for Unit 4. Treatment of cooling water systems only occurs during the scheduled intervals and is restricted to those generating units that are in operation.

2.8.2 Methods

As part of its ongoing permit-required chlorine-monitoring program, SBPP sampled for TRC twice per month during the study period. One sample was collected between the 1st and the 15th of each month, and the second was taken between the 15th and the end of the month. Samples were collected at least 6 days apart. On the days when samples were collected, an injection cycle was chosen (either the 0815 PDT or 1215 PDT cycle), and water samples were taken 15 minutes after initiation of the 20 minute treatment, when maximum TRC would be expected.

Water samples were collected from a floating sampling station located in the discharge channel on the SBPP property line. Water samples were pumped to shore and tested for TRC with a Hach® colorimeter. Baseline reference samples were collected from the intake channel on the same date and analyzed for TRC using the same methods (**Figure 2.8-1**).

2.8.3 Results

The TRC levels measured in the discharge channel during the monitored chlorinations during summer 2003 are summarized in (**Figure 2.8-2**). The TRC detection limit specified in the NPDES permit is 40 ppb. Measurements below 40 ppb are considered background variation and are attributed to other halides (e.g. bromine, fluorine, iodine) that interfere with the colorimeter measurements. From the figure it is apparent that the SBPP does little to increase TRC levels above the detection limit. The data indicate that background TRC levels are similar between the intake and discharge channels. Variation in the data were likely due to instrument interference from other halides occurring in seawater. Examination of the error bars indicates that TRC was rarely measured above 60 ppb (**Figure 2.8-2**). Thus, given the maximum allowable discharge level of 85 ppb when all four generating units are in operation, the power plant was consistently within the guidelines established by NPDES permit 96-05. Additionally, the SBPP maintained its discharge below 85 ppb TRC for over 60% of the sampling events with only three units in operation.

Analysis of the impacts of cooling water chlorination on organisms as an isolated stressor in the receiving waters is not possible in a field research context because the measured concentrations were close to or below detectable levels and would not be expected to produce any measurable changes in receiving water biota. However, it is possible that TRC, in concert with other SBPP discharge factors such as elevated temperatures, may have some small additional effect on biotic distributions in the receiving waters. It is this sum total of impacts due to environmental stresses created by the SBPP may reduce the fitness of organisms in the discharge channel. Thus, the data on biological communities presented in **Sections 3.2, 3.3,** and **3.4** should be interpreted in the context of a single water body influenced by the SBPP discharge. An integrated discussion of the various physical parameters of the discharge on biotic distributions is discussed in **Section 4.0**.

DRAFT

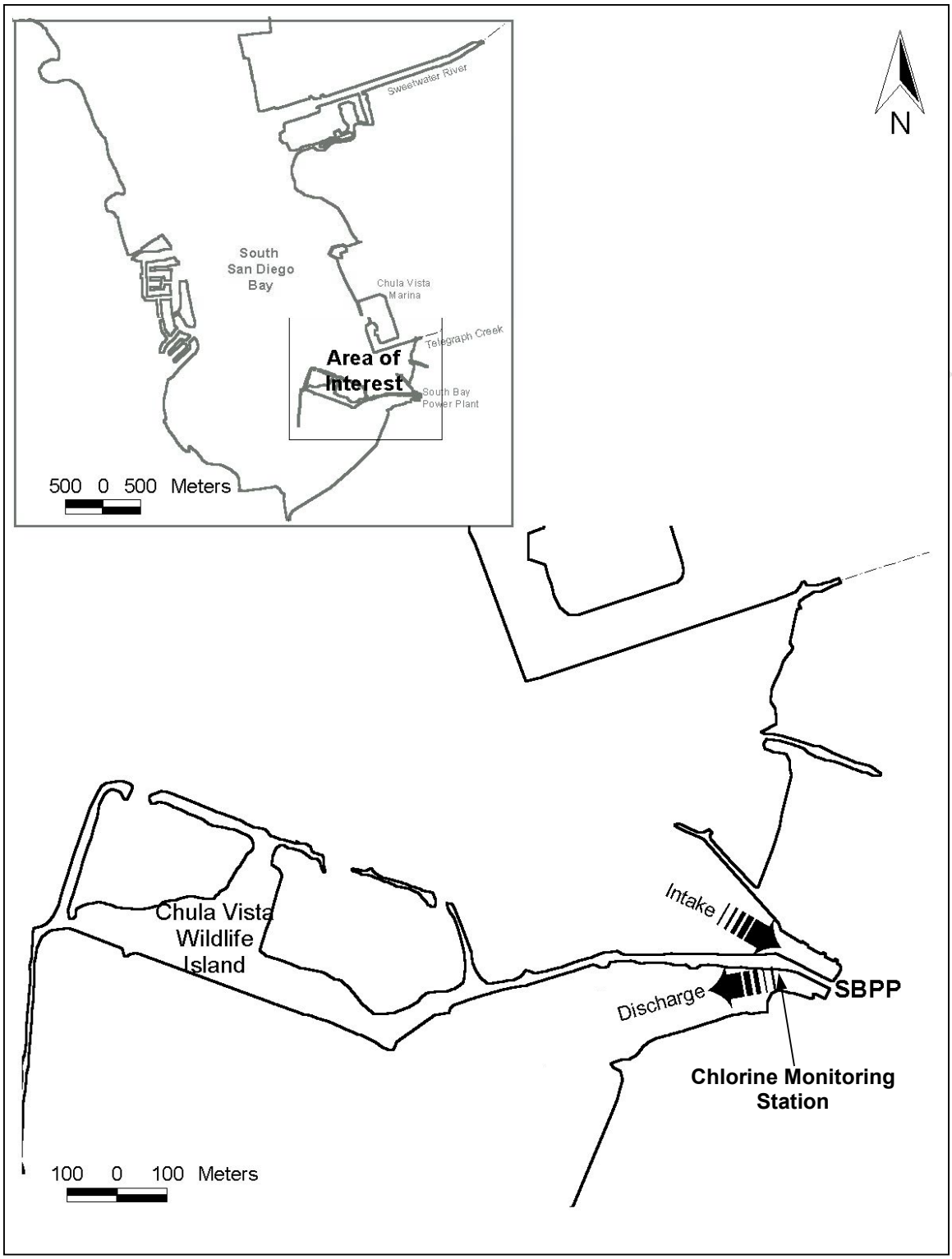

Figure 2.8-1. Location of chlorine monitoring station in relation to the cooling water intake and discharge channels for the South Bay Power Plant.

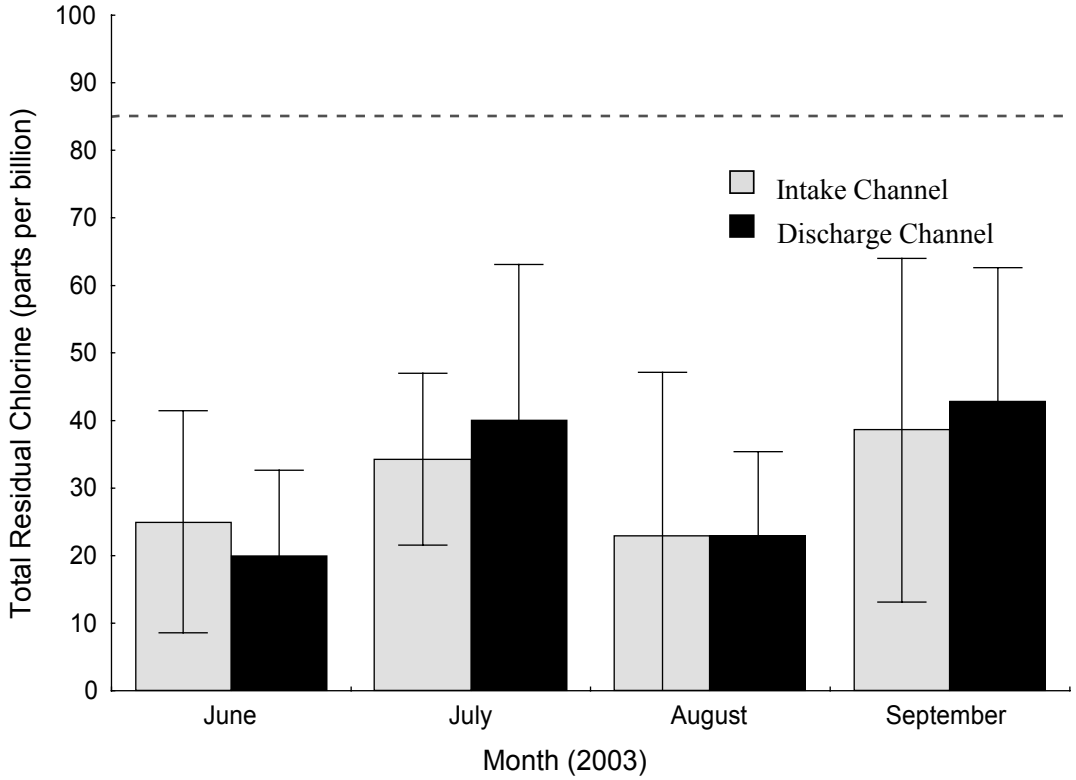

Figure 2.8-2. Total residual chlorine levels for the cooling water intake and discharge channels for the South Bay Power Plant. Error bars are ± 1 standard deviation. The dashed horizontal bar is the maximum allowable discharge limit when all cooling water pumps are operating

3.0 Biological Studies

This section describes the biological studies completed in 2003 to address the RWQCB questions regarding impacts of the SBPP discharge. The three main studies included an updated analysis of eelgrass distribution in south San Diego Bay in relation to abiotic factors, effects of the discharge on intertidal and subtidal benthic infauna, and examination of the relationship between fish abundance, dissolved oxygen, and water temperature in the SBPP discharge channel.

3.1 Introduction

Earlier studies concluded that the existing elevated-temperature cooling water discharged from SBPP had caused no appreciable harm to the aquatic biological community of San Diego Bay or to the beneficial uses of those waters (Ford et al. 1973). However, the study also concluded that the discharge did have adverse effects on the benthic invertebrate community within the discharge channel, which, for the purpose of that study, was not considered to be part of San Diego Bay. A subsequent data review of annual summer benthic studies conducted from 1977–1994 concluded that no appreciable long-term upward or downward trends in species diversity or abundance had occurred within the discharge channel (Ogden 1994). In 1996, SDG&E was required to conduct further effluent studies on eelgrass and fishes, which were completed in 2000 and submitted to the RWQCB (Merkel & Associates, Inc. 2000a, 2001, respectively).

Although the intake and discharge structures at SBPP remain unchanged since the previous studies, the RWQCB has moved the point of compliance for discharge temperature 4,000 feet closer to the point of discharge. The designated point of compliance in the existing NPDES permit (issued under Order No. 96-05) is approximately 1,000 ft beyond the SBPP discharge basin. SBPP is required to monitor water temperatures at this point and the results are submitted to the RWQCB monthly. Section 316(a) of the CWA requires that States impose an effluent limitation with respect to the thermal component of a discharge that will assure the protection and propagation of a balanced, indigenous population of shellfish, fish, and wildlife in the receiving water.

Based on this change of the point of compliance and the impacts to biological communities within the eastern portion of the discharge channel identified in previous studies, the Board requested that studies be designed to address the following questions:

1. *What are the effects of the cooling water discharge on aquatic and benthic species during the days when the water temperature is highest in the discharge channel? Are these effects permanent or temporary?*

2. *Does temperature, dissolved oxygen (DO), and/or chemical makeup (chlorine, metals, toxicity, etc.) have a combined effect on the species abundance and diversity in the discharge channel?*

3. *What portion, areal extent, of the discharge channel does not support beneficial uses, due to elevated temperatures? What are the affected species, and do these species exist in other parts of the discharge channel and in south San Diego Bay?*

The studies described in this section were performed mainly during the period of July through September when the greatest heat stress is imposed on the biota. These biological data are used along with the physical data described in Section 2.0—*Characteristics of the Source Water Body* and existing information to assess the magnitude of discharge impacts from SBPP which are described in Section 4.0—*Integrated Discussion*.

DRAFT

3.2 Eelgrass

3.2.1 Introduction

This section describes the results of an eelgrass (*Zostera marina*) mapping survey conducted in South Bay in May 2003. The results are later incorporated with receiving water turbidity monitoring and temperature modeling results in Section 4.0–*Integrated Discussion: Eelgrass* to evaluate the influence of the SBPP on the distribution and abundance of this habitat-forming species.

Eelgrass is a native marine vascular plant indigenous to the soft-bottom bays and estuaries of the Northern Hemisphere. The species is found from middle Baja California and the Sea of Cortez to northern Alaska along the West Coast of North America and is common in healthy shallow bays and estuaries. Within the southern portion of its range, eelgrass growth is generally limited at the shore by desiccation stress at low tides. Throughout its range, eelgrass is generally limited along its deeper fringe by light reduction to a level below which photosynthesis is unable to meet the metabolic demands of the plant to sustain net growth (the photo-compensation depth). Eelgrass is considered to be a habitat forming species that creates unique biological environments when it occurs in the forms of submerged or intertidal aquatic beds or larger meadows. As submerged aquatic beds, eelgrass is given special status under the Clean Water Act, 1972 (as amended), Section 404(b)(1), "Guidelines for Specification of Disposal Sites for Dredged or Fill Material," Subpart E, "Potential Impacts on Special Aquatic Sites."

Eelgrass plays many important roles in estuarine systems. It clarifies water through sediment trapping and stabilization. It also provides the benefits of nutrient transformation and water oxygenation. Eelgrass serves as a primary producer in a detrital-based food-web, and is further directly grazed upon by invertebrates, fish, and birds, thus contributing to eco-system health at multiple trophic levels. Additionally, it provides physical structure in the form of habitat to the community, and supports epiphytic plants and animals, which in turn are grazed upon by other invertebrates, fish, and birds. It is also nursery area for many commercially and recreationally important finfish and shellfish; those that are resident within the bays and estuaries, including oceanic species that enter the estuaries to breed or spawn. Among recreationally important species, sandbass and California lobster make uses of eelgrass beds as bay habitat. Besides providing important habitat for fish, eelgrass is also considered an important food resource supporting migratory birds during critical life stages, including migratory periods. Black brandt, a migratory species that occurs in San Diego Bay during winter months, is almost exclusively dependant upon eelgrass as a food resource.

This species can forage widely on intertidal and shallow subtidal beds throughout the south bay.

In addition to its high ecological value, eelgrass is also a valuable tool for examining long-term trends in a given eco-system associated with water quality improvements or deterioration. It has ideal characteristics for monitoring eco-system change. Eelgrass responds to persistent water quality conditions rather than short duration fluctuations. Eelgrass is adapted to a wide range of tolerances, and is capable of "averaging" exposure conditions, including temperature, turbidity, seasonal light levels, sedimentation rates, etc., that result in either positive growth or a gradual decline in the resource. As a result, day-to-day or hour-to-hour variability, as what can be seen in water quality testing, is of relatively little consequence to eelgrass. The ability of eelgrass to weather short-term stressful environments has been demonstrated on a number of occasions through natural and experimental restriction of resource availability. A more biologically meaningful measure of long-term trends in eco-system health can be seen in the response of eelgrass to chronic exposures to the ambient environment. For example, prolonged stresses, such as consistent light limitation, will result in a decline of eelgrass habitat.

Within San Diego Bay, eelgrass occurs in the low intertidal and shallow subtidal, from +0.3 m (+1.0 ft) MLLW to –5.2 m (–17.0 ft) MLLW. In 2003, eelgrass covered approximately 15 percent of San Diego Bay. The majority occurs within the South Bay eco-region located south of the Sweetwater River channel.

3.2.2 Review of Eelgrass Studies in south San Diego Bay

Eelgrass has been the focus of regulatory attention and resource management since the mid-1970s. As a result, there is greater documentation of eelgrass distribution and abundance than for most bay species and bay habitats. The following literature sources were reviewed to develop a chronology of changes in eelgrass distribution in South Bay:

1975-1979	San Diego Unified Port District. San Diego Bay Eelgrass Distribution 1975-1979. Draft Environmental Impact Report, Master Plan San Diego Unified Port District. September 1979.
1979	Lockheed Center for Marine Research. Biological Reconnaissance of Selected Sites of San Diego Bay. March 1979.
1979	Lockheed Center for Marine Research. Preliminary Report on Spatial Distribution of *Zoobotryon verticillatum*, *Zostera marina*, and *Ulva* spp. in South Bay. Sept. 1979.
1988	San Diego Unified Port District. Algae and Eelgrass Distribution, September 1988, South Bay Enhancement Plan. March 1990.

1993 SWDIV, Natural Resources, USN. San Diego Bay Eelgrass Beds. 1993.

1999 SWDIV, Natural Resources, USN. San Diego Bay Eelgrass Beds. 1999.

The efficacy of comparisons between eelgrass surveys is affected by advancements in technology and the resulting improvements in precision and accuracy of mapping capabilities. Surveys done in the 1970s, were performed by a variety of techniques, such as trawl and grab sampling and diver transects. Locations of eelgrass were mapped by estimating positions from landmarks, and on rare occasion, from controlled survey points to approximate positions. In the late 1970s and through the 1980s, larger spatial-scale eelgrass mapping was conducted using mainly true color and infrared aerial imagery. This provided more accurate maps of surface cover compared to earlier efforts. However, the aerial imagery was not consistently capable of detecting eelgrass beneath the water level. As a result, the emergent and very shallow water eelgrass beds were generally well mapped, but eelgrass beds that were well underneath the water surface were often under reported or missed entirely.

Side-scan sonar can be used to overcome this problem of detecting subsurface eelgrass beds, and was first used in the San Diego area in neighboring Mission Bay in 1988. The boat trackline was plotted using microwave navigation and eelgrass density was determined from sonagraphic charts. Diver transects were then used to ground-truth the sonagraphic charts (Merkel 1988). This approach was subsequently improved by using real-time differential GPS to plot the centerline boat position and using CAD software to create the maps (Merkel 1992). In 1993, the U.S. Navy applied this technology to San Diego Bay (Natural Resources, SWDiv, USN 1993).

From these mapping efforts, the eelgrass present within the bay ranges markedly from as little as about 200 acres in March 1979 to as great as 1,260 acres in 1993. It is generally believed that prior to the 1970s eelgrass within the bay had declined significantly due to heavy nutrient enrichment and subsequent plankton and macroalgal blooms associated with in-bay sewage discharges. While eelgrass maps appear to be relatively consistent in where eelgrass is located, the aerial coverage within these locations varies significantly between years and mapping efforts. Much of this may be related to survey methods.

From approximately 1985 through the early 1990s, southern California bays and estuaries as a whole experienced a tremendous expansion of eelgrass. In general, eelgrass expanded mostly in deeper waters in the various bays and estuaries. This was presumably from increases in water clarity associated with both a prolonged drought condition and a decline in watershed erosion from a slowdown in the southern California real estate development market. The continued lack of a sewage outfall in San Diego Bay also likely contributed to further increases in eelgrass habitat in the bay. Other expansions in San Diego County occurred in Agua Hedionda Lagoon and in Mission Bay

(Merkel 1992). Expansions also occurred in other bay and estuary systems northward to central California in Morro Bay (R. Hoffman, pers. comm.).

Baywide eelgrass surveys conducted within San Diego Bay included surveys performed by the U. S. Navy in 1993 and 1999. These surveys inventoried the eelgrass resources and presence/absence distribution within all of San Diego Bay; the 1993 survey also included bathymetric data. During the 1993 eelgrass survey there was a total of 509.9 ha (1,260 ac) of eelgrass observed within all of San Diego Bay. Of that total, 207.3 ha (512.2 ac) of eelgrass was noted within the current survey area for this study, which covered the majority of the South Bay eco-region. During the 1999 survey there was a total of 661.1 ha (1,633.6 ac) of eelgrass detected within San Diego Bay, of that total, 369.6 ha (913.3 ac) of eelgrass was mapped within the current survey area.

Within Mission Bay the City of San Diego has conducted baywide eelgrass surveys approximately every four years starting in 1988, then 1992, 1997, and 2001. Over those four monitoring intervals the total amount of eelgrass coverage within Mission Bay was 384.2 ha (949.3 ac), 454.0 ha (1,121.9 ac), 528.8 ha (1,306.6 ac), and 489.8 ha (1,210.4 ac) respectively. This trend over time, from 1988 through 1997 indicates a noticeable increase in eelgrass coverage, while the 2001 total is slightly lower than 1997. The overall trend observed within Mission Bay is similar to the increase in eelgrass coverage observed in San Diego Bay during the 1993 to 1999 time interval.

Eelgrass within South Bay follows similar distribution patterns from year to year and has not significantly changed in predicted locations of occurrence over time. Eelgrass has, however, likely expanded both more extensively to the south, along the Chula Vista Wildlife Island (CVWI), and into deeper fringes of existing beds from its distribution in the 1970's.

System-wide and regional conditions appear to play a major role in structuring eelgrass communities. Trends of expansion and contraction can be seen throughout a system and between systems within the southern bight of California. Watershed controls may be an important factor in structuring some systems while local conditions may play a major role in structuring other systems.

3.2.3 Methods

An eelgrass mapping survey was completed in 2003 to obtain updated information on eelgrass in South Bay. The survey was conducted in late May 2003 to take advantage of the yearly emerging growing season in this species. The survey used the combination of boat-towed side-scan sonar, similar to the U.S. Navy method, and single-beam sonar acoustic survey methods. The survey was done during the highest tides in the survey period for sampling shallow habitats.

3.2.2.1 Survey Area

The survey area was approximately 935 ha (2,310 ac), which was the portion of San Diego Bay south of the Sweetwater River Channel (**Figure 3.2-1**). Water depths during the survey ranged from +0.6 m (+2 ft) to –7.6 m (–25 ft) MLLW.

Portions of South Bay not covered in the survey included the shallow area north of Crown Isle, at the Loews Coronado Bay Resort, the channels of the Coronado Cays, the Chula Vista Marina, the tidal mud flat area between the SBPP and the Chula Vista Marina, where Telegraph Creek enters the bay, and the tidal flats of the historical Sweetwater River mouth. Boat access to these tidal areas was limited due to lack of adequate water depth.

3.2.2.2 Acoustic Field Survey Methods

Navigation

The acoustic surveys involved the integration of a differential global positioning system (dGPS) with 600 kHz side-scan sonar and fathometer systems. Navigation and positioning data for the survey were collected using a Leica MX400 GPS receiver equipped with a differential correction receiver, which utilized the U.S. Coast Guard FM correction beacon. Vessel position and direction data were linked to an on-board PC and integrated with on-screen navigation monitors. Survey trackline positional fixes were saved to the computer hard drive, and were simultaneously applied to side-scan record plots. The horizontal system resolution was ±1.5 m (±5 ft); the combined error of the navigation system and side-scan equipment.

All data were collected in decimal degrees latitude and longitude using the North American Datum of 1983 in meters (NAD 83). The data were then subsequently converted and plotted on a coordinate grid using UTM coordinates in meters (NAD 83).

The surveys were conducted aboard the 21 ft *R/V Merkel Johnson-150*, operated by Merkel & Associates. The research vessel ran a series of parallel north-northwest to south-southeast oriented tracklines within the northern portion of the survey area and northwest to southeast transect lines in the southern portion. The transects were spaced approximately 38 m apart. These tracklines were oriented roughly parallel to the orientation of the bay and the CVWI, respectively. A navigation fix was collected every second during data collection. Vessel position was maintained along the tracklines using the on-board, real-time dGPS display.

Side-Scan Sonar

Sonar data were collected using a side-scan sonar operating at 600 kHz. The towfish was positioned approximately 0.5 to 1.0 m (1.6 to 3.3 ft) below the water surface, depending on the distance between the surface and bay bottom. To obtain good coverage and resolution, given the average water depth, the side-scan recorder was configured to

survey a width of 20 m per channel (port and starboard). This configuration allowed for the neighboring trackline path widths to overlap by approximately two meters (transects were spaced 38 meters apart).

Fathometer

Bathymetric data were collected using a single-beam fathometer operating at a frequency of 200 kHz. The echo-sounder was mounted on the port side of the vessel, with the 15 degree beam width transducer located approximately half a foot (0.15 m) below the water surface. All fathometer data were recorded onto the side-scan data and stored in the computer with time stamps and x-y coordinate data.

Eelgrass Mapping-Data Post Processing

Following the completion of the acoustic survey, the stored side-scan data was post-processed into a series of geo-rectified mosaic images using UTM, Zone 11, NAD 83, meters, covering all surveyed areas of the south bay. The images were imported into ArcView 3.2a for delineation of eelgrass and classification into percent bottom cover categories.

3.2.4 Results

The majority of the eelgrass identified in South Bay during this study fell in the percent bottom coverages of 26-50% and 76%-100%. Represented in smaller amounts were sparse eelgrass beds (<25% coverage), and beds in the highest coverage category (76-100%). Of the 935 ha (2,310 ac) surveyed, 442 ha (1,094 ac) supported eelgrass, which generally occurred as contiguous, mature beds (**Figure 3.2-2**). The total areal coverage of the eelgrass beds categorized by percent bottom cover are presented in **Table 3.2-1**.

Eelgrass within the eelgrass survey area was found to occur as elevations as high as +0.3 m (+1 ft) MLLW within the southern portions of the survey area and as deep as -3.0 m (-10 ft) MLLW, typically noted near the edge of channels in the northern regions of the survey area. Nearly 80% of all the eelgrass mapped within the survey area fell within the intermediate percent bottom cover categories.

Within the survey area there are several channels, both dredged and natural. The dredged channels include the existing and previous Chula Vista Marina channels, the SBPP seawater intake and discharge channels, the Emory Cove channel, and the Coronado Cays channel. The natural bay channel is within the middle portion of the survey area. These channels were not found to support eelgrass due to their depth, which are too deep to provide the light required for eelgrass growth in back bay environments.

In the northern portion of the study area, eelgrass distribution is generally dictated by bathymetry, with deeper areas devoid of eelgrass, while slightly shallower areas support

large, contiguous beds. The depth range of eelgrass occurrence in this region is from +0.3 m (+1 foot) to approximately –1.8 m (–6 ft) MLLW.

In the lower reaches of the south bay, eelgrass is most widespread in the large area west of CVWI (**Figure 3.2-2**) Eelgrass here falls predominantly in the 26-50% bottom cover range. There is a particularly robust bed near the mouth of the Otay River, with 76-100% bottom cover. The depth range of eelgrass occurrence in this region is from +0.3 m (+1 foot) to approximately –1.2 m (–4 ft) MLLW.

Immediately to the west and south of CVWI there is almost no eelgrass growing. The predominately bare area to the west of the wildlife island extends out from the natural channel, which is also bare, and continues further north through the center of the study area. To the south of CVWI there is a small occurrence of eelgrass, consisting of sparse, isolated patches, covering less than 25% of the bottom. This area has not been previously noted to support eelgrass year round, and it is anticipated that the current occurrence is likely the result of spring recruitment and is unlikely to have persisted through the summer months as water temperatures increased.

Table 3.2-1. Eelgrass coverage categories and acreages in study area.

Coverage Category	Amount of Eelgrass Within Survey Area Hectares (Acres), % of Total Area
<25% coverage	58.48 (144.5), 13.2%
26-50% coverage	215.87 (533.4), 48.8%.
51-75% coverage	139.44 (344.6), 31.5%
76-100% coverage	28.84 (71.3), 6.5%
TOTAL	**442.63** (1,093.8), 100%

3.2.4.1 Comparison of the Recent Survey to Prior Surveys

The eelgrass maps produced by the U.S. Navy in 1993 and 1999 and those from the present study represent the most comprehensive sets of maps for San Diego Bay, and are the most comparable because the surveys utilized similar methods. The results of the present study overlain on eelgrass maps from the U.S. Navy reveal a continued increase in eelgrass from 1993 to 2003 in the South Bay region (**Figure 3.2-3**). The 1993 survey mapped a total of 207.3 ha (512.2 ac) of eelgrass, the 1998 survey 369.6 ha (913.3 ac), and the present study 442.6 ha (1,093.8 ac). The increase in coverage over the last ten years is generally accounted for by an expansion of these beds into slightly deeper water, possibly as a result of improved water quality.

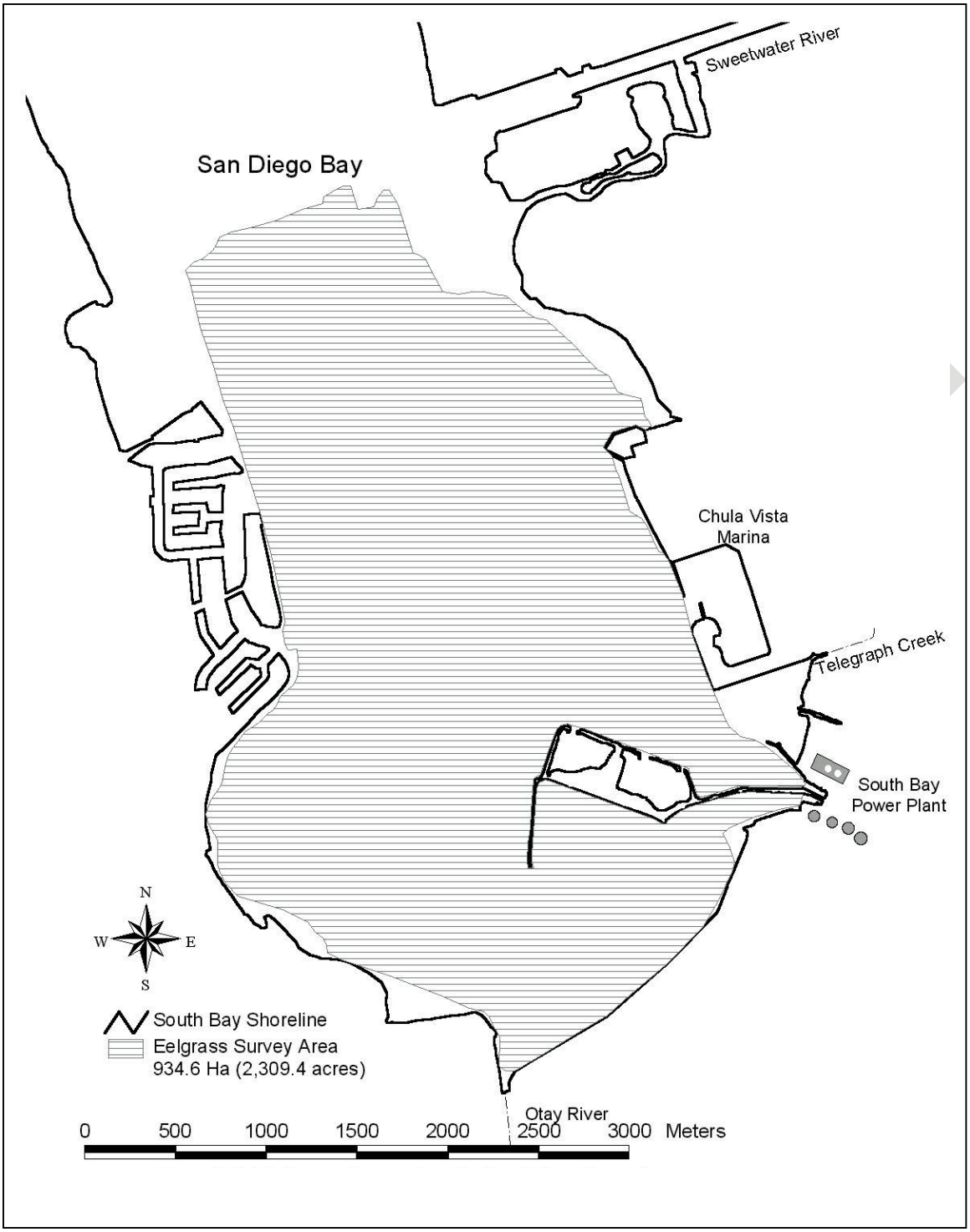

Figure 3.2-1. Eelgrass survey area in South Bay.

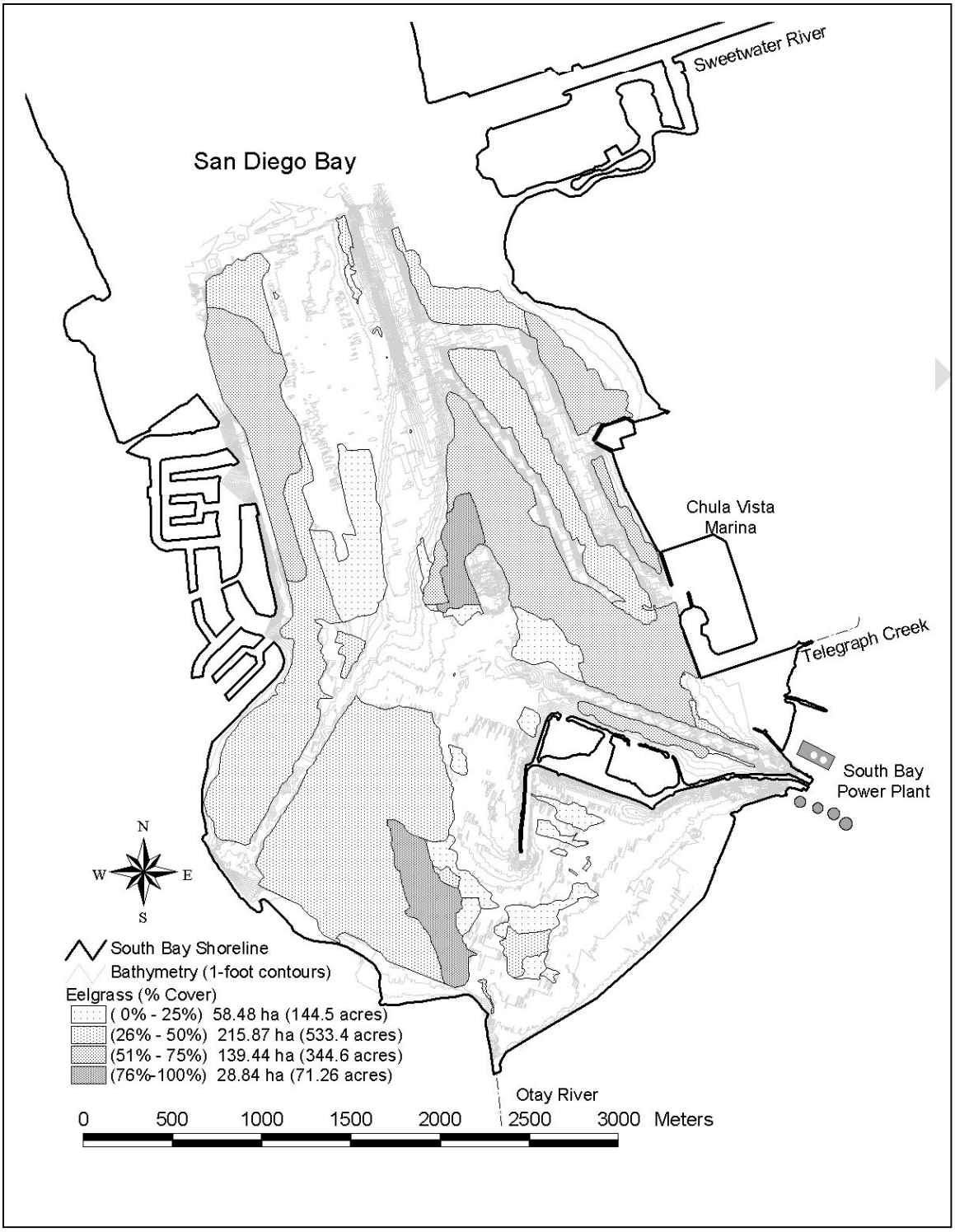

Figure 3.2-2. Eelgrass coverage in South Bay, May 2003.

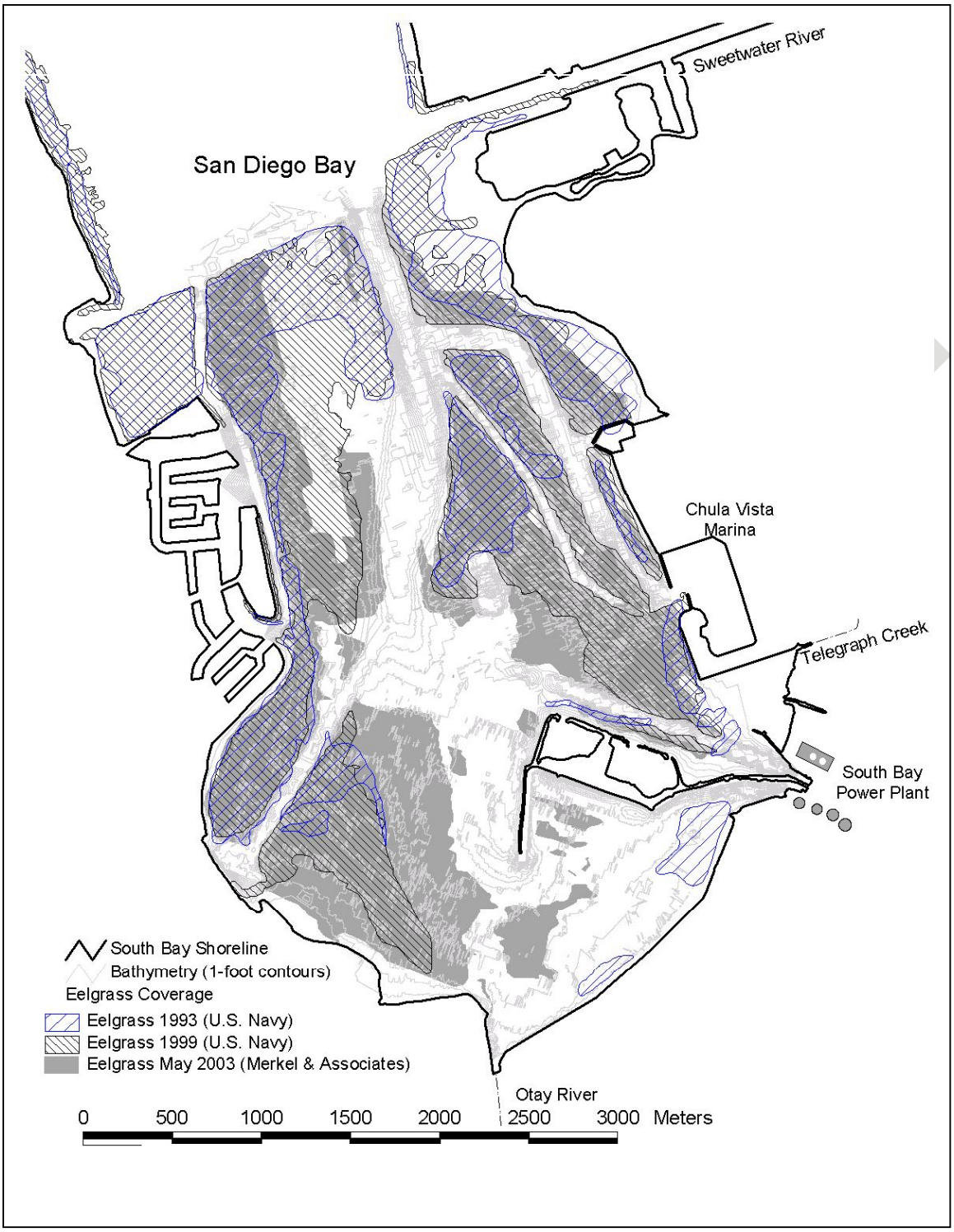

Figure 3.2-3. Comparisons of eelgrass coverage in South Bay (1993, 1999, 2003).

3.3 Benthic Invertebrates

3.3.1 Introduction

Benthic marine invertebrates reside within and on the surface of soft substrates and are also associated with benthic algae and seagrasses. The fauna typically includes numerous species of annelid worms, bivalve and gastropod mollusks, various types of crustaceans, echinoderms, and lesser known but equally important groups such as nematodes, nemerteans and phoronids. Together they comprise an important food source for higher trophic level predators such as fishes and shorebirds. Changes in the productivity and persistence of benthic infauna are related to natural and anthropogenic factors such as water quality, pollutant loading, substrate composition, organic matter content, temperature, oxygen concentration, and interspecific community interactions (Weisberg et al. 1997). Benthic infauna have been widely used as pollution indicators because populations are sedentary and respond to local changes in ambient conditions (Smith et al. 2001). The benthic studies reported in this report supplement earlier monitoring work performed for SBPP from 1968–1994, and further delineate the area affected by discharges from SBPP.

3.3.2 Review of Benthic Invertebrate Studies in South Bay

Benthic invertebrate populations in south San Diego Bay have been quantified in various studies since 1968. The first studies were conducted by Ford (1968), and Ford et al. (1970, 1972, 1973). The sampling design consisted of a grid of subtidal stations in the area directly influenced by the discharge, the general area of the intake channel, and other areas outside the influence of the thermal plume but within the South Bay ecoregion. Samples were collected mainly in summer with a Hayward "Orange Peel" grab that sampled a surface area of approximately 1,060 cm^2 (164.3 in^2). Samples were washed through a 0.75 mm (0.03 in) mesh nylon screen cloth. Some intertidal core samples were also collected but the data set was not analyzed because the sampling pattern was deemed inadequate to describe any potential gradient of power plant effects.

Data were analyzed using non-parametric statistical tests to compare faunal characteristics of discharge and control stations. The main conclusion from this series of studies was that significant effects on benthic invertebrate assemblages were "restricted primarily to the cooling channel area and to warmer periods of the year" (Ford et al. 1973). The evidence included lower numbers of invertebrate species and reduced invertebrate richness and diversity in the discharge channel. Numbers of algal species,

however, were greater in the outer discharge area than the control area, which was interpreted as a possible beneficial effect of the thermal plume.

Biomass was found to be significantly reduced for almost all major taxonomic groups at inner discharge channel stations as compared to control stations. There were some significant increases in invertebrate and plant biomass in the outer discharge area stations compared to the control area in winter and spring, but not in summer. Of the taxonomic groups tested, only polychaetes worms and bivalve mollusks had no significant differences between the outer discharge stations and the control stations. Comparisons between years (1968, 1970, 1972) indicated that numbers of invertebrate species and all species were significantly different among years.

An annual benthic monitoring program was conducted in the receiving waters of SBPP from 1977–1993. The station array consisted of a subset of 11 locations from the original 28 stations established by Ford (1972). An analysis of data collected from 1977–1980 concluded that there were "no undesirable or adverse ecological effects to the soft bottom benthos associated with the operation of the SBPP" (LES 1981). The stations within the discharge channel and nearest the power plant (E5 and E7) (see **Figure 2.3-1**) had lower numbers of infaunal taxa and lower species diversity than control stations, indicating a localized effect of the power plant. Differences in species composition between discharge and control stations were also attributed to a pattern of increasing sediment temperatures, increasing concentrations of chemical oxygen demand (COD) and total kjeldahl nitrogen (TKN), and higher proportions of silt and clay occurring from the station nearest the plant to the stations furthest from the plant. Four of the common polychaete worm species recorded from the discharge channel, *Capitella capitata, Streblospio benedicti, Polydora ligni,* and *Fabricia limnicola,* were characteristic of benthic environments with high proportions of silt and clay and high organic content.

A complete review of the long-term receiving water monitoring was done in 1994 included surveys over a 17-year period from 1977–1993 (Ogden Environmental and Energy Services Co., Inc. 1994). The data were first standardized taxonomically because different groups of researchers had conducted the work over the years. The infaunal data were analyzed for trends in numbers of taxa, species densities, species diversity and evenness, biomass, and correlations between environmental conditions and species' abundances. As with the 4-year analysis (LES 1981), temperature and sediment characteristics proved to be the most important abiotic factors determining the distribution of invertebrate fauna. It was concluded that the biota were biologically richer (greater diversity and numbers of species) at the far-field stations than at the discharge channel and transition stations. The assemblage that predominated in the discharge channel area was generally comprised of opportunistic species with life history characteristics allowing them to readily colonize a disturbed or thermally-stressed environment. In addition to the polychaete species identified in the 4-year study as being relatively more abundant in the discharge as compared to control areas, other abundant

species included the polychaete worms *Marphysa sanguinea*, *Typosyllis armillaris, Cirriformia* sp., unidentified oligochaetes, and the gastropod *Cylichnella inculta*. Two species common throughout the entire study area, the polychaete *Mediomastus* sp. and the caprellid crustacean *Mayerella banksia*, had depressed abundances at the two stations closest to the power plant. The general conclusions of the 17-year analysis concurred with earlier reviews that power plant effects were confined to the discharge area southeast of the separation dike.

Other studies of benthic fauna have been done in San Diego Bay to identify areas potentially affected by accumulated pollutants. In one such study, the Bay Protection and Toxic Cleanup Program (BPTCP) sponsored by the SWRCB, 75 stations were sampled in San Diego Bay and vicinity (CSWRCB et al. 1996, 1998). The research involved analysis of sediment chemistry, benthic fauna, and toxicity testing of sediments and sediment pore water. Core samples were sieved through 0.5-mm mesh screens and the specimens identified to the lowest practical taxon.

Benthic habitats were classified as degraded, undegraded, or transitional using measures of species diversity and evenness, analyses of habitat and species composition, construction of dissimilarity matrices for pattern testing, assessment of indicator species, and development of a benthic index, cluster analyses, and ordination analyses. When combined with data from chemical testing and toxicity studies, it was determined that 23 stations (31 percent) in San Diego Bay were undegraded, 43 (57 percent) were degraded and 9 (12 percent) were in a transitional condition. Of 15 stations sampled in South Bay, 8 were classified as degraded, 2 were in a transitional condition, and 5 stations (all on the west side of the bay) were undegraded.

Another wide area study, which included San Diego Bay, was the Bight'98 sampling program organized by the Southern California Coastal Water Research Project. The primary objective of the study was to assess the extent of the area in the Southern California Bight (SCB) with benthic assemblages that were altered by pollution from point or non-point sources (SCCWRP 2003). Benthic grab samples were collected at 46 stations in San Diego Bay as part of the cooperative project in which over 323 stations along the SCB were sampled. There were 341 invertebrate taxa identified in the San Diego Bay samples. An important product of the research was the development of a benthic response index (BRI) that assigned habitat-specific pollution index values to each invertebrate taxon (Smith et al. 2003). The indices were then applied to the abundances of taxa comprising individual core or grab sample assemblages to produce pollution response threshold categories. This approach was used in the present analysis to describe the condition of benthic infauna as a function of distance from the SBPP discharge.

3.3.3 Methods

3.3.3.1 Benthic Sampling and Laboratory Procedures

Replicate benthic samples (n=3) were obtained by hand core at 21 subtidal stations and 10 intertidal stations (see **Figure 2.3-1a** and **2.3-1b**) during July, August, and September 2003. The warmest water temperatures of the year typically occur during this time period, so the sampling was intended to bracket a period in which infauna would be exposed to these maximum temperatures. Permanent marker buoys were established at each location using a dGPS to locate previously assigned lat/long coordinates. Locations (latitude and longitude) of the subtidal and intertidal stations are shown in **Table 2.3-1**, and the distance of the stations from the SBPP discharge are shown in **Table 2.3-2**. The measured distances are the shortest drift path to the station from the plant discharge. Eleven of the subtidal stations were at locations sampled in earlier benthic monitoring studies (Ogden 1994) and in ongoing monthly water quality studies (MEC Analytical Systems, Inc. 2003). Ten new intertidal stations and 10 new subtidal stations were established for the present study at discharge and reference sites.

The same collection methods were used for both the intertidal and subtidal samples. A hand-held coring device was used measuring 15 cm (5.9 in) in diameter and 15 cm in height, enclosing a 0.018 m^2 (0.19 ft^2) area. Samples were collected at points within 3 m (9.8 ft) of the station marker. Patches of algae or eelgrass were avoided. Corers were placed into the sediment with a minimum disruption of the surface sediments, capturing both surface fauna as well as species living deeper in the sediment. Corers were slowly pushed into the sediment, retrieved by digging along one side, and the core vent plug and end cap were replaced. Core samples were sieved through a 0.5-mm mesh screen and residues (e.g., organisms and remaining sediments) were rinsed into pre-labeled jars and preserved with a 10 percent formalin solution.

After a minimum of one week, samples were rinsed and transferred into 70 percent ethanol and stored for future taxonomy and enumeration of fauna. Invertebrates were separated from the residual sediments using a dissecting microscope into major groupings of annelids, arthropods, mollusks, echinoderms, and all other phyla. Damp weight biomass for each of these groups was measured to the nearest 0.1 g using a calibrated digital balance. Individual specimens were identified to the lowest practical taxonomic level, usually species. Identifications were done by experts in each taxonomic group using nomenclature standardized by the Southern California Association of Marine Invertebrate Taxonomists. All laboratory data were reviewed and entered into a Microsoft Access® database in accordance with applicable quality control procedures to ensure data accuracy. Residual sediment samples and all organisms were archived for any further analysis or quality control checks.

3.3.3.2 Analysis Methods

Analysis of infaunal intertidal and subtidal invertebrate data focused on detecting changes in communities or species abundances that may be related to proximity to the power plant discharge. Although monitoring of infaunal communities in the vicinity of the SBPP discharge occurred from 1977–1994 (Ogden Environmental and Energy Services Co., Inc. 1994) there were no data prior to plant operation that would provide a rigorous statistical evaluation of power plant effects in the absence of discharges. Therefore, differences in species composition and abundance between discharge and reference areas were used to determine the effects of the discharge. Typically large natural variation in biological communities makes these types of comparisons problematical, but consistent change in communities with increasing distance from the discharge provides strong evidence of discharge effects especially if these changes occur in a large number of species (Green 1979). The previous array of NPDES monitoring stations included only two in the discharge channel, a design that did not allow a determination of a gradient in potential effects. The current study design added five more stations within the discharge and intake areas to better delineate any gradients.

Standard measures of community parameters were calculated for each station and included: (1) species (taxa) richness, number of taxa /0.018m^2; (2) total number of taxa per station (n=3 cores per station); (3) abundance, number of individuals/0.018m^2; (4) wet weight biomass, g/0.018m^2; (5) diversity (H') using the $\log_2$ formulation, and (6) Pielou's evenness index (J').

Multivariate analysis allowed us to examine entire species assemblages and provided a robust test of changes due to the discharge. Multivariate analysis using the non-metric multidimensional scaling (MDS) method of ordination available in PRIMER Ver. 5.2.0 (Primer-E Ltd. 2001) was used to detect community changes due to the discharge. The Bray-Curtis measure of dissimilarity was used in the MDS analyses. The abundances from invertebrate taxa used in the analyses were square root transformed prior to calculating the Bray-Curtis distance to help reduce the effects of the most abundant species on the analysis.

For the August survey, replicates were analyzed separately and the average abundance from the three replicates at each station was also analyzed. Data from all ten intertidal stations were used in both analyses. Only the reference and discharge area subtidal stations were analyzed with all of the replicates because the larger numbers of samples in the analysis when the transition stations were included would potentially affect the ability to detect differences between reference and discharge areas, which was the primary focus of the analysis. A separate analysis of the average abundances from all of the subtidal stations was also done. The analyses of the average abundances at the intertidal and subtidal stations were done to better show the differences among stations and provided a direct comparison with the July and September surveys where only one of the replicates from each survey was processed.

Results from the MDS analysis were analyzed using ANOSIM (Clarke and Warwick 2001) to determine if there was a significant difference between discharge and reference communities. ANOSIM generates a test statistic that is based on a comparison of the average rank similarity among replicates within groups to the average rank similarity among all pairs of samples between groups. The value of the test statistic calculated for the data is compared to a distribution of values generated by recalculating the test statistic numerous times with random permutations of the group assignments for each sample. A significant difference exists among groups if the value of the test statistic is outside the range of some percentage (usually 95 percent) of the values generated during the randomization routine. ANOSIM was calculated using a one-way design using the stations within groups as replicates, and also as a two-way nested design with replicates nested within the stations within each group.

Taxa contributions to the pattern in the MDS analyses were examined using the SIMPER routine in PRIMER (Clarke and Gorley 2001). This program computes the average dissimilarity between all pairs of samples between groups and then breaks this average down into the separate contributions from each species.

Other environmental data that were collected with the infaunal samples were analyzed to determine their relationship to the observed biological patterns. These relationships were analyzed in the Ogden (1994) summary report using regression analysis of individual species abundances and biological indices with various physical parameters, including sediment grain size, sediment chemistry, temperature, depth, and distance from discharge. Sediment grain size, and variables for mean, maximum temperature and temperature range and variance were also measured at each of the stations during these surveys and were evaluated using principal components analysis (PCA) and other multivariate methods described in Clarke and Warwick (2001). PCA was used to describe the major patterns of variation among the stations and the physical variables responsible for the patterns. The correspondence between the biological community and physical variables was analyzed using the rank correlation between the dissimilarity matrices among sites derived from biological and physical data. A similar analysis was used to determine the set of physical variables that best groups the sites in a pattern consistent with the biological data. The average of the three replicate samples from each station was used in these analyses because only single values for temperature were available for each station.

A benthic response index (BRI) (SCCWRP 2003) was also calculated for each sample based on taxa abundances and associated pollution tolerance indices (p_i). The index was developed by SCCWRP from empirical data on the abundances of species most likely to occur in polluted or non-polluted areas. Pollution was defined in terms of sediment contaminants, proximity to wastewater outfalls, and other industrialized coastal areas, but did not include a thermal discharge component. The indices were specific to embayment habitats between Dana Point Harbor and the Mexican border and were developed partly

with data collected in San Diego Bay between 1993 and 1998. Only taxa with assigned (p_i) indices specifically developed for southern California bays were used in the present analysis. An index value was calculated for each benthic station based on the mean abundances of taxa with assigned indices at that station.

3.3.4 Results

Replicate samples were collected at 21 subtidal stations and 10 intertidal stations during July, August, and September 2003. Samples were prioritized for sorting and identification because the large volumes of retained sediments and high abundances of infauna precluded the complete processing of all samples within a specified period. The following results are from one replicate of 31 samples from July 2003, one complete survey (3 replicates per station) of 93 samples from August 2003, and one replicate of 31 samples from September 2003. Concurrent temperature records at each station from July through September and continuous temperature records from SBPP NPDES monitoring indicated that the month of August 2003 had the warmest monthly mean water temperatures in the discharge channel and warmest bay-wide ambient temperatures. Therefore, benthic sampling results from August would be representative of the greatest temperature stress on infaunal communities and highlight any differences in faunal distributions influenced by power plant discharges. The surveys from July and September were confirmatory and bracketed the results from the August survey. Mean abundances and counts of all taxa sampled per station by survey are presented in **Appendix I**.

3.3.4.1 Community Parameters

A summary of community parameters including species richness, total number of taxa, biomass, diversity, evenness, and a benthic response index are presented for the subtidal and intertidal stations during July, August, and September 2003 in **Tables 3.3.1** and **3.3.2**.

Number of Species

A total of 189 invertebrate taxa was identified from 105 subtidal and 50 intertidal core samples collected in the SBPP discharge channel and receiving waters of South Bay. The best estimates of total numbers of taxa at subtidal stations were from the August survey with data from three replicate cores. Values ranged from a low of 22 taxa at Stations SR1 and SR3 in the intake channel to a high of 58 taxa at Station SF4 near the south end of the CVWI. The average number of taxa per station was 38.1. The July survey had a low of 8 taxa at Station ST3 in the discharge channel and a high of 36 taxa at Station SF2 in the south end of the bay with an average of 23.3 taxa per station. There was an average of 26.5 taxa per station in the September survey. Intertidal stations had fewer numbers of

taxa overall than subtidal stations, averaging 22.5, 33.9, and 19.1 taxa per station for the July, August, and September surveys, respectively.

Subtidal samples included 166 taxa and intertidal samples had 113 taxa. Annelid worms were the most diverse taxonomic group overall with 66 taxa represented. Arthropods (mainly amphipods) were the next most speciose group with 64 taxa, followed by mollusks (clams and snails) with 23 taxa. Other phyla, including echinoderms, coelenterates, nematodes and phoronid worms, contributed 36 taxa to the overall numbers for all surveys combined.

There was no clear gradient in total number of taxa per station as a function of distance from the discharge at subtidal stations. The station nearest the discharge, SE7, had a relatively high number of taxa (46) in August compared to the average at all stations for the same period (38.1 per station) (**Table 3.3.1**). Intertidal stations, however, did exhibit a significant increase in taxa richness as a function of distance from the point of discharge during the August and September surveys ($p<0.01$) but not in July (**Table 3.3-2**, **Figure 3.3-1**).

Infaunal Abundance

Mean abundance of invertebrates per subtidal sample ranged from 6,171 at Station SE7 in September to 21 at Station ST3 in July. The high total abundances at Station E7 in all surveys was due to high numbers of nematodes and oligochaetes associated with high concentrations of organic debris in the samples. These two taxa generally comprised over 75 percent of the individuals at the station. There was no clear gradient in total numbers of individuals per station as a function of distance from the discharge at subtidal stations.

There were significantly lower abundances of infaunal invertebrates at intertidal stations nearer to the discharge during August and September (regression test, $p<0.05$), but no significant difference among stations in July. Station IT2 generally had depressed abundances of invertebrates compared to other stations, and the highest densities of invertebrates generally occurred at Stations IR4 and IR5 near the Chula Vista Marina. Abundances at the four stations closest to the discharge were generally less than half those of the reference stations (**Table 3.3-2**).

Biomass

Mean biomass varied considerably among subtidal stations and ranged from a high of 48.3 g/ sample at Station E7 in September to less than 0.1 g/sample at several stations during all three surveys (**Table 3.3-1**). The high values at Station E7 and several of the other stations were largely due to shell biomass of the bivalve *Musculista senhousia*, a small non-native species that can form dense aggregations in some areas. Polychaete and nematode worms contributed to most of the remainder of the biomass in the samples.

Amphipods, though sometimes numerous, comprised only a small fraction of the invertebrate biomass.

There was no consistent pattern in the distribution of total biomass and no obvious gradient as a function of distance from the discharge. However, when the biomass of polychaete worms was considered separately, there was a trend toward higher biomass values for polychaetes at stations farther from the discharge (**Figure 3.3-2**). The other main taxonomic groups, mollusks and arthropods, did not have any apparent gradients in biomass. Intertidal biomass showed no consistent trends related to distance from the discharge.

Species Diversity and Evenness

Mean diversity at subtidal stations was generally low at the two stations closest to the discharge, SE7 and ST1, and high at Station SF4 near the south end of the CVWI. During all months sampled there was a significant trend of decreasing diversity within the discharge channel as distance from the discharge decreased ($p<0.05$; **Figure 3.3-3**). A low evenness index in July, August and September at Station E7 was mainly due to the dominance of nematodes, oligochaetes, and *Musculista senhousia* in the samples even though the overall number of taxa was higher than the average. The lowest intertidal faunal diversities were also recorded at stations closest to discharge (**Table 3.3-2**), but there was no significant trend among sampling stations as a function of distance from the discharge.

DRAFT

Table 3.3-1. Benthic infaunal community parameters at SBPP subtidal stations sampled during July–September 2003. Data are: (1) species (taxa) richness, no. taxa /0.018m^2; (2) abundance, no. individuals/0.018m^2;(3) biomass, g/0.018m^2; (4) diversity (H'); (5) evenness (J'); (6) benthic response index (BRI) for southern bays. (n=1 core per station for July and September, and n=3 cores per station for August. Stations are ordered in increasing distance from the discharge.

	Total Taxa			Abundance			Biomass (g)			Diversity (H')			Evenness (J')			Benthic Index		
Station	**Jul**	**Aug**	**Sep**	**Jul**	**Aug**	**Sep**	**Jul**	**Aug**	**Sep**	**Jul**	**Aug**	**Sep**	**Jul**	**Aug**	**Sep**	**Jul**	**Aug**	**Sep**
SE7	26	46	41	965	1156	6171	3.1	23.2	48.3	1.85	2.31	1.59	0.39	0.48	0.30	30	43	50
ST1	20	31	28	296	399	1028	1.2	0.6	2.5	2.68	2.34	2.84	0.62	0.72	0.59	25	34	47
ST2	17	29	21	93	174	159	<0.1	0.2	0.2	3.10	3.27	3.44	0.76	0.76	0.78	21	36	33
ST3	8	28	16	21	122	76	<0.1	0.6	<0.1	2.42	3.38	3.31	0.81	0.80	0.83	28	29	35
ST4	21	33	24	103	224	393	0.8	0.7	0.3	3.21	3.52	2.95	0.73	0.76	0.64	27	32	27
SE5	24	31	20	135	211	250	0.4	0.3	<0.1	3.95	3.05	2.86	0.86	0.72	0.66	29	32	48
ST5	20	37	20	94	181	179	0.4	<0.1	<0.1	3.09	3.36	3.54	0.72	0.76	0.82	40	34	33
SF4	32	58	33	196	818	338	1.6	12.6	7.2	4.24	3.68	4.26	0.85	0.70	0.84	19	20	15
SF3	22	32	21	77	130	328	0.5	0.6	0.5	3.74	3.26	3.26	0.84	0.76	0.74	27	25	18
SE3	25	44	25	117	313	201	0.5	1.0	0.2	3.43	3.94	3.75	0.74	0.78	0.81	32	24	31
SE4	22	32	20	117	94	110	0.8	0.7	0.3	3.43	3.42	3.69	0.77	0.78	0.85	32	29	31
SF2	37	48	40	378	498	341	1.5	2.4	0.8	4.26	3.91	4.13	0.82	0.77	0.78	33	33	31
SD4	22	42	23	206	160	176	0.5	0.7	0.9	3.11	3.48	3.26	0.70	0.77	0.72	44	29	34
SR3	18	22	11	167	78	54	0.6	0.2	<0.1	2.48	2.51	2.61	0.59	0.67	0.76	38	34	15
SC3	32	46	31	460	239	372	12.0	0.7	1.6	3.19	3.56	3.28	0.64	0.75	0.66	35	30	33
SR2	28	38	19	364	252	68	1.2	1.9	3.1	3.30	3.40	3.68	0.69	0.72	0.87	29	32	23
SR1	10	22	18	110	102	161	0.5	0.2	0.2	2.07	2.52	2.94	0.62	0.68	0.70	40	43	26
SR4	29	53	34	511	530	665	2.2	2.0	1.7	2.80	4.10	3.39	0.58	0.77	0.67	39	34	31
SR5	36	50	42	600	322	1303	1.0	3.6	17.2	3.71	3.78	3.15	0.72	0.74	0.58	41	30	34
SA3	26	28	35	264	92	395	8.7	5.9	23.1	3.35	2.79	3.28	0.71	0.71	0.64	39	36	33
SN2	35	50	34	309	210	149	2.0	1.3	<0.1	3.70	3.40	4.23	0.72	0.70	0.83	32	35	25

DRAFT

Table 3.3-2. Benthic infaunal community parameters at SBPP intertidal stations sampled during July–September 2003. Data are: (1) species (taxa) richness, no. taxa /0.018m^2; (2) abundance, no. individuals/0.018m^2;(3) biomass, g/0.018m^2; (4) diversity (H'); (5) evenness (J'); (6) benthic response index (BRI) for southern bays. (n=1 core per station for July and September, and n=3 cores per station for August. Stations are ordered in increasing distance from the discharge.

	Total Taxa			Abundance			Biomass (g)			Diversity (H')			Evenness (J')			Benthic Index		
Station	**Jul**	**Aug**	**Sep**	**Jul**	**Aug**	**Sep**	**Jul**	**Aug**	**Sep**	**Jul**	**Aug**	**Sep**	**Jul**	**Aug**	**Sep**	**Jul**	**Aug**	**Sep**
T1	25	23	12	229	115	178	1.3	0.4	<0.1	2.77	2.59	1.43	0.60	0.68	0.40	46	47	-13
T2	17	21	13	224	46	51	0.2	<0.1	<0.1	2.20	3.19	3.22	0.54	0.86	0.87	43	26	20
T3	17	29	20	420	161	126	0.4	0.3	<0.1	2.71	2.80	3.47	0.66	0.68	0.80	27	30	25
T4	22	29	12	88	186	43	0.8	1.5	0.2	3.72	3.11	2.97	0.84	0.71	0.83	27	31	9
T5	23	38	17	694	531	113	0.1	<0.1	<0.1	2.72	3.28	2.48	0.60	0.70	0.61	41	25	2
R3	18	44	16	202	345	47	0.1	0.6	0.5	2.88	3.33	3.27	0.69	0.72	0.82	24	25	20
R2	24	30	22	217	292	486	0.5	0.3	3.4	3.19	2.60	2.48	0.70	0.60	0.56	20	19	19
R1	28	42	29	654	297	450	0.3	<0.1	1.1	3.16	3.22	3.45	0.66	0.70	0.71	20	22	22
R5	28	47	25	674	466	499	1.6	0.8	<0.1	2.69	3.17	3.33	0.56	0.63	0.72	25	24	12
R4	33	36	25	820	374	367	0.6	0.5	2.9	3.60	2.65	2.26	0.71	0.59	0.49	29	24	23

DRAFT

Benthic Response Index

Approximately 40 percent of the taxa sampled during the study had a pollution tolerance index (p_i) associated with them based on earlier studies by SCCWRP (2003). Only these taxa were used in the calculation of the BRI. A listing of the sampled taxa that had the highest (most pollution tolerant) and lowest (least pollution tolerant) scores is presented in **Table 3.3-3**. The highest subtidal BRI scores in August, the month with the warmest mean temperatures, occurred at Stations SE7 and SR1 (43), and the lowest score (20) occurred at Station SF4 (**Table 3.3-1**). Subtidal scores from the September samples were highest at Station SE7 and lowest at Stations SF4 and SR3 (**Table 3.3-1**). The highest intertidal score in August was at Station IT2 (47), nearest the discharge, and the lowest was at reference Station IR2 (19) (**Table 3.3-2**); September intertidal scores were generally lower than those in August (**Table 3.3-2**). Stations with a BRI threshold less than 31 are relatively unpolluted and are considered reference stations unaffected by pollutants and higher scores are classified into response levels based on loss of biodiversity and increases in pollution-tolerant taxa (**Table 3.3-4**). A greater percentage of the subtidal and intertidal stations classified at Level 2 occurred in the discharge channel than in South Bay as a whole, although most stations in both areas were classified as unpolluted or Level 1 (**Figure 3.3-4**).

Table 3.3-3. Taxa with the 20 highest and 20 lowest pollution tolerance indices (p_i) for southern California bays (from Smith et al. 2003), for taxa enumerated in SBPP benthic core samples.

Sampled taxa with highest pollution tolerance scores			Sampled taxa with lowest pollution tolerance scores		
Phylum	**Taxon**	p_i	**Phylum**	**Taxon**	p_i
Annelida	Cirratulidae	162.865	Arthropoda	*Erichthonius brasiliensis*	-75.217
Mollusca	*Macoma* sp.	150.473	Annelida	*Polyophthalmus pictus*	-70.708
Annelida	*Marphysa* sp.	150.452	Mollusca	*Acteocina inculta*	-57.035
Arthropoda	*Hyale* sp.	109.003	Mollusca	*Barleeia* sp.	-54.511
Annelida	*Leitoscoloplos pugettensis*	94.277	Mollusca	*Mytilus* sp.	-48.531
Annelida	*Dorvillea (Schistomeringos)* sp	90.093	Mollusca	*Ostrea conchaphila*	-31.128
Annelida	*Neanthes acuminata* Cmplx	89.682	Mollusca	*Chione californiensis*	-28.846
Annelida	*Capitella capitata* Cmplx	88.339	Annelida	*Scoloplos acmeceps*	-28.300
Annelida	*Caulleriella sp.*	84.393	Annelida	*Piromis* sp SD1	-22.455
Annelida	*Streblospio benedicti*	71.422	Mollusca	*Crucibulum spinosum*	-16.324
Mollusca	*Musculista senhousia*	69.863	Arthropoda	*Acuminodeutopus heteruropus*	-13.494
Arthropoda	*Schmittius politus*	68.492	Mollusca	*Solen rostriformis*	-12.356
Annelida	*Pista agassizi*	65.688	Annelida	*Pionosyllis* sp SD1	-10.139
Annelida	*Typosyllis* sp.	64.715	Mollusca	*Tagelus subteres*	-9.515
Arthropoda	*Oxyurostylis pacifica*	61.628	Mollusca	*Tellina meropsis*	-7.542
Arthropoda	*Paracerceis sculpta*	57.289	Annelida	*Notomastus* sp	-6.496
Mollusca	*Theora lubrica*	55.417	Arthropoda	*Cumella* sp. D	-5.010
Annelida	*Odontosyllis phosphorea*	52.772	Arthropoda	Neotrypaea californiensis	-4.874
Mollusca	*Nassarius tiarula*	52.640	Arthropoda	*Corophium* sp.	0.356
Annelida	*Exogone lourei*	48.162	Arthropoda	*Leptochelia dubia*	0.733

There was no trend of decreasing BRI scores as distance from the discharge increased, as might be expected if some physical or chemical factors associated with the discharge were affecting infaunal composition. The relatively high abundances of *Musculus senhousia*, at Stations SE7 and IT1 were the main factor contributing to the higher scores at these sites. However, other taxa with relatively high pollution tolerance indices such as the polychaete *Leitoscoloplos pugettensis* were absent at the stations closest to the discharge and most abundant at reference stations beyond the discharge channel. This varied assemblage composition contributed to the lack of any clear gradients in this index among the sampled stations.

Table 3.3-4. Description of bay benthic response index (BRI) assessment thresholds.

Level	Characterization	Definition	BRI Thresholds
Reference	Reference		<31
Response Level 1	Marginal deviation	>5% of reference species lost	31–42
Response Level 2	Biodiversity loss	>25% of reference species lost	42–53
Response Level 3	Community function loss	>50% of reference species lost	53–73
Response Level 4	Defaunation	>80% of reference species lost	>73

3.3.4.2 Spatial Patterns of Taxa Densities

The density of several of the most abundant and frequently occurring invertebrate taxa were examined for spatial trends related to proximity to the SBPP discharge. An earlier analysis of benthic data from a 17-year data set that included 11 of the stations sampled in the present study (Ogden 1994) identified several taxa that had distributions with higher densities at reference stations located furthest from the discharge or higher densities at stations located nearer to the discharge. Many species, particularly those with low abundances, could not be categorized with respect to these trends, or had variable abundances that demonstrated no spatial trends in relation to the discharge.

The intertidal and subtidal data sets were divided into discharge stations and non-discharge (or reference) stations to compare lists of the more abundant species comprising each set. Discharge stations had varying thermal exposures with the inner stations receiving a greater thermal dose than outer stations (see Section 2.3–*Receiving Water Temperature Monitoring*). Nematodes and oligochaetes comprised nearly half the numbers of invertebrates at subtidal discharge stations, although nematodes were also abundant at non-discharge stations (**Table 3.3-5**). The polychaete *Mediomastus* sp. was the most abundant taxon at non-discharge stations.

Regression analyses between taxa densities and mean monthly station temperatures showed that the following example taxa had significant ($p<0.05$) positive associations with temperature. Among the more abundant subtidal taxa with distributions skewed toward the discharge channel, including high abundances at the warmest station, SE7, were *Musculista senhousia*, *Capitella capitata*, nematodes and oligochaetes (**Figure 3.3-5**). *Rhynchospio glutaea, Exogone* sp. 1, *Streblospio benedicti*, and *Leptochelia dubia,* also tended to be more abundant at discharge stations than other stations, but had depressed abundances at the innermost discharge station SE7 (**Figure 3.3-6**). Peak abundances at certain discharge channel stations and gradations in their abundances between stations suggested points at which the most favorable environmental conditions existed in the channel for their local populations. Most of these taxa, except *Leptochelia dubia*, increased in abundance from July through September at many stations.

Other taxa had distributions with negative spatial correlations in relation to the discharge and significant negative regressions with temperature. Abundant subtidal species with distributions skewed away from or largely absent from the discharge channel included *Leitoscoloplos pugettensis, Scoletoma* sp. C*, Mediomastus* sp., and *Acuminodeutopus heteruropus* (**Figure 3.3-7**). These species tended to be more abundant at discharge stations in July and declined as water temperatures increased through September. Phoronids, *Mayerella acanthopoda*, *Armandia brevis* and *Tellina meropsis* were examples of taxa that were abundant at some stations and uncommon at others within both the discharge and non-discharge station groups, displaying no definitive spatial distribution pattern (**Figure 3.3-8**). These taxa had no statistically significant relationship with temperature. Most of the taxa sampled in the study had a low frequency of occurrence among all of the stations or low overall densities and consequently their distributions could not be accurately classified according to proximity to the discharge or relationship to temperature variables.

One specimen of note, the polychaete *Naineris* cf. *laevigata*, was identified from subtidal discharge Station E7, and represents a new occurrence of this species in San Diego Bay. This species has a cosmopolitan distribution, but typically in warm waters, and its nearest previously recorded occurrence in the Pacific is from the Galapagos Islands[1]. As with many other non-native species in San Diego Bay its occurrence may have resulted from an accidental introduction through ship's ballast water or hull fouling.

The tanaid crustacean *Leptochelia dubia* was the most abundant intertidal species among both the discharge station and reference groups, with nematodes and oligochaetes also abundant at most stations (**Table 3.3-6**). Several intertidal taxa were more abundant at discharge stations than at reference stations, but only *Musculista senhousia* and Phoronida had highest abundances at the warmest station, IT1. Several others, however, had higher abundances at intermediate stations in the discharge channel, including

[1] Dr. Gene Ruff, personal communication.

Grandidierella japonica, *Acteocina inculta*, *Polydora* spp., and *Marphysa* sp. (**Figure 3.3-9**). Taxa with intertidal distributions skewed away from the inner discharge stations included *Leptochelia dubia, Scoloplos acmeceps, Euphilomedes carcarodonta,* and *Fabricinuda limnicola* (**Figure 3.3-10**). As with some of the thermally sensitive subtidal species, the distributions of these intertidal taxa appeared to gradually shift away from the discharge as temperatures warmed from July through September. *Tellina meropsis*, *Corophium* spp., *Tagelus subteres* and Phoronida were examples of taxa that were abundant at some intertidal stations and uncommon at others within both the discharge and non-discharge station groups, displaying no definitive spatial distribution pattern (**Figure 3.3-11**). *Tagelus subteres* was absent from stations in July and recruited into the study area in August and September.

Table 3.3-5. Comparison of ten most abundant invertebrate taxa at the subtidal discharge channel stations (ST1–5, SE7, SE5 and F4) (n=8), and other subtidal benthic stations (n=13) in South Bay for August 2003. Mean abundance is #/0.018 m^2 within each station grouping.

Taxon	Description	Mean	Cum. %
Discharge stations			
1. Nematoda	Nematode	125.58	30.6%
2. Oligochaeta	Oligochaete	61.29	45.5%
3. *Musculista senhousia*	Bivalve	28.96	52.6%
4. *Mayerella acanthopoda*	Caprellid amphipod	24.75	58.6%
5. *Leptochelia dubia*	Tanaid crustacean	22.54	64.1%
6. *Corophium* sp.	Gammaridean amphipod	20.92	69.2%
7. Phoronida unid.	Phononid	15.08	72.9%
8. *Streblospio benedicti*	Polychaete	13.00	76.0%
9. *Exogone* sp. 1	Polychaete	11.79	78.9%
10. *Capitella capitata*	Polychaete	9.08	81.1%
Other stations			
1. *Mediomastus* sp.	Polychaete	55.54	23.9%
2. Nematoda	Nematode	17.38	31.4%
3. *Leitoscoloplos pugettensis*	Polychaete	13.92	37.4%
4. Oligochaeta	Oligochaete	12.15	42.6%
5. *Mayerella acanthopoda*	Caprellid amphipod	12.05	47.8%
6. *Scoletoma* sp. C	Polychaete	9.13	51.8%
7. *Armandia brevis*	Polychaete	8.13	55.3%
8. *Fabricinuda limnicola*	Polychaete	7.23	58.4%
9. Phoronida unid.	Phononid	7.00	61.4%
10. *Tellina meropsis*	Bivalve	5.95	63.9%

DRAFT

Table 3.3-6. Comparison of ten most abundant invertebrate taxa at the intertidal discharge stations (IT1–5) and reference intertidal stations (IR1–5) in South Bay in August 2003. Mean abundance is #/0.018 m^2 within each station grouping.

Taxon	Description	Mean	Cum. %
Discharge stations			
1. *Leptochelia dubia*	Tanaid crustacean	36.5	17.6%
2. Nematoda	Nematode	27.1	30.6%
3. Oligochaeta	Oligochaete	25.5	42.9%
4. *Grandidierella japonica*	Gammaridean amphipod	19.7	52.4%
5. *Mayerella acanthopoda*	Caprellid amphipod	16.7	60.5%
6. *Corophium* sp.	Gammaridean amphipod	11.7	66.1%
7. *Exogone* sp. 1	Polychaete	11.0	71.4%
8. *Musculista senhousia*	Bivalve	10.0	76.3%
9. Leptocheliidae	Tanaid crustacean	5.5	78.9%
10. *Streblospio benedicti*	Polychaete	5.1	81.4%
Reference stations			
1. *Leptochelia dubia*	Tanaid crustacean	99.5	28.0%
2. *Fabricinuda limnicola*	Polychaete	72.4	48.4%
3. *Euphilomedes carcarodonta*	Ostracod crustacean	38.8	59.4%
4. Nematoda	Nematode	24.7	66.3%
5. Leptocheliidae	Tanaid crustacean	14.3	70.3%
6. *Parasterope bamesi*	Ostracod crustacean	11.3	73.5%
7. Oligochaeta	Oligochaete	9.6	76.2%
8. *Mayerella acanthopoda*	Caprellid amphipod	9.0	78.8%
9. *Barleeia* sp./*Assiminea californica*	Gastropod mollusk	7.7	80.9%
10. *Corophium* sp.	Gammaridean amphipod	6.7	82.8%

3.3.4.3 Multivariate Analysis of Invertebrate Assemblages

Subtidal Data Set

The MDS analysis of 139 taxa from all the replicates at the discharge and reference stations for the August 2003 survey shows a clear separation between areas. As expected, the replicates for most stations were generally less variable in faunal composition within stations, and consequently more tightly grouped in the analysis, than they are among stations (**Figure 3.3-12**). An exception is the results for replicate A from Station T1, that had only four individuals from two taxa. This sample had the fewest taxa and total individuals of any of the samples. The MDS pattern between areas is reflected in the results of the two-way nested ANOSIM that detected a statistically significant difference (p=0.017) between discharge and reference station groups.

The average abundances of 145 taxa at all of the stations during the August survey were analyzed to better show the pattern of community and species differences among stations (**Figure 3.3-13**). The transition stations (D4, E3, E4, and F3) were included in this analysis. The results are similar to the analysis of the replicates from the discharge and

reference area stations in showing the separation between areas. The analysis indicates that communities at the transition stations share faunal characteristics with both reference and discharge area stations. The discharge area stations furthest from the discharge (T4, E5, and T5) are more similar to the transition stations than the other discharge area stations, but it is also clear that the differences from the reference stations do not necessarily increase linearly for stations that are closest to the discharge. This is especially true for Station F4. Station F4 appears to be more similar to Station E7, which is the station closest to the discharge, than it is to the transition stations that are located much closer.

The SIMPER analysis shows that the similarity among stations is greater for the transition (58 percent) than for the reference (46 percent) and discharge (48 percent) station groups (**Table 3.3-7**). The increased similarity among transition stations is most likely due to the lower number of stations in that group. Taxa contributions to the similarity among stations show that the transition stations share taxa with the two other groups. Most notably, the polychaete worm *Mediomastus* sp. had the largest contribution to the similarity among the reference and transition station groups, but contributed much less to the similarity among the discharge stations. Conversely, phoronid worms had large contributions to the similarities among transition and reference stations, but contributed much less to the similarity among the reference stations. These results confirm our characterization of these stations as being intermediate between the discharge and reference groups. The taxa contributing the most to the differences between reference and discharge stations include nematode and oligochaete worms, and *Mediomastus* sp. (**Table 3.3-8**). The analysis indicates that a large number of taxa contribute to the difference between areas and that no single taxon characterizes either group.

The data from 96 taxa from one replicate from each of the 21 stations in the July survey, and 105 taxa from one replicate from 21 stations in the September survey were analyzed using MDS (**Figures 3.3-14** and **3.3-15**) and SIMPER (**Tables 3.3-9** and **3.3-10**). The results of the MDS for both of these months are similar to the results from the August survey (**Figure 3.3-13**) in that discharge and reference stations are separated along a gradient of faunal change with transition stations intermediate between the groups. The ANOSIM test detected a statistically significant difference between the discharge and reference station groups for both surveys. The SIMPER analysis showed that the three taxa most responsible for the differences between the reference and discharge groups (*Mediomastus* sp., nematodes and oligochaetes) were generally the same among surveys, although in the July survey oligochaetes were relatively less important. The relative contributions for many of the taxa changed among surveys because the contributions for a large number of taxa were very similar in value and would be expected to vary in response to changing environmental conditions.

Table 3.3-7. Results of SIMPER analysis showing taxa and their relative contributions to the similarity among subtidal stations within a) discharge areas b) transition, and c) reference, based on Bray-Curtis distances of average station abundances during the August 2003 survey.

Species	% Contribution	Cumulative %
a) Discharge Group - average similarity: 48 %		
Nematoda	12.83	12.83
Oligochaeta	10.67	23.50
Phoronida	8.08	31.58
Exogone sp. 1	7.70	39.28
Capitella capitata	6.47	45.74
Leptochelia dubia	5.93	51.68
Mediomastus sp.	5.19	56.87
Mayerella acanthopoda	4.75	61.61
Corophium sp.	4.51	66.13
Streblospio benedicti	4.09	70.22
b) Transition Group - average similarity: 58 %		
Mediomastus sp.	12.39	12.39
Phoronida	11.28	23.67
Mayerella acanthopoda	9.25	32.91
Megalomma pigmentum	7.36	40.27
Leitoscoloplos pugettensis	5.99	46.26
Oligochaeta	5.88	52.14
Nematoda	5.20	57.34
Exogone sp. 1	4.76	62.10
Tellina meropsis	4.38	66.48
Amphideutopus oculatus	2.65	69.14
Scoletoma sp. C	2.56	71.70
c) Reference Group - average similarity: 46 %		
Mediomastus sp.	22.13	22.13
Leitoscoloplos pugettensis	8.12	30.25
Scoletoma sp. C	7.58	37.83
Oligochaeta	6.81	44.65
Nematoda	4.76	49.40
Acuminodeutopus heteruropus	4.58	53.99
Mayerella acanthopoda	3.93	57.91
Tellina meropsis	3.92	61.83
Prionospio heterobranchia	2.54	64.37
Armandia brevis	2.19	66.56
Musculista senhousia	2.05	68.61
Phoronida	1.89	70.50

DRAFT

Table 3.3-8. Results of SIMPER analysis showing taxa and their relative contributions to the dissimilarity between subtidal stations in the reference and discharge areas based on Bray-Curtis distances of average station abundances during the August 2003 survey.

Species	% Contribution	Cumulative %
Nematoda	5.86	5.86
Mediomastus sp.	5.72	11.58
Oligochaeta	4.53	16.12
Leptochelia dubia	3.76	19.88
Corophium sp.	3.19	23.07
Scoletoma sp. C	3.16	26.24
Leitoscoloplos pugettensis	3.10	29.34
Mayerella acanthopoda	3.05	32.39
Streblospio benedicti	2.93	35.32
Musculista senhousia	2.78	38.10
Phoronida	2.73	40.84
Capitella capitata	2.71	43.54
Exogone sp. 1	2.60	46.14
Armandia brevis	1.77	47.92
Neanthes acuminata complex	1.72	49.63
Acuminodeutopus heteruropus	1.66	51.29
Rhynchospio glutaea	1.59	52.88
Exogone lourei	1.52	54.40
Leptocheliidae	1.46	55.86
Rutiderma judayi	1.46	57.32
Fabricinuda limnicola	1.38	58.70
Megalomma pigmentum	1.33	60.03
Prionospio heterobranchia	1.32	61.34
Tellina meropsis	1.26	62.60
Nemertea	1.19	63.79
Parasterope bamesi	1.11	64.90
Paracerceis sculpta	1.10	66.00
Rudilemboides stenopropodus	1.09	67.09
Bemlos macromanus	1.05	68.14
Theora lubrica	1.05	69.18
Diadumene spp.	1.04	70.22

DRAFT

Table 3.3-9. Results of SIMPER analysis showing taxa and their relative contributions to the dissimilarity between subtidal stations in the reference and discharge areas based on Bray-Curtis distances of average station abundances during the July 2003 survey.

Species	% Contribution	Cumulative %
Mediomastus sp.	9.98	9.98
Nematoda	7.39	17.37
Leitoscolopios pugettensis	4.78	22.15
Mayerella acanthopoda	3.99	26.14
Scoletoma sp. C	3.97	30.11
Leptochelia dubia	3.44	33.55
Musculista senhousia	2.74	36.29
Exogone lourei	2.60	38.88
Oligochaeta	2.58	41.46
Exogone sp. 1	2.50	43.96
Megalomma pigmentum	2.38	46.34
Prionospio heterobranchia	2.31	48.64
Fabricinuda limnicola	2.19	50.83
Scoloplos acmeceps	1.94	52.77
Acuminodeutopus heteruropus	1.91	54.68
Neanthes acuminata Cmplx.	1.81	56.49
Corophium sp.	1.66	58.15
Capitella capitata	1.63	59.77
Parasterope bamesi	1.57	61.35
Euphilomedes carcarodonta	1.38	62.73
Leptocheliidae	1.35	64.08
Tellina meropsis	1.34	65.42
Rudilemboides stenopropodus	1.32	66.74
Streblospio benedicti	1.21	67.95
Solen rostriformis	1.16	69.11
Lyonsia californica	1.15	70.26

DRAFT

Table 3.3-10. Results of SIMPER analysis showing taxa and their relative contributions to the dissimilarity between subtidal stations in the reference and discharge areas based on Bray-Curtis distances of average station abundances during the September 2003 survey.

Species	% Contribution	Cumulative %
Nematoda	9.48	9.48
Oligochaeta	5.96	15.44
Mediomastus sp.	4.92	20.36
Capitella capitata cmplx	4.37	24.73
Exogone sp. 1	3.45	28.18
Scoletoma sp. C	3.14	31.32
Phoronida	3.04	34.35
Leitoscoloplos pugettensis	3.03	37.38
Streblospio benedicti	3.02	40.40
Ctenodrilus serratus	2.80	43.19
Musculista senhousia	2.76	45.95
Acuminodeutopus heteruropus	2.73	48.68
Tellina meropsis	2.38	51.06
Mayerella acanthopoda	2.29	53.35
Leptochelia dubia	2.03	55.38
Rhynchospio glutaea	1.86	57.25
Rudilemboides stenopropodus	1.86	59.11
Corophium sp.	1.80	60.91
Rutiderma judayi	1.33	62.24
Armandia brevis	1.29	63.53
Scolelepis sp.	1.24	64.78
Exogone lourei	1.22	66.00
Fabricinuda limnicola	1.12	67.12
Megalomma pigmentum	1.11	68.23
Odontosyllis phosphorea	1.11	69.34
Neanthes acuminata cmplx	1.08	70.41

Intertidal Data Set

The MDS analysis of 100 taxa from all the replicates at each of the 10 stations for the August 2003 survey shows a clear separation between reference and discharge stations (**Figure 3.3-16**). The variation among replicates for each station is also generally less than the variation among stations. The results also show that stations T1 and T2, closest to the discharge, have the greatest differences with the other stations. The MDS pattern is reflected in the statistically significant difference (p=0.008) between discharge and reference station groups detected using a two-way nested ANOSIM.

The average abundances at the stations during the August 2003 survey were also analyzed to show the pattern of community and species differences more clearly among stations (**Figure 3.3-17**). The results are similar to the analysis of all the replicates showing that the communities at intertidal stations T1 and T2, closest to the discharge,

have the greatest differences with the other stations. The results show that the differences from the reference stations do not necessarily increase linearly for stations that are closest to the discharge. The differences between the reference stations and stations T1 and T2 are similar and Station T4 is more similar to the reference stations than Station T5, which is further from the discharge.

The SIMPER analysis shows that the similarity among stations was greater for the reference (59 percent) than for the discharge stations (45 percent) (**Table 3.3-11**). This is also evident in the dispersion of the stations in the MDS analysis (**Figure 3.3-17**). Taxa contributions to the similarity among stations show that different taxa characterize the stations within the two groups even though nematode worms (Nematoda) and the tanaid crustacean *Leptochelia dubia* are in the top five taxa within each group. The taxa contributing to the differences between groups include many of the same taxa that characterize the station groups (**Table 3.3-11**). The taxa with the greatest contribution to differences between reference and discharge stations also include the species *Fabricinuda limnicola*, *Euphilomedes carcarodonta* and *Parasterope bamesi*. *F. limnicola* was more abundant at the reference stations and the other two species were not collected at the discharge stations (**Table 3.3-12**).

The data for 65 taxa from one replicate from each of the 10 stations in the July survey and 57 taxa from one replicate from 10 stations in the September survey were analyzed using MDS (**Figures 3.3-18** and **3.3-19**) and SIMPER (**Tables 3.3-13** and **3.3-14**). The results of the MDS show a separation of reference and discharge stations for both months similar to the August results. The ANOSIM test detected a statistically significant difference between the discharge and reference station groups for both surveys. Differences in the absolute positions of stations between the July and September analyses are a consequence of the analysis routine and of no significance, but both plots clearly demonstrate the separation between discharge and reference stations.

The SIMPER analysis showed that the same three species most responsible for the differences between the discharge and reference groups for the August survey (**Table 3.3-12**) were also responsible for differences during the September survey. One exception was the bubble shell *Acteocina inculta*, which was collected in very low abundances during the August survey at the discharge stations. This species increased in abundance between surveys especially at the discharge stations.

DRAFT

Table 3.3-11. Results of SIMPER analysis showing taxa and their relative contributions to the similarity among intertidal stations within the a) discharge and b) reference areas and based on Bray-Curtis distances of average station abundances during the August 2003 survey.

Species	% Contribution	Cumulative %
a) Discharge Group - average similarity: 45 %		
Oligochaeta	15.8	15.8
Grandidierella japonica	8.4	24.2
Nematoda	7.4	31.6
Corophium sp.	7.1	38.7
Leptochelia dubia	6.3	45.0
Phoronida	5.3	50.2
Streblospio benedicti	5.3	55.5
Tellina meropsis	5.2	60.7
Polydora websteri	5.1	65.8
Capitella capitata	4.7	70.5
Musculista senhousia	3.4	73.9
Tagelus subteres	3.2	77.1
b) Reference Group - average similarity: 59 %		
Leptochelia dubia	18.4	18.4
Euphilomedes carcarodonta	9.1	27.4
Fabricinuda limnicola	8.8	36.3
Nematoda	7.0	43.3
Leptocheliidae	6.3	49.5
Parasterope bamesi	4.3	53.9
Oligochaeta	4.2	58.0
Mayerella acanthopoda	3.9	61.9
Scoloplos acmeceps	3.7	65.7
Capitella capitata	3.2	68.9
Corophium sp.	2.8	71.7
Grandidierella japonica	2.5	74.1
Acuminodeutopus heteruropus	2.4	76.5

DRAFT

Table 3.3-12. Results of SIMPER analysis showing taxa and their relative contributions to the dissimilarity between intertidal stations in the reference and discharge areas based on Bray-Curtis distances of average station abundances during the August 2003 survey.

Species	% Contribution	Cumulative %
Fabricinuda limnicola	8.0	8.0
Leptochelia dubia	7.4	15.4
Euphilomedes carcarodonta	7.3	22.7
Nematoda	4.3	26.9
Parasterope bamesi	3.6	30.6
Mayerella acanthopoda	3.6	34.2
Grandidierella japonica	2.9	37.1
Leptocheliidae	2.8	39.9
Oligochaeta	2.6	42.5
Barleeia sp./*Assiminea californica*	2.4	44.9
Acuminodeutopus heteruropus	2.3	47.2
Corophium sp.	2.3	49.5
Polydora websteri	2.2	51.7
Musculista senhousia	2.1	53.8
Exogone sp.	2.1	55.9
Rutiderma judayi	2.0	57.9
Scoloplos acmeceps	1.9	59.8
Streblospio benedicti	1.8	61.6
Brania mediodentata	1.7	63.4
Mediomastus sp.	1.6	64.9
Tellina meropsis	1.5	66.5
Capitella capitata	1.5	68.0
Phoronida	1.2	69.2
Podocerus spp.	1.2	70.3
Tagelus subteres	1.2	71.5
Armandia brevis	1.1	72.6
Rutiderma lomae	1.0	73.6
Cirriformia moorei	1.0	74.6
Acteocina inculta	0.9	75.5

DRAFT

Table 3.3-13. Results of SIMPER analysis showing taxa and their relative contributions to the dissimilarity between intertidal stations in the reference and discharge areas based on Bray-Curtis distances of one replicate from the July 2003 survey.

Species	% Contribution	Cumulative %
Fabricinuda limnicola	10.44	10.44
Euphilomedes carcarodonta	7.66	18.09
Oligochaeta	7.56	25.65
Leptochelia dubia	5.73	31.39
Nematoda	5.12	36.51
Streblospio benedicti	3.85	40.35
Corophium sp.	3.69	44.04
Capitella capitata	3.09	47.13
Leptocheliidae	2.60	49.73
Pseudopolydora paucibranchiata	2.48	52.20
Acuminodeutopus heteruropus	2.37	54.58
Grandidierella japonica	2.36	56.94
Mediomastus sp.	2.30	59.24
Exogone sp. *1*	2.25	61.49
Scoloplos acmeceps	2.23	63.72
Mayerella acanthopoda	2.22	65.94
Rhynchospio glutaea	2.04	67.98
Tellina meropsis	1.81	69.79
Parasterope bamesi	1.74	71.53

DRAFT

Table 3.3-14. Results of SIMPER analysis showing taxa and their relative contributions to the dissimilarity between intertidal stations in the reference and discharge areas based on Bray-Curtis distances of one replicate from the September 2003 survey.

Species	% Contribution	Cumulative %
Leptochelia dubia	12.26	12.26
Acteocina inculta	6.59	18.86
Fabricinuda limnicola	6.33	25.19
Euphilomedes carcarodonta	5.39	30.57
Nematoda	4.42	34.99
Parasterope bamesi	3.90	38.89
Leptocheliidae	3.65	42.54
Oligochaeta	3.16	45.70
Acuminodeutopus heteruropus	2.76	48.47
Dipolydora socialis	2.74	51.20
Grandidierella japonica	2.69	53.90
Rutiderma judayi	2.53	56.43
Corophium sp.	2.35	58.79
Scoloplos acmeceps	2.22	61.00
Mediomastus sp.	2.20	63.21
Tagelus subteres	2.19	65.40
Capitella capitata	2.17	67.57
Mayerella acanthopoda	2.10	69.68
Musculista senhousia	1.73	71.40
Marphysa nr. sanguinea	1.71	73.11
Phoronida	1.62	74.74
Chione californiensis	1.61	76.34

3.3.4.4 Invertebrate Assemblages and Environmental Conditions

Subtidal Data Set

The PCA analysis of the physical data from the same set of stations for the August survey shows two patterns that account for 95 percent of the variation among the stations (**Figure 3.3-20**). The first PCA axis accounts for 80 percent of the variation and the variable loadings (**Table 3.3-15**) indicate that the axis is accounting for variation among variables for temperature. The first axis separates the stations into two groups: those located closest to the discharge, and those located past the small point on the southern boundary of the Chula Vista Wildlife Island. In this second group of stations there is a gradient of change representing decreased temperature exposure from the discharge and transition stations to the reference stations. The second axis describes variation in percentages of silt-clay sediments among stations. Stations T1 and R3 had much larger percentages of silt-clay sediments than stations such as N2.

A statistically significant relationship (p>0.001) was detected between station distances calculated using the physical variables and distances calculated using the taxa abundances. An iterative procedure was used to determine the suite of physical variables that provided the highest rank correlation between sample distances based on the infaunal and environmental data. Sample distances based on average temperature resulted in a statistically significant (p>0.01) rank correlation of 61 percent with the Bray-Curtis distances for the biotic data. The subsets of variables that provided the highest correlations with the biological data did not include the variable for percent silt-clay. This indicates that temperature is by far the most important variable affecting biological differences among stations.

Table 3.3-15. Variable loadings for PCA analysis of physical variables measured at subtidal reference, transition, and discharge stations for the August 2003 survey.

Variable	Principal Component One	Principal Component Two
Average Temperature	-0.455	-0.250
Maximum Temperature	-0.492	-0.175
Temperature Range	-0.483	-0.065
Temperature Standard Deviation	-0.484	-0.091
Percent Silt/Clay	0.291	-0.946

Intertidal Data Set

The PCA analysis of the physical data from the same set of stations for the August survey shows two patterns that account for 98 percent of the variation among the stations (**Figure 3.3-21**). The first PCA axis accounts for 91 percent of the variation and the variable loadings (**Table 3.3-16**) indicate that the axis is accounting for variation in temperature. As a result there is a clear gradient across the axis representing temperature differences among the discharge stations. The reference stations are all relatively similar compared to the discharge stations. The second axis describes variation in percentages of silt-clay sediments among the discharge stations. Stations T4 and T5 had much smaller percentages of silt-clay sediments than the other discharge stations. There was much less variation in the percentage of fine sediments among the reference stations.

An iterative procedure was used to determine the suite of physical variables that provided the highest rank correlation between sample distances based on the infaunal and environmental data. Sample distances based on two variables, average temperature and temperature standard deviation, resulted in a rank correlation of 83 percent with the Bray-

Table 3.3-16. Variable loadings for PCA analysis of physical variables measured at intertidal reference and discharge stations during the August 2003 survey.

Variable	Principal Component One	Principal Component Two
Average Temperature	0.457	0.268
Maximum Temperature	0.451	0.411
Temperature Range	0.455	0.256
Temperature Standard Deviation	0.462	0.208
Percent Silt/Clay	0.408	0.806

Curtis distances for the biotic data. All of the subsets of variables that provided the highest correlations with the biological data did not include the variable for percent silt-clay. This indicates that temperature is by far the most important variable affecting biological differences among stations.

DRAFT

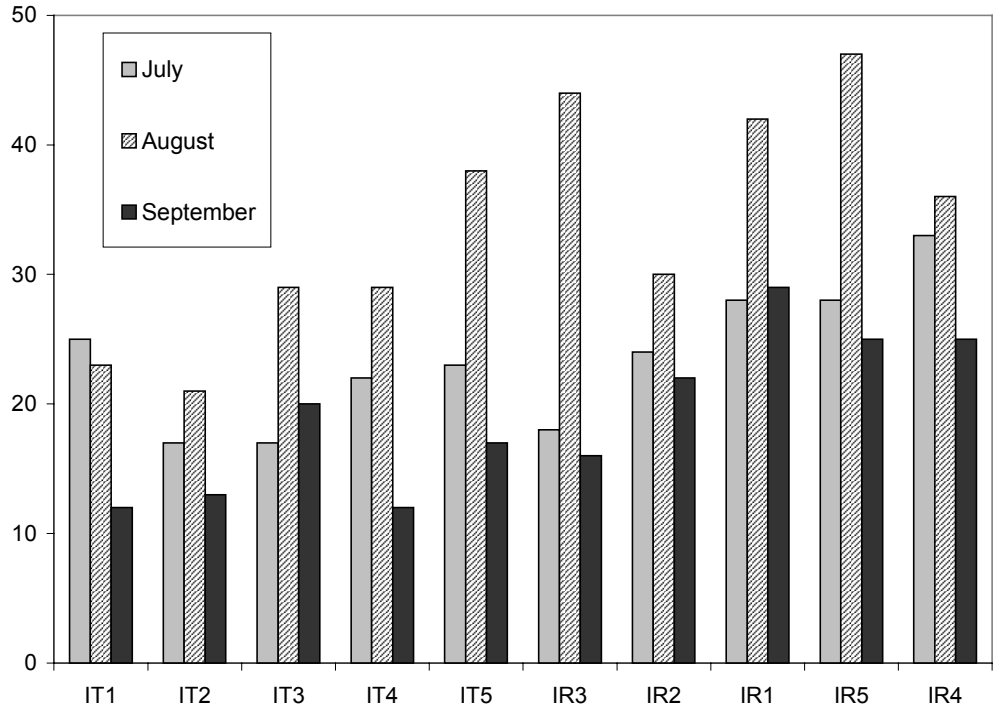

Figure 3.3-1. Total number of taxa per station at intertidal discharge (Series IT) and reference (Series IR) stations for July, August and September 2003. Totals based on one 0.018 m^2 core sample per station for July and September, and three 0.018 m^2 core samples per station for August. Stations are arranged in order of increasing distance from the station nearest the discharge (IT1).

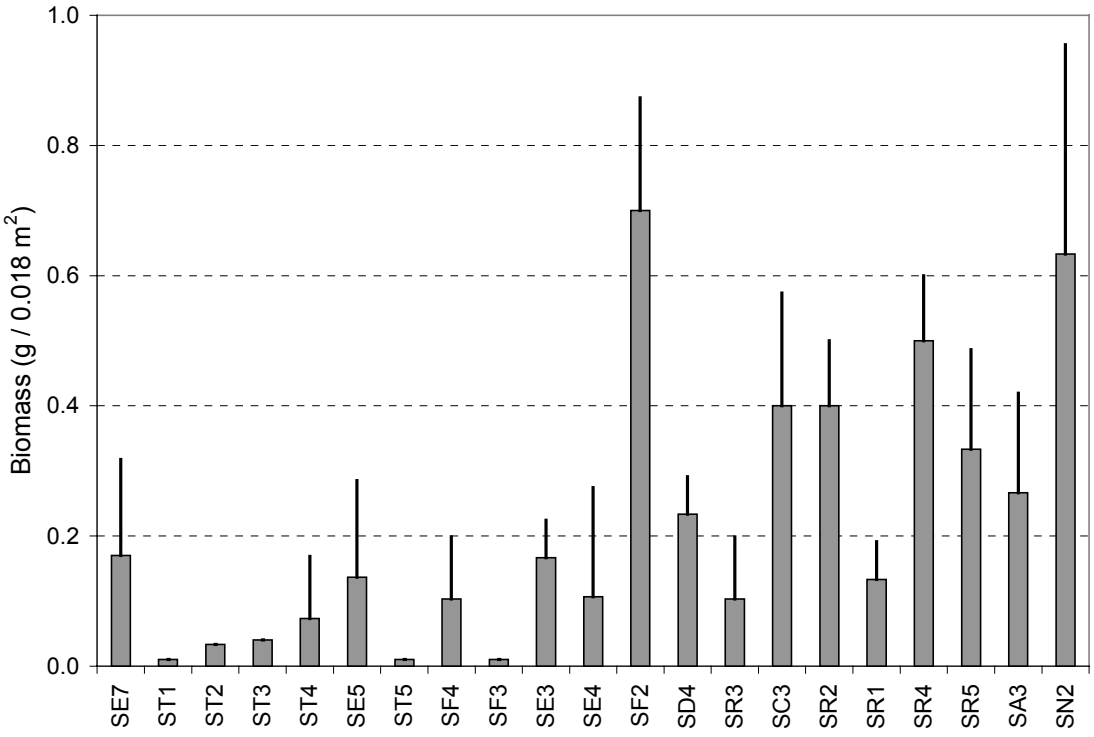

Figure 3.3-2. Polychaete biomass (g / 0.018 m^2) mean and standard deviation at subtidal stations in south San Diego Bay in August 2003. Stations are plotted in order of increasing distance from the station nearest the discharge (SE7).

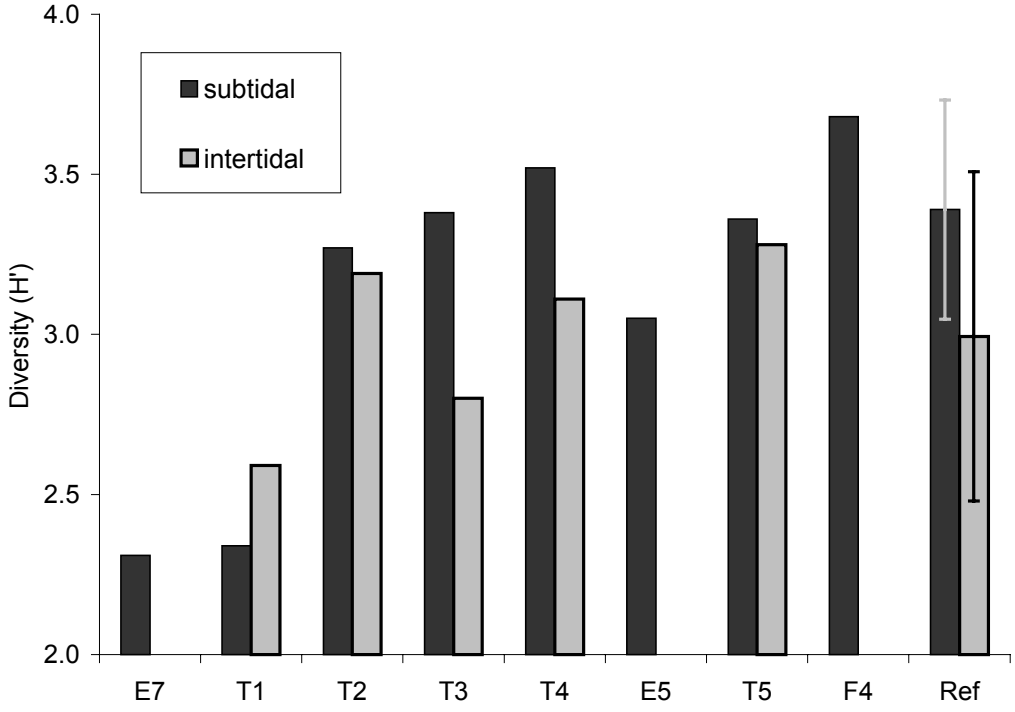

Figure 3.3-3. Infaunal diversity (H') mean per station at SBPP discharge channel stations, August 2003. Reference diversity values are the mean and standard deviation of other sampled subtidal (n=13) and intertidal (n=5) stations in south San Diego Bay.

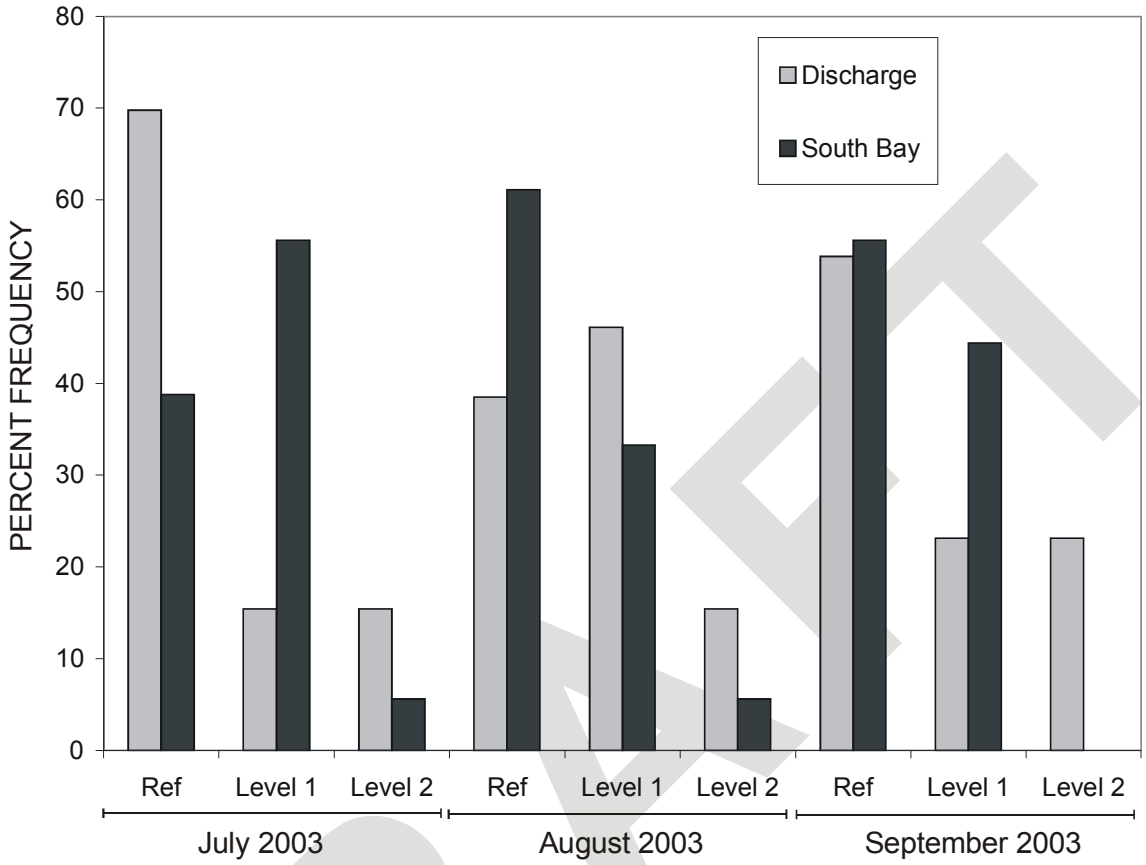

Figure 3.3-4. Benthic response index (BRI) levels as percent of stations in discharge channel (13 stations) and south San Diego Bay (18 stations) for July–September 2003 sampling periods. Refer to Table 3.3-4 for BRI response level descriptions.

DRAFT

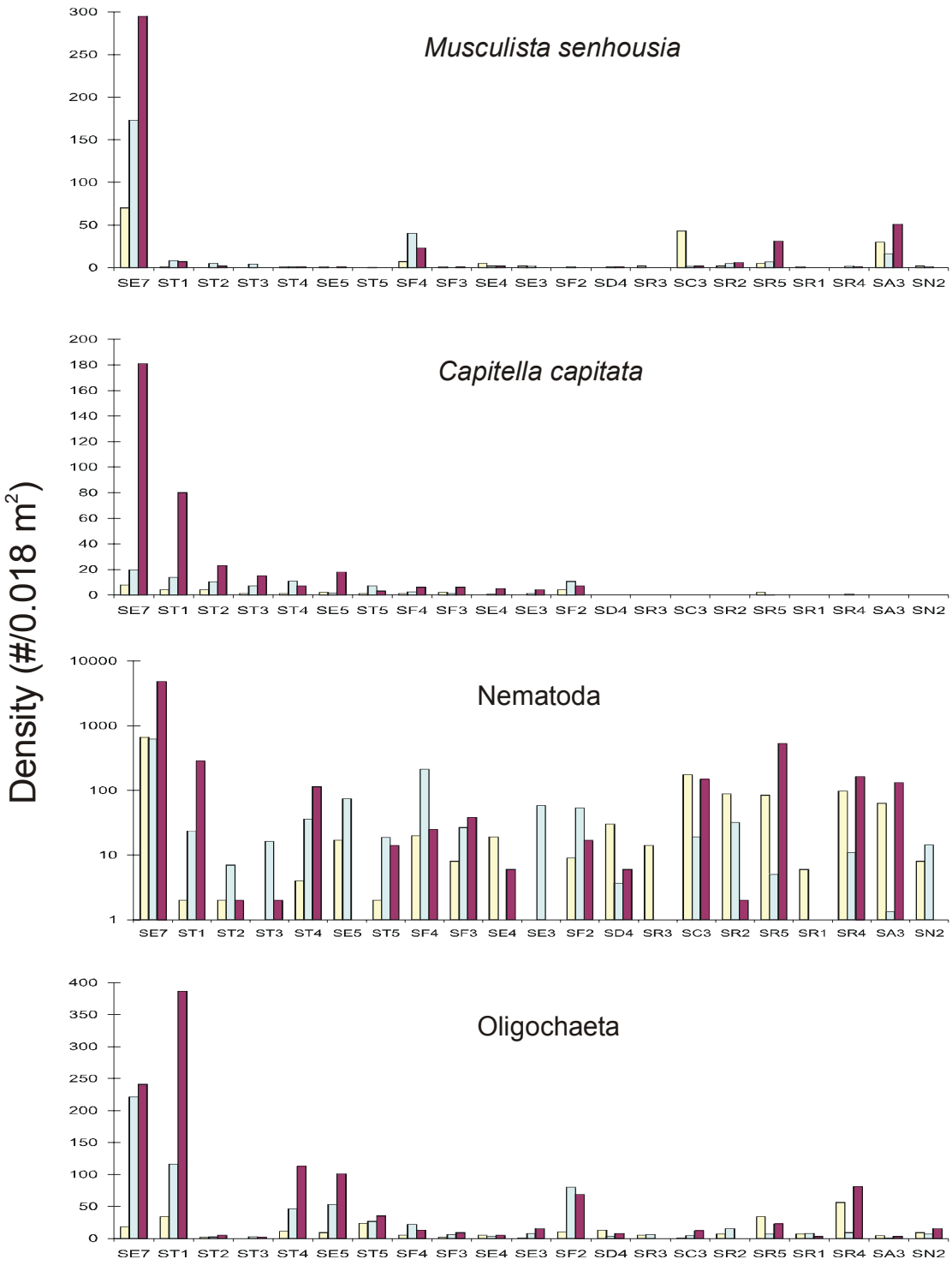

Figure 3.3-5. Subtidal invertebrate density per station for example taxa with distributions skewed toward the SBPP discharge (Station SE7) for July, August and September 2003 (yellow, blue, and red bars, respectively).

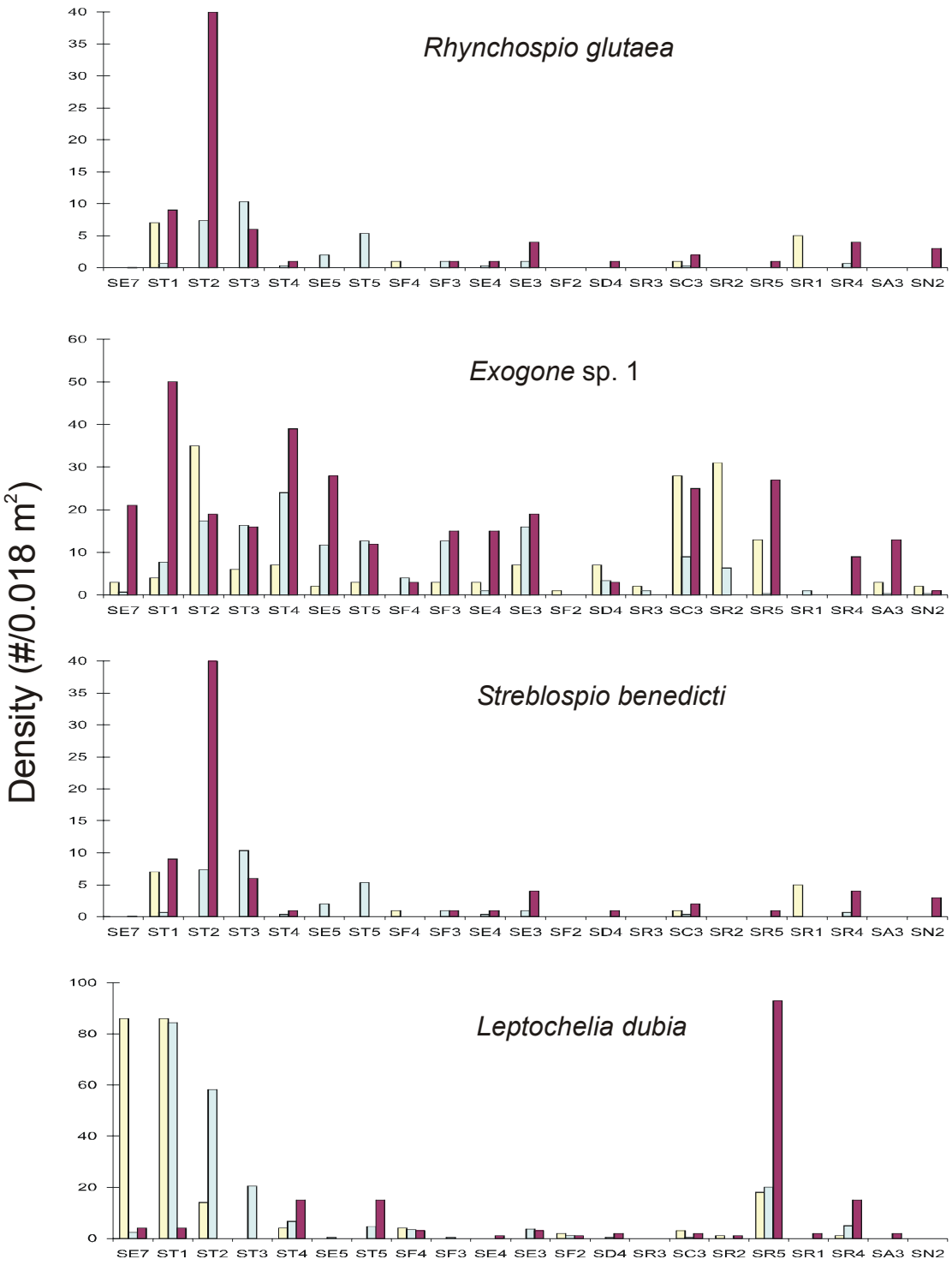

Figure 3.3-6. Subtidal invertebrate density per station for example taxa with distributions generally skewed toward the SBPP discharge stations but with depressed abundances at the station closest to the discharge (SE7) for July, August and September 2003.

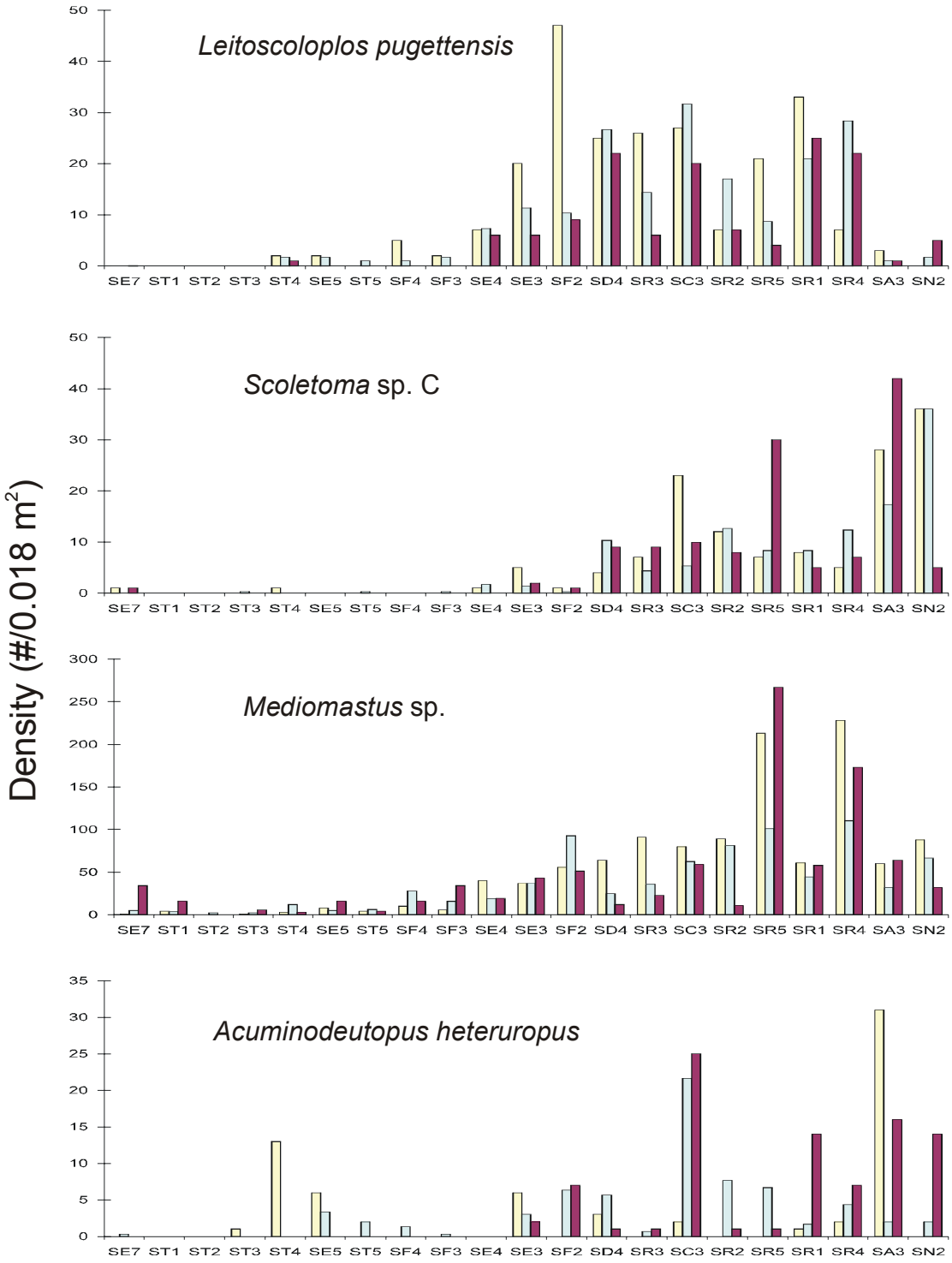

Figure 3.3-7. Subtidal invertebrate density per station for example taxa with distributions generally skewed away from the SBPP discharge (Station SE7) for July, August and September 2003.

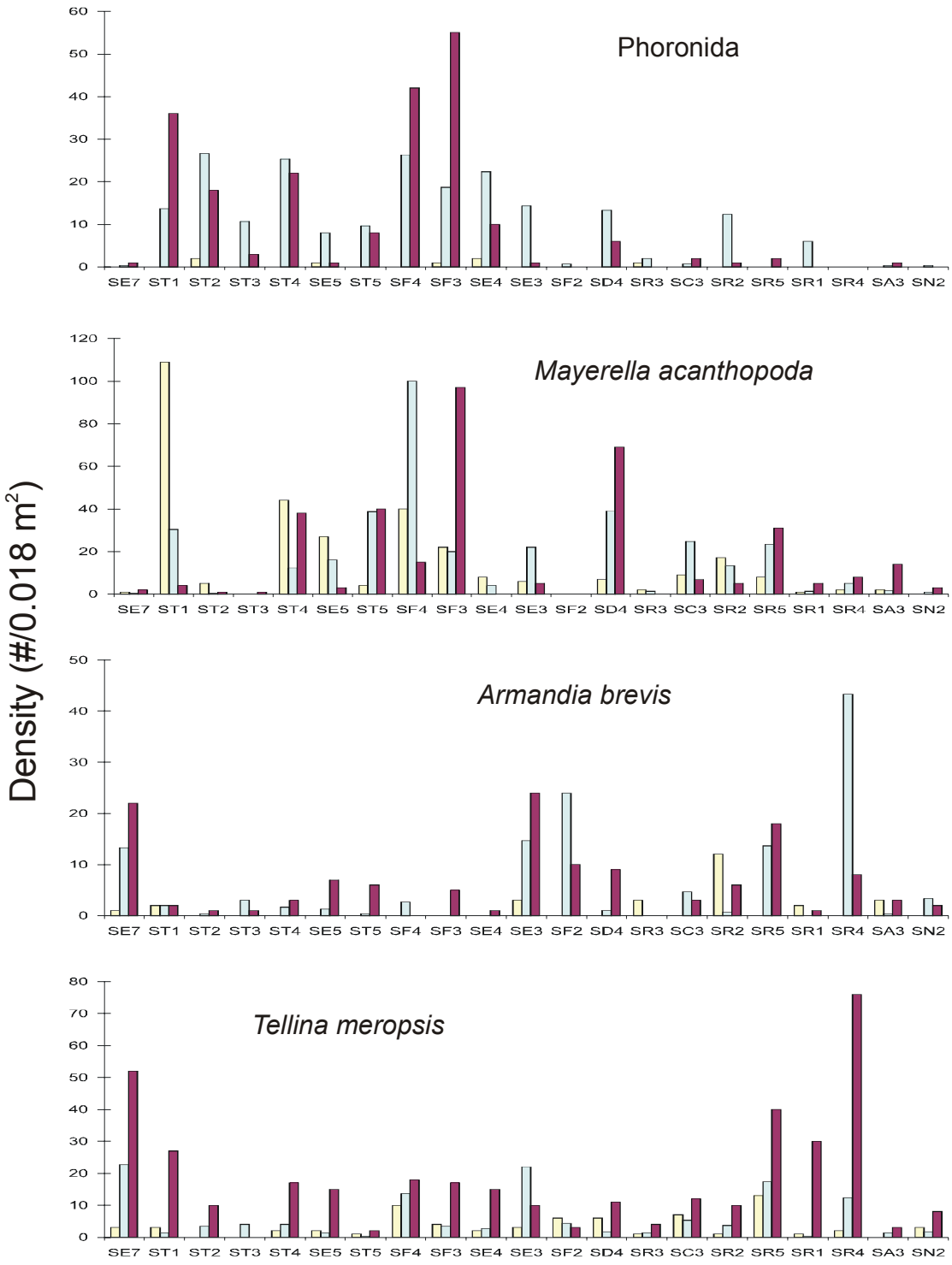

Figure 3.3-8. Subtidal invertebrate density per station for example taxa with no definitive distribution pattern relative to the SBPP discharge (Station SE7) for July, August and September 2003.

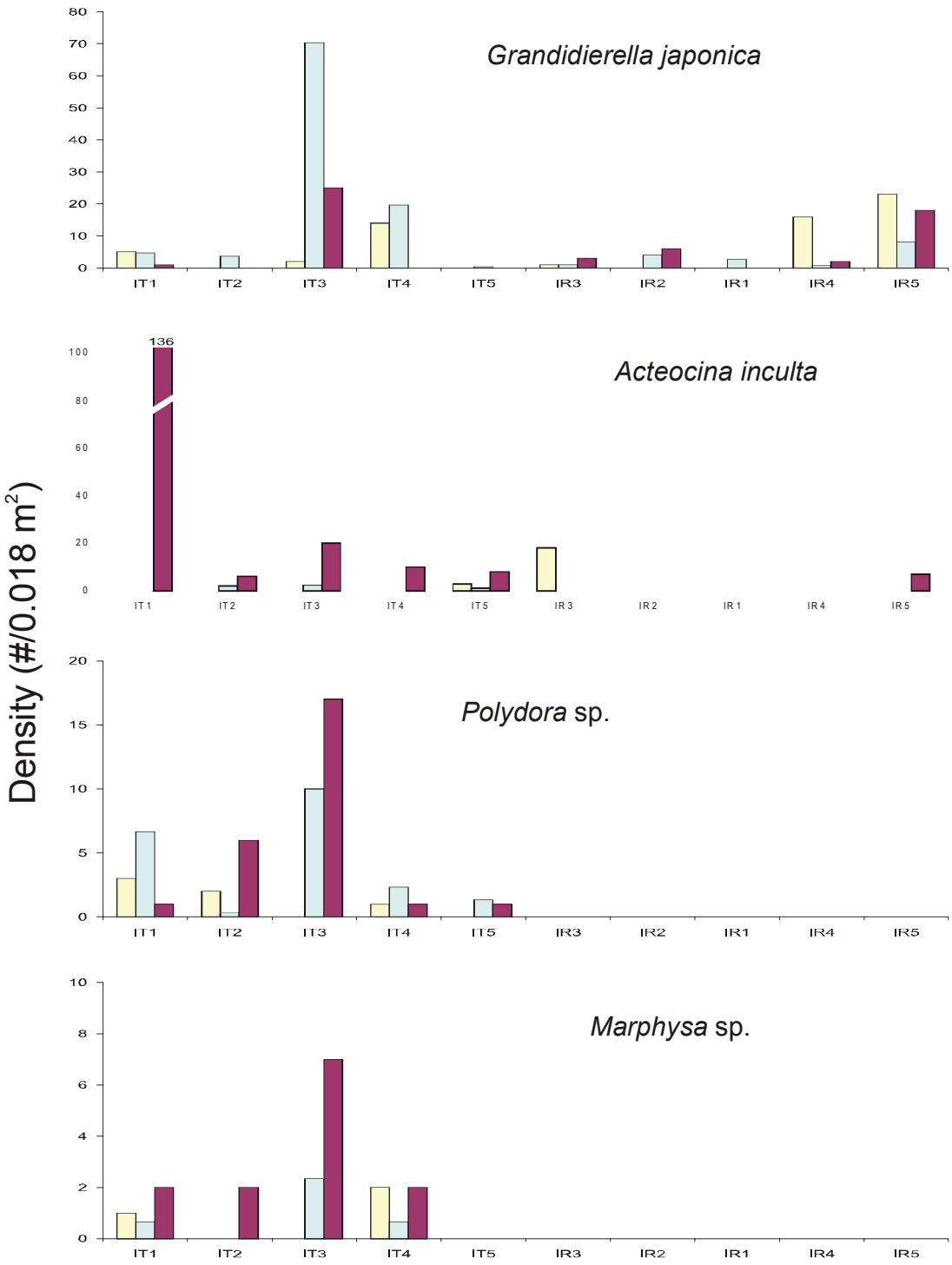

Figure 3.3-9. Intertidal invertebrate density per station for example taxa with greater abundances at discharge stations than reference stations for July, August and September 2003.

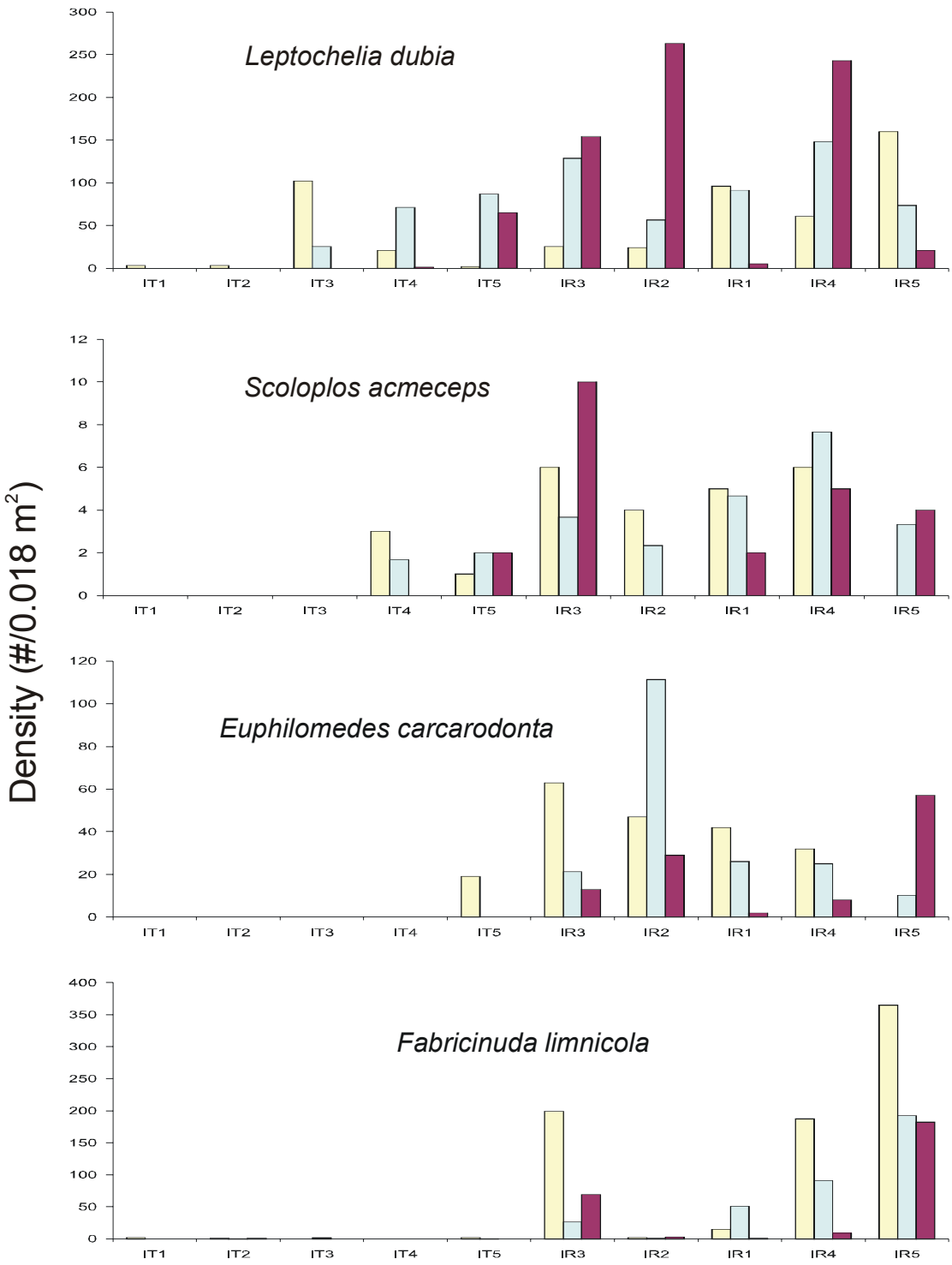

Figure 3.3-10. Intertidal invertebrate density per station for example taxa with greater abundances at reference stations than discharge stations for July, August and September 2003.

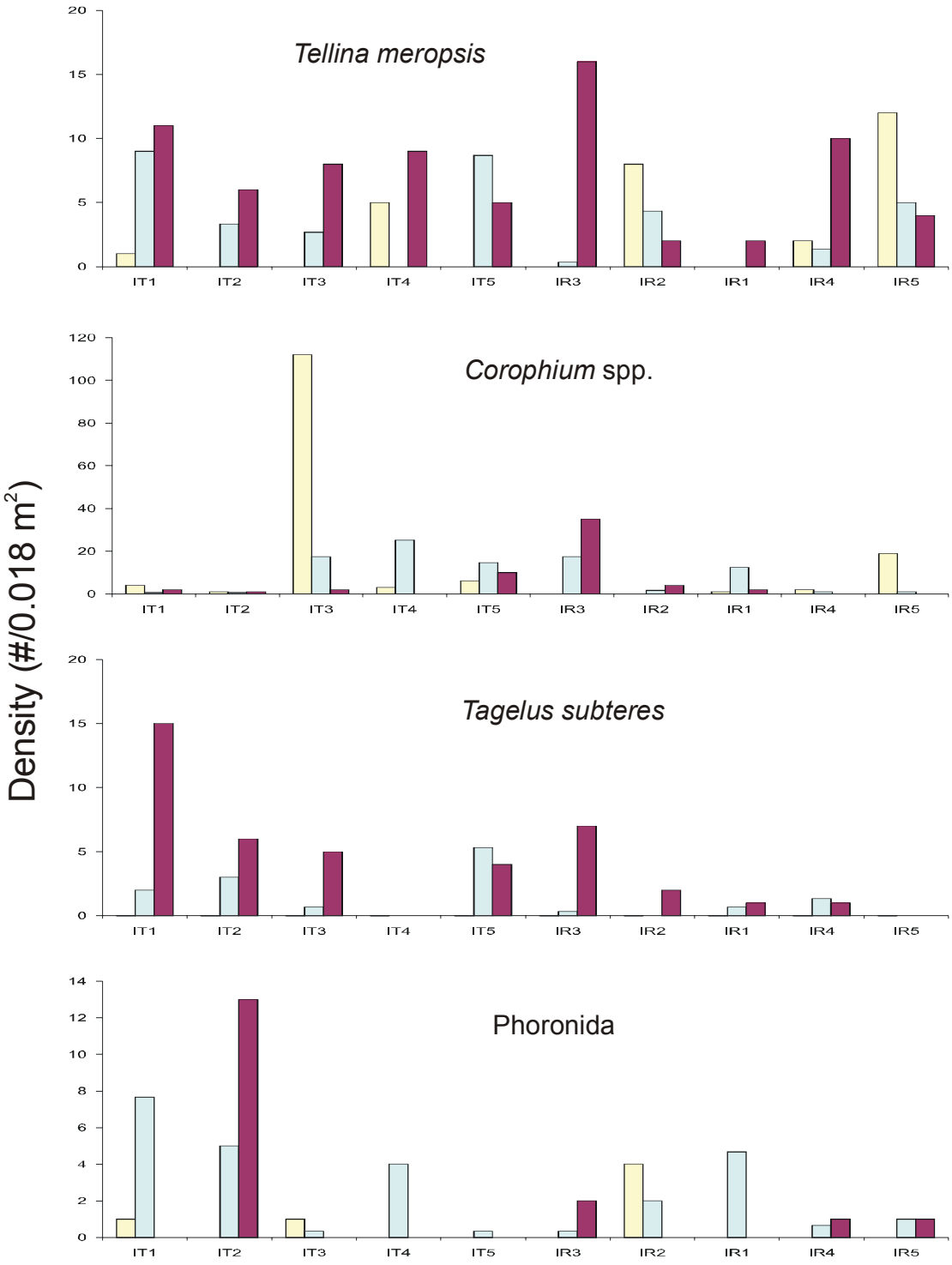

Figure 3.3-11. Intertidal invertebrate density per station for example taxa with no definitive distribution pattern relative to the SBPP discharge (Station IT1) for July, August and September 2003.

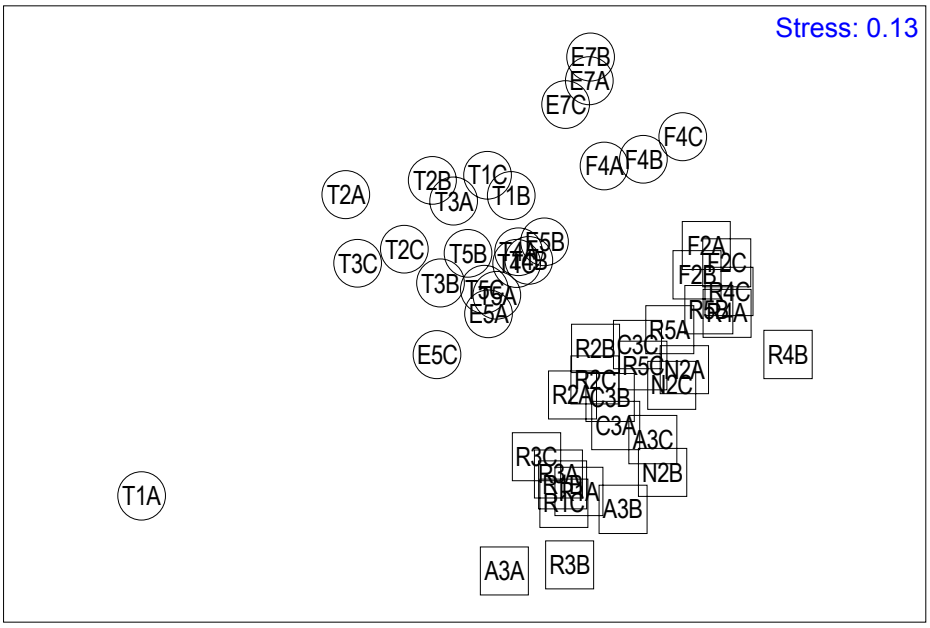

Figure 3.3-12. MDS analysis of infaunal abundances from 139 invertebrate taxa for subtidal benthic core samples in reference (A3, C3, F2, N2, R1–R5 squares) and discharge (E5, E7, F4, T1–T5 circles) areas during the August 2003 survey. The three replicate cores at each station are indicated by the A, B, and C in the last letter of the station name.

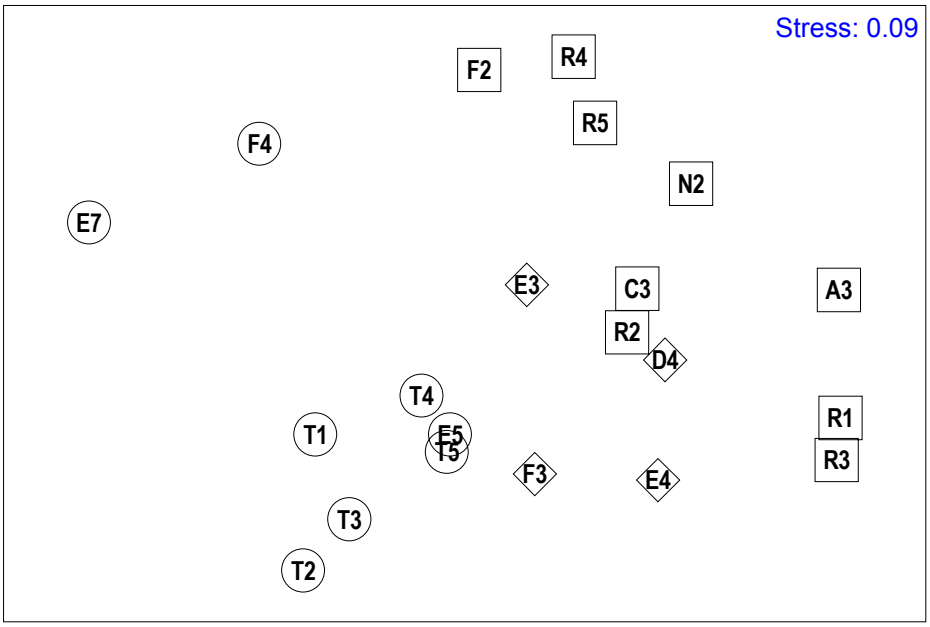

Figure 3.3-13. MDS analysis of average infaunal abundances from 145 invertebrate taxa at subtidal benthic stations in reference (A3, C3, F2, N2, R1–R5 squares), transition (D4, E3, E4, and F3 diamonds), and discharge (E5, E7, F4, T1–T5 circles) areas during the August 2003 survey.

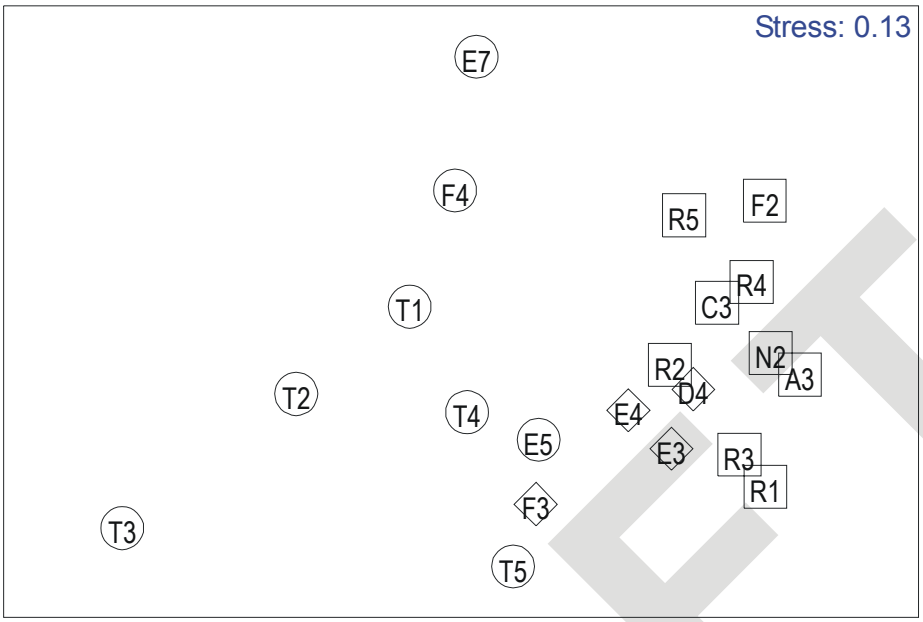

Figure 3.3-14. MDS analysis of average infaunal abundances from 95 invertebrate taxa at subtidal benthic stations in reference (A3, C3, F2, N2, R1–R5 squares), transition (D4, E3, E4, and F3 diamonds), and discharge (E5, E7, F4, T1–T5 circles) areas during the July 2003 survey.

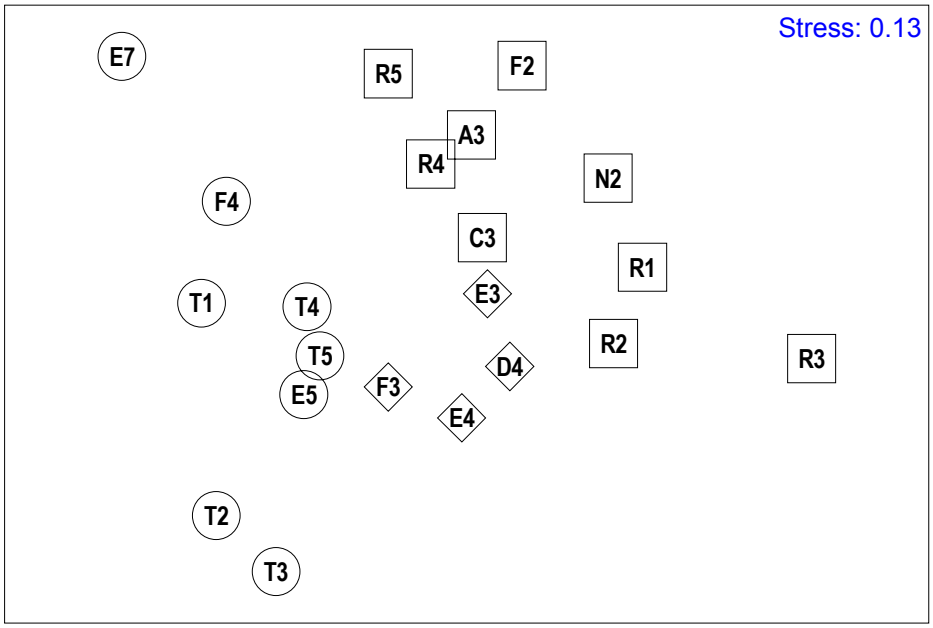

Figure 3.3-15. MDS analysis of average infaunal abundances from 105 invertebrate taxa at subtidal benthic stations in reference (A3, C3, F2, N2, R1–R5 squares), transition (D4, E3, E4, and F3 diamonds), and discharge (E5, E7, F4, T1–T5 circles) areas during the September 2003 survey.

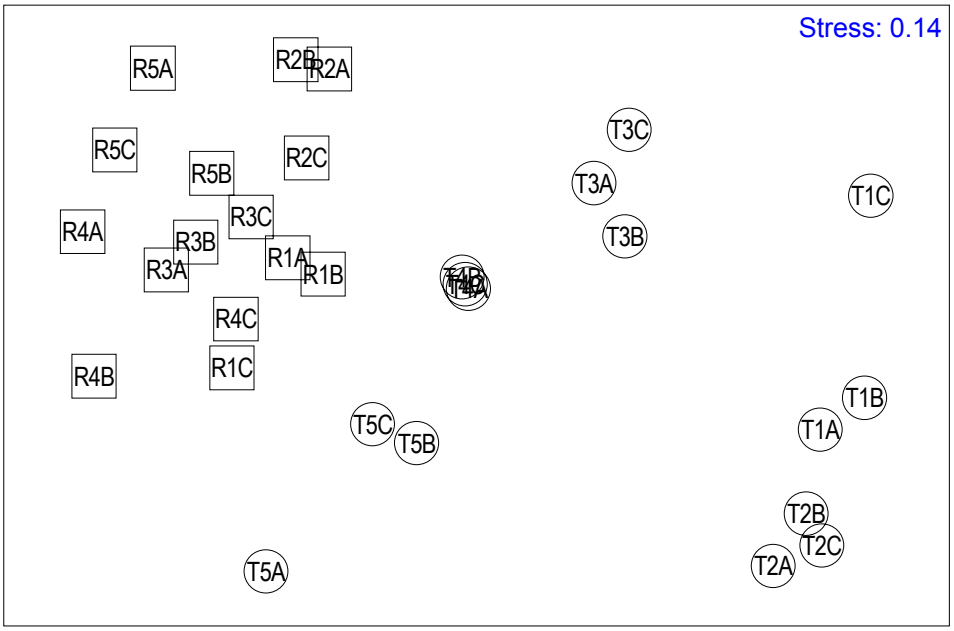

Figure 3.3-16. MDS analysis of infaunal abundances from 100 invertebrate taxa for intertidal benthic core samples in reference (R1–R5 squares) and discharge (T1–T5 circles) areas during the August 2003 survey. The three replicate samples at each station are indicated by the A, B, and C in the last letter of the station name.

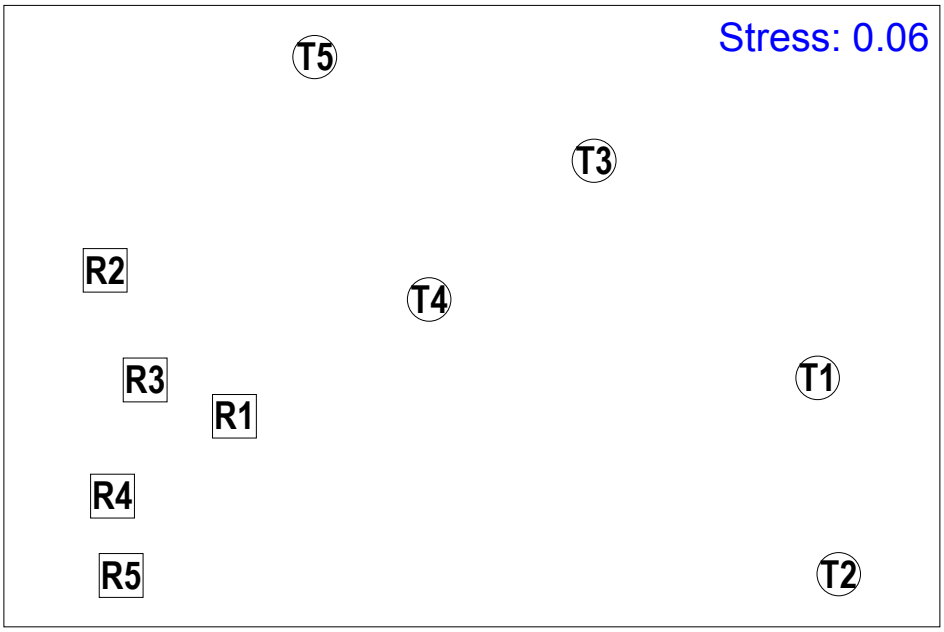

Figure 3.3-17. MDS analysis of average infaunal abundances from 100 invertebrate taxa at intertidal benthic stations in reference (R1–R5 squares) and discharge (T1–T5 circles) areas during the August 2003 survey.

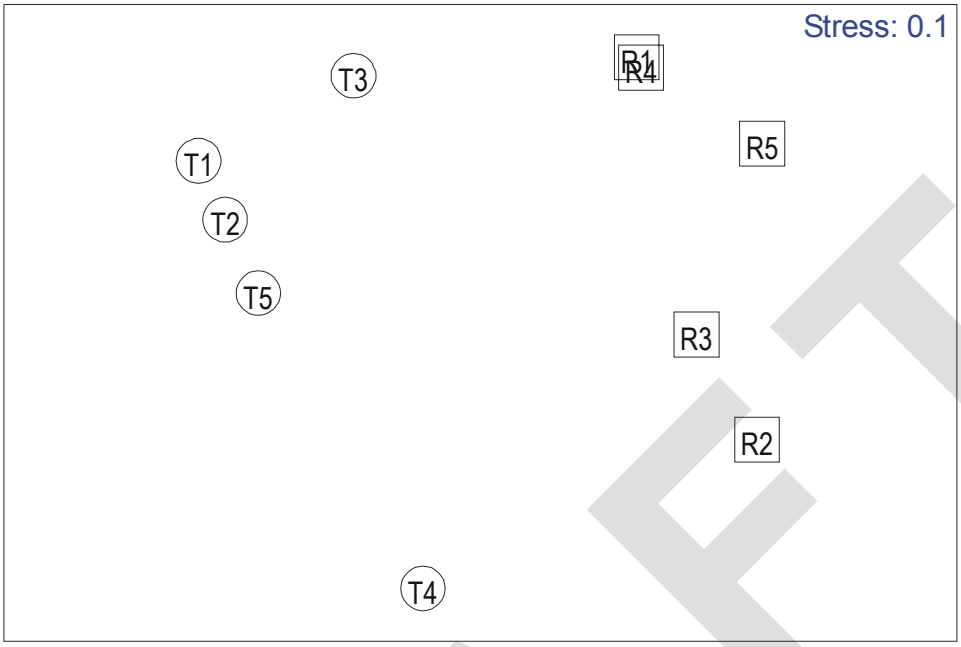

Figure 3.3-18. MDS analysis of average infaunal abundances from 57 invertebrate taxa at intertidal benthic stations in reference (R1–R5 squares) and discharge (T1–T5 circles) areas during the July 2003 survey.

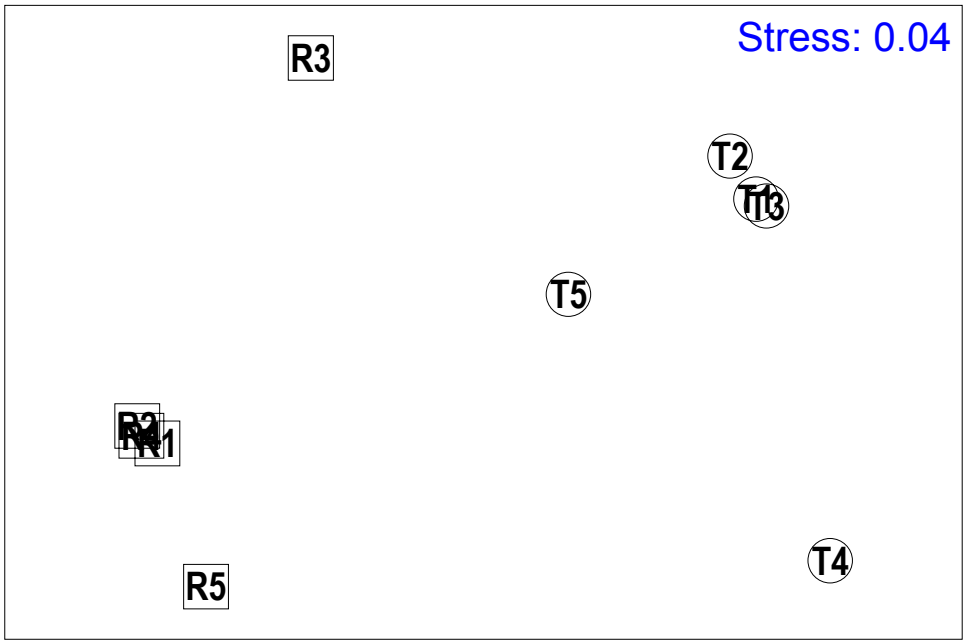

Figure 3.3-19. MDS analysis of average infaunal abundances from 57 invertebrate taxa at intertidal benthic stations in reference (R1–R5 squares) and discharge (T1–T5 circles) areas during the September 2003 survey.

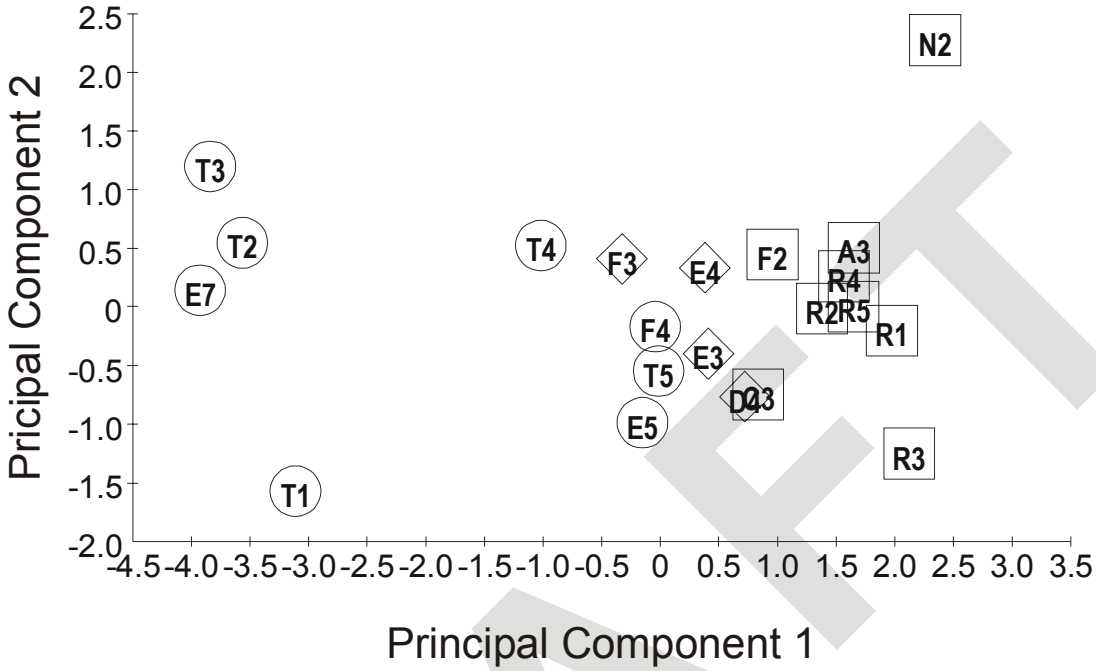

Figure 3.3-20. PCA analysis of physical data parameters from subtidal benthic stations in reference (A3, C3, F2, N2, R1–R5 squares), transition (D4, E3, E4, and F3 diamonds), and discharge (E5, E7, F4, T1–T5 circles) areas during the August 2003 survey.

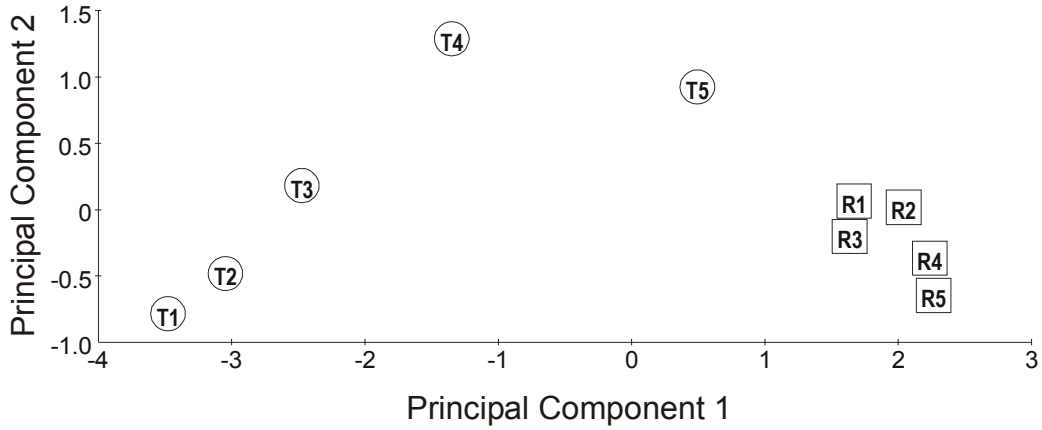

Figure 3.3-21. PCA analysis of physical data parameters from intertidal benthic stations in reference (R1–R5 squares) and discharge (T1–T5 circles) areas for the August 2003 survey.

3.4 Fish Communities

3.4.1 Introduction

The present study was designed to compare fish communities between the discharge channel and a reference site during the warmest months of the year (July–September). The reference site selected was in the nearby Sweetwater River channel, a shallow, warm site subject to seasonal freshwater input, and with periodically reduced DO levels. Fish sampling was conducted at the SBPP discharge channel and Sweetwater River on August 27, September 12, and September 29. To make additional comparisons, several past fish studies conducted in other back-bay environments were reviewed for diversity, density and biomass data for comparison to results of the current study.

3.4.2 Review of Fish Studies in South San Diego Bay

Few studies of fish communities within the southern end of San Diego Bay have been conducted in past years. Ford and Chambers (1968) conducted the most comprehensive early investigation; however this study pre-dated some significant environmental changes including the construction of the San Diego Unified Port District's Chula Vista Wildlife Island (CVWI), and the CDFG's authorization of an experimental mullet fishery within south San Diego Bay (a fishery that subsequently ended in the late 1990s).

Ford and Chambers (1968) sampled 36 stations throughout the south bay (including 10 stations in the SBPP discharge channel) in July and August 1968. They used a 1.5 m (4.9 ft) beam trawl at 26 stations, and a 15.2 m (50 ft) bag seine and a 4.6 m (15 ft) minnow seine at 10 stations. They collected 21 species of bony fishes and elasmobranchs, among which were six that were considered important as recreational fishery species: black croaker *Cheilotrema saturnum*, California halibut *Paralichthys californicus*, diamond turbot *Hypsopsetta guttulata*, barred sand bass *Paralabrax nebulifer*, spotted sand bass *P. maculatofasciatus*, and striped mullet *Mugil cephalus*. There were significantly fewer species and numbers of fishes at stations in the inner portion of the cooling water discharge channel as compared to reference stations, with only four species sampled: black croaker, striped mullet, California killifish *Fundulus parvipinnis*, and longjaw mudsucker *Gillichthys mirabilis*. They noted that black croaker and striped mullet are fast swimming pelagic species that could make excursions into the warmest areas of the plume, and the California killifish and longjaw mudsucker are species that are naturally tolerant of very warm water conditions.

Additional data on fish abundances in the vicinity of SBPP were collected as part of cooling water system impact studies during 1979–1980 (SDG&E 1980). It was concluded that SBPP impingement losses were insignificant to the adult fish populations of San Diego Bay. Four 'critical' species (topsmelt *Atherinops affinis,* slough anchovy *Anchoa delicatissima,* round stingray *Urolophus halleri,* and California halibut) and one 'non-critical' species (deepbody anchovy *A. compressa*) were included in the analysis. An estimated 28,174 fishes were impinged annually during the study.

From 1994 to 1999, a bay-wide fish study was conducted by the U.S. Navy, the San Diego Unified Port District, and NOAA Fisheries (Allen 1999, Allen et al. 2002). This study included quarterly sampling within four bay ecoregions, using six gear types including a large beach seine, small seine, 1 m^2 square enclosure, beam trawl, purse seine, and otter trawl. Sampling was done in the south San Diego Bay ecoregion but the SBPP discharge channel was not among the areas sampled. The study did, however, more fully characterize the composition and seasonal changes in the south San Diego Bay fish community than any of the earlier studies. A total of 51 species was recorded from the south ecoregion, substantially expanding the list of species found in the Ford and Chambers (1968) study. Slough anchovy, topsmelt, arrow goby *Clevelandia ios*, round stingray, northern anchovy *Engraulis mordax*, and shiner surfperch *Cymatogaster aggregata* were the most abundant species while round stingray, spotted sand bass, barred sand bass, and bat ray *Myliobatis californicus* dominated in biomass. Allen (1999) also noted several species that were characteristic of the warm waters of south San Diego Bay including striped mullet, California halfbeak *Hyporhamphus rosae*, bonefish *Albula vulpes*, and Pacific seahorse *Hippocampus ingens*. Approximately 70 percent of all fishes captured in San Diego Bay during this study were juveniles emphasizing the importance of the bay as a nursery area for young fishes. A comparison of areas with dense eelgrass cover and areas with sparse eelgrass cover yielded no significant differences in the total numbers of fishes sampled during the five-year study.

An agreement was reached in 1997 between interested state and federal resource agencies and SDG&E to conduct a study that documented the existing fish communities of the SBPP discharge channel. As a formal requirement, the discharge channel fish study was incorporated into the NPDES permit renewal process by the RWQCB (Order 96-05). The three-year study provided baseline information for characterization of the beneficial uses (related to fisheries) that existed within the cooling water discharge channel (Merkel & Associates 2000a). The study, conducted quarterly from 1997 through 1999 employed methods comparable to those used in the overlapping bay-wide fish study (Allen 1999).

Merkel & Associates (2000a) recorded 38 species in the discharge channel during the 12 quarterly sampling periods. Slough anchovy numerically dominated most catches (91 percent overall) and most were juveniles. The mean density of fishes was 2.6 times higher at the outer station (approximately 1.3 km [0.8 mi] from the point of discharge) than the inner station (approximately 0.5 km [0.3 mi] from the point of discharge).

Sharks and rays accounted for over 76 percent of the total biomass of fishes captured at both stations. Biomass in their study was highest during cool water months (January) and lowest during the warm water months (July and October). The overall conclusion of the study was that the discharge channel supported a high density of fishes, particularly anchovies, that was greater than San Diego Bay as a whole, and that these fishes comprised the principal forage base for piscivorous birds, such as terns and skimmers, feeding within the channel.

In another study, Williams and Zedler (1999) compared fish assemblages in natural and constructed wetlands in the Sweetwater Marsh National Wildlife Refuge, approximately 3.5 km (2.2 mi) north of SBPP. In this wetland habitat, characteristic of several shoreline areas on the southeastern margin of San Diego Bay, they found that California killifish, topsmelt, longjaw mudsucker, arrow goby, bay pipefish *Syngnathus leptorhynchus*, and yellowfin goby *Acanthogobius flavimanus* were the most abundant species.

3.4.3 Methods

3.4.3.1 Study Sites

The fish study sites were located in south San Diego Bay in the Sweetwater River Channel and the SBPP discharge channel (**Figure 3.4-1**). The 116 ha (287 ac) discharge channel area consists of a shallow triangular portion of the bay under marine tidal influence. The CVWI to the north, the northern-most dikes of the Western Saltworks evaporator ponds to the south, and an extension of the southern arm of the intake/discharge dividing dike south to the mouth of the Otay River geographically define the channel. Most of the discharge channel is an extensive intertidal mudflat extending northward from the dikes of the Western Saltworks. A deeper channel follows along the southern edge of the CVWI dike, which is bordered by a narrow beach along the northern channel edge that is exposed during low tides. The environmental setting of SBPP, operating characteristics of the power plant, and a description of the discharge are presented in Section 2.0–*Description of the South Bay Power Plant and Characteristics of the Source Water Body*.

The SBPP discharge channel study site was located in the channel, inside of the southerly arm of the original intake/discharge separator dike. Shore-based sampling was conducted at low tide over a stretch of beach along the north shore of the channel (**Figure 3.4-2**). The sampling area had a cobblestone bottom at higher tidal elevations and a firm mud bottom at the lower tidal elevations. Boat-based sampling was conducted adjacent to the onshore sampling stations within the deeper channel and flats of the discharge channel. Because it was anticipated that the fish assemblage of the discharge channel varied along a thermal gradient, samples were collected at three sites in the channel: one near the bend in the earthen dike, one at the western end of the discharge channel, and one in-between.

The Sweetwater River sampling site was located in the lower Sweetwater River, approximately 0.8 km (0.5 mi) upstream of the Interstate 5 overpass (**Figure 3.4-2**). Shore-based sampling was conducted at medium tide along a stretch of rip-rap riverbank. The samples were collected over mud bottom, partially vegetated by ditch grass *Ruppia maritima* and eelgrass. Boat-based sampling was conducted adjacent to the onshore sampling stations within the deeper river channel. Three replicate samples were collected from shore and a boat along an east-west gradient, similar to the discharge channel sampling site.

3.4.3.2 Data Collection

Previous efforts to characterize the fish community in the discharge channel used a variety of sampling equipment. The prior discharge channel fish study completed in 1999 (Merkel & Associates 2000a) and the bay-wide study (Allen 1999) found that the beach and purse seine effectively caught representative samples of the various fish guilds occurring in south San Diego Bay. Based on these results, a large beach seine and a purse seine were used in the current investigation. Hauls with each gear type from each of these areas were treated as three replicate samples for that sampling site.

Large Seine

The large seine was used to sample schooling and benthic fishes in the nearshore portion of a station. The seine consisted of a 15.5 m (50.9 ft) x 1.8 m (5.9 ft) net fitted with a 1.8 m x 1.8 m x 1.8 m bag; it had 1.2 cm (0.5 in) mesh in the main body and 0.6 cm (0.25 in) mesh in the bag. The seine was deployed in waters between 0 m and 1.7 m (5.6 ft) MLLW and set parallel to shore. After waiting for 3 min, a crew hauled the seine to shore being careful to keep the weighted edge of the net in contact with the bottom. An average area of 275 m^2 (2,970 ft^2)was sampled per haul.

Purse Seine

The purse seine was used to sample juvenile and adult fishes in the water column of the nearshore portions of each station. The purse seine also samples demersal species when it is deployed in shallow water where the net reaches the bay bottom, as in the present study. A 66 m (217 ft) x 6 m (20 ft) seine with 1.2 cm (0.5 in) mesh in the wings and 0.6 cm (0.25 in) mesh in the bag was pulled with a skiff or other larger draft vessel. The area of bottom coverage by the seine was calculated as 347 m^2 (3,735 ft^2).

Threefold replication was completed for each gear type at each sampling site. Sampling was conducted on August 27, September 12, and September 29, 2003. Fishes collected in each haul were identified, weighed to the nearest gram, and standard length (SL) measured to the nearest millimeter. If more than 100 individuals of a species were caught in a replicate of any gear type, a batch sampling procedure was utilized. First, the SL and weight were determined for 30 randomly selected individuals. Second, a batch weight was determined for 100 additional randomly selected individuals. Finally, the batch

weight was determined for all of the remaining, uncounted individuals. The number of uncounted individuals was then estimated by using the batch weight of the 100 randomly selected individuals as a known fraction of the total sample.

All project data were initially recorded on hard copy original datasheets and then transferred in the laboratory to digital database files. IDS Ecological Survey©, an ecological information management program, was used to manage relational data from the project surveys. For each sampling event, data on abundance, density, and biomass at each site were compiled. Means were reported as means $\pm$ 1 standard deviation.

3.4.4 Results

3.4.4.1 SBPP Discharge Channel

A total of twenty species, represented by a combined total of 26,672 fish, was captured during the summer 2003 study (**Table 3.4-1**) (**Appendix J**), in a sampling area totaling 5,465 m^2 (58,825 ft^2)over the course of the three sampling events. The most abundant fishes were juvenile slough and deepbody anchovy, that represented 96 percent of the total individuals caught. The next most abundant was adult slough anchovy, representing 2 percent of the total individuals caught, followed by topsmelt representing 1 percent of the total individuals caught. All other species were caught in numbers of sixty or less, including nine species represented by less than 10 individuals. Commonly captured species included California halfbeak, round stingray, queenfish *Seriphus politus*, barred pipefish *Syngnathus auliscus*, bay pipefish and three species of goby: arrow goby, cheekspot goby *Ilypnus gilberti*, and yellowfin goby. Of note was the capture of a large California butterfly ray *Gymnura marmorata* weighing 20 kg (44 lb).

The majority of the fish caught was juvenile anchovy, composed of a mix of slough and deepbody anchovy. The fish were too abundant and small to all be identified in the field. A subsample was collected and identified later in the laboratory. Based on this analysis, it was assumed that the juveniles were 83 percent slough anchovy and 17 percent deepbody anchovy.

During each of the three sampling events, 15 species were captured in the discharge channel. Variation in the number of fishes caught during each event was driven primarily by the abundance of adult and juvenile anchovy. Abundances of fishes for the August 27, September 12, and September 29 sampling were 12,603, 3,925, and 10,144 fish, respectively (**Table 3.4-1**). With anchovy counts removed, total abundance of all other species combined was 126, 202, and 125, respectively. This illustrates the clear dominance of the numeric count by anchovies and the more consistent count figures for the other fish from survey to survey.

Table 3.4-1. Summary of fish abundance (# of individuals) and density (#/m^2) by sampling period and station.

SPECIES	Survey 1 (27Aug03)		Survey 2 (12Sept03)		Survey 3 (29Sept03)		Mean abundance	
	SBPP	Sweet-water	SBPP	Sweet-water	SBPP	Sweet-water	**SBPP**	**Sweet-water**
Anchovy, unid. juvenile	12,316		3,633		9,787		**8,578.7**	**-**
Slough Anchovy	158	168	62	744	214	254	**144.7**	**388.7**
Topsmelt	37	1,378	104	598	44	444	**61.7**	**806.7**
California Halfbeak	20	20	17	16	23	37	**20.0**	**24.3**
Round Stingray	11	4	29	2	11	2	**17.0**	**2.7**
Deepbody Anchovy	3		28	1	18		**16.3**	**0.3**
Arrow Goby	8	2	12		11		**10.3**	**0.7**
Bay Pipefish	2		14	2	12	1	**9.3**	**1.0**
Queenfish	10		10		8		**9.3**	**-**
Barred Pipefish	22	2	3				**8.3**	**0.7**
Diamond Turbot	2		5		4	1	**3.7**	**0.3**
California Needlefish	8	3		2			**2.7**	**1.7**
Cheekspot Goby			2		3		**1.7**	**-**
Bat Ray			1		3		**1.3**	**-**
California Killifish	2	1	2				**1.3**	**0.3**
Yellowfin Goby	1	1	2		1	5	**1.3**	**2.0**
Bonefish					2		**0.7**	**-**
Spotted Sand Bass		2		5	2	1	**0.7**	**2.7**
Striped Mullet	2						**0.7**	**-**
California Butterfly Ray					1		**0.3**	**-**
Shortfin Corvina	1	2		3			**0.3**	**1.7**
Shadow Goby			1				**0.3**	**-**
Total Abundance (Indiv.)	12,603	1,583	3,925	1,373	10,144	745	**8,890.7**	**1,233.7**
Mean Density (Indiv./m^2)	7.04	0.77	2.10	0.77	5.95	0.39	**5.0**	**0.6**

The total mean density (number of individuals/m^2) during the study was 5.03 $\pm$ 3.0 indiv/m^2 (**Table 3.4-1**). Mean density of all six hauls (3 large seine, 3 purse seine) during the August 27, September 12, and September 29 sampling was 7.04 $\pm$ 0.81, 2.10 $\pm$ 0.62, and 5.95 $\pm$ 3.85 indiv/m^2, respectively. Variations in density were attributable to variations in abundance of juvenile anchovy.

A total of 39.2 kg (86.4 lb) of fish was captured at this site during the study. This weight was dominated by the single California butterfly ray, which accounted for more than half of the total weight caught. Other species composing large portions of the total weight were round stingray (16 percent), juvenile anchovy (9 percent), bat ray (7 percent), and striped mullet (6 percent).

The total mean biomass (g/m^2) in the discharge channel during the study was 8.31 $\pm$ 15.93 g/m^2 (**Table 3.4-2**). The high variation in the mean biomass was due largely to the 20 kg California butterfly ray captured during the September 29 sampling. (If the large California butterfly ray is removed from calculations, the total mean biomass was 3.63 $\pm$2.73 g/m^2).

Table 3.4-2. Summary of fish weight (g) by sampling period and station.

SPECIES	Survey 1 (27Aug03)		Survey 2 (12Sept03)		Survey 3 (29Sept03)		Mean weight (g)	
	SBPP	Sweet-water	SBPP	Sweet-water	SBPP	Sweet-water	**SBPP**	**Sweet-water**
California Butterfly Ray					20,000		**6,666.7**	**-**
Round Stingray	990	755	3,594	386	1,578	427	**2,054.0**	**522.7**
Anchovy, unid. juvenile	1,571		580		1,503		**1,217.9**	**-**
Bat Ray			528		2,300		**942.7**	**-**
Striped Mullet	2,200						**733.3**	**-**
Bonefish					1,301		**433.7**	**-**
Topsmelt	119	3,454	430	1,746	217	1,428	**255.6**	**2,209.4**
Spotted Sand Bass		641		1,650	503	304	**167.7**	**865.0**
Slough Anchovy	158	235	57	1,108	257	341	**157.6**	**561.4**
Deepbody Anchovy	45		281	4	77		**134.3**	**1.4**
Shortfin Corvina	372	1,021		1,436			**124.0**	**819.0**
Diamond Turbot	56		180		73	150	**102.7**	**50.0**
Yellowfin Goby	22	3	53		1	3	**25.5**	**1.8**
Queenfish	14		8		36		**19.5**	**-**
California Halfbeak	9	7	8	9	18	28	**11.4**	**14.7**
Arrow Goby	5	1	11		10		**8.5**	**0.3**
Barred Pipefish	8	2	2				**3.2**	**0.5**
California Killifish	4	2	2				**2.0**	**0.6**
Bay Pipefish	1		2	1	1	0	**1.1**	**0.5**
Cheekspot Goby	1	1	1		1		**0.8**	**0.2**
Shadow Goby			1				**0.3**	**-**
California Needlefish				444			**-**	**148.0**
Total Biomass (g)	5,575	6,121	5,738	6,785	27,875	2,681	**13,062.5**	**5,195.4**
Mean Biomass (g/m2)	3.25	2.97	2.82	3.82	18.87	1.42	**8.3**	**2.7**

The mean biomass of all six hauls during the August 27, September 12, and September 29 sampling was 3.25 $\pm$ 1.16, 2.82 $\pm$ 3.13, and 5.95 $\pm$ 3.85 g/m^2, respectively. Variations in biomass were largely driven by the capture of round stingray, striped mullet, and bat ray.

Measurements of water quality parameters during the sampling in the discharge channel were as follows:

- August 27—temperature 26.9°C – DO 5.1 mg/l – salinity 35.8 ppt,
- September 12—temperature 26.9°C – DO 5.1 mg/l – salinity 36.1 ppt, and
- September 29—temperature 25.2°C – DO 5.5 mg/l – salinity 35.6 ppt.

DRAFT

3.4.4.2 Sweetwater River Channel

A total of 14 species, represented by a combined total of 3,701 fishes, was captured in the Sweetwater River channel (**Table 3.4-2**) (**Appendix J**), in a sampling area totaling 5,736 m^2 (61,741 ft^2). The most abundant fish was topsmelt, representing 65 percent of the total catch. The next most abundant fishes were slough anchovy (32 percent), followed by California halfbeak (2 percent). Less than 10 individuals of all other species comprised the remainder of the catch. Other species regularly captured included round stingray, California needlefish *Strongylura exilis*, bay pipefish, spotted sand bass, shortfin corvina *Cynoscion parvipinnis*, and yellowfin goby.

During each of the three sampling events, eleven, nine, and seven species were captured. Variation in the number of fishes caught during each event was driven primarily by the amount of topsmelt captured. Abundance of fishes for the August 27, September 12, and September 29 sampling was 1,583, 1,373, and 745 fishes, respectively (**Table 3.4-2**).

The total mean density (number of individuals/m^2) during the study was 0.65 $\pm$ 0.30 indiv/m^2 (**Table 3.4-2**). Mean density of all six hauls (3 large seine, 3 purse seine) during the August 27, September 12, and September 29 sampling was 0.77 $\pm$ 0.42, 0.77 $\pm$ 0.16, and 0.39 $\pm$ 0.15 indiv/m^2, respectively.

A total of 15.6 kg of fish was captured at this site during the study. The majority of the weight was attributable to topsmelt (43 percent). Other major contributors were spotted sand bass (17 percent), shortfin corvina (16 percent), slough anchovy (11 percent), and round stingray (10 percent).

The total mean biomass (g/m^2) in the Sweetwater River channel during the study was 2.73 $\pm$ 1.50 g/m^2 (**Table 3.4-2**). The mean biomass of all six hauls during the August 27, September 12, and September 29 sampling was 2.96 $\pm$ 1.64, 3.82 $\pm$ 1.06, and 1.42 $\pm$ 0.83 g/m^2, respectively. Variations in biomass were largely driven by the capture of slough anchovy, topsmelt, and spotted sand bass.

Measurements of water quality parameters during the sampling in Sweetwater River channel were as follows:

- August 27—temperature 25.4°C – DO 4.8 mg/l – salinity 34.0 ppt,
- September 12—temperature 24.3°C – DO 4.6 mg/l – salinity 32.6 ppt, and
- September 29—temperature 23.1°C – DO 6.2 mg/l – salinity 34.9 ppt.

3.4.4.3 SBPP Discharge Channel and Sweetwater River Channel Comparisons

A total of 20 species was caught in the SBPP discharge channel during this study, and 14 were caught in Sweetwater River (**Appendix J**). The seven species not found in

Sweetwater River were bat ray, California butterfly ray, queenfish, striped mullet, shadow goby, diamond turbot, and bonefish. All of these species except the bonefish are either known or expected to occur in the Sweetwater River channel with some regularity. The bonefish is a species typically distributed in warmer waters and regularly found only in the far southern portions of San Diego Bay around the SBPP. The only species found in Sweetwater River that was not observed in the discharge channel was California needlefish. This species has been captured within the discharge channel during prior fish studies (Merkel & Associates 2000a).

The SBPP discharge channel had considerably higher fish densities than Sweetwater River during each sampling, with a mean density over seven times that of Sweetwater River (**Figure 3.4-3**). The large numbers of juvenile anchovy captured in the discharge channel drove this disparity. Nearly three times as many adult anchovy were found in Sweetwater River than in the discharge channel, suggesting anchovy may move out of the channel as they mature, thus resulting in the demographics observed in the channel.

Mean biomass was higher in the discharge channel than in Sweetwater River during the first and third sampling, and slightly lower during the second sampling (**Figure 3.4-3**). Across all sampling events, mean biomass was three times higher in the discharge channel than in Sweetwater River. If the large California butterfly ray that accounted for over half the biomass in the channel is removed, the mean biomass in the channel was still greater than in Sweetwater River. Much of the mass was due to the round stingrays and bat rays that were much more abundant in the discharge channel, as well as the juvenile anchovies.

The notably large disparity in density between sites during the first (August 27) sampling contrasts with the biomass data, which are similar between the two sites. This is due to the capture of thousands of juvenile anchovy of very small weight (about 0.1g each) in the discharge channel during this sampling. Fish this small were not captured in the Sweetwater River. These observations of large numbers of small anchovies during the summer months suggest that the SPBB discharge channel may sustain a well-developed forage base of suitable type and size of fish for piscivorous birds. The small fish also provide abundant prey species for larger foraging fish. The regular capture of sub-adult fish suggests the area may provide a nursery area for some fish species.

Comparison of the water quality data at the two sites shows temperature and salinity to be slightly higher in the discharge channel at the time of sampling. Dissolved oxygen was slightly lower at the Sweetwater River site during the instantaneous sampling performed coincident with fish sampling. These parameters vary at both sites throughout each day, and these sites in general have similar temperature, DO, and salinity. This is confirmed not only by long-term monitoring, but also by the similar species composition at both sites.

3.4.4.4 SBPP Discharge Channel and Other Reference Site Comparisons

For the purposes of comparison of this study to other back-bay sites, data have been examined from single summer samplings at each of the reference sites. These sites are located in Anaheim Bay, Agua Hedionda Lagoon, and Batiquitos Lagoon.

The 1994 and 1995 Field Survey Report of the Ecological Resources of Agua Hedionda Lagoon (MEC 1995a) reported results including a fish survey of the east inner lagoon in July 1994. Water quality parameters measured during this survey included: temperature 24.7°C, DO 9.0–9.8 mg/l, and salinity 32.5 ppt. Sampling with a beam trawl and beach seine captured 16 species at a combined density of 2.12 indiv/m^2 (**Figure 3.4-4**). Catch was dominated by topsmelt and gobies. Biomass was not reported in the MEC study. Despite favorable water quality at the site, these fish indices all have values lower than those found in the SBPP discharge channel.

Data were examined from the Anaheim Bay Biological Monitoring Project – Final Report (MEC 1995b). The reference site was the station called Case Road in the Seal Beach National Wildlife Refuge. This site is a large tidal basin that was characterized as having late summer water quality parameters generally within the following range: temperature 22–25°C, DO 5.5–7.0 mg/l, and salinity 33.5–34.5 ppt. Seven species of fish were captured with a beach seine in September 1994. Topsmelt and anchovy dominated the catch. Mean density was 0.75 individuals/m^2 and mean biomass was 2.26 g/m^2 (**Figure 3.4-4**). These density and biomass values were much lower than those observed in the SBPP discharge channel. They are, however, similar to the results observed in Sweetwater River, suggesting this site selection can provide useful information as a reference site.

The results of the July 2003 fish sampling at Batiquitos Lagoon were reviewed for comparison (Merkel & Associates, in prep.). The station at the far-east end of the lagoon was sampled using purse seine and large seine. Water quality observations at the time of sampling measured: temperature 24.6°C, DO 3.3 mg/l, and salinity 31.8 ppt. A total of 17 species was captured at a density of 0.76 individual/m^2 and a biomass of 8.26 g/m^2 (**Figure 3.4-4**). Catch was also dominated by topsmelt and gobies. The small number of fish captured is reflected in the low density, however the capture of numerous round stingray yielded a high biomass. The species count and biomass were nearly the same as those in the discharge channel. The density was much lower due to much greater abundances in the discharge channel.

It is also useful to make broader, long-term comparisons between sites as well. The same reports discussed above were reviewed to find a total species count, density, and biomass for sampling conducted at the target station throughout the year and for the length of each study. Calculations generally include many sampling events over several years (**Table 3.4-3**). For comparison with the discharge channel, the results of the three-year study conducted in the SBPP discharge channel from 1997–2000 have been used.

The SBPP Cooling Water Discharge Channel Fish Community Characterization Study (Merkel & Associates 2000) included sampling for three years at two stations in the discharge channel. A total of 38 species was captured. The mean fish density for the study was 1.35 indiv/m^2 and mean biomass was 5.48 g/m^2. Samples were dominated in number by slough anchovy, which represented 91 percent of the individuals captured, and dominated in weight by sharks and rays.

The 2.5-year monitoring program at Anaheim Bay (MEC 1995b) reported a total of 33 species at Case Road (**Table 3.4-3**). The density of fish captured throughout the length of the study at this site was 0.40 indiv/m^2 and the biomass was 1.27 g/m^2. This site showed similar diversity as the SBPP discharge channel but had much lower fish density and biomass.

The 1994 and 1995 Field Survey Report of the Ecological Resources of Agua Hedionda Lagoon (MEC 1995a) reported a total of 17 species captured at the east inner lagoon station during the length of the study. Also reported was a mean density of 5.01 indiv/m^2. Biomass (g/m^2) was not reported. The high mean density is due to the capture of thousands of small juvenile topsmelt and juvenile gobies. With the exception of queenfish (present at Agua Hedionda Lagoon, but not in the discharge channel), the sampled community at Agua Hedionda Lagoon represents a subsample of the species found within the SBPP discharge channel.

An additional study that can be reviewed for comparison is the U.S. Navy Study conducted from 1994 through 1999 (Allen 1999). Samples collected at the southern station were intended to characterize the fish community of the south bay. Water quality fell within the following ranges during the sampling: temperature 15–26°C, DO 6.5–11 mg/l, and salinity 32.5–40 ppt. A total of 51 species was captured at this station. Individual station density and biomass figures were not reported, however density throughout San Diego Bay was reported to be 1.36 indiv/m^2 and a biomass of 2.03 g/m^2.

DRAFT

Table 3.4-3. List of fish species observed in long term studies at SBPP discharge and other southern California reference sites.

Common Name	Scientific Name	SBPP Discharge Channel 1997-2000*	South San Diego Bay 1994-99 *	Agua Hedionda 1994-95***	Anaheim Bay 1990-95+	Batiquitos Lagoon 1997-2001 ++
Gray smoothhound	*Mustelus californicus*	X	X	X	X	X
Brown smoothhound	*Mustelus henlei*					X
Leopard shark	*Triakis semifasciata*				X	
Shovelnose guitarfish	*Rhinobatos productus*	X	X			X
Bat ray	*Myliobatis californica*	X	X			X
Round stingray	*Urolophus halleri*	X	X		X	X
California butterfly ray	*Gymnura marmorata*	X	X	X		X
Diamond stingray	*Dasyatis dipterura*	X				
Bonefish	*Albula vulpes*	X	X			X
Pacific worm eel	*Myrophis vafer*					X
Threadfin shad	*Dorosoma petenense*	X	X			X
Pacific herring	*Clupea harengus*				X	X
Pacific sardine	*Sardinops sagax*	X	X		X	X
Northern anchovy	*Engraulis mordax*	X	X	X	X	X
Slough anchovy	*Anchoa delicatissima*	X	X		X	X
Deepbody anchovy	*Anchoa compressa*	X	X	X	X	X
California lizardfish	*Synodus lucioceps*		X			
Specklefin midshipman	*Porichthys myriaster*	X	X		X	
Plainfin midshipman	*Porichthys notatus*		X			
California needlefish	*Strongylura exilis*	X	X			X
California halfbeak	*Hyporhamphus rosae*	X	X			
California killifish	*Fundulus parvipinnis*	X	X	X	X	X
Topsmelt	*Atherinops affinis*	X	X	X	X	X
Jacksmelt	*Atherinopsis californiensis*		X			
California grunion	*Leuresthes tenuis*				X	X
Snubnose pipefish	*Bryx arctos*		X			
Bay pipefish	*Syngnathus leptorhynchus*	X	X		X	X
Barred pipefish	*Syngnathus auliscus*	X	X	X	X	X
Barcheek pipefish	*Syngnathus exilis*		X			
Kelp pipefish	*Syngnathus californiensis*		X			
Pacific seahorse	*Hippocampus ingens*		X			
Spotted scorpionfish	*Scorpaena guttata*		X			
Staghorn sculpin	*Leptocottus armatus*	X	X	X	X	X
Spotted sand bass	*Paralabrax maculatofasciatus*	X	X		X	X
Barred sand bass	*Paralabrax nebulifer*	X	X	X		X
Kelp bass	*Paralabrax clathratus*		X			
Salema	*Xenistius californiensis*		X			X
Sargo	*Anisotremus davidsonii*				X	X
Bigscale goatfish	*Pseudupeneus grandisquamis*	X				
Lookdown	*Selene vomer*	X				
Queenfish	*Seriphus politus*			X	X	X
White seabass	*Atractoscion nobilis*	X	X		X	X
California corbina	*Menticirrhus undulatus*		X			X
White croaker	*Genyonemus lineatus*				X	
Spotfin croaker	*Roncador stearnsii*	X	X			X
Yellowfin croaker	*Umbrina roncador*	X	X		X	X
Black croaker	*Cheilotrema saturnum*		X		X	
Shortfin corvina	*Cynoscion parvipinnis*	X	X			
Shiner surfperch	*Cymatogaster aggregata*	X	X	X		X
Striped mullet	*Mugil cephalus*	X	X		X	X
California barracuda	*Sphyraena argentea*				X	X

(table continued)

Table 3.4-3 *(continued).* List of fish species observed in long term studies at SBPP discharge and other southern California reference sites.

Common Name	Scientific Name	SBPP Discharge Channel 1997-2000*	South San Diego Bay 1994-99 **	Agua Hedionda 1994-95***	Anaheim Bay 1990-95+	Batiquitos Lagoon 1997-2001 ++
Blue bobo	*Polydactylus approximans*	X				
Bay blenny	*Hypsoblennius gentilis*		X			
Spotted kelpfish	*Gibbonsia elgans*		X			
Giant kelpfish	*Heterostichus rostratus*		X		X	
Longtail goby	*Gobionellus sagittula*	X				X
Longjaw mudsucker	*Gillichthys mirabilis*	X	X	X	X	X
Bay goby	*Lepidogobius lepidus*					X
Yellowfin goby	*Acanthogobius flavimanus*	X	X	X	X	X
Cheekspot goby	*Ilypnus gilberti*	X	X		X	X
Arrow goby	*Clevlandia ios*	X	X	X	X	X
Shadow goby	*Quietula y-cauda*	X	X	X	X	X
California halibut	*Paralichthys californicus*	X	X	X	X	X
Bigmouth sole	*Hippoglossina stomata*				X	
Fantail sole	*Xystreurys liolepis*		X			
Spotted turbot	*Pleuronichthys ritteri*		X			
Diamond turbot	*Hypsopsetta guttulata*	X	X	X	X	X
	Total species count	**38**	**51**	**17**	**33**	**42**
	Total density (individuals/m^2)	**1.35**	**1.36****	**5.01**	**0.40**	**0.51**
	Total biomass (g/m^2)	**5.48**	**2.03****	**NR**	**1.27**	**5.01**

* – SBPP Cooling Water Discharge Channel Fish Community Characterization Study, Merkel & Associates 2000.

** – Station 4 (South) from Fisheries Inventory and Utilization of San Diego Bay, 3rd Annual Report, CSU Northridge 1997 (density and biomass are bay-wide).

*** – East Inner Lagoon Station, from 1994 and 1995 Field Survey Report of the Ecological Resources of Agua Hedionda Lagoon, MEC Analytical Systems 1995.

+ – Case Road Station, from Anaheim Bay Biological Monitoring, MEC Analytical Systems 1995.

++ – Station 1 (east lagoon) from Long Term Monitoring and Pilot Vegetation for the Batiquitos Lagoon Enhancement Project, Merkel & Associates 2001.

NR – Not reported.

The greater number of fish species observed by Allen (2002) than found in the discharge channel in the present study is due principally to the greater area of San Diego Bay surveyed in his study. This larger area encompassed more diverse habitats capable of supporting a greater number of fish species. In addition, Allen identified more species of pipefishes and gobies than were identified in any of the other studies, including the SBPP discharge channel study. Variations in the species lists can often be accounted for by the treatment of fish groups where taxonomy is difficult and not well defined. Multiple species have overlapping characteristics that can lead to variations in species counts. These species are notoriously difficult to distinguish in field identifications and it is possible that misidentification of some fish played a role in either artificially depressing the species list in other studies or elevating that within the San Diego Bay-wide study.

To a large degree, the discharge channel features a fish community comprised of species very similar to the other back-bay sites examined. All species caught in the highest abundance at each of the reference sites were also caught in the discharge channel. A review of **Table 3.4-3** shows that all major guilds are represented in the discharge channel, and that gaps in the discharge channel species list fall within groups of fish represented by similar species occupying a similar niche. For example, white croaker were found in Anaheim Bay but not in the discharge channel. However, three other species of croakers did occur in the discharge channel.

The discharge channel is notable for its high abundance of elasmobranchs including stingray, bat ray, smoothhound sharks, butterfly ray, and guitarfish. These species are found in very high numbers in all but the warmest months of the year, when they likely move out into cooler portions of the bay. Juvenile anchovies and topsmelt likely provide a significant food source to the high concentrations of piscivorous birds known to frequent and/or nest near the discharge channel. These fish undoubtedly serve as a prey base for larger fish in the channel as well.

The discharge channel is a unique environment that shows some similarity to other back-bay environments, while also providing conditions that allow for unusual species occurrences, atypical juvenile abundances, and seasonal use patterns. The unique temperature environment of the channel may provide a warm water refuge area for several bay species during the winter, but may similarly preclude some species from full use of the area during the hottest portions of the summer months. The site provides a warm haven for fish and for green sea turtles in winter, as well as for interesting Panamic province species such as the diamond stingray, California halfbeak, California needlefish, bonefish, and shortfin corvina.

DRAFT

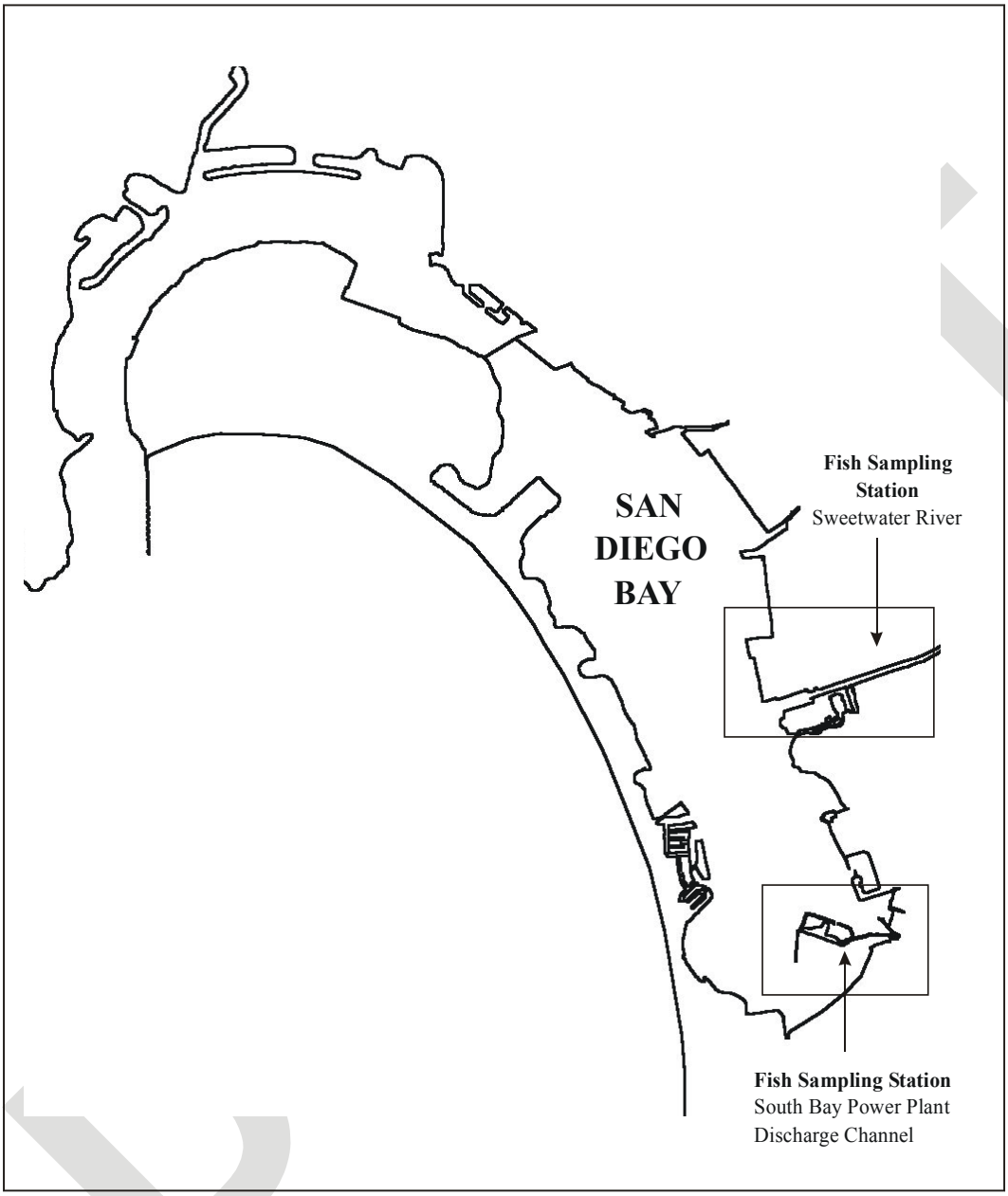

Figure 3.4-1. Location map of fish study sampling stations in San Diego Bay. Refer to Figure 3.4-2 for area detail.

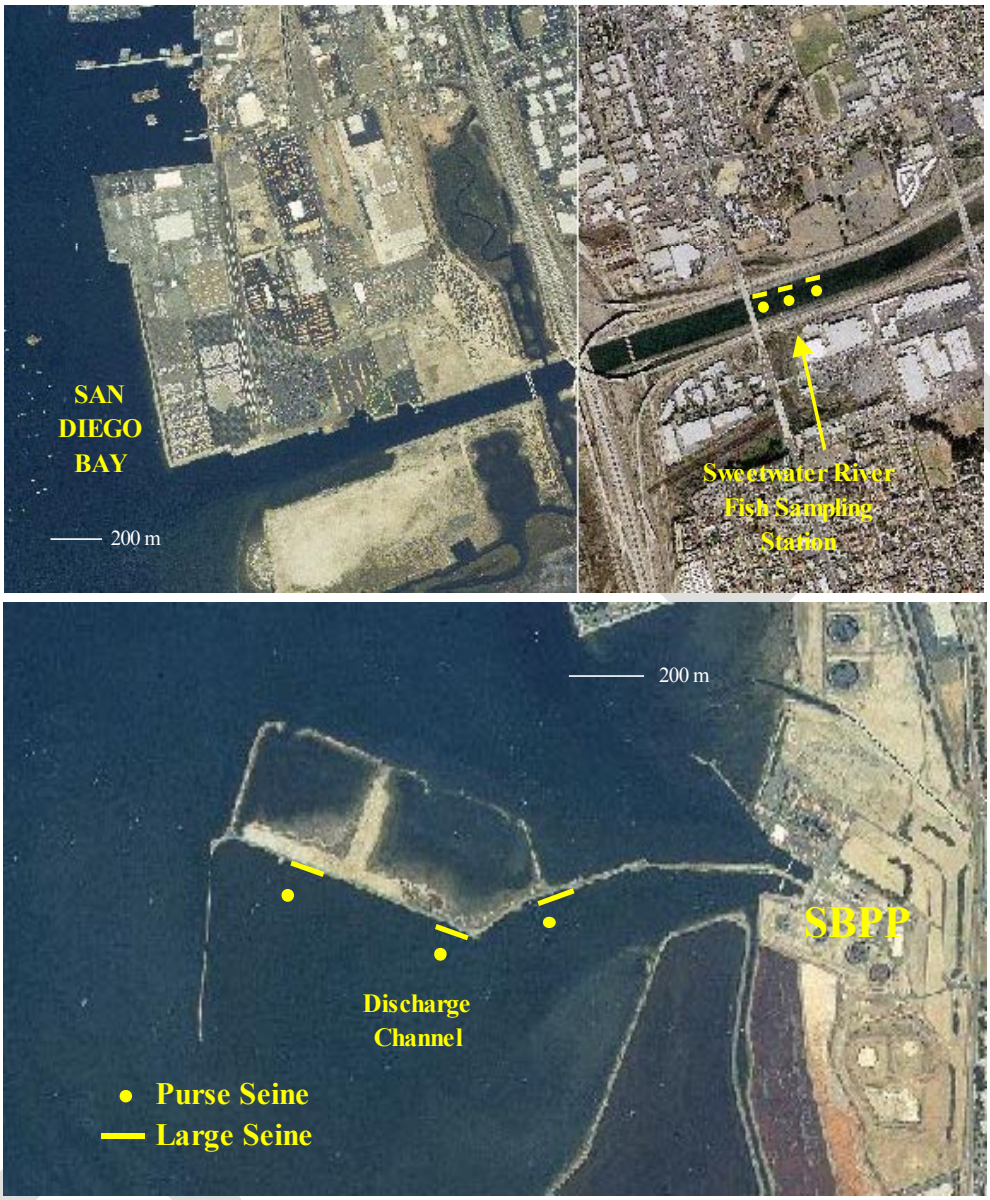

Figure 3.4-2. Fish study sampling stations in SBPP discharge channel and Sweetwater River channel.

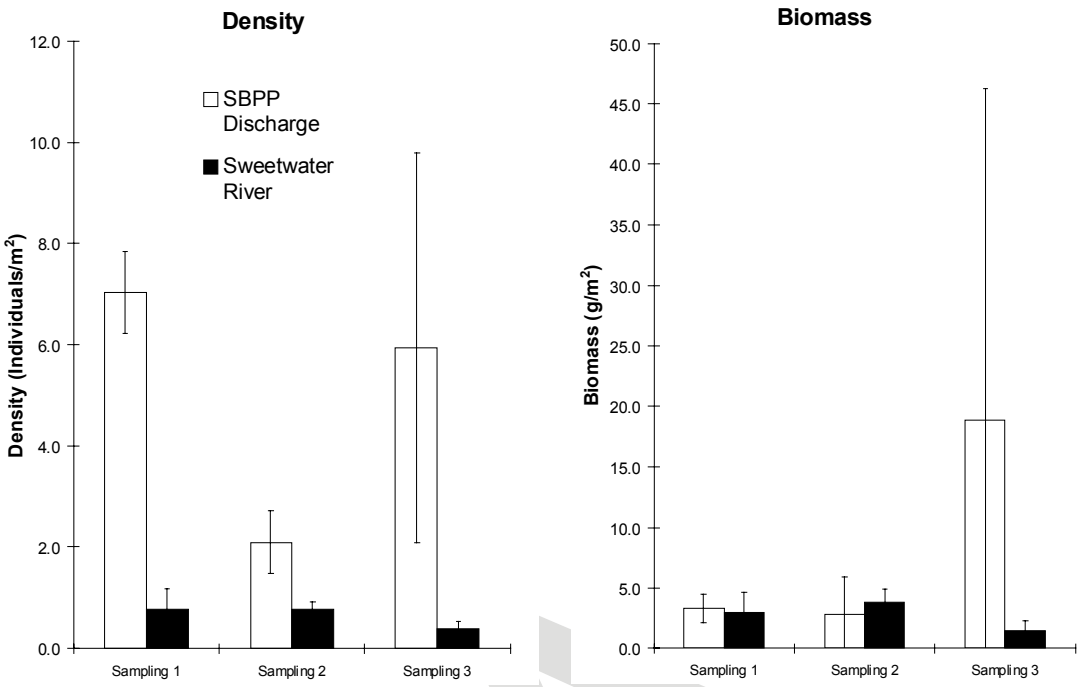

Figure 3.4-3. Density and biomass of fish caught in SBPP discharge channel and Sweetwater River during three sampling events, Summer 2003.

DRAFT

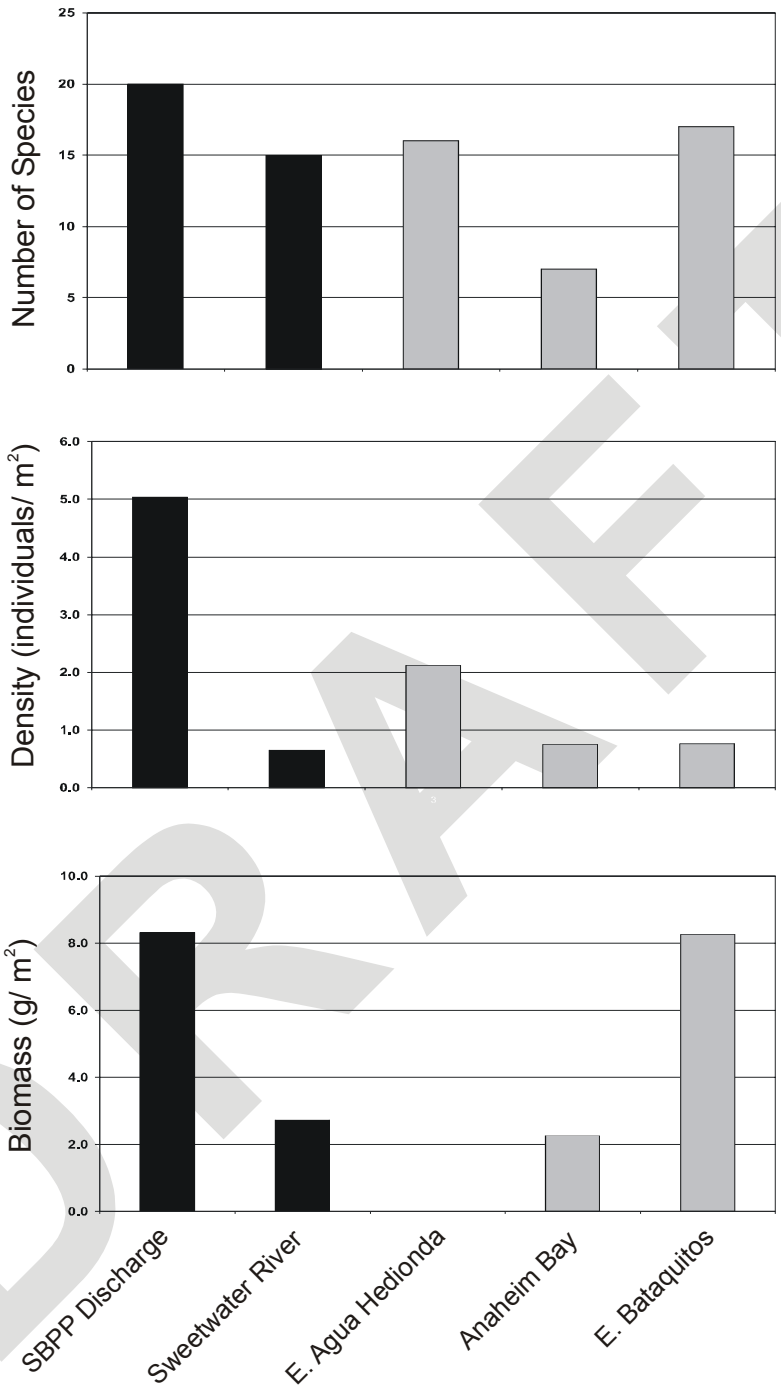

Figure 3.4-4. Number of fish species, density, and biomass at study sites and three reference sites. Agua Hedionda Lagoon data from July 1994 (MEC Analytical Systems 1995) (no biomass reported); Anaheim Bay data from Sept. 1994 (MEC Analytical Systems 1995); Batiquitos Lagoon data from July 2003 (Merkel & Associates 2003, unpublished data).

DRAFT

4.0 Integrated Discussion

4.1 Introduction

This integrated discussion is a synthesis of the physical and biological data that were collected during this study to address the objectives described in the introductory section. The following sections relate the study findings to the questions posed by the RWQCB. For eelgrass, this includes an explanation of the effects of increased temperature and turbidity associated with SBPP operation on the potential distribution of this habitat-forming plant in South Bay. The conclusions are derived from a complex modeling approach that predicted the response of eelgrass growth to various light regimes under simulated power plant operational modes.

Benthic invertebrate populations are discussed mainly in terms of the gradient of effects related to bottom temperatures in the discharge channel and the sediment quality that can affect infaunal composition. The conclusions are based on a combination of multivariate analysis, species distributions in relation to their distances from the SBPP discharge basin, variations in community measures such as diversity, species richness, biomass, and a calculated benthic pollution index for each sampling station.

Fish abundance and species composition in the discharge channel is described in relation to the dissolved oxygen characteristics of the receiving water, but also to discharge temperatures. This analysis combines existing data on fish resources with new data collected in this study. By comparing the physical characteristics and fish assemblages of several bays and estuaries in southern California, the fish assemblage of the SBPP discharge can be evaluated as to its trophic functions in the food web of the bay.

DRAFT

4.2 Eelgrass

Previous studies of controls on the distribution of eelgrass determined that light, not temperature, was the principal factor controlling eelgrass distribution within South Bay (Merkel & Associates 2000a). The Merkel & Associates (2000a) study determined that eelgrass beds were located in habitats that received greater photosynthetically active radiation (PAR) than similar habitats without eelgrass. It was also found that sites supporting eelgrass experienced both greater accumulated daily light levels and longer durations of photosynthesis-saturating irradiation. The study suggested that sediments re-suspended and transported by wind generated waves dictate the South Bay turbidity environment. Differential light attenuation and bathymetry control the amount of PAR reaching the bottom.

Accepting the basic conclusions from the Merkel & Associates (2000a) study that turbidity in the South Bay controls the ambient light environment and ultimately is the primary controlling factor to the distribution of eelgrass, the Regional Board has requested further information as follows:

- *Does the discharge volume and velocity from the SBPP contribute to the generation of turbidity due to disturbance of bottom sediments?*
- *Does the SBPP discharge move or redistribute the turbidity caused naturally by wave or wind action?*
- *What is the impact of the turbidity generated and redistributed by the SBPP on the survivability and distribution of eelgrass in South Bay?*
- *Does the combined impact of turbidity and temperature impact eelgrass distribution and survivability?*

Using the Board's questions to guide the discussion, the present section explores the relationships between the SBPP, turbidity, and combined turbidity/temperature and ultimately the distribution of eelgrass in South Bay.

The approach taken in the present study was to further develop and calibrate a numeric model to predict patterns of turbidity, light at depth, and ultimately eelgrass in the south Bay. Such linked physical and biological models have been employed at various times in prior efforts to explore the effects of changing environmental parameters on submerged aquatic vegetation (Smith 1976, Ward et al. 1984, Gallegos et al. 1990, Bach 1993, Miller and McPherson 1995, Pederson et al. 1995). By using this modeling approach, SBPP cooling water flows may be altered or eliminated within the model and the results evaluated. The drawback to this study approach is that numeric modeling of natural

systems is not an exact science, and conclusions must be cautiously interpreted as they provide insights but not evidence as to what affects may exist. However, given the inability to significantly alter the SBPP flows for extended periods to empirically assess effects of the SBPP on the parameters of interest, a modeling approach offers the best means to predict turbidity patterns and the amount of light available to eelgrass . Prior sections of this report have documented the recent and presently known distribution of eelgrass in the South Bay (**Section 3.2**), as well as the hydrodynamic, turbidity, and light environments of the South Bay (**Sections 2.5** and **2.6**). This section relies heavily on results within these prior sections.

4.2.1 SBPP Influence on Turbidity

South San Diego Bay spatial turbidity trends were consistent among sampling periods. Turbidity was generally low in the north and increased toward the south through the South Bay. Within the southern portion of the Bay, turbidity increased dramatically moving towards the east with the greatest turbidity being found to the southeast of the Chula Vista Wildlife Island (CVWI).

Results of bottom-shear modeling support the hypothesis that the SBPP does not contribute to the generation of turbidity in south San Diego Bay. Although the spatial distribution of turbidity appears correlated with the SBPP discharge channel, the generation of turbidity is almost exclusively explained by wind wave re-suspension of bottom sediments (**Figure 2.6-20**). The results of bottom-shear modeling combined with bottom-sediment characteristics suggest wind-driven waves account for most of the turbidity generated in the South Bay. Shallow portions of the South Bay occurring in areas with extended wind fetch are subjected to high levels of bottom shear. This is especially true where shallows occur beyond deeper upwind areas where wave environments can freely build. When areas of high bottom shear also contain sediments prone to suspension, a turbidity source is created. The shallow waters to the southeast of the CVWI are probably the single greatest source for turbidity in the southern portion of the South Bay. Long fetch distances from the west-southwest combine with non-cohesive, fine-grained sediments (silts) in shallow water to create turbidity in this portion of the South Bay.

Although the results of turbidity monitoring and modeling do not indicate the SBPP is a major source of turbidity, the SBPP cooling water flows do affect the distribution of turbidity in the South Bay. As indicated in **Figures 2.6-21** and **2.6-22**, changing cooling water flow rates results in changes to the turbidity environment within South Bay. The power plant cooling water flows contribute to South Bay turbidity distribution by drawing clearer waters southward along the deeper navigational channels on the eastern portion of the bay and expanding natural turbidity plumes along the western portion of

the South Bay. The power plant flows counteract tidal inflow into the far end of the Bay (SBPP discharge channel and adjacent waters) by filling the discharge channel via the SBPP cooling water system and thus limiting the tidal waters penetration from the west. Because the SBPP cooling water system generally draws clearer water from the north side of the discharge dike and discharges this clearer water to the southern side of the dike, the more turbid water that is generated on the shallow mudflats by wind wave re-suspension is ejected further out into the South Bay adjacent to the Chula Vista Wildlife Island. In addition, because the SBPP increases the rate of flow down the deeper navigation channels on the east side of the Bay, there is less extensive penetration onto the western shallows by clearer waters of the south-central ecoregion. This is evident in **Figures 2.6-20** and **2.6-21**.

The results of numeric hydrodynamic and turbidity modeling reject the hypothesis that the SBPP does not distribute turbidity created by the natural environment in the South Bay. Current and turbidity modeling support the idea that discharged cooling water from the SBPP plays an important role in the distribution of naturally generated turbidity in South Bay near the Chula Vista Wildlife Island.

4.2.2 SBPP Influence on Eelgrass Distribution

Turbidity causes a decrease in light available to photosynthetic organisms due to scattering and reflection of incident light by particulates in the water. In south San Diego Bay, eelgrass (*Zostera marina*) is the principal organism of concern in relation to primary productivity and habitat structure in the South Bay. Previous studies on eelgrass distribution in the South Bay indicated that light regime had predictive power in determining the presence of eelgrass in the greater South Bay ecoregion, whereas water temperature did not (Merkel & Associates 2000a). Unfortunately, the Merkel & Associates (2000a) study was not designed to explicitly explore the spatial relationship between light, temperature, and eelgrass abundance on a fine scale. Moreover, the study excluded the discharge channel under an assumption that the temperatures within this channel would exclude eelgrass irrespective of what light environment existed.

In the present study, eelgrass was mapped throughout most of the South Bay Ecoregion to compare the distribution of eelgrass to the turbidity environment, which was directly under investigation. Eelgrass was generally found to occur throughout much of the shallow-bottom habitats in South Bay where it had been observed in past surveys (see **Section 3.2**). The present and past eelgrass surveys have revealed the absence of eelgrass from a central portion of South Bay shallows, although the most recent survey located more extensive eelgrass within portions of this area than had been previously noted. Another interesting observation of eelgrass was that found in the SBPP discharge channel during the 2003 surveys. As discussed in **Section 3.2**, the occurrence of eelgrass within

this area has not been previously documented and was unexpected during the present survey since the summer temperatures within the discharge channel are generally too high to support eelgrass year-round. Because prior surveys have generally been conducted during late summer months, it is possible that the presence of eelgrass in this area is seasonal, much as eelgrass occurs within populations of the Sea of Cortez (Phillips 1990).

The power of turbidity and light measurements to predict eelgrass distribution was illustrated by mapping the number of hours for which regions of the South Bay experienced a favorable light environment for eelgrass at the canopy level. The photosynthetic saturation point is the amount of photosynthetically active radiation that results in the most efficient conversion of sunlight into plant energy. Radiation above saturation results in no further gain for the plant, whereas radiation below that level results in a decreased ratio of photosynthesis to respiration. The saturation point for *Z. marina* in California has been hypothesized to range between 50 and150 $\mu E/m^2/s$ (Zimmerman et al. 1990). Merkel & Associates (2000a) demonstrated that light demands for eelgrass in San Diego Bay were typically higher relative to eelgrass populations in more northern climates. This is not unexpected given longer day lengths during the growing season and higher sun angles than found at more northerly latitudes. The number of hours a portion of the South Bay is at or above the eelgrass saturation point (H_{sat}) is obtained from the photosynthetic saturation point, canopy depth, DAC, average surface PAR at noon, and applying the sinoidal relationship representing light levels throughout daylight hours (refer to Zimmerman et al. 1990, 1994). The H_{sat} formula used in this study is as follows:

$$Hsat = D \times \left[1 - \frac{2}{p} \left(\arcsin \frac{150}{I_z} \right) \right]$$

Where D is the available photoperiod in hours, 150 is the saturating PAR for *Z. marina* in South Bay, I_z is the maximum irradiance at depth z at noon using the 2003 average summer water surface irradiation at noon of 1,849 $\mu E/m^2/s$.

Applying the equations and relationships identified here and in **Section 3.6** and plotting the results analogously to the prior spatial modeling, maps of H_{sat} were obtained for the South Bay study area (**Figure 4.2-1**). This figure illustrates the interpolated H_{sat} results of field data collection based on the towed-transect derived DAC as discussed in **Section 3.6** compared to the numerical model based results with the SBPP operating at the 441 mgd (the average cooling water flows observed during the 2003 summer months). The results of the empirical interpolation and the numeric model are in agreement regarding H_{sat} and support the modeling approach.

The empirical interpolation of H_{sat} was used as a basis for evaluation of the distribution of 2003 eelgrass across hours of photosynthesis saturating PAR (**Figure 4.2-2)**. **Figure 4.2-2** illustrates the importance of hours of adequate saturating PAR in supporting eelgrass communities in the South Bay. From the charts, it is clear that most eelgrass in the bay occurs in regions receiving greater hours of saturating light per day. These visual results are strongly supported by the cumulative eelgrass plot, which shows the cumulative proportion of eelgrass cover as a function of the number of hours of saturating PAR and which suggests that a threshold of approximately 9.5 hours of H_{sat} in September is required for predictable eelgrass occurrence through the year.

Using the numeric model, the influence of SBPP cooling water flows on turbidity have already been demonstrated. Given the relationships between turbidity and H_{sat}, it is possible to evaluate the influence of SBPP flows on H_{sat} and ultimately eelgrass through the use of a threshold estimator of 9.5 hours in September at or above saturating PAR levels being required to support eelgrass growth. **Figure 4.2-3** illustrates the results of numeric model runs with differing cooling water flows to predict H_{sat}. The flow regimes employed in this figure are the same as those employed in **Figure 3.6-21** and include no cooling water flows, the 2003 average flows of 441 mgd, and the maximum operational limit of 601 mgd. The figure also includes an overlay of 2003-mapped eelgrass. The results of the modeling suggest a high degree of similarity exists between H_{sat} levels throughout most of the South Bay both with and without the SBPP flows. The modeling also predicts conditions where progressive reduction of cooling water flows increases H_{sat} levels and, where changes result in H_{sat} values exceeding 9.5 hours, the occurrence of new eelgrass beds is predicted.

Within **Figure 4.2-3** the greatest SBPP effects on H_{sat} are seen in the region of the bay immediately west of the CVWI. In this region, H_{sat} increases substantially with reduction or elimination of cooling water flows. Far less evident are increases and decreases in H_{sat} within the larger western and eastern portions of the Bay, respectively. These are identified by subtraction of the no cooling water flow condition from the respective cooling water flow conditions of 441 mgd and 601 mgd to generate the net effects of SBPP cooling water discharge on H_{sat} levels (**Figure 4.2-4**). The effects of changing cooling water discharge are also clear from a review of a plot of the areal extent of the South Bay as a function of H_{sat} (**Figure 4.2-5**). In this plot, the spike in area at zero hours accounts for deep channels while the relatively flat shallow South Bay bottom accounts for the lack of significant area at other low H_{sat} levels. The plot also illustrates the correlation between the field interpolation and numeric modeling approaches to determining H_{sat}.

The effect of the SBPP on H_{sat} can be traced directly to the discharge effects on turbidity distribution as discussed previously. However, the influence of H_{sat} on eelgrass distribution is not linear, but rather is dictated by threshold exceedance. While greater

durations of saturated photosynthesis generally impart increased stability and density to eelgrass beds, this level of prediction falls below the resolution of the present model. For this reason, only H_{sat} effects that alter values across the accumulated time threshold are considered to result in predictable changes in eelgrass habitat. To highlight the importance of the duration threshold, **Figure 4.2-3** employs a color change from browns to greens at this value. To further investigate the magnitude of difference in eelgrass predictions between the various flow regimes, those areas of the South Bay that are predicted to exceed an H_{sat} accumulation threshold were identified and plotted along with the extent of eelgrass mapped in 2003 (**Figure 4.2-6**). In addition, the areal extent of eelgrass coverage predicted under each condition was determined. The results of this analysis predict differing amounts of eelgrass based on power plant flows (**Table 4.2-1**).

Table 4.2-1. Numeric Model predictions of eelgrass areal coverage based on application of H_{sat} thresholds.

Condition	Predicted Eelgrass Coverage	
	Spring Tide	Neap Tide
2003 Surveyed Eelgrass	442.6 ha (1,093.7 ac)	442.6 ha (1,093.7 ac)
SBPP @ 601 mgd	454.1 ha (1,122.1 ac)	----
SBPP @ 441 mgd	467.1 ha (1,154.2 ac)	448.8 ha (1,109.0 ac)
No SBPP Flow	496.0 ha (1,225.6 ac)	----

Table 4.2-1 and **Figure 4.2-7** identify the predicted turbidity effects of the SBPP cooling water flows on eelgrass within South Bay. The predicted effects suggest that the SBPP, operating at maximum allowed cooling water circulation rate of 601 mgd, would preclude eelgrass from approximately 41.9 hectares (103.5 acres) of South Bay based on a spring tidal period analysis. At the mean summer 2003 operating conditions of 441 mgd, the SBPP is predicted to preclude eelgrass from approximately 28.9 hectares (71.4 acres) of the South Bay through its cooling water discharge effects on naturally generated turbidity based on a spring tidal period analysis.

Because the actual effects of the SBPP on turbidity distribution and ultimately H_{sat} are dependent on temporally variable tidal conditions as well as cooling water discharge volumes, it is not possible to predict the absolute effects of the SBPP on eelgrass distribution. To evaluate specific effects, variable flow rates would need to be modeled along with increased length of model runs. At the present time, this has not been done. However, to better assess the magnitude of the range of effects, a neap tide period was investigated at a static cooling water flow rate of 441 mgd (**Table 4.2-1**).

The combined effects of turbidity and heat are more difficult to address and are generally more ambiguously defined. The prior Merkel & Associates (2000a) investigation of temperature and turbidity focused on determining which of the two parameters (temperature or turbidity) was primarily responsible for the patterns of eelgrass distribution observed in the South Bay ecoregion. The study found no relationship between temperature and eelgrass, but strong relationships between PAR and eelgrass. However, this study was designed to explore eelgrass distribution patterns in the entirety of the South Bay ecoregion rather than eelgrass distribution patterns near the SBPP discharge. This was because concerns over potential SBPP effects on eelgrass focused on the absence of eelgrass through the central portion of the South Bay. The prior investigation dismissed the discharge channel as being unsuitable to support eelgrass due to high summer temperatures associated with cooling water discharge.

As discussed earlier in this section and in Section 3.2, the current 2003 survey found low-density eelgrass beds to the southeast of the CVWI within the SBPP discharge channel and more extensive beds to the west of the Wildlife Island than noted in prior surveys. Interestingly, this study found that although turbidity is high in this region, the shallow water results in a light regime that is adequate to support eelgrass. The presence of eelgrass in this area during the Spring 2003 surveys and the absence of eelgrass during summer 2003 field sampling and prior studies suggest that presence of eelgrass within the discharge channel and near field discharge plume is ephemeral but not restricted by the ambient light environment. This determination begs the question of what other factors may be contributing to the absence of eelgrass in this region. Prior reviews of aerial photographs pre-dating the operations of the SBPP suggest that eelgrass was absent from the extensive mudflats now described as the cooling water discharge channel. The prior presumption was that low light resulting from turbidity and perhaps elevated temperatures from solar heating may account for this absence. The present modeling effort suggests that light may not be a major factor restricting eelgrass from this area. The 2003 spring season occurrence of eelgrass within the discharge channel suggests that prior presumption that temperatures would preclude eelgrass within the discharge channel may also be an over simplification of the conditions of the discharge channel.

While neither turbidity, nor temperature individually account for the absence of eelgrass within the discharge channel, there may be synergistic effects of these two factors combined. This does not rule out the potential for other factors to also be involved, however, no other physical or biological factors are presently known that would be expected to control eelgrass distribution in this area. To evaluate the potential thermal contribution to eelgrass limitation in the South Bay, areas within the cooling water discharge plume (**Figures 2.6-13** through **2.6-16**) were examined to determine the extent to which eelgrass was predicted to occur based on H_{sat} but was not present in prior summer surveys. These areas include the cooling water discharge channel and portions of the South Bay west of the CVWI (**Figure 4.2-7**). Where the SBPP cooling water plume extends beyond the first persistent occurrence of eelgrass over prior summer

survey periods (**Section 3.2**), the effects of temperature were considered not to play a substantive role in dictating eelgrass dynamics. This area does not regularly exceed what has been considered to be preclusionary temperatures for eelgrass (see below). As such, it is possible that temperature stress combines with turbidity influences to limit eelgrass in these areas.

Within the proximate turbidity/thermal effects zones, the spring 2003 eelgrass survey detected 54.2 ha. (135.6 acres). Later in the summer of 2003, the eelgrass within the discharge channel was not detected; the status of eelgrass west of the CVWI was not documented. Based on the observations of eelgrass during spring, but not summer, and the absence of eelgrass during prior summer surveys, it is anticipated that eelgrass recruits to these regions of the South Bay but does not regularly persist through warmer summer months. Given the shallow bathymetry of flats within the discharge channel, natural solar warming of waters in this area may also inhibit eelgrass growth and survival.

The nature of eelgrass within the near-field turbidity/thermal effects zones is not dissimilar to that of other areas including the Sea of Cortez where eelgrass has adopted a truly annual strategy with summer season die-off. Zimmerman et al. (1990) notes that high temperatures may stress plants and thus influence the hours of H_{sat} required to sustain eelgrass. Numerous authors have noted that high temperatures can restrict the occurrence of eelgrass and can influence the species metabolism (Biebl and McRoy 1971, Marsh et al. 1986, Bulthuis 1987, Masini et al. 1995) or can lead to un-seasonal diebacks (Phillips and Backman 1983, Phillips 1984). Although relatively high thermal tolerances have been reported for eelgrass (30ºC Setchell 1929, 27-40ºC – Phillips 1974, 27.5-34ºC – Penhale 1977, 24-32ºC – Phillips and Backman 1983, and 30-35ºC – Wetzel and Penhale 1983), several studies have noted that photosynthetic capacity of plants is strongly influenced by temperature due to increased reaction rates, and most particularly reaction rates in the dark reaction of photosynthesis. Bulthuis (1987) noted temperature optima for photosynthesis has been reported in the 30-35ºC range. However, Marsh et al. (1986) pointed out that optimal temperatures for photosynthesis are not necessarily the same as those required for whole-plant growth. Given that increased temperature also results in increased respiratory demand, the optimal range for whole-plant growth typically occurs at lower temperatures than for gross photosynthesis. Thus, plants may grow better at lower temperatures, even though they are less efficient at photosynthesis. In field studies in North Carolina estuaries, Penhale (1977) found eelgrass growth rates to be higher in 15ºC water than at higher temperatures of 22ºC and 29ºC. At 29ºC Penhale noted a decline in eelgrass biomass.

The relationships between photosynthesis, respiration, and optimal carbon uptake are complex. However, relative consistency in the literature persists regarding photosynthetic optima and plant response to short and long-term high temperature exposures. Many authors (Biebl and McRoy 1971, Drew 1979, Bulthuis 1983, and

Marsh et al. 1986) have noted that respiration rates continue to climb with increasing temperatures above 30ºC while photosynthetic activity begins to decline somewhere between 30ºC and 40ºC. At extreme temperatures, eelgrass respiratory demand may exceed photosynthesis and plants will experience a negative growth condition (Dennison et al. 1993). While these conditions can clearly lead to an adverse impact on eelgrass if prolonged, Marsh (1986) notes that seagrasses go through a rapid temperature equilibration with the ambient water and respond accordingly to short-term temperature changes. Thus short-term exposures to high temperatures tend not to result in mortality from heat stress, but rather a condition of negative growth that, if prolonged, may ultimately result in mortality.

Within the near-field environment of the SBPP, the non-summer temperatures fall below the extreme temperatures expressed as limiting in various studies on thermal stress in eelgrass. In prior deployed-instrument investigations, Stations 5A (in eelgrass) and 5B (outside of eelgrass), occurring to the west of the discharge channel and occurring near the boundary of the near-field turbidity/thermal effects zones, exceeded average weekly temperatures above 28ºC during the summers of 1997 and 1998 without loss of eelgrass at Station 5A (Merkel & Associates 2000a). These stations were the warmest stations employed in the 2000 study. While the average temperatures at Station 5A and 5B differed by less than 0.5°C, the present numeric model suggests that Station 5B occurs within more direct influence of the turbidity plume influenced by power plant flows. As a result, the region where Station 5B was located is predicted to receive fewer hours of saturated photosynthesis. With lower values of H_{sat} being received at Station 5B than at Station 5A, it is believed that similar respiratory demands were not being similarly balanced by photosynthesis. At lower temperatures, the respiratory demand of eelgrass would be reduced and it is anticipated that adequate H_{sat} would be achieved within the near-field turbidity/thermal effects zones.

The present studies offer unique insight into the role of the SBPP in the distribution and dynamics of eelgrass habitat within South Bay. Because turbidity is generated by winds on a year-round basis, the effects of the SBPP cooling water flows on H_{sat} are expected to track the long-term mean flows. The resultant impacts to eelgrass would be expected to be greatest during the winter months when light levels are normally low and day-lengths are shortest. Within the near-field influence of the SBPP cooling water discharge, it is anticipated that summer temperature plays a role in limiting the extent of eelgrass, either on an on-going or intermittent basis.

The prior conclusions that areas within the defined discharge channel are wholly unsuitable to support eelgrass due to high temperatures have been called into question by the spring 2003 occurrence of eelgrass in this area. At least portions of the discharge channel appear to be capable of supporting eelgrass for portions of the year. The cumulative conclusions derived from the present and prior Merkel & Associates (2000a) study indicate that while turbidity plays the primary role in dictating the distribution of

eelgrass in South Bay, the SBPP plays a role in distributing naturally generated turbidity and thus, influencing the distribution of eelgrass. Further, the two studies suggest that there are collective effects of turbidity and temperature within near-field portions of the thermal plume of the SBPP. These effects may result in either an absence of eelgrass, or seasonal die-off or die-back of eelgrass. In the area of the discharge channel nearest the SBPP, it is still believed that summer season discharge temperatures alone may limit the occurrence of eelgrass, and turbidity may not be a significant factor in structuring eelgrass habitat within these areas.

Comparisons of H_{sat} (Field vs. Model)

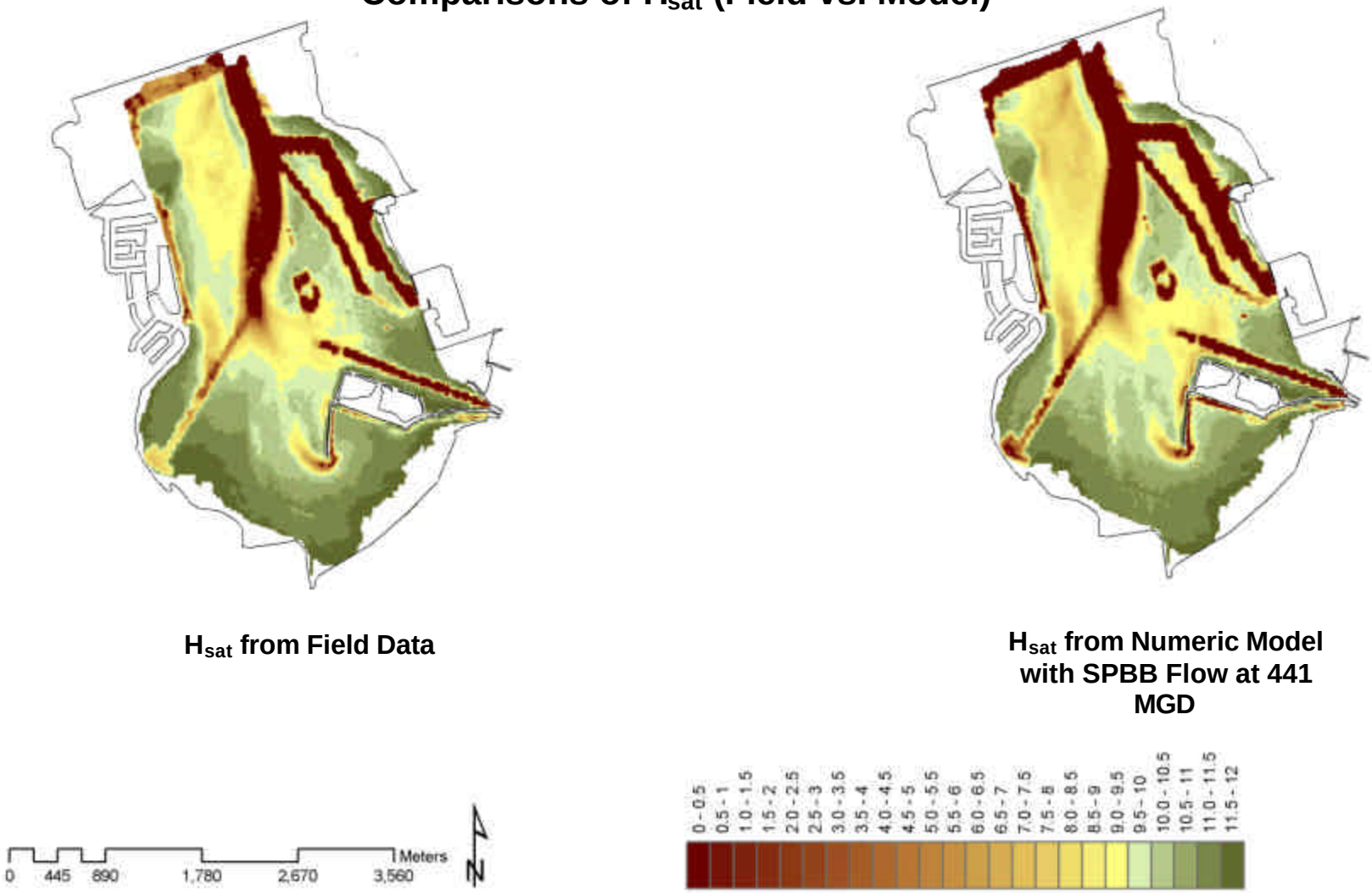

Figure 4.2-1. Calculated hours of saturating PAR received (H_{sat}) from field collected turbidity data (left) and numerically modeled turbidity (right) for South San Diego Bay, summer 2003.

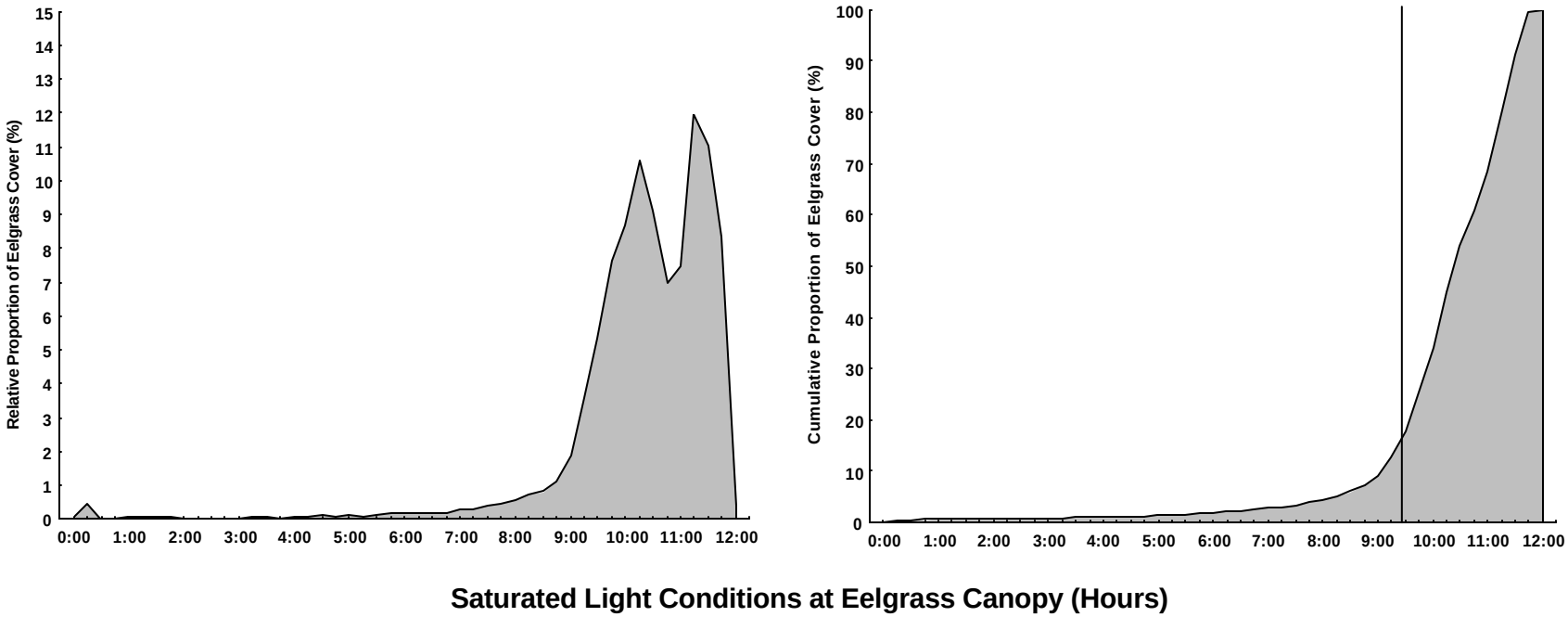

Figure 4.2-2. Relative proportion of eelgrass cover (left) and cumulative proportion cover (right) for South San Diego Bay expressed as a function of the number of hours of saturating PAR received. Vertical bar represents a predicted 9.5-hour threshold of saturating PAR required for *Z. marina* growth in South San Diego Bay.

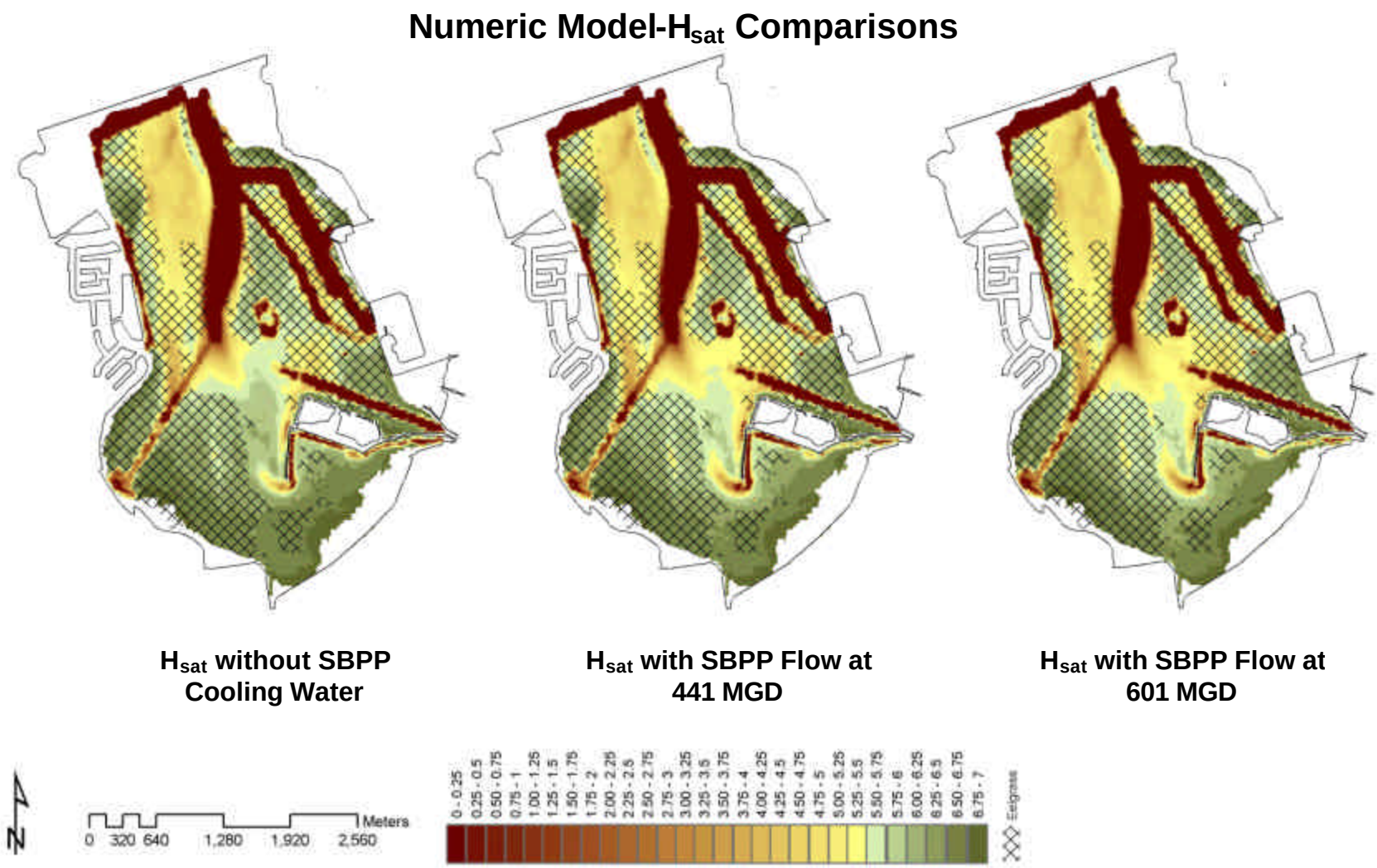

Figure 4.2-3. Numeric model of H_{sat} without SBPP cooling water (left), with SBPP cooling water flow of 441 mgd (middle), and with SBPP cooling water flow at 601 mgd (right). Data derived from model runs of average turbidity (NTU) during a 72-hour spring tidal cycle. Cross-hatched area represents mapped eelgrass, summer 2003.

Numeric Model-H_{sat} Comparisons

Net H_{sat} Effect of SBPP with Flow at 441 mgd

Net H_{sat} Effect of SBPP with Flow at 601 mgd

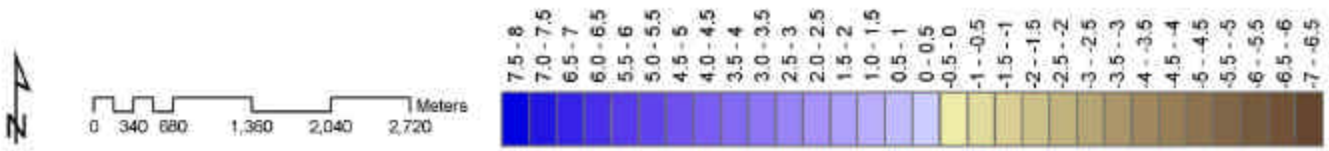

Figure 4.2-4. Numeric model of net effect of 441 mgd cooling water flow versus no SBPP cooling flow (left), and 601 mgd cooling flow versus no SBPP cooling flow (right). Net H_{sat} values derived from model runs of average turbidity (NTU) during a 72-hour spring tidal cycle.

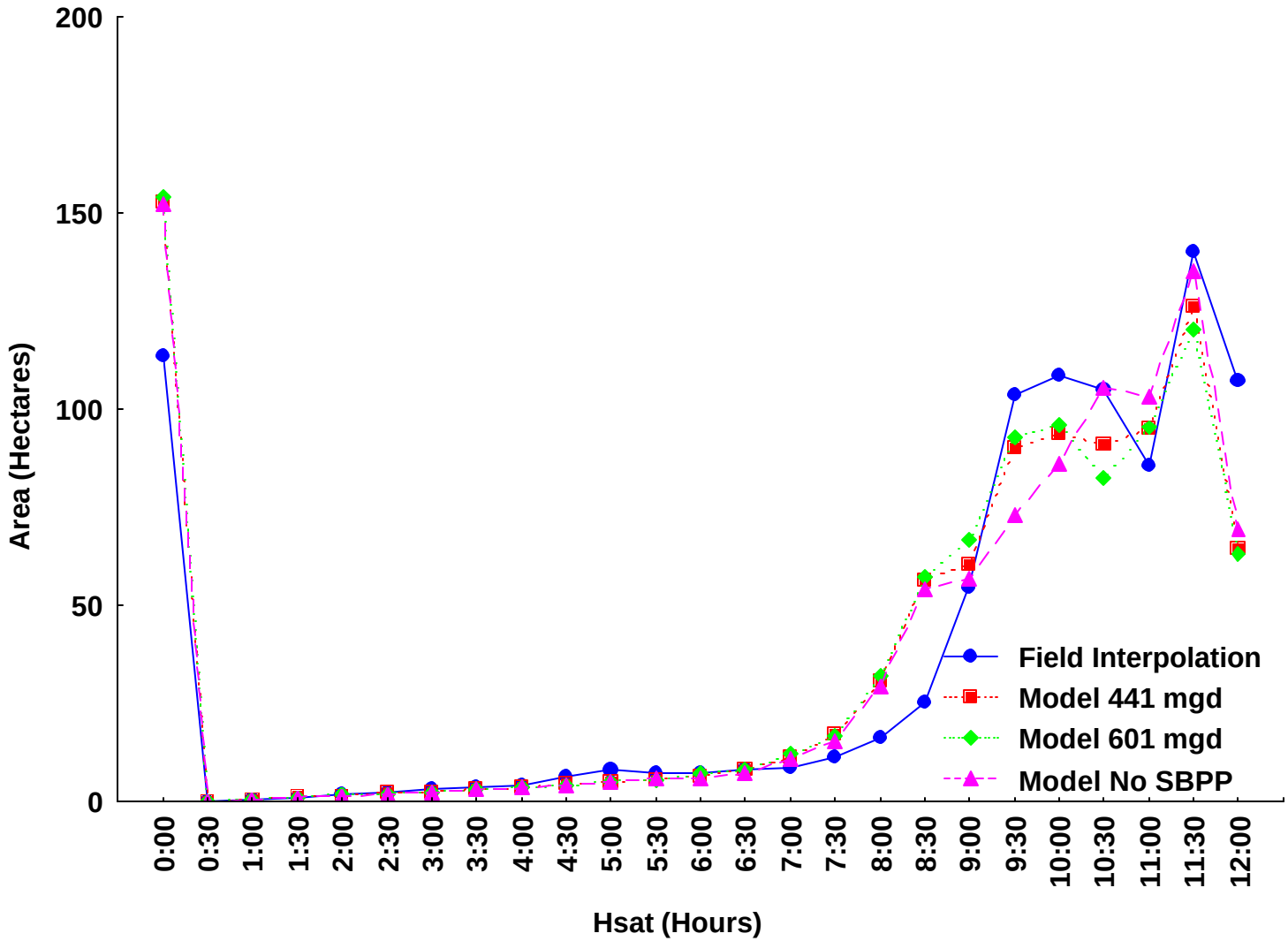

Figure 4.2-5. Plot of bay area by hours of photosynthesis saturating PAR received at the eelgrass canopy level for the field interpolated data, and the numerical model with SBPP cooling water flows at 441 mgd, 601, mgd, and 0 mgd.

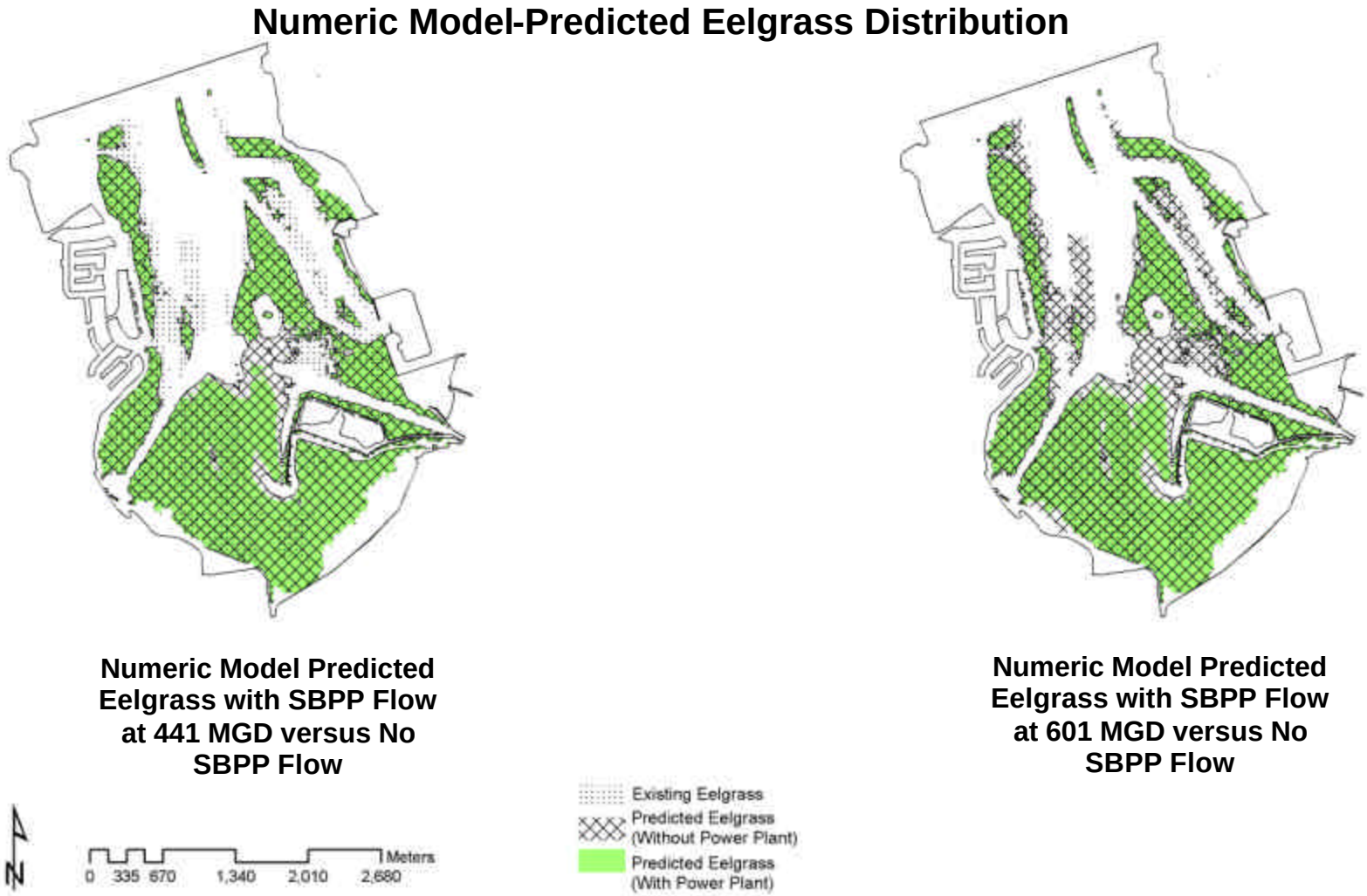

Figure 4.2-6. Predicted eelgrass distribution for south San Diego Bay with SBPP running at 441 mgd (left) and 601 mgd (right). Both figures include predicted eelgrass distribution without the effect of the SBPP (hatched area), and observed eelgrass, summer 2003 (stippled area).

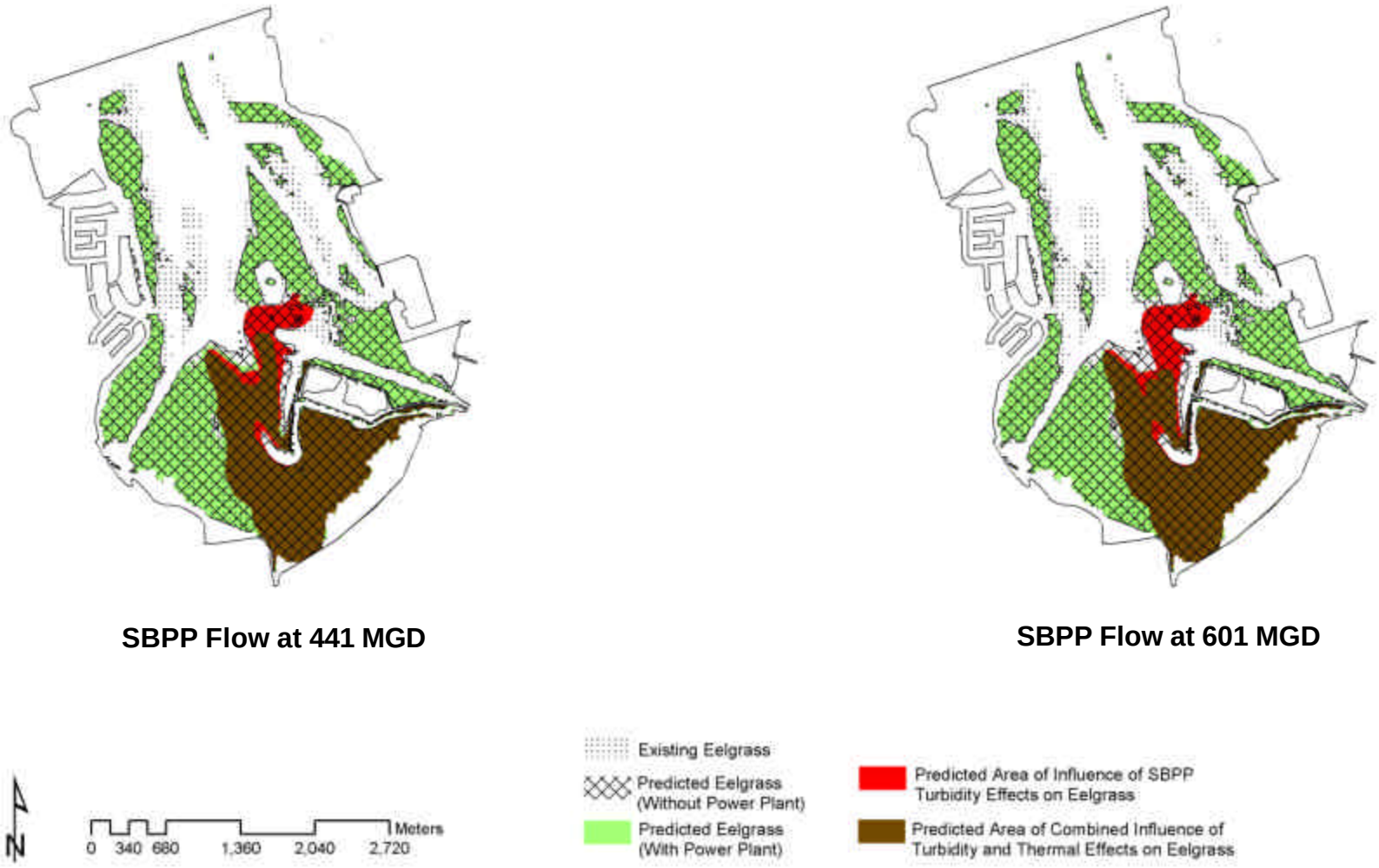

Figure 4.2-7. Predicted effects of temperature and turbidity on the distribution of eelgrass in south San Diego Bay with the SBPP cooling water flow at 441 mgd (left) and 601 mgd (right).

4.3 Benthic Invertebrates

Earlier studies concluded that the existing elevated-temperature cooling water discharged from SBPP had caused no prior appreciable harm to the aquatic biological community of San Diego Bay or to the beneficial uses of those waters (Ford et al. 1973). However, the study also concluded that the discharge did have adverse effects on the benthic invertebrate community within the discharge channel. The effects appeared to be seasonal and related mainly to temperature distribution because several species tended to become established progressively closer to the source of the thermal effluent as temperatures declined from summer highs to lows in winter and spring. A subsequent data review of annual summer benthic studies conducted between 1977 and 1993 concluded that no appreciable long-term upward or downward trends in species diversity or abundance had occurred within the discharge channel (Ogden 1994).

The studies described in Section 3.3–*Benthic Invertebrates* were done in July, August and September 2003 to include the period when biota experience the greatest heat stress in South Bay. Based on earlier studies of infaunal distributions, it was reasoned that any temperature-related effects of the discharge would be greatest at that time of the year, including any lag time in responses, thus defining the maximum spatial extent of effects on infaunal invertebrates. The analysis approach was to classify the sampled stations based on similarity of their infaunal composition to test the hypothesis that discharge and reference stations differed at the community level. These included multivariate tests with all taxa and comparisons of community attributes such as diversity and species richness at each station. A benthic response index (BRI) (SCCWRP 2003) was also calculated that classified the samples based on the abundances of known pollution-tolerant indicator species. Community faunal differences were examined more closely within the discharge channel to describe any gradient of effects that may have been correlated with proximity to the discharge. Densities of some of the more abundant individual taxa at each station were also examined for patterns related to the discharge. Finally, a multivariate analysis was used to identify the relative effects of temperature and sediment grain size composition on benthic community composition and to examine the grouping of stations in relation to these physical and biological variables.

4.3.1 Discrimination of Discharge and Reference Assemblages

Compared to the earlier monitoring studies conducted from 1977–1993, this study provided a more complete description of benthic communities in South Bay during the warmest months of the year. In addition to the core group of 11 monitoring stations sampled in previous years, we included 10 additional subtidal and 10 additional intertidal stations. In the August 2003 survey we identified a total of 141 taxa compared to an

average of 79.7 taxa per survey during the previous 17 annual monitoring efforts (Ogden 1994). This was largely due to improved spatial coverage and was expected based on species-area accumulation curves. By increasing the spatial coverage within the discharge zone, we were able to describe response gradients using both univariate and multivariate statistical techniques.

Reference and discharge infaunal communities had many taxa in common, but their relative abundances were substantially different, and this was revealed by the MDS analysis. The inner discharge station, SE7, (see map **Figure 2.3-1b**), had a higher number of taxa (46) than the average (38) of all stations in August but the assemblage was dominated by a few taxa including the small non-native mussel *Musculista senhousia*, the polychaetes *Capitella capitata* and *Streblospio benedicti*, nematodes, and oligochaetes. The relative abundances of these five taxa at Station ST2 located 369 m (1,299 ft) from the discharge, and other stations farther from the discharge were within the range of values at the reference stations, but the higher absolute abundance of the faunal group at the discharge distinguished it from the same grouping at both reference and transition station groups. The SIMPER species analysis showed that a large number of taxa contributed to within-group differences at the reference stations, and that small shifts in the abundances of a few species would affect the MDS results and the relationship among of the stations. These types of shifts in abundance would be expected in a diverse infaunal community. This is contrasted with the stations closest to the discharge that typically were dominated by a few species adapted to the more varied environmental conditions near the discharge, which may change to a lesser degree over short time periods.

Discharge and reference stations differed only minimally in terms of the benthic response index (BRI) analysis, which categorizes stations based on the relative abundances of pollution tolerant taxa. The discharge stations tended towards a higher pollution grouping than the reference stations due to the high pollution tolerance scores of *Musculista*, *Capitella*, and *Streblospio*. Some reference stations, however, actually had higher BRIs than discharge stations. This was not unexpected since the index was not specifically developed to identify benthic responses to thermal stress but responses to chemical pollutant loadings. For example, one common species with a high pollution tolerance score, the polychaete *Leitoscoplos pugettensis*, was significantly more abundant at reference stations than discharge stations, demonstrating that the BRI analysis was not an effective approach to differentiating potentially polluted sites within a thermal gradient.

The subtidal discharge stations as a group had the lowest taxa diversity, but some individual stations in the discharge channel were actually more diverse and had a greater total number of taxa than some individual reference stations. Benthic communities are typically very patchy, and some of these differences are due to the inherent variation within stations that is expected in a fine-scale faunal distribution study. Similar variation

among far-field sites and near-field sites was observed in a previous analysis of benthic communities in South Bay (Ogden 1994), although that study also concluded that the two discharge channel stations (E7 and E5) had faunal assemblages that differentiated them from the far-field station group.

For intertidal stations, the analysis of August and September surveys shows that the biological communities at Stations T1, T2, and T3 closest to the discharge had a close faunal similarity that was different from either the discharge Stations T4 and T5, or the reference stations. This was especially evident from our analyses of the September survey. Similarity analysis of August and September data showed that the reference stations clustered together and were distinct from the discharge stations. Some taxa were unique to either the discharge or reference stations which contributed to the cluster separation of the two groups. Earlier studies (Ford et al. 1973, Ogden 1994) did not include intertidal stations in their analyses. In this study it was expected that the intertidal fauna, although not as diverse as the subtidal fauna, would be a good response indicator because of the greater temperature fluctuations that occur at intertidal sites compared to subtidal sites.

4.3.2 Discharge Effects Gradients

The differences in the biological assemblages among the discharge channel stations did not occur along a linear gradient with increasing distance from the discharge, but rather segregated into two groups of stations consistent with the pattern of variation for the physical variables. Stations T1, T2, T3, and E7 are all located inside the small point on the southern boundary of the CVWI and have the most frequent and warmest exposure. The other stations are all located beyond this point and receive reduced plume exposure. A gradient of biological change is evident within this group of stations. The discharge stations that receive reduced plume contact are more similar to the other stations closer to the discharge, than the reference stations further away. Considered separately, none of the community parameters such as diversity or species richness showed a consistent linear gradient with proximity to the discharge even though as a group the discharge stations showed a trend toward reduced diversity and species richness.

Total biomass per station was highly variable largely due to high densities of the mussel *Musculista senhousia* at several stations, including Station E7 closest to the discharge, and therefore no conclusions could be drawn concerning discharge effects on total biomass. The biomass of individual phyletic groups was also generally not abundant enough or too variable to draw any conclusions about discharge effects, except that polychaete biomass did show a gradual reduction as a function of proximity to the discharge. This occurred despite high densities of *Capitella* at Station E7, but most of these individuals were small compared to larger species such as *Mediomastus* that were

characteristic of the transition and reference stations. An earlier review of a 17-year time series of benthic monitoring studies (Ogden 1994) concluded that there were no trends in biomass attributable to the discharge. However, Ford et al. (1973) found that for almost all groups of organisms, except oligochaetes and phoronids, biomass was lower in the discharge channel than at references stations. Given the inherently high variation in this measure, it is understandable why these conclusions differed.

Some individual species showed clear gradients in abundance relative to the discharge although most did not. During the September 2003 survey, for example, *Capitella* and *Acteocina* increased almost exponentially near the discharge whereas the tanaid crustacean *Leptochelia* and the polychaete *Scoloplos acmeceps* declined at intertidal stations close to the discharge. The more typical response for taxa that had clear differences in overall abundance between discharge and reference stations was not a linear increase or decrease between adjacent stations, but it was a variable response in abundances that produced trends among groups of stations. Several taxa had maximum abundances at the inner discharge stations, and at the same time exhibited depressed abundances at Station E7 closest to the discharge and at reference stations outside of the discharge channel. This suggests that some populations were responding to an area of preferred environmental conditions in the discharge channel that was defined by elevated temperatures closest to the discharge and cooler temperatures in reference areas away from the discharge.

4.3.3 Faunal Associations with Physical Factors

Sediment grain size, sediment (bottom) temperature, and depth were measured at each benthic collection station, and dissolved oxygen characteristics were measured at several intermediate stations. All intertidal stations were positioned at the (+0.3 m) (+1.0 ft) MLLW elevation and subtidal stations were all less than 4.3 m (13.9 ft) deep. Because all subtidal stations were relatively shallow, this was not considered to be a significant variable that would influence assemblages, especially in the typically calm bay environment. Sediment grain size is known to correlate with assemblage attributes under natural conditions, with finer particle sizes associated with higher organic content and a greater diversity of deposit feeding and suspension feeding taxa. In the analysis, the silt/clay size fraction was used as the tested variable because differences in this fraction tend to exert a greater influence over assemblage composition than coarser fractions. Several measures of temperature were used (mean, standard deviation, range, and maximum) to test the relationship between assemblage attributes and water temperature. Dissolved oxygen was not found to be a limiting factor for fish assemblages in the discharge channel and DO concentrations would also not be a factor limiting the distributions of invertebrate species.

The principal component analysis results showed that temperature was by far the most important variable affecting biological differences among both subtidal and intertidal stations. Sample distances based on average temperature resulted in a statistically significant ($p>0.01$) rank correlation of 61 percent with the Bray-Curtis distances for the biotic data. The subsets of variables that provided the highest correlations with the biological data did not include the variable for percent silt-clay. This finding was consistent with the earlier analysis of relationships between several physical variables and infaunal data by Ogden (1994) that concluded temperature exposure was the single most important variable controlling the infaunal distributions in the SBPP discharge channel. That analysis also found that factors such as grain size and sediment organics, which typically exert major influence on assemblage structure, were only weakly correlated with faunal distributions where temperatures varied widely among sites. An analysis of SBPP benthic data from 1977 through 1980 by LES (1981) attributed a greater effect on benthic structure to sediment composition than temperature. We found that only one of the species that was abundant in the discharge channel, the polychaete *Capitella capitata*, had a statistically significant positive correlation with silt/clay sediment fractions and that the majority of taxa distributions were related to temperature differences, not sediment composition. In the present study we found that differences up to 8.3°C (15°F) sometimes occurred between inner discharge stations and reference stations during plant operation, and absolute temperatures at near-field stations could reach 37°C (98.6°F) for short periods of time. Mean temperatures, of course, were much lower, but the fact that assemblages were exposed to an intermittent regime that included physiological stressful periods of high temperature may explain why many taxa were unable to colonize the discharge channel habitat.

General conclusions from earlier studies (Ogden 1994) concerning the importance of temperature in defining assemblages were substantiated in this study, although several of the specific conclusions regarding temperature responses of individual taxa differed between the two studies. Based on regression analysis, Ogden (1994) found a significant positive relationship between temperature and infaunal density (i.e., taxa increased in abundance as temperatures increased) for the following taxa: *Armandia, Capitella, Marphysa, Neanthes*, *Streblospio*, Oligochaeta, and *Paracereis*. From this list, *Capitella*, *Streblospio* and Oligochaeta showed a significant positive relationship with temperature in the present study and *Paracereis* had a negative relationship. The other taxa were not abundant enough to draw any conclusions about their relationship to temperature. The earlier study identified significant negative relationships between temperature and infaunal density (i.e., taxa decreased in abundance as temperatures increased) for the following taxa: *Leitoscoloplos, Mayerella, Acteocina* (*Cylichnella*), *Solen, Tagelus*, and Phoronida. Of these taxa, the present analysis confirmed that only *Leitoscoloplos* followed this relationship between temperature and abundance, with *Tagelus, Acteocina* (*Cylichnella*), and Phoronida showing a statistically significant opposite response. The distributions of *Solen* and *Mayerella* had no significant relationship to temperature. The

present study also identified other positive and negative relationships between temperature and faunal abundances that were not seen in the earlier studies. The differences between the results in the two studies was probably due to the lack of spatial resolution within the discharge zone in the earlier study which was unable to measure infaunal densities where the greatest temperature changes occurred. The weighting of the station array in far-field and reference areas in the Ogden (1994) analysis masked the relationship between temperature and faunal distributions, or in some cases, yielded contradictory results. By increasing the number of stations from 11 to 21, we could delineate temperature-faunal relationships for some taxa more accurately than in the previous study design.

The segregation of the inner intertidal Stations T1, T2, and T3 from Stations T4 and T5, which was particularly evident in the intertidal MDS analysis for September 2003, may be partially explained by the location of Stations T4 and T5 beyond the small point on the southern boundary of the CVWI. This point partially deflects the discharge plume away from these stations (see **Figure 2.5-9**), reducing the period of time they are exposed to the plume. Temperature records confirm that there was a small but noticeable break at this point where temperatures were lower than on the eastern side (see **Figures 2.3-3** and **2.3-9**). Some of the differences may also be explained by the sediment composition that had a higher silt/clay fraction at the three inner stations than at the outer discharge and reference stations.

In an earlier analysis (Ogden 1994), it was speculated that the configuration of the separation dike of CVWI and the outflow currents of the discharge would create flow conditions in the discharge embayment that would restrict colonization by some species with planktonic larvae and favor species with non-planktonic larvae. This idea, however, was based on an incomplete understanding of currents in the discharge channel and also on the assumption that any planktonic larvae colonizing the channel would have to survive transit through the SBPP cooling water system. Based on ADP current measurements in the present study (see Section 2.5—*Receiving Water Currents and Bathymetry*), it was evident that under certain high tide and plant operational conditions a near-bottom countercurrent entrained cooler water toward the plant. Coupled with the presence of a periodic counterclockwise gyre in the larger discharge embayment during flood tides and periodic shutdown of the SBPP circulating water pumps, sufficient conditions should exist to allow dispersal and potential colonization of all parts of the discharge channel by invertebrate larvae from throughout South Bay. Although the current regimes could favor opportunistic species with extended spawning periods, post-settlement environmental conditions and processes would mainly determine the abundance and distribution of species in the discharge channel.

4.3.4 Conclusions

Results from this study confirm the general conclusions of Ford et al. (1973) and Ogden (1994) that differences in patterns in species composition between the discharge sites and reference (far-field) sites indicate that the SBPP discharge creates a highly variable environment that favors opportunistic species adapted to a wide range of temperatures. Among these are several species of annelid worms, nematodes, and an introduced bivalve species (*Musculista senhousi*). Multivariate statistical analysis clearly demonstrated the dissimilarity among discharge and reference stations at both intertidal and subtidal depths, and also separated stations along a gradient consistent with changes in water temperature resulting from the SBPP discharge. Although there are numerous physical and biological factors that regulate the abundance and distribution of benthic communities, the delineation of sites along a general gradient related to the presence of the SBPP discharge suggests that one or more factors related to the discharge caused the observed patterns. Differences in sediment type contributed to some of the observed variation in faunal composition, but physiological stresses on organisms caused by elevated bottom temperatures is likely the most important factor in determining faunal composition. There were many species in common between the discharge and reference areas suggesting that conditions at the inner discharge stations were not inhibiting the propagation and colonization of these species.

It is important to consider the faunal characteristics of groups of stations rather than individual stations when drawing conclusions about discharge effects. Benthic communities are spatially patchy, and replicate samples can vary considerably in attributes such as diversity and total number of species. Some discharge stations were similar to reference stations in community attributes, even exceeding certain reference stations in measures such as diversity and species richness that would be considered indicative of a balanced and indigenous ecological community. However, when analyzed in terms of area characteristics, and not only individual station characteristics or individual species abundances, the inner discharge channel stations trended toward reduced diversity and a benthic community with more opportunistic species that had high temperature tolerances (e.g., *Capitella* complex).

There have been no investigations concerning the physiological tolerances of the invertebrate species sampled in this study that would explain their persistence in the discharge channel to the exclusion of other species, or how settling larvae of those species respond to the variable thermal regimes encountered in the discharge. Furthermore, it is not understood which aspects of thermal exposure (e.g., maximum temperature, average temperature, daily range) are most important to organism growth and survival. Investigations on rocky shore invertebrates have found that the exposure history of body temperature and acclimation effects are important factors in determining levels of thermal stress (Helmuth and Hoffman 2001), and that “snapshot” sampling of temperature and biochemical indices may not always be a reliable method for defining

thermal stress. One of the main goals of current research is to address how spatial and temporal heterogeneity in thermal stress translates into ecological effects.

Earlier analyses concluded that power plant effects on benthic fauna were confined to the discharge channel and were less well defined during winter and spring as water temperatures cooled from summer maxima. Ford et al. (1973) found that several species became established at locations progressively closer to the source of thermal effluent as seasonal temperatures declined. These conclusions could not be confirmed in the present study because samples were only collected during a single summer season, but the gradient of effects we observed between the discharge and reference areas would be expected to diminish as average water temperatures cooled. Therefore, the extent of effects described in this study represents a maximum effects range that was still confined to the discharge channel area. The most noticeable subtidal differences occurred at the four innermost stations that were within 1.0 km of the SBPP discharge and were east of a point of land midway along the southern margin of the CVWI. Modeling of thermal conditions during the study period indicated that this zone would be exposed to a temperature increase of 4°F (2.2°C) above ambient at least 50 percent of the time. Intertidal effects were also most distinguishable along this adjacent reach of shoreline, although all intertidal stations in the discharge zone, including those beyond the point, showed differences in faunal composition from the reference stations on the north side of CVWI.

We did not delineate a physical area of affected bay bottom because the nature of discharge effects depends on how departures from the reference area are defined. Examination of the August 2003 MDS and PCA analyses show a greater separation from reference assemblages in the intertidal zone than subtidal zone which is consistent with the assumption that temperature was the most important physical factor affecting the infauna. Variation among the reference sites probably resulted from a combination of differences in sediment parameters, biological interactions, and differential settlement or colonization patterns, all of which would occur in the absence of any discharges. Superimposing the added source of variation from discharges on this natural variation creates an overlapping margin within which community responses grade both spatially and temporally. In all cases the effects would appear to be confined to the discharge channel area. The presence of cooler countercurrents along the southeastern margin of this discharge area, particularly on flood tides, would tend to further diminish any far-field effects on shallow water assemblages.

The near-field station array in earlier studies was inadequate for defining the magnitude of change along the discharge gradient. The general conclusion of Ford et al. (1974) and Ogden (1994) that adverse effects of the discharge were confined to the larger discharge area was confirmed in the present study. Even with a trend toward diminished diversity and biomass, the discharge supports a relatively high density of infaunal organisms that functionally provide food resources to species at higher trophic levels, such as fishes and

shorebirds, in South Bay. However, by sampling at a finer spatial scale we were able to delineate a gradient of discharge effects on several individual infaunal taxa, and provide evidence that the greatest departures from the reference communities occurred within a near-field zone (primarily within 305 m [1000 ft] of the discharge point) that is smaller than the effects area defined in previous studies.

DRAFT

4.4 Effect of Cooling Water Discharges on Fish Communities: Role of Dissolved Oxygen

The primary focus of the fish studies, in response to RWQCB questions, was to investigate fish assemblage composition in the SBPP discharge channel in relation to dissolved oxygen regimes by comparing habitat and assemblage characteristics to a nearby reference site. A previous study (Merkel & Associates, Inc. 2000b) provided a detailed description of seasonal and interannual changes in the SBPP discharge channel fish assemblages. The fewest numbers of fishes were generally found during the summer months when temperatures were highest, but overall the channel supported a diverse fish assemblage that was dominated by juvenile anchovies. Based on purse seine data the discharge channel supported an average of 9.8 times the density of slough anchovies compared to greater San Diego Bay, providing a rich forage base for terns, skimmers, and other avian predators. The study concluded that species representing all fish guilds typical of coastal bays were regularly captured during the surveys although some taxa such as northern anchovy, surfperches, and giant kelpfish were under-represented due to a combination of thermal preferences and lack of structural habitat.

The monitoring conducted in the present study demonstrated that during the 2003 summer months DO concentrations within the SBPP discharge channel were within the range observed at the sampled reference sites (**Figure 2.3-7**). As discussed previously, the combined mean daily DO concentration for the reference sites was 5.38 mg/l with a maximum hourly mean of 7.06 mg/l and minimum hourly mean of 4.02 mg/l. The mean daily DO concentration in the discharge channel was of 4.99 mg/l, with a mean hourly peak of 5.51 mg/l and minimum of 4.47 mg/l. The diurnal variation in DO in the discharge channel is muted in comparison to the reference sites, with reduced fluctuation throughout the day. Mean daily hourly DO in the discharge channel does not fall above or below the range seen at the other back-bay sites.

The reference sites support communities of fish that are adapted to the DO, salinity and temperature regimes typically found in back-bay waterbodies. Because DO in the discharge channel is comparable to other back-bay sites in southern California, it would be expected that DO concentrations would not be a limiting factor for supporting a typical back-bay fish assemblage in the discharge channel. As presented in Section 3.4–*Fish Communities*, the discharge channel does in fact support a diverse and abundant native fish community. Although sampling methods varied across the reference sites, a best effort was made to use the most comparable data from previously conducted studies, based on seasonal timing, geographical location, physical characteristics, and methodology. Making these general comparisons, the SBPP discharge channel was found to have a higher species count, density, and biomass than the four reference sites (Sweetwater River, Seal Beach NWR, Batiquitos Lagoon, and Agua Hedionda

Lagoon)(**Figure 3.4-4**). This suggests that the SBPP discharge channel provides a suitable environment for a diverse, back bay fish community.

While sites with extremely low DO levels can preclude most species of fish, the discharge channel and reference sites have been shown to have sufficient ranges of DO to support diverse communities of fish adapted to back-bay environments. If the diversity, density, or biomass of the fish communities were strongly determined by DO levels, it would be predicted that a correlation between DO and these population parameters could be seen in the accumulated data. This hypothesis is investigated in **Figure 4.4-1** in which these parameters are plotted against DO. DO concentrations in the discharge channel and at reference sites are plotted in ascending order. The number of fish species, density, and biomass reported in other summer fish sampling studies at each site is shown on the right vertical axis.

These figures do not reveal a correlative trend between DO and the parameters of species count, density, and biomass. Although the reference site at Seal Beach NWR had the highest DO, fish data collected at the site had very low diversity, low density, and the lowest biomass. The station with the lowest DO, eastern Batiquitos Lagoon, supported a large number of back-bay species with a very high biomass. Density at this site was low, due to the capture of primarily large fish in small numbers. Within the back-bay fish communities of the sites studied, increased DO did not appear to be linked to more robust fish populations. This lack of correlation suggests that other factors, such as habitat quality, food availability, and water temperature, are more important than DO to the variation between sites.

It is important that the conclusions here not be construed as meaning that DO concentrations are not relevant to fish or other biota. Rather, the conclusions suggest that within the range of DO conditions encountered within the SBPP discharge channel, fish communities were not substantially different from what would be expected in such environments. The results of the investigations further show that the fish species comprising the various sampled communities are highly consistent and predictable with few deviations that are reflective of the different systems. This observation is important in that it provides definition to what would be considered a balanced indigenous community for these back-bay waters. The species list along with the other community parameters previously discussed also suggests that a balanced indigenous community is being maintained within the discharge channel. It is equally important to note that, while the DO conditions of the SBPP discharge channel and the reference areas are supportive of the needs of the native fish community, they would not necessarily be expected to support a differing community with differing physiological tolerances and adaptations to such environments as found in the highly variable waters of shallow back-bay environments.

DRAFT

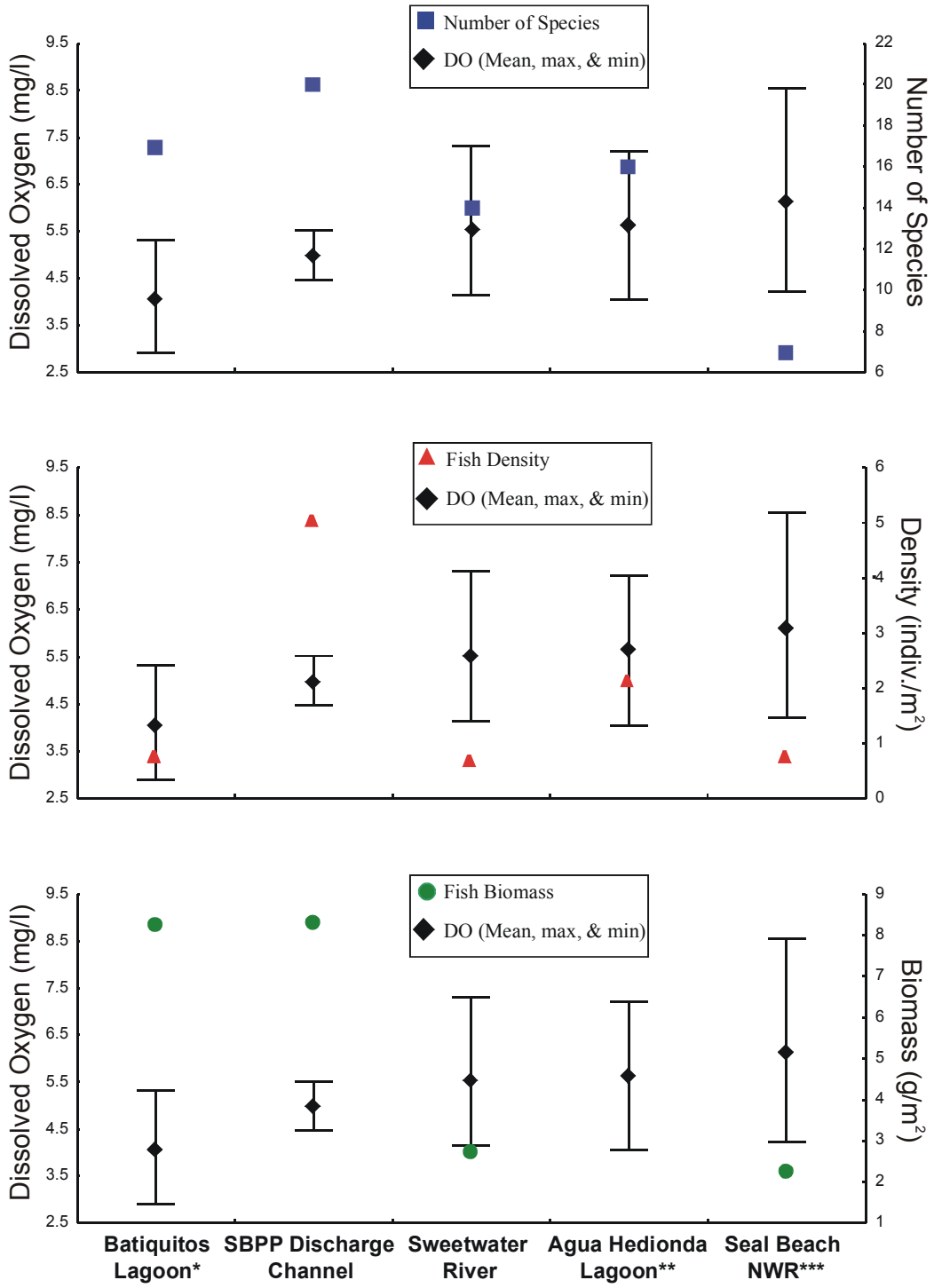

Figure 4.4-1. Dissolved oxygen at each study site plotted in increasing value, against number of fish species, density, and biomass at study sites and three reference sites. Error bars are the average hourly minimum and maximum dissolved oxygen levels.

* July 2003, Merkel & Associates (2003).
** July 1994, MEC Analytical Systems, Agua Hedionda Lagoon Fish Surveys, (1995) (no biomass reported)
*** Sept. 1994, MEC Analytical Systems, Anaheim Bay Biological Monitoring Report (1995).

5.0 Literature Cited

Adams, J. 1975. The influence of thermal discharges on the distribution of macroflora and fauna, Humboldt Bay Nuclear Power Plant, California. Ph.D. Thesis. University of Washington.

Allan, L. G. 1999. Fisheries Inventory and Utilization of San Diego Bay, San Diego, California. Final Report: Sampling Period July 1994 to April 1999. Prepared for U.S. Navy and the San Diego Unified Port District.

Allen, L. G., A. M. Findlay, and C. M. Phalen. 2002. Structure and standing stock of the fish assemblages of San Diego Bay, California from 1994 to 1999. Bull. So. Cal. Acad. Sci. 101(2):49–85.

Bach, H. K. 1993. A dynamic model describing the seasonal variations in growth and the distribution of eelgrass (*Zostera marina* L.). I. Model theory. Ecological Modeling 65:31-50.

Backman, T. W. and D. C. Bairilotti. 1976. Irradiance reduction: effects on standing crops of the eelgrass *Zostera marina* in a coastal lagoon. Marine Biology 34:33-40.

Bergen, M., S. B. Weisberg, R. W. Smith, D. B. Cadien, A. Dalkey, D. E. Montagne, J. K. Stull, R. G. Velarde, J. A. Ranasinghe. 2001. Relationship between depth, sediment, latitude, and the structure of benthic infaunal assemblages on the mainland shelf of southern California. Mar. Biol. 138:637–647.

Biebl, R. and C. P. McRoy. 1971. Plasmatic resistance and rate of respiration and photosynthesis of *Zostera marina* at different salinities and temperatures. Mar. Biol. 8:48-56.

Browning, B. M., J. W. Speth, and W. Gayman. 1973. The natural resources of San Diego Bay: Their status and future. CA Dept. Fish Game. Coastal Wetlands Series #5. 105 pp.

Buthuis, D. A. 1987. Effects of temperature on photosynthesis and growth of seagrass. Aquatic Botany 27:27-40.

California State Water Resources Quality Control Board (SWRCB). 1975. Water Quality Control Plan for Control of Temperature in the Coastal and Interstate Waters and Enclosed Bays and Estuaries of California (Thermal Plan).

California State Water Resources Quality Control Board (SWRCB). 2001. California Ocean Plan.

Casulli, V. and E. Cattanni. 1994. Stability, accuracy and efficiency of a semi-implicit method for three-dimensional shallow water flow. Computers Math. Applic. 27:99-112.

DRAFT

Chadwick, D. B., J. L. Largier, and R. T. Cheng. 1996. The role of thermal stratification in tidal exchange at the mouth of San Diego Bay. Proceedings of the 7th International Conference on the Physics of Estuaries and Coastal Seas, American Geophysical Union.

Cheng, R. T., V. Casulli, and J. W. Gartner. 1993. Tidal, residual, intertidal mudflat (TRIM) model and its applications to San Francisco Bay, California. Estuarine, Coastal and Shelf Science 36:235-280.

Clarke, K. R. and R. M. Warwick. 2001 Change in marine communities: an approach to statistical analysis and interpretation. PRIMER-E, Plymouth, England.

Clarke, K. R. and R. N. Gorley. 2001 PRIMER Version 5.0: User Manual/Tutorial. PRIMER-E, Plymouth, England.

Coutant, C. C. and A. J. Brook. 1970. Biological aspects of thermal pollution. I. Entrainment and discharge canal effects. CRC Critical Reviews in Environmental Control. p. 341–380.

Dennison, W. C. 1987. Effects of light on seagrass photosynthesis, growth and depth distribution. Aquatic Botany 27:15-26.

Dennison, W. C. and R. S. Alberte. 1985. Role of daily light period in the depth distribution of *Zostera marina* (eelgrass). Marine Ecology Progress Series 25:51-61.

Eckert, S. A. 1994. Results of trawling for sea turtles in the South San Diego power plant intake channel. Unpublished report prepared for SDG&E.

ESA, Environmental Science Associates. 1997. Initial Study for San Diego Gas & Electric Company's Application No. 97-12-039.

Ford, R. F. 1968. Marine organisms of south San Diego Bay and the ecological effects of power station cooling water discharge. Environmental Engineering Laboratory Tech. Report. 278 pp.

Ford, R. F., R. L. Chambers, and J. Merino. 1970. Ecological effects of power station cooling water discharge in south San Diego Bay during August 1970. Environmental Engineering Laboratory Tech. Report. 92 pp.

Ford, R. F., R. L. Chambers, and J. Merino. 1973. Thermal distribution and biological studies for the South Bay Power Plant. Final Report. Volume 5a Biological Measurements. Environmental Engineering Laboratory Tech. Report. 188 pp.

Gallegos, C. L., D. L. Correll, and J. W. Pierce. 1990. Modeling spectral diffuse attenuation, absorption, and scattering coefficients in a turbid estuary. Limnology and Oceanography 35:1486-1502.

Green, R. H. 1979. Sampling design and statistical methods for environmental biologists. Wiley and Sons, New York. 257 pp.

DRAFT

Helmuth B. and G. E. Hoffman. 2001. Microhabitats, thermal heterogeneity and physiological gradients of stress in the rocky intertidal zone. Biological Bulletin 201:374-384.

Iannuzzi, T. J., M. P. Weinstein, K. G. Sellner and J. C. Barrett. 1996. Habitat disturbance and marina development: an assessment of ecological effects. I. Changes in primary production due to dredging and marina construction. Estuaries 19(2A):257-271.

Kenworthy, W. J. and M. S. Fonseca. 1996. Light requirements of seagrasses *Halodule wrightii* and *Syringodium filiforme* derived from the relationship between diffuse light attenuation and maximum depth distribution. Estuaries 19(3):740-750.

Kinne, O. 1963. The effects of temperature and salinity on marine and brackish water animals. Oceanogr. Mar. Biol. Ann. Rev. 1:301-340.

Largier, J. L. 1995. San Diego Bay circulation: a study of the circulation of water in San Diego Bay for the purpose of assessing, monitoring and managing the transport and potential accumulation of pollutants and sediment in San Diego Bay. Scripps Institution of Oceanography Tech. Rep. # 1-188-190-0. Final Report prepared for Calif. State Water Res. Control Board and the Calif. Reg. Water Quality Control Board, San Diego Region.

Lerberg, S. B., A. F. Holland, and D. M. Sanger. 2000. Responses of tidal creek macrobenthic communities to the effects of watershed development. Estuaries 23(6):838-853.

Lockheed Environmental Sciences (LES). 1981. South Bay Power Plant Receiving Water Monitoring Program - A Four-Year Cumulative Analysis Report (1977-1980). Carlsbad, CA.

Lüning, K. and M. Neushul. 1978. Light and temperature demands for growth and reproduction of laminarian gametophytes in southern and central California. Mar. Biol. 45:297–309.

Marsh, J. A., W. C. Dennison, and R. S. Alberte. 1986. Effects of temperature on photosynthesis and respiration in eelgrass (*Zostera marina* L.). Journal of Experimental Marine Biology and Ecology 101:257-267.

Masini, R. J., J. L. Cary, C. J. Simpson, and A. J. McComb. 1995. Effects of light and temperature on the photosynthesis of temperate meadow-forming seagrasses in Western Australia. Aquatic Botany 49:239-254.

McDuff, R.E. 2002. Settling of particles; threshold of motion. Univ. Washington Marine Geological Processes Lecture Notes. Figure 1 after F. Hjulstorm. [Cited 13 January 2004 at: www2.ocean.washington.edu/oc540/lec02-25/].

MEC Analytical Systems, Inc. 1995a. 1994 and 1995 Field Survey Report of the Ecological Resources of Agua Hedionda Lagoon. Prepared for SDGE. Carlsbad, CA.

DRAFT

MEC Analytical Systems, Inc. 1995b. Anaheim Bay Biological Monitoring Project. Final Report. Prepared for the Port of Long Beach. Carlsbad, CA.

MEC Analytical Systems, Inc. 2003. South Bay Power Plant monthly intake and receiving water monitoring study. September 2003. Prepared for Duke Energy Power Services. 10 p.

Meldrim, J.W. and J.J. Gift. 1971. Temperature preference, avoidance and shock experiments with estuarine fishes. Ichthyological Associates Bulletin, Ithaca, New York.

Merkel & Associates, Inc. 2002. Long-term Monitoring and Pilot Revegetation Program for the Batiquitos Lagoon Enhancement Project Annual Report, January–December 2001. Prepared for City of Carlsbad Planning Department and Port of Los Angeles, Environmental Management Division. San Diego, CA.

Merkel & Associates, Inc. 2000a. Environmental controls on the distribution of eelgrass (*Zostera marina* L.) in south San Diego Bay: An assessment of the relative roles of light, temperature, and turbidity in dictating the development and persistence of seagrass in a shallow back-bay environment. Prepared for Duke Energy North America. 81 p. + App.

Merkel & Associates, Inc. 2000b. South Bay Power Plant cooling water discharge channel fish community characterization study: April 1997 through January 2000 – Final Report. Prepared for Duke Energy North America. 55 p. + App.

Merkel, K. W. and D. Sutton. 2000. Development of a numeric model for explaining eelgrass distribution in south San Diego Bay. Appendix E *in* Environmental Controls on the Distribution of Eelgrass (*Zostera marina* L.) in south San Diego Bay: An Assessment of the Relative Roles of Light, Temperature, and Turbidity in Dictating the Development and Persistence of Seagrass in a Shallow Back-bay Environment. Prepared for Duke Energy North America. 81 p. + App.

Miller, R. L. and B. F. McPherson. 1995. Modeling photosynthetically active radiation in water of Tampa Bay, Florida, with emphasis on the geometry of incident irradiance. Estuarine, Coastal and Shelf Science 40:359-377.

Norris, K. S. 1963. The functions of temperature in the ecology of the percoid fish *Girella nigricans* (Ayres). Ecol. Monogr. 33:23–62.

Ogden Environmental and Energy Services Co., Inc. 1994. Review of the long-term receiving water monitoring done for the South Bay San Diego Bay Power Plant. Prepared for San Diego Gas & Electric. 29 p. + App.

Pederson, O. B., C. Christiansen, and M. B. Laursen. 1995. Wind-induced long term increase and short term fluctuations of shallow water suspended matter and nutrient concentrations, Ringkobing Fjord, Denmark. Ophelia 41:49-66.

DRAFT

Penhale, P. A. 1977. Macrophyte-epiphyte biomass and productivity in an eelgrass community. J. Exp. Mar. Biol. Ecol., Vol. 26, pp. 211–224.

Phillips, R C. 1984. The ecology of eelgrass meadows in the Pacific northwest: a community profile. U.S. Fish Wildl. Serv. OBS 84/24, 85p.

Phillips, R.C. and T.W. Backman. 1983. Phenology and reproductive ecology of eelgrass (*Zostera marina* L.) at Bahia Kino, Sea of Cortez, Mexico. Aquatic Botany 17:85-90.

Phillips, R. C., W. S. Grant, and C. P. McRoy. 1983. Reproductive strategies of eelgrass (*Zostera marina*). Aquat. Bot. 16:1-20.

Pulich, W. M., Jr. and W. A. White. 1991. Decline of submerged vegetation in the Galveston Bay system: chronology and relationships to physical processes. Journal of Coastal Research 7:1125-1138.

San Diego Gas & Electric Co. (SDG&E). 1973. Thermal distribution and biological studies for the South Bay Power Plant. Final Report. Vol. 1: Summary and Conclusions. Pioneer Service and Engineering Company. 54 p.

San Diego Gas & Electric Co. (SDG&E). 1980. South Bay Power Plant Cooling Water Intake System Demonstration Summary. Prepared for: California Regional Water Quality Control Board San Diego Region, San Diego CA.

San Diego Regional Water Quality Control Board (SDRWQCB). 1994. Water Quality Control Plan for the San Diego Basin (Basin Plan).

SDUPD (San Diego Unified Port District) and California State Coastal Conservancy. 1990. South San Diego Bay Enhancement Plan. 4 volumes. Prepared by Michael Brandman Associates, Inc.

SDUPD (San Diego Unified Port District). 1976. Master Plan (1972) amendment submitted to State Lands Commission as required by Public Resources Code 63.

Smith, R. W., J. A. Ranasinghe, S. B. Weisberg, D. E. Montagne, D. B. Cadien, T. K. Mikel, R. G. Velarde, and A. Dalkey. 2003. Extending the southern California benthic response index to assess benthic condition in bays. Appendix C *in* Southern California Bight 1998 Regional Monitoring Program, Vol. VII: Benthic Macrofauna. Southern California Coastal Water Research Project, Westminster, CA. 280 p.

Smith, R. W., M. Bergen, S. B. Weisberg, D. Cadien, A. Dalkey, D. Montagne, J. K. Stull, and R. G. Velarde. 2001. Benthic response index for assessing infaunal communities on the southern California mainland shelf. Ecological Applications 11:1073–1087.

Smith, W. H. B. 1976. Productivity measurements and simulation models of a shallow estuarine ecosystem receiving a thermal plume at Crystal River, Florida. Ph.D. Dissertation, University of Florida, Gainesville, FL.

DRAFT

Southern California Coastal Water Research Project (SCCWRP). 2003. Southern California Bight 1998 Regional Monitoring Program: VII. Benthic Macrofauna. 280 pp. *ftp://ftp.sccwrp.org/pub/download/PDFs/bight98benthic.pdf*

Stephens, J. S. Jr., and K. Zerba. 1981. Factors affecting fish diversity on a temperate reef. Envir. Biol. Fish. 6: 111–121.

Stephens, J. S. Jr., P. A. Morris, D. J. Pondella, T. A. Koonce, and G. A. Jordan. 1994. Overview of the dynamics of an urban artificial reef fish assemblage at King Harbor, California, USA, 1974-1991: A recruitment driven system. Bull. Mar. Sci. 55:1224 (abstract).

U. S. Fish and Wildlife Service. 1998. Proposed South San Diego Bay Unit, National Wildlife Refuge. Draft Environmental and Land Protection Plan. U.S. Fish Wild. Serv. 89 p.

U. S. Navy, Southwest Div. Nat. Resource Branch. 1994. San Diego Bay Eelgrass Survey. Jan. 1, 1994.

United States Environmental Protection Agency (EPA). 1974. 316(a) Technical Guidance Manual–Thermal Discharges. Water Planning Division, Office of Water and Hazardous Materials, U.S. EPA, Washington, D.C. Draft of September 30, 1974.

Wang, P. F., R. T. Cheng, K. Richter, E. S. Gross, D. Sutton, J. W. Gartner. 1998. Modeling tidal hydrodynamics of San Diego Bay, California. J. Am. Water Res. Assoc. 34(5):1123–1140.

Ward, L. G., W. M. Kemp, and W. C. Boynton. 1984. The influence of waves and seagrass communities on suspended particulates in an estuarine embayment. Marine Geology 59:58–103.

Weisberg, S. B., J. A. Ranasinghe, D. M. Dauer, L. C. Schaffner, R. J. Diaz, and J. B. Frithsen. 1997. An estuarine benthic index of biotic integrity (B-IBI) for Chesapeake Bay. Estuaries 20:149–158.

Weiss, R. F. 1970. Solubility of nitrogen, oxygen and argon in water and seawater. Deep-Sea Res. 17:721-735.

Williams, G. D. and J. B. Zedler. 1999. Fish assemblage composition in constructed and natural tidal marshes of San Diego Bay: relative influence of channel morphology and restoration history. Estuaries 22:702–716.

Zimmerman, R. C., A. Cabello-Pasini, and R.S. Alberte. 1994. Modeling daily production of aquatic macrophytes from irradiance measurements: A comparative analysis. Marine Ecology (Progress Series) 114:185-196.

Zimmerman, R. C., R. D. Smith, and R. S. Alberte. 1990. Seagrass revegetation: Developing a predictive model of light requirements for *Zostera marina*. *In:* Proceedings of the California Eelgrass Symposium, May 1988, Chula Vista, California. Merkel, K. W. and R. S. Hoffman, eds. Sweetwater River Press, National City, CA.

DRAFT